

Comparisons of Carbon and Water Fluxes of Pine Forests  
in Boreal and Temperate Climatic Zones

by

Pantana Tor-ngern

Department of Environment  
Duke University

Date: \_\_\_\_\_

Approved:

\_\_\_\_\_  
Ram Oren, Supervisor

\_\_\_\_\_  
Sari Palmroth

\_\_\_\_\_  
Jean-Christophe Domec

\_\_\_\_\_  
Danielle Way

Dissertation submitted in partial fulfillment of  
the requirements for the degree of Doctor  
of Philosophy in the Department of  
Environment  
of Duke University

2015

ABSTRACT

Comparisons of Carbon and Water Fluxes of Pine Forests  
in Boreal and Temperate Climatic Zones

by

Pantana Tor-ngern

Department of Environment  
Duke University

Date: \_\_\_\_\_

Approved:

\_\_\_\_\_  
Ram Oren, Supervisor

\_\_\_\_\_  
Sari Palmroth

\_\_\_\_\_  
Jean-Christophe Domec

\_\_\_\_\_  
Danielle Way

An abstract of a dissertation submitted in partial  
fulfillment of the requirements for the degree  
of Doctor of Philosophy, in the Department of  
Environment in the Graduate School of  
Duke University

2015

Copyright by  
Pantana Tor-ngern  
2015

## **Abstract**

Quantifying carbon fluxes and pools of forest ecosystems is an active research area in global climate study, particularly in the currently and projected increasing atmospheric carbon dioxide concentration environment. Forest carbon dynamics are closely linked to the water cycle through plant stomata which are regulated by environmental conditions associated with atmospheric and soil humidity, CO<sub>2</sub>, air temperature and light. Thus, it is imperative to study both carbon and water fluxes of a forest ecosystem to be able to assess the impact of environmental changes, including those resulting from climate change, on global carbon and hydrologic cycles. However, challenges hampering such global study lie in the spatial and temporal variability of fluxes in forests around the globe. Moreover, continuous, long-term monitoring and measurements of fluxes are not feasible at global forest scale. Therefore, the need to quantify carbon and water fluxes and to identify key variables controlling them at multiple stands and time scales is growing. Such analyses will benefit the upscaling of stand-level observations to ecosystem or global-scale modelling approaches.

I performed a series of studies investigating carbon and water fluxes in pine forests of various site characteristics, conditions and latitudes. The common techniques used in these studies largely involved sap flux sensors to measure tree-level water flow, which is scaled up to stand-level transpiration, and a process-based model, which

calculates canopy light absorption and carbon assimilation constrained by the sap-flux based canopy stomatal conductance (called Canopy Conductance Constrained Carbon Assimilation, or the 4C-A model). I collected and analyzed sap flux data from pine forests of two major species: *Pinus taeda* in temperate sites (36 °N) and *Pinus sylvestris* in boreal (64 °N) climatic zones. These forests had different stage-related canopy leaf area and some were under treatments for elevated atmospheric CO<sub>2</sub> concentration or fertilization.

I found that (**Chapter 2**) the 17-year long free-air CO<sub>2</sub> enrichment (FACE) had little effect on canopy transpiration of a mixed forest dominated by *P. taeda* and with other broadleaved species as the understory in North Carolina, USA (Duke FACE). The result was due to the compensation of an elevated [CO<sub>2</sub>]-induced increase of canopy leaf area for the reduction of mean canopy stomatal conductance. My next theoretical study (**Chapter 3**), comparing *P. taeda* (native at 36 °N in North Carolina), *P. sylvestris* (native at 64 °N in northern Sweden) and *Pinus contorta* (native at 58 °N in British Columbia, Canada) canopies, revealed that the interaction between crown architecture and solar elevation associated with site latitude of pine canopies affected the distribution and total amount of canopy light absorption and potential photosynthesis, such that the latitudinally prescribed needle organization of a pine canopy is optimal for light interception and survival in its native location. Then, I quantified and analyzed water fluxes in four pine forests: one composed of *P. taeda* in North Carolina and three

containing *P. sylvestris* in northern Sweden (**Chapter 4**). The latter forests consisted of various stage-related canopy leaf area and nutrient status. Combining my estimates with other published results from forests of various types and latitudinal locations, I derived an approach to estimate daily canopy transpiration during the growing season based on a few environmental variables including atmospheric and soil humidity and canopy leaf area. Moreover, based on a water budget analysis, I discovered that the intra-annual variation of precipitation in a forest has a small effect on evapotranspiration and primarily affects outflow; however, variation of precipitation across latitudes proportionally influences annual evapotranspiration and outflow. Furthermore, the hydrologic analyses implied the 'disequilibrium' of forest water cycling during the growing season when forests may use less and more water in dry and wet regions, respectively, than the incoming precipitation. Nevertheless, at annual timescales, most forests became in 'equilibrium' by using a similar proportion of incoming precipitation. Finally, (**Chapter 5**) I estimated and analyzed the temporal and spatial variabilities of carbon fluxes of the same four forests measured in Chapter 4 using the 4C-A computational approach and analyzed their resource-use efficiencies. I concluded that, based on my results and others as available, despite differences in species clumping and latitude (which influence growing season length and solar elevation), the gross primary productivity of the forests is linearly related to the canopy light absorption. However,

based on previous findings from a global study, different allocation of the acquired carbon to the above- and belowground is regulated by soil nutrient status.

Overall, the findings in this dissertation offer new insights into the impacts of environmental changes on carbon and water dynamics in forests across multiple sites and temporal scales which will be useful for larger-scale analyses such as those pertaining to global climate projection.

## **Dedication**

For my first teachers, Mr. & Mrs. Tor-ngern.

# Contents

Abstract .....	iv
List of Tables .....	xiv
List of Figures .....	xvi
Acknowledgements .....	xviii
1. Introduction .....	1
1.1 Carbon in Forests .....	1
1.2 Water in Forests .....	5
1.3 Carbon and Water in Forests .....	8
1.4 Boreal and Temperate Forests .....	9
1.5 The Studies .....	11
2. Increases in atmospheric CO <sub>2</sub> have little influence on transpiration of a temperate forest canopy .....	16
2.1 Introduction .....	16
2.2 Materials and Methods .....	18
2.2.1 Settings .....	18
2.2.2 Long- and short-term [CO <sub>2</sub> ] manipulation experiments .....	19
2.2.3 Measurements and calculations of variables .....	20
2.2.4 Tests for significant elevated-[CO <sub>2</sub> ] effects .....	22
2.3 Results and Discussion .....	22
2.4 Appendix .....	33

2.4.1 Additional Materials and Methods.....	33
2.4.1.1 Data for the interannual elevated-[CO <sub>2</sub> ] effects on $G_s$ , $L_D$ and $E_c$ at Duke FACE.....	33
2.4.1.2 Hierarchical Bayesian scaling approach.....	34
2.4.1.3 Calculations of daily $E_c$ and $G_s$ .....	35
2.4.1.4 Analysis of the Elevated- to-Ambient-[CO <sub>2</sub> ] ratio of $G_s$ ( $G_s^E:G_s^A$ ).....	36
2.4.1.5 Leaf hydraulic conductance ( $K_{leaf}$ ).....	40
2.4.1.6 Long-term response of $Q$ to increasing [CO <sub>2</sub> ] .....	41
3. Adaptation of pine crown architecture to growing season solar elevation supports low branches and prevents extra light from reaching competing subcanopy species .....	48
3.1 Introduction.....	48
3.2 Materials and Methods .....	54
3.2.1 Settings.....	54
3.2.2 Canopy structure .....	56
3.2.3 Absorbed Photosynthetically Active Radiation (APAR).....	58
3.2.4 Cost-benefit analysis of light absorption/crown carbon investment .....	60
3.3 Results .....	62
3.4 Discussion.....	68
3.5 Concluding remarks.....	76
3.6 Appendix .....	87
3.6.1 Calculation of total carbon cost in the crown for estimating light-capturing efficiency (LCE).....	87

4. Daily transpiration of forests is controlled spatially by variation of canopy leaf area and soil texture and temporally by variation in atmospheric and soil humidity: Synthesis of new and published results .....	91
4.1 Introduction.....	91
4.2 Materials and Methods .....	95
4.2.1 Settings.....	95
4.2.2 Environmental measurements.....	97
4.2.3 Estimation of sapwood area and leaf area index .....	99
4.2.4 Sap flux measurements and scaling to the canopies .....	99
4.2.5 Hydrologic balance .....	104
4.2.6 Statistical analyses.....	106
4.3 Results .....	107
4.3.1 Environmental conditions.....	107
4.3.2 Daily sap flux density and transpiration .....	108
4.3.3 Canopy transpiration in relation to atmospheric, soil and stand conditions .	109
4.3.4 Hydrologic balance across study sites.....	111
4.4 Discussion.....	114
4.4.1 Sensitivity of forest hydrologic components to climate.....	117
4.5 Concluding remarks.....	118
4.6 Supplementary Data .....	129
4.6.1 Appendix S1 .....	129
4.6.1.1 Derivation of gapfilling functions for $J_{SD,Out}$ .....	129

4.6.1.2 Literature review for $E_c$ versus $D_z$ response and hydrologic components .....	130
4.6.1.3 Literature review for soil moisture effect .....	131
5. Estimates of gross primary productivity (GPP) and resource-use efficiencies of <i>Pinus taeda</i> and <i>Pinus sylvestris</i> forests in temperate and boreal zones.....	148
5.1 Introduction.....	148
5.2 Materials and Methods .....	153
5.2.1 Settings.....	153
5.2.2 Biometric measurements .....	154
5.2.3 Environmental measurements.....	155
5.2.4 Calculating mean canopy stomatal conductance ( $G_s$ ) .....	157
5.2.5 Estimating gross primary productivity (GPP) .....	158
5.2.6 Estimating net primary productivity (NPP).....	161
5.2.7 Statistical Analyses.....	163
5.3 Results .....	163
5.3.1 Environmental conditions and variable estimates .....	163
5.3.2 Temporal responses of photosynthesis to environmental variation.....	166
5.3.3 Resource-use efficiencies .....	169
5.4 Discussion.....	170
5.4.1 Spatio-temporal variations of GPP at half-hourly timescale.....	170
5.4.2 Total growing season GPP .....	172
5.4.3 Analyses of the resource-use efficiencies .....	173
5.5 Conclusion.....	176

5.6 Supplementary Data .....	189
6. Concluding Remarks .....	205
References .....	206
Biography .....	251

## List of Tables

Table A2.4.1: Regression statistics of <i>Indirect Ec</i> response to $D_z$ .....	43
Table A2.4.2: $P$ values from a Student's $t$ -test.....	44
Table A2.4.3: Results from Randomized Intervention Analyses (RIA).....	45
Table 3.1: Site and stand information.....	78
Table A3.6.1: Components of cost estimates of the crown.....	90
Table 4.1: Definitions .....	120
Table 4.6.1: Site characteristics of surveyed forests used to derive the functions for estimating daily canopy transpiration (Fig. 4.4).....	132
Table 4.6.2: Summary of instrumentation for environmental measurements at the study sites.....	136
Table 4.6.3: Summary of empirical functions.....	139
Table 4.6.4: Summary of regression statistics.....	140
Table 4.6.5: Site characteristics of forests used to determine soil drying effect on canopy transpiration (Fig. 4.5c) .....	141
Table 4.6.6: Growing season water balance of the study sites.....	142
Table 4.6.7: Site characteristics of forests used for the analysis of hydrologic components (Fig. 4.7) .....	143
Table 5.1: Definitions .....	178
Table 5.2: Summary of characteristics of the study forests .....	180
Table 5.3: $C_i/C_a$ ratios.....	181
Table 5.4: Summary of growing season estimates of variables used in the analyses.....	182
Table A5.6.1: Summary of instrumentation for environmental measurements at the study sites.....	189

Table A5.6.2: Summary of components of the net primary productivity (NPP). .....	191
Table A5.6.3: Summary of regression statistics.....	192
Table A5.6.4: Literature survey of water-use efficiency (WUE) in $\text{gC mm}^{-1}$ . .....	193
Table A5.6.5: Literature survey for light-use efficiency (LUE) analysis (Figure 5.6a).....	196
Table A5.6.6: Literature survey for carbon-use efficiency (CUE) analysis (Figure 5.6b).	199

## List of Figures

Figure 1.1: Carbon cycle in a forest.....	4
Figure 1.2: Water cycle in a forest.....	7
Figure 2.1: Site conditions.....	29
Figure 2.2: Elevated-[CO <sub>2</sub> ] effect on canopy transpiration at Duke FACE.....	30
Figure 2.3: Mean canopy stomatal conductance response to elevated [CO <sub>2</sub> ].....	31
Figure 2.4: The elevated-[CO <sub>2</sub> ] effects for +200 μmol mol <sup>-1</sup> enrichment.....	32
Figure A2.4.1: Results from Randomized Intervention Analysis (RIA).....	46
Figure A2.4.2: Elevated-to-Ambient [CO <sub>2</sub> ] ratios of $K_{leaf}$ .....	47
Figure 3.1: Settings.....	79
Figure 3.2: Canopy structures.....	80
Figure 3.3: Daily growing season average absorbed photosynthetically active radiation, APAR, profiles.....	81
Figure 3.4: Comparisons of vertical distribution of APAR within crown.....	82
Figure 3.5: Total absorbed photosynthetically active radiation (APAR) in the crown.....	83
Figure 3.6: Comparison of light-capturing efficiency (LCE) and its components between exotic and native species at a given latitude.....	84
Figure 3.7: Comparison of <i>P. contorta</i> and <i>P. sylvestris</i> in Sweden in silvicultural context.....	85
Figure 3.8: Summary of findings.....	86
Figure 4.1: Environmental conditions.....	122
Figure 4.2: Variables for scaling to the canopy.....	123
Figure 4.3: Responses of canopy transpiration to environmental conditions.....	124

Figure 4.4: Functions to estimate daily canopy transpiration of forests .....	125
Figure 4.5: Incorporating soil drying effect.....	126
Figure 4.6: Water balance of the mature pine forests in the present study.....	127
Figure 4.7: Synthesis analysis of hydrologic components of forests.....	128
Figure 5.1: Environmental conditions .....	183
Figure 5.2: Estimates of the variables.....	184
Figure 5.3: Environmental responses of half-hourly variables.....	185
Figure 5.4: Spatial variation of the half-hourly variables.....	186
Figure 5.5: Total growing season GPP .....	187
Figure 5.6: The synthetic analyses of light- and carbon-use efficiencies.....	188

## Acknowledgements

First of all, I would like to thank my advisor, Ram, who teaches me that anything is possible ever since the first day I asked for his supervision for my PhD degree. I wouldn't have made it this far without all his thorough help and coaching throughout the process of academic research. I sincerely thank Eric Ward and Chris Oishi for their teaching and support, especially during my first year in the Oren group, even when they were so busy with their dissertation. Their help then had established the foundations for my research for later years and I would like to let both of you know that you'll make great advisors in the future! Many thanks to Sari, Dani and JC for serving as my committee members and for their prompt and helpful advice. I would like to express my gratitude to Professor Torgny Näsholm of Swedish University of Agricultural Sciences (SLU) for giving me the opportunity to do research in Umeå, Sweden and for all the help and advice during the three summers that I was there. I'd like to thank all my colleagues from both Duke and SLU: Dohyoung Kim, Henry Berghoff, Melissa Chernick, Jeff Phippen, Nils Henriksson, Hyungwoo Lim, Lasse Tarvainen and others that I have worked with. I really appreciate your help and support both academically and socially.

But none of this would have happened, if it wasn't for my parents who always support and respect my decision. Thank you for allowing your only child to come to America 11 years ago. I have become what I am today because of you two. Finally, I also

wouldn't have made it through the long years of study without mental support from friends and family. Thank you everyone for believing in me and loving me for who I am.

# 1. Introduction

## 1.1 *Carbon in Forests*

Global climate change is a growing concern that has become central to international discussions and negotiations. Responses to this issue have concentrated on decreasing emissions of greenhouse gases, particularly carbon dioxide (CO<sub>2</sub>), the most abundant greenhouse gas produced by humans and the gas that contributes the most to climate change (Trenberth *et al.*, 2007; Forster *et al.*, 2007). Under the 1997 Kyoto Protocol, the developed nations agreed to specified reductions in their greenhouse gas emissions (Böhringer, 2003). In calculating overall carbon emissions, the Protocol permits removals of carbon by a nation's forests and soils, which are the mostly carbon sinks, to be deducted from emissions (UNFCCC, 1997). Consequently, one approach to slow down the rate of increasing atmospheric CO<sub>2</sub> concentration, and therefore mitigating climate change, is to enhance the amount of atmospheric carbon removed by and stored in forests, *i.e.* the forest carbon sequestration (Dixon *et al.*, 1993; Sampson & Sedjo, 1997; Marland & Schlamadinger, 1999). Mitigating climate change through increasing forest carbon sequestration is an economical option but faces many challenges involving tracking the amount of sequestered carbon and verifying the results from measuring carbon fluxes and their responses to environmental changes (Sedjo & Macauley, 2011). Thus, several issues regarding monitoring levels and changes in forest

carbon and the scientific uncertainties about the interrelationships among forests, carbon and climate change are ongoing subjects of research.

Forest carbon is linked to the atmosphere through photosynthesis and respiration. During the process of photosynthesis, plants utilize sunlight to convert nutrients into sugars and carbohydrates. These products are subsequently used to build leaves, roots, stems and other essential elements for plant growth. Therefore, the more photosynthesis occurs, and the more atmospheric CO<sub>2</sub> is removed for the synthesis of slow turnover biomass, the slower will be the increase of CO<sub>2</sub> level in the atmosphere. This fundamental principle underlies the use of forests for climate change mitigation.

To understand the interaction between carbon fluxes of forests and the atmosphere and the sensitivity of forest carbon pool and fluxes to changing environmental conditions, it is imperative to evaluate principal processes within the forest, combined into the overall net ecosystem production (NEP). The interaction among these processes, the rate of response and the sensitivity of environmental changes determine the future and long-term potential of carbon sequestration by forests.

In a forest ecosystem, annual carbon fluxes can be written as

$$NEP = GPP - R_p - R_h \quad (1.1)$$

where NEP is the net ecosystem primary production, GPP is the gross primary production representing the total amount of CO<sub>2</sub> fixed by photosynthetic organisms

through photosynthesis,  $R_p$  and  $R_h$  refer to the amount of  $CO_2$  released from plants and decomposers, respectively, through respiration. All components are expressed in units of mass of carbon per unit ground area per unit time. Considering the plant component only, the NEP reduces to net primary production (NPP) which is

$$NPP = GPP - R_p \quad (1.2)$$

Equation (1.2) is of significance for plant physiologists and ecophysiologists studying the influence of environmental changes on plants and trees in forests. Figure 1.1 illustrates the carbon fluxes in a forest.

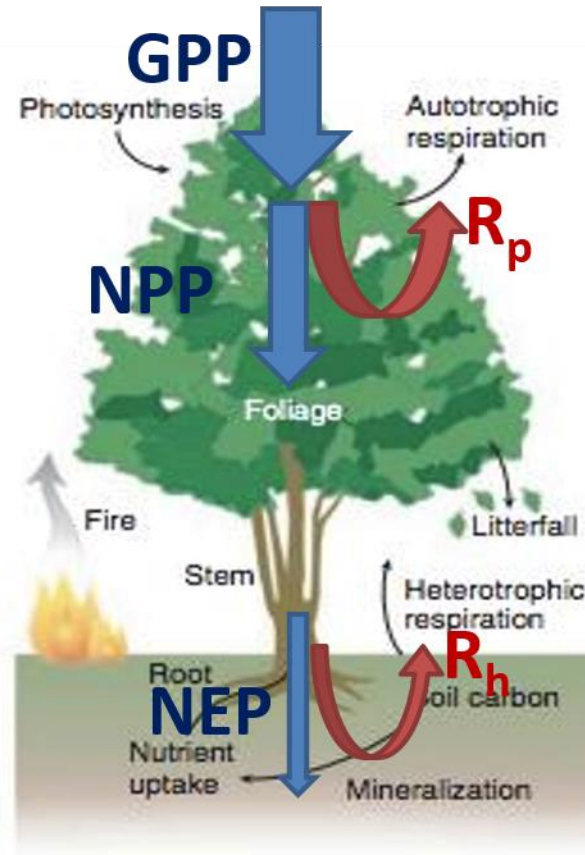


**Figure 1.1: Carbon cycle in a forest** (adapted from Bonan, 2008). In a forest ecosystem, plants draw atmospheric  $\text{CO}_2$  for photosynthesis and obtain carbon known as Gross Primary Production (GPP). Some of this carbon is used for plant growth (*i.e.* Net Primary Productivity; NPP) while the rest is utilized through respiration (*i.e.* plant respiration;  $R_p$ ). Some of the NPP is distributed to heterotrophs which respire as heterotrophic respiration ( $R_h$ ). The net amount of carbon left in the forest is Net Ecosystem Production or NEP. Blue (red) arrows and texts represent carbon inflow (outflow) of a forest.

## ***1.2 Water in Forests***

Recent evidence shows that the Earth's climate has warmed rapidly during the 20<sup>th</sup> century (Solomon *et al.*, 2007), resulting in significant changes in the hydrologic cycle (Ohamura & Wild, 2002; Huntington, 2006). Such changes are expected to intensify and to exert large impacts on forests (*e.g.* Boisvenue & Running, 2006; Soja *et al.*, 2007) and, in turn, the water services that they provide (*e.g.* Betts *et al.*, 2007). Temperature rises occur all over the globe, but with the greatest increases at the high northern latitudes (Solomon *et al.*, 2007). Of all changes in the water cycle, precipitation has been the most discussed component. Total global precipitation has increased (Nicholls *et al.*, 1996) but not in all areas. For example, significant decreases have been observed in mid-latitudinal areas (Bates *et al.*, 2008) while an increasing amount is seen at high latitudes (Trenberth *et al.*, 2007). In addition, drought events have aggravated in some and affected more areas (Solomon *et al.*, 2007; Trenberth *et al.*, 2007). Overall, the observed global warming is connected to changing precipitation patterns as well as sea level rise, reductions in snow and ice extent, and changes in the intensity and frequency of extreme events such as droughts, heat waves and heavy rainfall.

Forests contribute to the water cycle through transpiration, which is the major component of total water loss (*i.e.* evapotranspiration) from an ecosystem (Lawrence *et al.*, 2007). The hydrologic cycle of a forest ecosystem is illustrated in Figure 1.2.

Precipitation ( $P$ ) reaches the forest in the form of rainfall or snow, depending on seasons and geographical locations. A fraction of the incoming  $P$  is intercepted by tree leaves in the canopy ( $I_c$ ), letting some fraction reach the forest floor (*i.e.* throughfall,  $P_t$ ) and flow down the stem (*i.e.* stemflow, SF). However, SF has been observed to be small and often neglected in the hydrologic budget analysis (Delfs, 1967; Viville *et al.*, 1993; Uebelherr, 2008; Oishi *et al.*, 2010). Some of this water is used and released back to the atmosphere by plants as transpiration ( $E_c$ ). Water that reaches the ground is also evaporated and thus travels back to the atmosphere as soil evaporation ( $E_s$ ). Finally, the residual water not intercepted or cycled through plant and soil will flow out of the forest as runoff ( $R_o$ ) or percolated through deep soil as drainage ( $Q$ ). In other words, assuming no change in water storage in the system over long periods, the water balance of a forest is expressed as

$$P = I_c + E_c + E_s + R_o + Q \quad (1.3)$$

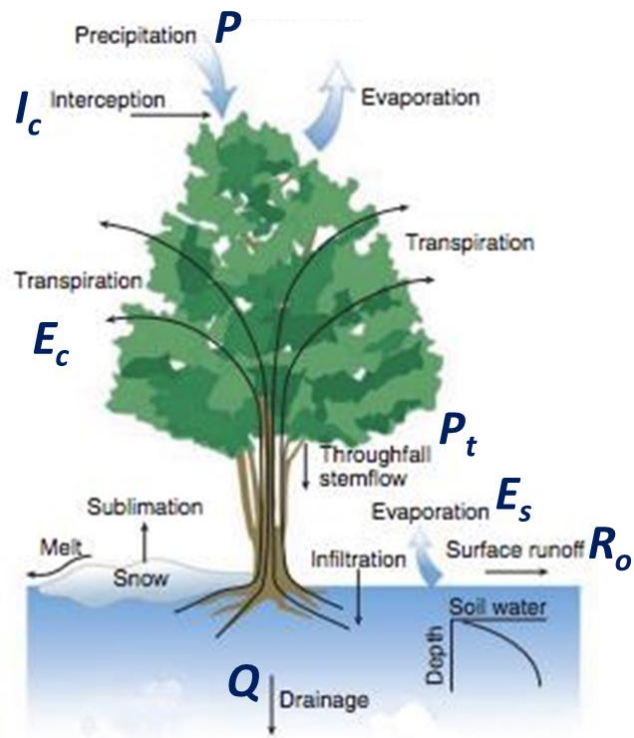


**Figure 1.2: Water cycle in a forest** (adapted from Bonan, 2008). Some of the incoming precipitation ( $P$ ) is intercepted by forest canopy ( $I_c$ ), leaving the rest reaching the subcanopy as throughfall ( $P_t$ ). Trees draw water from the soil and release it as canopy transpiration ( $E_c$ ). Water also evaporates from the subcanopy community and soil ( $E_s$ ). The residual  $P$  that is not intercepted by the canopy or evaporated will leave the system as surface runoff ( $R_o$ ) and/or drainage below the plant rooting zone ( $Q$ ), depending on soil texture.

### ***1.3 Carbon and Water in Forests***

In forest ecosystems, water and carbon fluxes are intrinsically linked through plant stomata which are tiny pores in leaves controlling gas exchange. Specifically, via stomatal opening, atmospheric CO<sub>2</sub> diffuses into leaves and is used for photosynthesis while water vapor is released to the atmosphere as transpiration. Consequently, stomata mainly regulate how plants respond to environmental conditions. For example, a high atmospheric CO<sub>2</sub> concentration may lead to stomatal closure, resulting in decreased transpiration in most deciduous, broadleaved species but the stomata of conifers are less sensitive to CO<sub>2</sub> as shown by leaf-scale gas exchange measurements (*e.g.* Medlyn *et al.*, 2001; Ellsworth, 1999). However, at the canopy scale, long-term exposure to elevated atmospheric CO<sub>2</sub> concentration induced stomatal closure in both coniferous and broadleaved species in a temperate forest via changes in hydraulic allometry (Tor-ngern *et al.*, 2014). Under drought stress, stomata close to minimize water loss from the plants (Alder *et al.*, 1996; Cochard *et al.*, 1996; Sperry *et al.*, 1998) and consequently limit photosynthesis and growth (Cornic, 2000). In general, stomata respond to various climatic factors including atmospheric water demand, light, temperature and soil water availability (Jarvis, 1976). However, the responses are even more complex when moving from leaf to forest scale as other structural factors can influence stomatal behavior. For

instance, increasing leaf area may lead to shading in the canopy, reducing light interception and consequently causing stomatal closure (Sellin & Kupper, 2005).

#### ***1.4 Boreal and Temperate Forests***

Forest regions are broadly divided into latitudinal zones: tropical, temperate and boreal, from low to high latitudes of both northern and southern hemispheres, respectively. However, the studies in this dissertation will only focus on forests in temperate and boreal zones in the northern hemisphere.

Temperate forests are located at approximately 25 – 50 °N and are primarily in developed countries. Human impacts have been found in almost all of these forests. About 20% of temperate forests are under management for wood production or other services and are affected by pollution, with potentially positive and some negative effects on growth (Innes, 1993). Standing biomass and carbon storage of temperate forests is currently increasing at 0.2 – 0.5 GtC yr<sup>-1</sup>, mostly resulting from reforestation, underharvesting and regrowth after wood removal (e.g. Dixon *et al.*, 1994; Galinski & Küpper, 1994; Kohlmaier *et al.*, 1995) and fertilization effects of nitrogen deposition (Kauppi *et al.*, 1992). The boreal and temperate forests are considered carbon sinks; however, the increasing demand for wood may change these forests to a net carbon source (Heath *et al.*, 1993).

Boreal forests are found at 50-70 °N latitudes, between the temperate and tundra zones and cover approximately 17% of the earth's land surface area (IPCC, 2014). They are estimated to be a carbon sink of 0.2 – 0.7 GtC yr<sup>-1</sup> (Apps *et al.*, 1993; Dixon *et al.*, 1994, Bradshaw & Warkentin, 2015). Growth and production of plants are restricted by low air temperature and small heat sums (Heide, 1974; Pohtila, 1980). In addition, low soil temperature and permafrosts have been shown to limit growth and nutrient availability (Van Cleve *et al.*, 1983; Van Cleve & Yarie, 1986; Jarvis & Linder, 2000). Moreover, litter in most coniferous boreal forest is relatively resistant to decomposition because of the generally low soil temperature and low nutrient content (Shaver *et al.*, 1992; Berg *et al.*, 1993; Kobak & Kondrasheva, 1993). Thus, boreal forests are the world's second largest carbon stock, after tropical forests, with carbon mostly stored in soil and litter.

Current knowledge of ecophysiological mechanisms governing carbon and water fluxes in forests facilitates the detailed study of forests at individual plant and stand scales with time resolution ranging from minutes to years (IPCC, 2014). When moving to the larger spatial scale (*e.g.* global) and longer timescale (*e.g.* decades to centuries), the analyses reduce to simplified plant characteristics, known as Plant Functional Types, with the focus on biospheric equilibrium; therefore, General Circulation Models (GCMs) for future climate scenarios only provide us with projected future responses as consequences of given assumptions rather than enabling precise forecasts (IPCC, 2014).

Because of great complexity generated by the contrasting characteristics of global forests under different climatic zones, it is difficult to study forests in specific details at the global scale. Therefore, field-based studies at forest scale across latitudinal locations are needed as the basis for improving current knowledge of ecosystem functioning and for validating current modelling schemes.

### ***1.5 The Studies***

Combining the above perspectives, this dissertation aims at investigating the sensitivity of carbon and water fluxes in forests to environmental changes, both temporally (from half-hourly to inter-annual growing season) and spatially (latitudinal variation). The spatial gradients consist of differences in latitudinal location and stand structure as characterized by the amount of canopy leaf area per unit ground area (leaf area index,  $L$ ). Besides the impacts of inter-annual variations of weather patterns and climatic difference with latitudes, the effects of elevated  $[\text{CO}_2]$  and nitrogen deposition through fertilization on forest structure and functions were also studied. Both field and modelling studies were conducted at four pine (*Pinus* genus) forest sites in the southeastern United States and northern Sweden. The research was divided into four specific projects. The main research tools used in these studies are thermal dissipation sensors (Granier, 1985) and a process-based canopy photosynthesis model (Schäfer *et al.*, 2003; Kim *et al.*, 2008). The Granier-type sensors measure water flow in trees by

detecting the changes in temperature difference in response to changing environmental conditions. This information, referred to as sap flux density ( $J_s$ ), can be scaled up from the tree level to the entire forest to determine canopy transpiration and mean stomatal conductance ( $G_s$ ), which is linked to canopy photosynthesis. The canopy photosynthesis model, titled Canopy-Constrained Carbon Assimilation (4C-A), incorporates canopy conductance constrained by the sap-flux-based  $G_s$  and the Farquhar model of photosynthesis (Farquhar *et al.*, 1980) to estimate canopy photosynthesis based on absorbed light distribution in the canopy. These techniques combined with other measurements such as those from the eddy covariance system and biometric estimates, allowed the investigations of carbon and water fluxes (*i.e.* Equation 1.2 and 1.3) of these forests with respect to spatio-temporal changes of environments.

In the temperate region of the southeastern United States, *Pinus taeda* (loblolly pine) is the dominant species of economic importance (Schultz, 1997; Fox *et al.*, 2004). Intensive forest management and tree genetic improvements have been employed to increase productivity of loblolly pine plantations. Therefore, studying environmental impacts, with the inference to climate change, on hydrology and productivity of loblolly pine forests will be useful for not only forests management but also climate change mitigation. In the first manuscript (Tor-ngern *et al.*, 2015), the long-term effects of elevated  $[CO_2]$  on forest transpiration of a loblolly pine-dominated forest which had

been subjected to enriched [CO<sub>2</sub>] treatment for 14-17 years (the Free-Air CO<sub>2</sub> Enrichment, FACE, experiment) were investigated. Because previous studies, which were based on small individuals and/or short-term measurements, showed mixed results, we separated the short-term, instantaneous effects of elevated [CO<sub>2</sub>] from the long-term ones and evaluated the impacts on G<sub>s</sub> which directly links to transpiration of the forest. The results from this study are of importance for modelling climate change impact on carbon, water and energy cycles.

The second manuscript theoretically explored how crown architecture and solar altitude, reflected by different latitudes of the sites, affect total and vertical distribution of canopy light absorption of a loblolly pine (*P. taeda*) canopy in North Carolina, USA (36 °N), a lodgepole pine (*P. contorta*) native to British Columbia (58 °N) and a Scots pine (*P. sylvestris*) canopy in northern Sweden (64 °N). The light module of the 4C-A model was used to simulate canopy light absorption of a hypothetical stand composed of either species. In the simulation, the hypothetical stand was characterized by real canopy structures and crown characteristics estimated from measurements at both sites. Specifically, the vertical distribution and total amount of light absorption of each species when subjected to its native and exotic latitudes were compared. The results rendered the significance of unique crown architecture of pines in their native latitudes allowing sufficient light absorption for growth and failure to survive in exotic, contrasting

latitudes due to physiological and ecological consequences. Moreover, the superior growth of lodgepole pine introduced to northern Sweden, as well as the effects on understory species composition, was explained by their greater light absorption than the native Scots pine.

The third manuscript studied canopy transpiration of four pine forests of various conditions involving age-difference, nutrient-balanced treatment and latitudinal locations. All stands were on sandy, poor soils. These forests include the 40-year-old *P. taeda* and the 80-year-old untreated *P. sylvestris* stands, previously studied in the second manuscript, and another mature *P. sylvestris* stand under long-term nitrogen fertilization in Rosinedal, Sweden. The last stand was a regenerating Scots pine forest with 13 - 30-year-old trees located ~7 km away from the Rosinedal sites. These forests were of different *L*. In particular, spatio-temporal controls of the environments on canopy transpiration were examined in these forests. Moreover, the interannual growing season variations of hydrologic components of the three mature sites were explored. Extending the results to include published estimates from other studies of various biomes, latitudes and soil nutrient conditions, simple relationships for estimating daily canopy transpiration and responses of other hydrologic components to incoming precipitation were obtained with significance implications for climate change impacts on global forest hydrology.

Finally, the last manuscript investigated carbon fluxes and resource-use efficiencies of the same four forests previously studied in the third manuscript. The study focused on temporal and spatial variations of canopy photosynthesis and GPP. The responses of the instantaneous canopy photosynthesis to environments were examined with the implications for the difference among growing seasons. The spatial analyses involved the investigation of the carbon fluxes in relation to leaf area index of the sites. In addition, water-, light- and carbon-use efficiencies of these forests were quantified. In particular, the light-use efficiency, defined as the ratio of GPP to canopy light absorption, was relatively constrained across forest types and latitudes regardless of the methods of estimating GPP, reflecting the conservative nature of these approaches.

## 2. Increases in atmospheric CO<sub>2</sub> have little influence on transpiration of a temperate forest canopy<sup>1</sup>

### 2.1 Introduction

In most forests, exchanges of energy and mass with the atmosphere are determined by fluxes of CO<sub>2</sub> and water between leaves and the canopy air volume, regulated by stomata. Models of these processes incorporate functions describing stomatal closure with increasing atmospheric CO<sub>2</sub> concentration [CO<sub>2</sub>] based on leaf-level measurements (Ball *et al.*, 1987; Sellers *et al.*, 1996; Douville *et al.*, 2000). Responses of forest canopies, however, may differ (Medlyn *et al.*, 2001; Wullschleger *et al.*, 2002; Ainsworth & Rogers, 2007), provoking debate regarding the consequences of elevated [CO<sub>2</sub>]-induced stomatal responses to ecosystem water use and supply to downstream users (Milly *et al.*, 2005; Gedney *et al.*, 2006; Betts *et al.*, 2007; De Boer *et al.*, 2011; Keenan *et al.*, 2013). Because leaves in most temperate forests are well-coupled to the atmosphere (Jarvis & McNaughton, 1986; Pataki *et al.*, 1998a; Ewers & Oren, 2000; Schäfer *et al.*, 2002), reductions in stomatal conductance should scale to canopy fluxes. However, in water limited ecosystems, canopy leaf area ( $L_D$ ) is predicted to increase with decreasing stomatal conductance, thus conserving canopy conductance and transpiration (Woodward, 1990). Even in moist ecosystems, elevated [CO<sub>2</sub>] may increase carbohydrate availability, potentially enlarging  $L_D$  (Palmroth *et al.*, 2006), and consequently lowering

---

<sup>1</sup> Published in *New Phytologist* 205(2), 518 – 525, January 2015, doi: 10.1111/nph.13148

canopy conductance per unit leaf area ( $G_s$ ) via light or hydraulic limitation (Schäfer *et al.*, 2002; Ward *et al.*, 2013), also leading to conserved transpiration. Where direct stomatal closure in response to elevated  $[CO_2]$  is not countered by increased  $L_D$ , and atmospheric demand for and soil supply of water remain unchanged, canopy transpiration should decrease. For example, no increase of  $L_D$  is likely if soil nitrogen is limiting (Ågren, 1983) or leaf loss is accelerated by heat damage (Warren *et al.* 2011).

Where elevated  $[CO_2]$  does not elicit a *direct* stomatal response through  $CO_2$  concentration in the leaf-internal air-space, it may do so *indirectly* by changing growth partitioning among leaves, stems, and roots, and by affecting the efficiency of water transport (Domec *et al.*, 2009; Brodribb & Field, 2010; Ward *et al.*, 2013), or by increasing self-shading of foliage with enhanced  $L_D$  (McCarthy *et al.*, 2007). Some global-scale models predict  $L_D$  enhancement under high  $[CO_2]$  (Douville *et al.*, 2000; Betts *et al.*, 2007), but none to date include an acclimation of the hydraulic system. Tree hydraulic properties often require an extended period for complete acclimation to stepwise  $[CO_2]$  changes (Domec *et al.*, 2009, 2010), which may not necessarily be accompanied by increased  $L_D$ .

To properly account for and model the effect of increasing  $[CO_2]$  on biosphere-atmosphere exchanges, it is necessary to identify all of the primary processes involved and quantify their effect on stomatal conductance of forest canopy that is fully acclimated to increased  $[CO_2]$ . Yet, Free-Air  $CO_2$  Enrichment (FACE) studies on intact, hydraulically acclimated canopies are rare, and have not previously been used to

separate variables responsible for *direct versus indirect* stomatal responses to elevated [CO<sub>2</sub>]. The underlying mechanisms for observed high [CO<sub>2</sub>] effect on stomatal conductance and, in turn, their effect on tree crown and stand canopy conductance may have been misidentified, leading to incorrect specification in some models.

We used the Duke University FACE experiment in a temperate forest dominated by *Pinus taeda* (L.) and *Liquidambar styraciflua* (L.), to evaluate the elevated [CO<sub>2</sub>] effects on variables underlying whole-canopy responses of transpiration (*i.e.*  $G_s$ ,  $L_D$ , and leaf hydraulic conductance). We used a 17-year long annually integrated dataset to quantify coarse-scale response, and performed a short-term elevated-[CO<sub>2</sub>] manipulation during the final phase of the experiment to distinguish the *direct* from *indirect* effects on  $G_s$ , providing insight for modelling of future water, energy and carbon cycles in forest ecosystems.

## ***2.2 Materials and Methods***

### ***2.2.1 Settings***

The Duke FACE experiment was in Duke Forest, North Carolina USA (35° 52' N, 79° 59' W; 130 m asl). The forest was 27-year-old and 25 m tall in 2010. The soil was an acidic, low fertility clay Hapludalf classified in the Enon Series. Mean annual temperature and precipitation were 15.5 °C and 1165 mm (Phillips & Oren, 2001). The forest was dominated by *P. taeda* and *L. styraciflua* with other 50 broadleaved deciduous species in the subcanopy (Schäfer *et al.*, 2002). Under ambient [CO<sub>2</sub>], mean annual  $L_D$  was  $5.4 \pm 0.26$  (standard error; SE), composed of  $55 \pm 1\%$  *P. taeda*, and  $17 \pm 2\%$  *L. styraciflua*,

which was assumed representative of the other broadleaved trees. The long-term elevated-[CO<sub>2</sub>] treatment was +200 above ambient (c. 385 μmol mol<sup>-1</sup> at the end of the study) since 1994 (*n*=1) and 1996 (*n*=4), using FACE technology on 30-m diameter plots (Hendrey *et al.*, 1999) with untreated plots as reference (Oren *et al.*, 2001; Ward *et al.*, 2013).

### 2.2.2 Long- and short-term [CO<sub>2</sub>] manipulation experiments

In 2010, we separated *direct versus indirect* mechanisms of elevated-[CO<sub>2</sub>] effect on *G<sub>s</sub>* by observing responses to stepwise [CO<sub>2</sub>] changes in the canopy air of the four elevated-[CO<sub>2</sub>] plots, using the four ambient-[CO<sub>2</sub>] plots as reference. Stomatal response to rising [CO<sub>2</sub>] may depend on soil water availability (Schäfer *et al.*, 2002; Domec *et al.*, 2009); we therefore performed the study over a soil dehydration-rehydration cycle (Figure 2.1a). Five [CO<sub>2</sub>] (ambient, +100, +150, +200 and +300 above ambient) were administered in eight 5-day periods (Figure 2.1b). We avoided potential confounding effects of [CO<sub>2</sub>] and soil moisture by allocating one of the four elevated-[CO<sub>2</sub>] plots to one of the five [CO<sub>2</sub>] treatments during each 5-day period. The four ambient-[CO<sub>2</sub>] plots permitted accounting for potential effects of the large variation in soil moisture (expressed as relative extractable water, REW; Pataki & Oren, 2003) on *G<sub>s</sub>* sensitivity to [CO<sub>2</sub>]. We partitioned the data into two periods in 2010 (Figure 2.1): *Direct* (late August to early October, Day of Year (DOY) 242-282) during which the canopy-scale stepwise [CO<sub>2</sub>] changes were implemented, and *Indirect* (May to August, DOY 142-241 and late October, DOY 283-304) in which enrichment followed the long-term experimental

protocol (+200; Oren *et al.*, 2001). The 17-year long annual values were obtained as described below.

### 2.2.3 Measurements and calculations of variables

Growing season averaged leaf area index ( $L_D$ ) and canopy-integrated stomatal conductance per unit leaf area ( $G_s$ ) through 2008 were synthesized from published data (Phillips & Oren, 2001; McCarthy *et al.*, 2007; Ward *et al.*, 2013), and used to calculate canopy transpiration ( $E_c$ ) (see Appendix 2.4.1.1). We generated similar values from unpublished data for 2009 and 2010.

In 2010, the half-hourly mean sap flux density ( $J_s$ ;  $\text{g m}^{-2}_{\text{sapwood}} \text{S}^{-1}$ ), measured at multiple sapwood depths using thermal dissipation probes (Granier, 1985) in 91 *P. taeda* and 45 *L. styraciflua* individuals distributed among the eight plots, was used for the daily analyses. We employed a scaling method utilizing random effects generated from an empirical dynamic model based on a hierarchical Bayesian statistical approach (Ward *et al.*, 2013; Appendix 2.4.1.2) to scale the point-measured  $J_s$  to sapwood-averaged values ( $\bar{J}_s$ ). Daily values were used to avoid issues related to tree water storage and measurement errors (Phillips & Oren, 1998). The daily  $E_c$  was computed from daily sum  $\bar{J}_s$  and total sapwood area per unit ground area (Oren *et al.*, 1998a).  $G_s$  of a canopy well-coupled to the atmosphere, as in this study, can be computed using the simplified Penman-Monteith equation (Appendix 2.4.1.3). In a similar *P. taeda* forest, no vertical gradient of vapor pressure deficit was observed within the canopy, and thus leaf-level

stomatal conductance scaled with vertical leaf area distribution was correlated without bias to sap-flux based mean canopy stomatal conductance (Ewers & Oren, 2000). We further verified the close leaf-atmosphere coupling by testing and finding no sensitivity of  $J_s$  to wind speed in all study plots (following Kim *et al.*, 2014,  $P = 0.66$ ,  $R^2 = 0.003$ ), consistent with previous findings (Domec *et al.*, 2009).

Leaf hydraulic conductance ( $K_{\text{leaf}}$ ;  $\text{mmol m}^{-2} \text{MPa}^{-1} \text{s}^{-1}$ ) was measured on single leaves/fascicles using the timed rehydration method (Brodribb & Holbrook, 2003). We selected an upper and mid-canopy branch from two representative *P. taeda* trees in each plot (sixteen branches per treatment). For *L. styraciflua*, sampling was based on the distribution of trees in plots with two branches from each of the six trees selected from each  $[\text{CO}_2]$  treatment (twelve branches per treatment). Branches, 30–50 cm long, were collected in early morning, sealed in plastic bags, transported to the laboratory, recut under water and allowed to rehydrate for 4 h. Pressure-volume analyses (Tyree & Hammel, 1972) were conducted on leaves/fascicles taken on the same branches used to determine  $K_{\text{leaf}}$  (Appendix 2.4.1.5).

The influence of canopy leaf area on  $G_s$  was inferred from shading effects in the canopy. We employed a one-dimensional, multi-species, multilayer radiative transfer model (Schäfer *et al.*, 2003; Kim *et al.*, 2011) to calculate the average light on leaf surfaces ( $Q$ ) of each dominant species and for the entire forest. We characterized canopy structure using vertical distributions of shoot clumping, leaf angle distribution, leaf area density and wood surface density of branch and stem based on field measurements

(Kim *et al.*, 2011). We partitioned the canopy into 1-m layers, and calculated mean light on leaf surfaces for each canopy layer and for the whole canopy (Appendix 2.4.1.6).

## **2.2.4 Tests for significant elevated-[CO<sub>2</sub>] effects**

In all analyses, we used data from ambient and elevated [CO<sub>2</sub>] plots (each,  $n=4$ ) during DOY 142-304 in 2010. For the long-term treatment data (*Indirect*; DOY 142-241 & 283-304), we employed regression analysis to analyze  $E_c$  response to daylength-normalized vapor pressure deficit ( $D_z = D_D \times (n_d/24)$  where  $D_D$  = daytime mean vapor pressure deficit,  $n_d$  = number of daylight hours; Phillips & Oren, 2001) and to evaluate the response of  $G_s$ , expressed as a ratio of elevated- relative to ambient-[CO<sub>2</sub>] values *versus* [CO<sub>2</sub>]-enhancement ratio. We performed  $F$ -tests for the elevated [CO<sub>2</sub>] effect on the  $E_c$  *versus*  $D_z$  response during *Indirect*. We applied Student's  $t$ -tests on the ratios of  $G_s$ ,  $K_{leaf}$  and  $Q$  to test for [CO<sub>2</sub>] effects on these variables. Retaining information in the temporal variation, we performed a Randomized Intervention Analysis (Carpenter *et al.*, 1989) on  $G_s$  to detect nonrandom change due to treatment effect in the series of observation made before and after treatment application (Appendix 2.4.1.4). All computations and analyses were conducted in MATLAB 7.6.0 R2008a (Natick, Massachusetts: The MathWorks Inc., 2008).

## **2.3 Results and Discussion**

Reviews assessing the response of tree species to elevated-[CO<sub>2</sub>], mostly based on seedlings, suggest that  $G_s$  would decrease and canopy leaf area would increase (Eamus

& Jarvis, 1989; Mousseau & Saugier, 1992; Medlyn *et al.*, 2001; Ainsworth & Long, 2005). These responses were observed at the mixed *P. taeda*-*L. styraciflua* FACE experiment during the early establishment period (Figure 2.2a-c). The long dataset produced two clear conclusions: (1) the increased  $L_D$  and decreased  $G_s$  of *P. taeda* resulted in  $E_c$  unaffected by  $[\text{CO}_2]$  (Figure 2.2a). Because *P. taeda* dominated the stand, these responses represent the entire canopy (Figure 2.2c). (2) In contrast, the increased  $L_D$  of *L. styraciflua* did not compensate for the larger decrease of its  $G_s$ , resulting in ~20% lower  $E_c$  under high  $[\text{CO}_2]$  (Figure 2.2b). This is consistent with syntheses showing that stomatal conductance of broadleaved species is more sensitive to elevated  $[\text{CO}_2]$  than that of conifers (Medlyn *et al.*, 2001).

Earlier in the experiment, it was uncertain whether the increased  $L_D$  was simply due to accelerated ontogeny or treatment effect (Gunderson & Wullschleger, 1994); now that  $L_D$  has stabilized in both treatments, it is clear that  $L_D$  enhancement was induced and maintained by increased  $[\text{CO}_2]$ . However, it has not been possible to determine whether the  $G_s$  and  $L_D$  trends reflect independent and direct responses to  $[\text{CO}_2]$ , or represent a feedback whereby one variable directly responded to high  $[\text{CO}_2]$ , and the other followed indirectly. Because the experiment is in a fairly moist environment, the occasional drought notwithstanding, a feedback of  $L_D$  to direct  $G_s$  decrease is not likely; a more likely feedback scenario is  $L_D$  increasing as a direct response to increasing  $[\text{CO}_2]$  and causing a decrease of  $G_s$  (due to more mutual shading in the canopy and reduced hydraulic conductance).

We used the latter part of the last [CO<sub>2</sub>] enrichment year (termed *Indirect* phase in 2010), focusing on a finer, daily scale, to assess the long-term  $E_c$  responses, and to set a baseline for examining the response to stepwise [CO<sub>2</sub>] changes (termed *Direct* phase; Figure 2.1). During *Indirect*, the analysis focused on  $E_c$  response to  $D_z$  under non-limiting light and water conditions, setting a clear baseline for evaluating *Direct* data. The long-term elevated [CO<sub>2</sub>] did not affect  $E_c$  of *P. taeda* and the canopy ( $P \geq 0.53$ ) but reduced that of *L. styraciflua* ( $P < 0.001$ ; see fit lines Figure 2.2d-f and Table A2.4.1 for statistics). We compared  $E_c$  data under varying soil moisture conditions during *Direct* to the baseline by plotting time-averaged values of each treatment in each elevated-[CO<sub>2</sub>] plot (Figure 2.2d-f; symbols). Most (90%) of these values lay within the 99% confidence bounds. Moreover, the  $E_c$  values from the *Direct* phase showed no systematic pattern in response to increasing [CO<sub>2</sub>] relative to the long-term fit, with data below the fit representing the *Direct* drought period, and above the fit representing the period immediately following drought-breaking rains. Therefore, we observed no [CO<sub>2</sub>] effect on  $E_c$  in *Direct* phase. To identify plausible causes for the  $E_c$  responses observed over the long term (Figure 2.2a-c), we focused further analyses on  $G_s$ .

The underlying causes of  $G_s$  reduction under rising [CO<sub>2</sub>] have been elusive (Ward *et al.*, 2013). The plausible causes are not necessarily distinct; *e.g.*, hydraulic architecture may acclimate to a long-term decrease in leaf-level stomatal conductance, which may be driven by the increased mutual shading accompanying higher  $L_D$  (Whitehead *et al.*, 1984; Tyree & Ewers, 1991; McDowell *et al.*, 2002; Mencuccini, 2002,

2003; Buckley & Roberts, 2005). To help assess the potential contribution to the  $E_c$  response of increased  $L_D$  and changes of hydraulic conductivity, we reanalyzed the data in Figure 2.2d-f in terms of  $G_s$ , assessing the long-term *indirect* response of  $G_s$  to  $[\text{CO}_2]$ -induced changes of  $L_D$  and  $K_{leaf}$ . During both *Indirect* and *Direct* phases,  $G_s$  was highly variable, reflecting mostly soil drying-rewetting cycles and associated atmospheric conditions (Figure 2.3a-c). *P. taeda* was more sensitive to drought than *L. styraciflua* (Schäfer *et al.*, 2002). The background conditions of  $[\text{CO}_2]$  enrichment ( $+200 \mu\text{mol mol}^{-1}$  above ambient) reduced the elevated-to-ambient  $[\text{CO}_2]$   $G_s$  ratio ( $G_s^E:G_s^A$ ) (*Indirect* phase) to 0.85, 0.67 and 0.79 of ambient  $[\text{CO}_2]$  for *P. taeda*, *L. styraciflua*, and the entire canopy (Figure 2.3d-f; horizontal solid lines), similar to results from an analysis of an 11-year long dataset (0.87 and 0.69 for the two species respectively; Ward *et al.*, 2013). We then related  $G_s^E:G_s^A$  of *Direct* to the enhancement ratio of  $[\text{CO}_2]$  ( $[\text{CO}_2]^E:[\text{CO}_2]^A$ ). As  $[\text{CO}_2]^E:[\text{CO}_2]^A$  increased,  $G_s^E:G_s^A$  of neither species, nor that of the canopy changed significantly (Figure 2.3d-f; least-square regression on plot-scale data). The apparent slight trend seen for *P. taeda* represented only a 1% decrease for a 10% increase of  $[\text{CO}_2]$ , with *L. styraciflua* showing a slight, opposite trend. These weak responses made the  $G_s$  of the canopy insensitive to short-term changes in  $[\text{CO}_2]$ . Testing (one-sample *t*-test) whether  $G_s^E:G_s^A$  at each  $\text{CO}_2$  level differed from the mean of *Indirect* data showed that there was a tendency for difference only under two  $[\text{CO}_2]$  levels for *L. styraciflua* and one level for the canopy (Table A2.4.2-A2.4.3). Testing individual plots in each enrichment period based on Randomized Intervention Analysis showed that none displayed a  $G_s^E:$

$G_s^A$  different from the *Indirect* values (Figure A2.4.1; tested against  $\alpha=0.05$ ). Thus, neither  $E_c$  nor  $G_s$  show evidence of direct response to increasing  $[\text{CO}_2]$ . We note that the finding of no  $G_s$  response can be accommodated within the Ball-Berry framework (Ball *et al.*, 1987) considering, *e.g.*, that net photosynthesis can increase proportionally with  $[\text{CO}_2]$ .

Because  $G_s$  reduction under high  $[\text{CO}_2]$  cannot be attributed to *direct* stomatal response, we assessed changes in hydraulic conductance (Domec *et al.*, 2010) and increased mutual shading (McCarthy *et al.*, 2007) as potential causes of the observed decline of  $G_s$ . Elevated- $[\text{CO}_2]$  induced reduction of  $K_{leaf}$  of both dominant species regardless of soil moisture (Figure 2.4a) or leaf water status (Figure A2.4.2), averaging  $25\pm 7\%$  and  $32\pm 5\%$  for *P. taeda* and *L. styraciflua*, respectively. These reductions are large enough to explain the observed long-term  $G_s^E: G_s^A$  (Figure 2.3d-f; horizontal solid lines) and reflect an *indirect* effect, because  $K_{leaf}$  represents the structural capacity of the leaf transport system to deliver water (Sack & Holbrook, 2006; Brodribb, 2009).

During *Indirect*,  $L_D$  averaged  $19\pm 9\%$  enhancement in the canopy, somewhat lower during severe drought years and years of acute weather events (Figure 2.2a-c; squares; McCarthy *et al.*, 2007). Elevated- $[\text{CO}_2]$ -induced  $L_D$  enhancement of *L. styraciflua* ( $24\pm 15\%$ ) was more pronounced than that of *P. taeda* ( $17\pm 8\%$ ). The enhanced  $L_D$  resulted in  $14 \pm 6\%$  decrease of  $Q$  of the upper canopy *P. taeda*, and  $6 \pm 2\%$  decrease for mid-canopy *L. styraciflua* (Figure 2.4b), less than the effect of the hydraulic acclimation (Figure 2.4c). However, hydraulic conductivity is not independent of light intensity, *i.e.* lower light levels can reduce hydraulic conductivity (Sellin & Kupper, 2005) making the

effect of higher  $L_D$  under elevated  $[\text{CO}_2]$  non-additive with the reduction in hydraulic efficiency.

Taken together, these analyses suggest little, if any, *direct*  $[\text{CO}_2]$  effect on  $G_s$  for either species, and appreciable *indirect*  $[\text{CO}_2]$ -induced  $G_s$  reduction in *P. taeda* and *L. styraciflua*, with the canopy response falling close to that of *P. taeda* (Figure 2.4c) due to its dominance of stand  $E_c$  (Figure 2.2). Assuming all hardwoods responded similarly to *L. styraciflua*, the combined effects of  $[\text{CO}_2]$  on  $G_s$  and  $L_D$  produced no reduction of total canopy  $E_c$  during *Indirect* of +200  $\mu\text{mol mol}^{-1}$   $[\text{CO}_2]$  ( $-4\pm 12\%$ ,  $P = 0.58$ ) as  $19\pm 9\%$  increase of  $L_D$  compensated for reduced  $G_s$ . Considering that higher  $L_D$  would also increase canopy rainfall interception, we conclude that water yield and export to rivers draining such ecosystems will not increase. There are conflicting predictions on the effects of reduced transpiration resulting from elevated- $[\text{CO}_2]$ -induced stomatal closure, ranging from increased stream flow observed during the past two decades (Gedney *et al.*, 2006) and projected from results of general circulation models (Milly *et al.*, 2005; Betts *et al.*, 2007; Cao *et al.*, 2010), to intensified droughts resulting from decreases in cloud formation and precipitation (Katul *et al.*, 2012). Unless our results are atypical for forested ecosystems, such projections must consider increases of  $L_D$  as well as decreases in  $G_s$  with increasing  $[\text{CO}_2]$ .

Whether stomatal responses to high  $[\text{CO}_2]$  are *direct* or *indirect* is important not only for proper modeling of ecosystem response to elevated  $[\text{CO}_2]$ , but also when considering investments in expensive forest FACE experiments, several of which have

recently come online or are in planning. Such experiments require an initial phase during which an existing stand must acclimate to elevated [CO<sub>2</sub>] or a newly established stand matures to a quasi-steady state. Information collected during this initial phase is of limited use for modeling the responses of forests to increasing [CO<sub>2</sub>]. Effects of high [CO<sub>2</sub>] on  $G_s$  may take longer to manifest in established coniferous forest than in broadleaved forest (Li *et al.*, 2003; Wang *et al.*, 2005), possibly because many conifers retain foliage many years. For species retaining hydroactive xylem in stems and needles for several years, especially when growing slowly in cold or dry climates, or poor soil, many years will be needed to transition to tissues whose function represent the new [CO<sub>2</sub>] regime. We hope that the results of this study will serve as a model for future experiments, so that elevated-[CO<sub>2</sub>] acclimation will enlarge our understanding and ability to predict ecosystem responses.

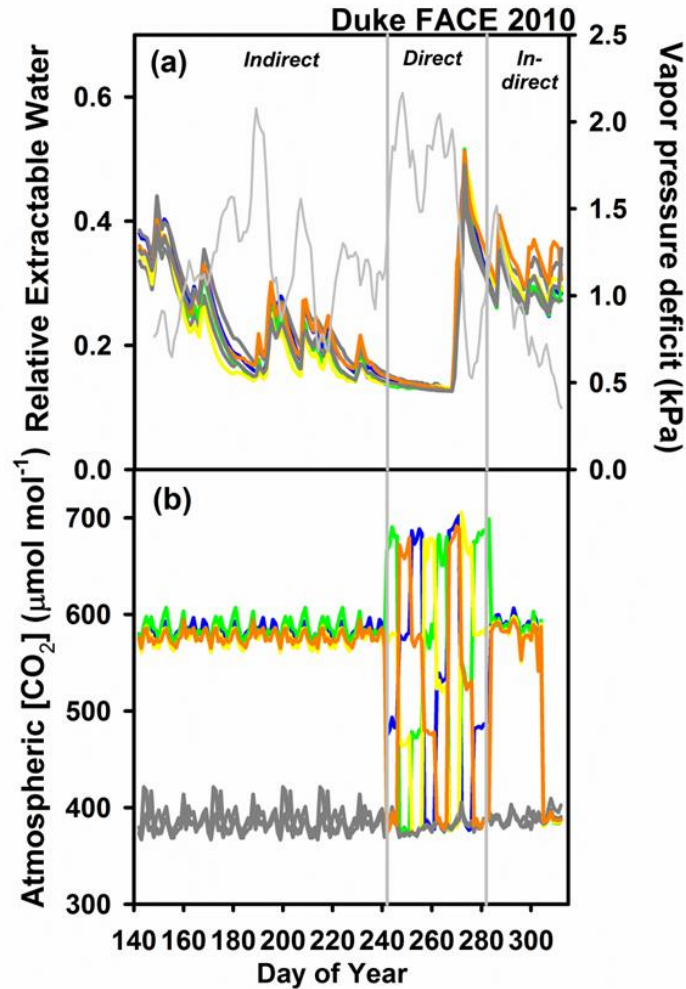


**Figure 2.1: Site conditions.** (a) Soil moisture, expressed as Relative Extractable Water (REW) in each of the eight plots (represented by different colors) and vapor pressure deficit (light gray) during the study period. (b) Atmospheric [CO<sub>2</sub>] in each plot during the study period. Ambient [CO<sub>2</sub>] in four reference plots are shown in gray, while that of the four elevated-[CO<sub>2</sub>] plots are in color. During *Indirect*, elevated-[CO<sub>2</sub>] plots were all subjected to +200 μmol mol<sup>-1</sup>. During *Direct*, [CO<sub>2</sub>] in each plot was varied independently for a five-day period to avoid confounding effects with REW. For example, in an elevated-[CO<sub>2</sub>] plot (orange line), [CO<sub>2</sub>] was decreased to ambient level during the first period, ramped up to +300 μmol mol<sup>-1</sup> above ambient in the second period, reduced to +200, +100 μmol mol<sup>-1</sup>, and to ambient level once again, followed by periods of +300 μmol mol<sup>-1</sup>, +150 μmol mol<sup>-1</sup> and finally to the ambient level in the last five-day period of *Direct* phase, before returning to the long-term enhancement of +200 μmol mol<sup>-1</sup>.

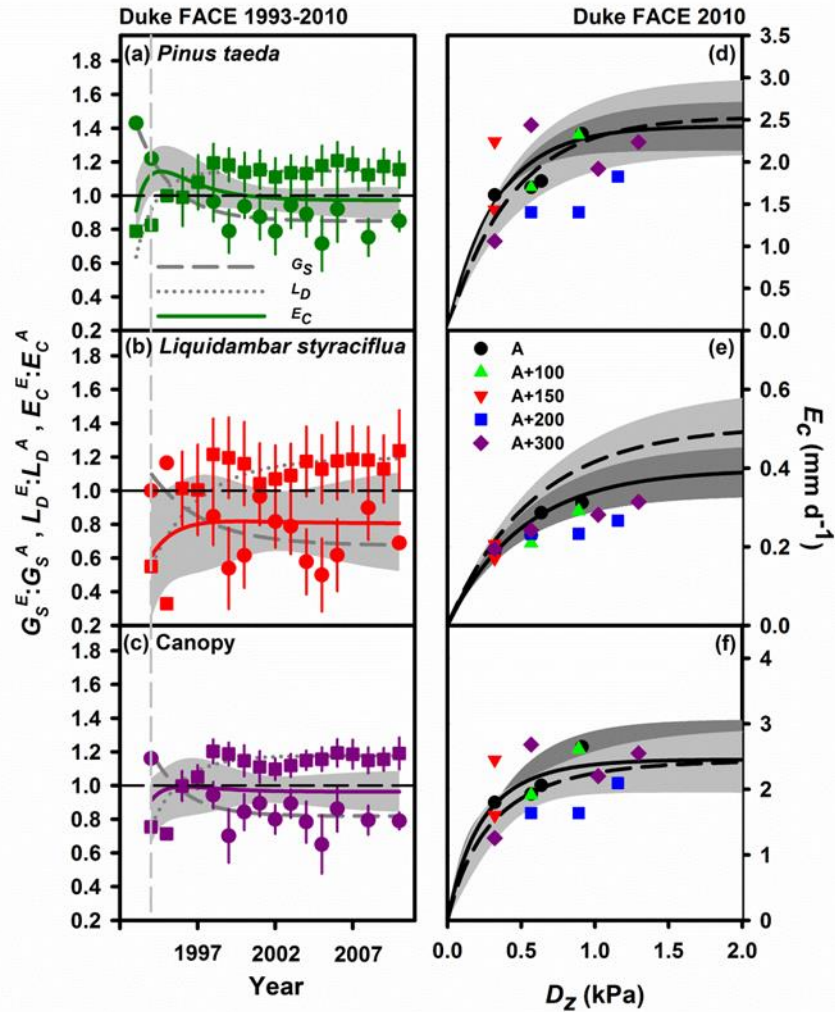


**Figure 2.2: Elevated-[CO<sub>2</sub>] effect on canopy transpiration at Duke FACE.** (a-c) Mean canopy stomatal conductance ( $G_s$ ; circles), mean growing season leaf area index ( $L_D$ ; squares) and canopy transpiration ( $E_c = G_s \times L_D$ ; colored solid lines) expressed as ratios of values in elevated-to-ambient [CO<sub>2</sub>] from 1993 to 2010 for each dominant species and the entire canopy. Shaded regions represent one SE of  $E_c$  (dashed and dotted lines, respectively). (d-f) Comparison of  $E_c$  response to  $D_z$  (daylength-normalized daytime vapor pressure deficit; see text) during the long-term elevated [CO<sub>2</sub>] treatment (*i.e.* +200  $\mu\text{mol mol}^{-1}$  during *Indirect* in 2010) under ambient- (dashed curves) and elevated-[CO<sub>2</sub>] (solid curves). Shaded regions are 95% confidence intervals associated with each curve (*e.g.*, light gray region corresponds to the fit for ambient-[CO<sub>2</sub>] data). Symbols represent the 5-day average data from elevated-[CO<sub>2</sub>] plot(s) during the short-term [CO<sub>2</sub>] manipulation (*Direct* phase).

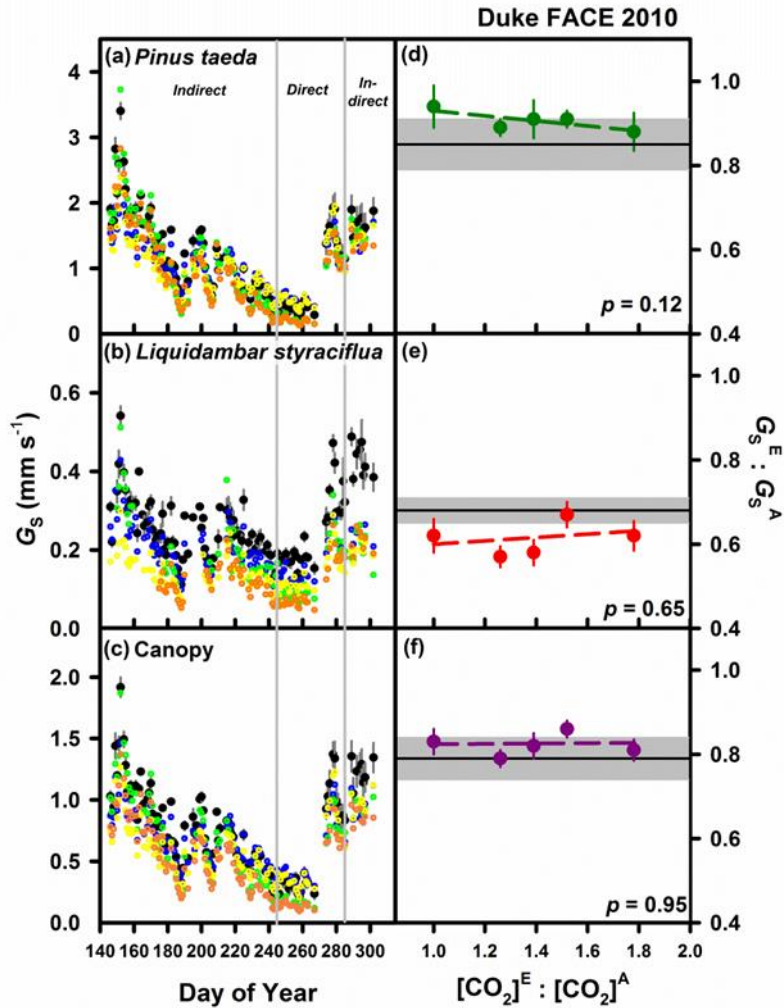


**Figure 2.3: Mean canopy stomatal conductance response to elevated  $[\text{CO}_2]$ .** (a-c) Time series of daily means of mean canopy stomatal conductance ( $G_s$ ) over the study period, including *Direct* and *Indirect* phases. Data for reference plots were averaged ( $n=4$ , black circles with 1 SE); data for each elevated- $[\text{CO}_2]$  plot are shown in different colors. (d-f) during *Direct*, the apparent decrease of  $G_s$  under elevated- relative to ambient- $[\text{CO}_2]$  ( $G_s^E : G_s^A$ ) with increasing  $[\text{CO}_2]$  was small,  $< 1\%$  per 10% increase of  $[\text{CO}_2]^E : [\text{CO}_2]^A$ , and insignificant in either major species or the entire canopy, indicating no direct response.  $P$  values are statistical results for  $t$ -tests on the regression slopes. The reduction of  $G_s$  observed during *Indirect* is depicted as a constant over the entire range of enhancement employed during the  $[\text{CO}_2]$ -response of *Direct* (horizontal solid lines, with 1 SE shown as a gray range). Because no direct response was detected in *Direct*, the reductions observed in *Indirect* are due to other mechanisms.

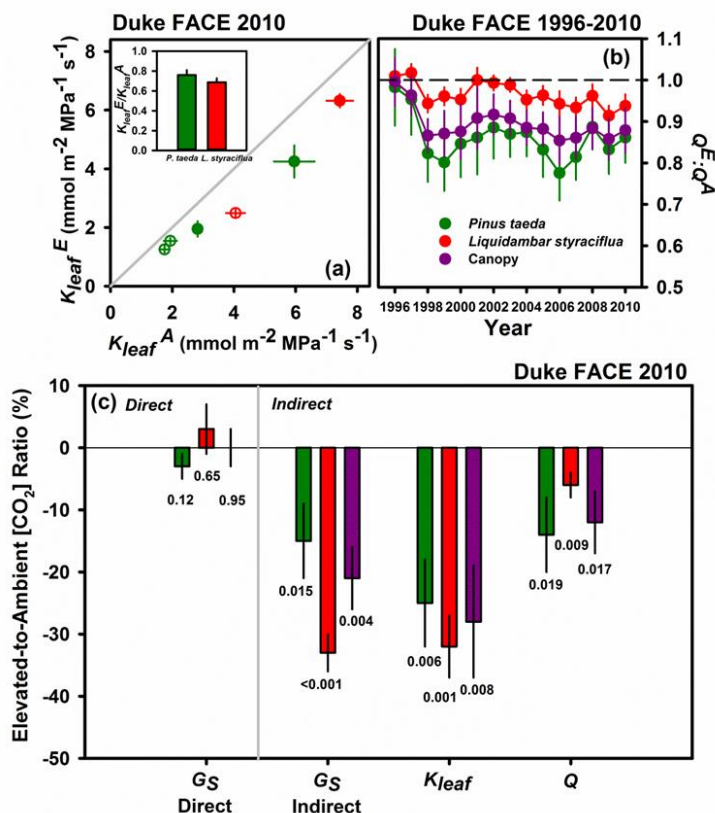


**Figure 2.4: The elevated-[CO<sub>2</sub>] effects for +200 μmol mol<sup>-1</sup> enrichment.** (a) Mean leaf hydraulic conductance ( $K_{leaf}$ , mmol s<sup>-1</sup> MPa<sup>-1</sup> m<sup>-2</sup>, with 1 SE) of the two dominant species measured at low (open circles) and high (filled circles) REW. Elevated-to-ambient [CO<sub>2</sub>] ratios of the mean annual  $K_{leaf}$  scaled from the two measurements in 2010 are presented in the inset. Repeated-measures ANOVA yielded significant reductions with  $P=0.029$  and  $P<0.001$  in *P. taeda* and *L. styraciflua*, respectively. (b) Responses of light intensity on leaf surfaces to high [CO<sub>2</sub>] through the increased-[CO<sub>2</sub>]-induced effect on  $L_D$  during the active FACE years ( $n = 4$  plots). Error bars represent one SE. The general decreasing trend of elevated-to-ambient [CO<sub>2</sub>] ratio of average light on leaf surfaces ( $Q^E:Q^A$ ) results from increasing mutual shading following the  $L_D$  enhancement (Figure 2.2a-c; squares). (c) The mean elevated-[CO<sub>2</sub>] impacts on stomatal conductance (with 1 SE) under stepwise [CO<sub>2</sub>] exposure (*Direct*, were calculated from the slopes in Figure 2.3d-f;  $G_{S,direct}$ ) and long-term elevated-[CO<sub>2</sub>] exposure (*Indirect*,  $G_{S,indirect}$ ). The results show non-significant direct and significant indirect  $G_S$  responses to high [CO<sub>2</sub>]. Leaf hydraulic conductance decreased ( $K_{leaf}$ ) through hydraulic acclimation, and reduced average light intensity on leaf surfaces through mutual shading caused by increased  $L_D$  contributed to  $G_{S,indirect}$ . Numbers under bars are  $P$  values from Student's  $t$ -tests ( $\alpha=0.05$ ). Color notations are the same as (b).

## 2.4 Appendix

### 2.4.1 Additional Materials and Methods

#### 2.4.1.1 Data for the interannual elevated-[CO<sub>2</sub>] effects on $G_s$ , $L_D$ and $E_c$ at Duke FACE (Figure 2.2a-c)

To illustrate the overall patterns of responses to high [CO<sub>2</sub>] treatment since the canopy establishment, we synthesized published data collected at the site since 1993. For the years of 1993-1996,  $G_s$  ratios were calculated from the ratios of canopy transpiration per unit leaf area at vapor pressure deficit of 1 kPa ( $E_{Lref}$ ) of *P.taeda* and *L.styraciflua* under elevated-[CO<sub>2</sub>] treatment relative to an untreated plot (Phillips & Oren, 2001). The ratios for entire canopy  $G_s$  was then computed as the average of these two species, weighted by their corresponding leaf area fraction of total canopy, assuming *L.styraciflua* represents other broadleaved subcanopy species. The leaf area data associated with those years were obtained from the same publication. We obtained  $G_s$  ratios for 1998-2008 from  $G_s$  at 1 kPa vapor pressure deficit ( $G_{Sref}$ ) data presented in Ward *et al.* (2013), focusing on the ambient- and elevated-[CO<sub>2</sub>] plots during non-drought years. The  $G_s$  ratios for 2010 were from the current study. Growing season averaged leaf area index ( $L_D$ ) from 1996-2010 was estimated from litterfall dynamics as described in McCarthy *et al.* (2007).  $E_c$  ratios were the product of the ratios of  $G_s$  and  $L_D$ .

### 2.4.1.2 Hierarchical Bayesian scaling approach

A scaling method is required to translate point measurements from sap flux density ( $J_s$ ) sensors to the forest canopy. Because a fertilization treatment has been conducted on all experimental plots since 2005 (Domec *et al.*, 2009; Ward *et al.*, 2013), we first performed the calculations of variables separately for each CO<sub>2</sub> × nitrogen (N) treatment. Later, we show that our analyses were not affected by nitrogen fertilization. We used random effects which were derived from a hierarchical Bayesian statistical model (Ward *et al.*, 2013) to simulate  $G_s$  of each species under each CO<sub>2</sub> × N treatment as a function of the responses to vapor pressure deficit ( $D$ ), soil moisture and photosynthetic photon flux density (PPFD), relative to a reference conductance.  $D$  was calculated from air temperature (°C) and relative humidity (%) measured at the site (Abteu & Melesse, 2013). Predicted  $G_s$  was then translated to transpiration per unit leaf area ( $E_L$ ) and finally to  $J_s$  after accounting for the water storage effect which causes a lag between transpiration and water flow in the stem. The random effects were derived by constraining the total amount of  $J_s$  to preserve the balance between  $J_s$  measured in the stem and transpiration. In particular, the following equation must be satisfied:

$$\sum_{d=1}^n \frac{A_{S(d)} \bar{\phi}_d}{\sum_{d=1}^n A_{S(d)}} = 1 \quad (\text{A2.1})$$

for each CO<sub>2</sub> × N treatment and species, where  $A_{S(d)}$  is sapwood area per unit ground area (cm<sup>2</sup> m<sup>-2</sup>) and  $\bar{\phi}_d$  is mean random effect at sapwood depth  $d$ . The measured  $J_s$  of

each sensor was divided by its corresponding  $\phi_d$ , resulting in mean  $J_s$  ( $\bar{J}_s$ ) for that sensor across the sapwood area. We used these half-hourly  $\bar{J}_s$  values to calculate daily  $E_c$  and  $G_s$ .

#### 2.4.1.3 Calculations of daily $E_c$ and $G_s$

The daily canopy transpiration ( $E_c$ ; mm d<sup>-1</sup>), presented in Figure 2.2d-f was computed from daily sum  $\bar{J}_s$  ( $\bar{J}_{SD}$ ; g<sub>H2O</sub> m<sup>-2</sup><sub>sapwood</sub> d<sup>-1</sup>) and total sapwood area per unit ground area ( $A_s$  in m<sup>2</sup> m<sup>-2</sup>) for each species and treatment (Oren *et al.*, 1998a). In other words,

$$E_C = 1 \times 10^{-3} \bar{J}_{SD} A_S \quad (\text{A2.2})$$

We calculated  $G_s$  (mm s<sup>-1</sup>) using the simplified Penman-Monteith equation

$$G_S = \frac{K_g(T) J_S A_S}{DL} \quad (\text{A2.3})$$

where  $K_g(T)$  is a conductance coefficient dependent on air temperature  $T$  in °C and equal to  $115.8 + 0.4226 T$  (kPa m<sup>3</sup> kg<sup>-1</sup>, Phillips and Oren 1998),  $D$  is vapor pressure deficit (kPa) and  $L$  is leaf area index (m<sup>2</sup> m<sup>-2</sup>). This equation assumes that boundary layer conductance exceeds  $G_s$ , consistent with the finding that the mean daytime boundary layer conductance was found to be 65 times  $G_s$  in this forest (Domec *et al.*, 2009). Thus, changes in  $G_s$  would reflect the response of the forest canopy to imposed changes of [CO<sub>2</sub>]. The analysis was performed on a daily-scale  $G_s$  to reduce the errors and noise created by water storage in trees. For each day, daily  $G_s$  was calculated by summing half-hourly  $\bar{J}_s$  over 24 hours (from 05:00 AM), to avoid large relative errors (Phillips & Oren, 1998), and using equation (3) with daytime average  $T$  and  $D$ . To avoid

uncertainties inherent in conductance calculations under low flux, we included only days in which daily average  $D$  was greater than 0.1 kPa (Phillips & Oren, 1998). We also excluded days in which daily photosynthetically active radiation (PAR) was  $<50 \text{ mol m}^{-2} \text{ d}^{-1}$  to avoid light limitation on  $G_s$ . Sapwood area was determined from an allometric relationship with diameter at breast height developed from trees harvested in 2011. Daily  $L$  was interpolated from bi-weekly values based on litterfall for all species, and including needle expansion for the pine (McCarthy *et al.*, 2007).

#### **2.4.1.4 Analysis of the Elevated- to-Ambient-[CO<sub>2</sub>] ratio of $G_s$ ( $G_s^E:G_s^A$ )**

In addition to variation in soil moisture,  $G_s$  response to elevated [CO<sub>2</sub>] might be affected by nutrition, altered by nitrogen fertilization since 1998 in two plots and in all plots in 2005 (Domec *et al.*, 2009; Ward *et al.*, 2013). We calculated the ratios of  $G_s$  in each of the elevated-[CO<sub>2</sub>] plots to the mean of the four ambient-[CO<sub>2</sub>] plots,  $G_s^E:G_s^A$  (see below for estimation of variance). To evaluate the direct elevated-[CO<sub>2</sub>] effect on  $G_s$ , we tested for differences between  $G_s^E:G_s^A$  obtained during each enrichment level of *Direct* (experimental period) and *Indirect* (reference period). We performed statistical tests (Student's *t*-test and least-square regression) using ratios produced by temporally averaging all available days for each plot within each [CO<sub>2</sub>] level after testing for interaction effects on  $G_s^E:G_s^A$  among high [CO<sub>2</sub>], soil moisture and N using daily values during the study period. A REW threshold of 0.3 (calculated as actual minus minimum soil moisture divided by maximum minus minimum moisture to 0.3 m depth; Pataki & Oren, 2003) was selected based on the REW profile during the study period and used to

partition data into dry and wet conditions. An Analysis of Covariance (ANCOVA) was applied to the ratios to test for elevated  $[\text{CO}_2] \times \text{N} \times \text{soil moisture}$  interaction effects using  $[\text{CO}_2]$  enhancement ratio ( $[\text{CO}_2]_E:[\text{CO}_2]_A$ ) or REW as covariate. We observed no significant interaction effect on  $G_s^E:G_s^A$  involving either soil factor and  $[\text{CO}_2]_E:[\text{CO}_2]_A$  for either species and the canopy ( $P \geq 0.12$ ). Thus, data were pooled for analyses regardless of soil moisture or fertilization treatment, *i.e.* we calculated a temporal average of daily  $G_s$  for each period in *Direct* and each plot of *Indirect*. We then divided the temporally averaged  $G_s$  of each elevated- $[\text{CO}_2]$  plot by the mean of the temporally averaged  $G_s$  of the ambient- $[\text{CO}_2]$  plots ( $n=4$ ), thus obtaining four  $G_s^E:G_s^A$  for analyses ( $n=4$ ). The least-square regression was based on the  $G_s^E:G_s^A$  values obtained for each plot in each  $[\text{CO}_2]$  level, testing for a response over the entire range of  $[\text{CO}_2]_E:[\text{CO}_2]_A$ . A Student's t-test was used to test for significance of the slopes. We also compared  $G_s^E:G_s^A$  of each  $[\text{CO}_2]$  treatment level during *Direct* with that obtained under  $+200 \mu\text{mol mol}^{-1}$  during *Indirect* using Student's t-test to test the hypothesis that there will be no difference in the ratio under a similar enrichment in *Direct*, but increased likelihood of higher ratio in lower  $[\text{CO}_2]$ , and *vice versa* under higher enrichment. For these analyses, we computed standard deviation ( $\sigma$ ) by considering the propagation of uncertainty in two steps:

**Step 1** Calculate  $\sigma$  of ratios between temporal average  $G_s$  of each elevated- $[\text{CO}_2]$  plot  $i$

( $\overline{G}_{Si}^E$ ) and average  $G_s$  across all ambient- $[\text{CO}_2]$  plots ( $\overline{G}_S^A$ )

The ratio can be written in terms of a function,  $f_i$ , of real variables  $\overline{G_{Si}^E}$  and  $\overline{G_S^A}$  with standard deviations of  $\sigma_{Ei}$  and  $\sigma_A$ , respectively (Fornasini, 2008). In other words,

$$f_i = \overline{G_{Si}^E} / \overline{G_S^A}$$

$$\sigma_{f_i} = f_i \frac{\sigma_A}{\overline{G_S^A}} \quad (\text{A2.4})$$

where  $\sigma_{f_i}$  is the standard deviation of the elevated- to ambient-[CO<sub>2</sub>]  $G_s$  ratio of each elevated-[CO<sub>2</sub>] plot  $i$ .

**Step 2 Calculate  $\sigma_R$  of  $G_{s^E}:G_{s^A}$**

For variables with equal sample size, the variance of the mean across these variables is equal to the mean of their variances. In this case, the sample size is 4 and therefore

$$\sigma_R^2 = \frac{\sum_{i=1}^4 \sigma_{f_i}^2}{4}$$

$$\sigma_R = \frac{\sqrt{\sum_{i=1}^4 \sigma_{f_i}^2}}{2} \quad (\text{A2.5})$$

where  $\sigma_R$  is the standard deviation of the mean ratio of  $G_{s^E}:G_{s^A}$  we used in the  $t$ -test.

The results show that  $G_{s^E}:G_{s^A}$  tended to be lower than the long-term mean of  $L$ .

*styraciflua* under +100 and +150  $\mu\text{mol mol}^{-1}$  ( $P = 0.08$  and  $0.10$ , respectively), and higher for the entire canopy under +200  $\mu\text{mol mol}^{-1}$  ( $P = 0.06$ ; Table A2.4.2), thus not consistent

with the hypothesized response, but consistent with the response seen in regression analyses.

We used Randomized Intervention Analysis (RIA) (Carpenter *et al.*, 1989) to retain temporal variation of  $G_s$  lost in the former approaches. RIA is a test designed to detect nonrandom change due to treatment effect in a series of observations made before and after the application of treatment. RIA utilizes randomization to derive error distribution from the data itself. This feature gives RIA the advantage of being unaffected by non-normality which usually exists in ecosystem experiments. In this study, the treatment difference was calculated by subtracting the averaged  $G_s$  of the ambient-[CO<sub>2</sub>] plots ( $n=4$ ) from  $G_s$  in each elevated-[CO<sub>2</sub>] plot on each day. The error distribution (*i.e.* daily difference between each [CO<sub>2</sub>] level of *Direct* and mean treatment difference during *Indirect*) was generated from 10,000 permutations of daily treatment differences. Then, we evaluated the significance of the treatment effect by comparing the frequency distribution of simulated error to the actual error observed in the original data (Carpenter *et al.*, 1989). Figure A2.4.1 illustrates the results from RIA by comparing the absolute difference of mean treatment difference during *Indirect* with that during *Direct* as observed in each plot and [CO<sub>2</sub>] treatment level ( $\left| \overline{\Delta_{Direct}} - \overline{\Delta_{Indirect}} \right|$ ) to that required for significant elevated-[CO<sub>2</sub>] effects ( $\alpha=0.05$ ). The data points in these figures lie below the 1:1 line, indicating non-significant difference in all [CO<sub>2</sub>] enrichment levels. The results from all analyses are consistent in finding  $G_s^E/G_s^A$  to be similar over the entire study period, showing no signs of response to fast changes of [CO<sub>2</sub>] treatment during *Direct*.

#### 2.4.1.5 Leaf hydraulic conductance ( $K_{leaf}$ )

Leaf hydraulic conductance  $K_{leaf}$  ( $\text{mmol m}^{-2} \text{MPa}^{-1} \text{s}^{-1}$ ) was measured on single leaves/fascicles by using the timed rehydration method (Brodribb & Holbrook, 2003) which is based on an analogy between rehydrating a leaf and recharging a capacitor:

$$K_{leaf} = C_{leaf} \frac{\ln \left[ \frac{\Psi_{leaf(o)}}{\Psi_{leaf(t)}} \right]}{t} \quad (\text{A2.6})$$

where:  $C_{leaf}$  ( $\text{mmol m}^{-2} \text{MPa}^{-1}$ ) is the leaf capacitance determined from the slope of relative water content to  $\Psi_{leaf}$  obtained from pressure-volume curves,  $\Psi_{leaf(o)}$  (MPa) is the leaf water potential prior to re-hydration,  $\Psi_{leaf(t)}$  is the leaf water potential after re-hydration, and  $t$  (s) is the duration of re-hydration of leaves/fascicles detached under water from the stem. For a given  $\Psi_{leaf}$ ,  $K_{leaf}$  values estimated using the timed rehydration method has been shown to be similar to values measured on intact plants (Domec *et al.*, 2009; Johnson *et al.*, 2009). Distilled water was used for rehydration of  $K_{leaf}$  samples, and water temperature was maintained between 21°C and 22°C. Pressure-volume analyses (Tyree & Hammel, 1972) were conducted on leaves/fascicles taken on the same branches used to determine  $K_{leaf}$ . Pressure-volume curves were initiated by first determining the fresh weight of the leaves/fascicles, and then measuring  $\Psi_{leaf}$  with a pressure chamber (PMS Instrument Company, Albany, OR). Alternate determinations of fresh weight and  $\Psi_{leaf}$  were repeated during slow dehydration on the laboratory bench until values of  $\Psi_{leaf}$  ranging from -3.0 MPa to -3.5 MPa were attained. The inverse of water potential was

plotted against relative water content to establish a pressure-volume curve and determine the water potential at turgor loss point. All capacitance values reported and used to calculate  $K_{\text{leaf}}$  corresponded to  $C_{\text{leaf}}$  determined before the water potential at turgor loss point (Brodribb & Holbrook, 2003).

On days 150-153 (where REW = 0.37) and on days 266-269 (where REW = 0.15), field  $K_{\text{leaf}}$  corresponding to the time of the day of maximum leaf stomatal conductance ( $g_s$ ; usually between 10:00 AM and 11:00 AM) was calculated from measured  $\Psi_{\text{leaf}}$  and the relationships between  $K_{\text{leaf}}$  and  $\Psi_{\text{leaf}}$  determined in the laboratory. Because  $\Psi_{\text{leaf}}$  measured at maximum  $g_s$  may underestimate  $\Psi_{\text{leaf}}$  at mean  $g_s$ , we calculated the ratio of  $K_{\text{leaf}}$  under ambient and elevated  $\text{CO}_2$  concentrations ( $K_{\text{leaf}}^{\text{E}}:K_{\text{leaf}}^{\text{A}}$ ) over a large range of  $\Psi_{\text{leaf}}$  to assess whether  $K_{\text{leaf}}^{\text{E}}:K_{\text{leaf}}^{\text{A}}$  was always below unity over the entire range of observed  $\Psi_{\text{leaf}}$  (Figure A2.4.2). A mean annual  $K_{\text{leaf}}$  for each treatment and each species was then determined using a linear fit between  $K_{\text{leaf}}$  and REW and the seasonal variation of REW. Measurements made on multiple dates were analyzed by repeated measure ANOVA. Statistical analyses were performed using SAS (Version 9.2, Cary, NC, USA) and curve fits were performed using Sigmaplot (version 12.3.0, SPSS Inc. San Rafael, CA, USA).

#### **2.4.1.6 Long-term response of $Q$ to increasing $[\text{CO}_2]$ (Figure 2.4b)**

We estimated the average light intensity on leaf surfaces ( $Q$ ) based on light absorption normalized by canopy leaf area. In other words,

$$Q = Q_0 \times (1 - \exp(-k_{eff}L_D)) / L_D \quad (A2.7)$$

where  $Q_0$  is the incident light intensity at the top of canopy,  $k_{eff}$  is the effective light extinction coefficient and  $L_D$  is the mean growing season leaf area index (same data as presented in Figure 2.2a-c; squares).  $k_{eff}$  was calculated using a one-dimensional radiative transfer model as explained in the Materials and Methods section. For each species and canopy, we took average of daytime  $k_{eff}$  values across the growing season (May to October of each year).  $Q$  values were determined for each study plot and averaged across ambient- and elevated-[CO<sub>2</sub>] plots (each,  $n = 4$ ) with one SE.

**Table A2.4.1: Regression statistics of *Indirect Ec* response to  $Dz$  (Curves in Figure 2.2d-f). The fitting equation is  $E_c = a(1 - e^{-bDz})$ . CO<sub>2</sub><sup>A</sup> and CO<sub>2</sub><sup>E</sup> plots refer to reference and [CO<sub>2</sub>] enrichment plots.**

<b>Species</b>	<b>Plot</b>	<b>a</b>	<b>b</b>	<b>R<sup>2</sup></b>	<b>P</b>
<i>P. taeda</i>	CO <sub>2</sub> <sup>A</sup> 1	2.313	2.293	0.50	<0.0001
	CO <sub>2</sub> <sup>A</sup> 2	2.770	2.325	0.49	<0.0001
	CO <sub>2</sub> <sup>A</sup> 3	2.841	2.461	0.38	<0.0001
	CO <sub>2</sub> <sup>A</sup> 4	1.927	3.581	0.06	0.016
	CO <sub>2</sub> <sup>E</sup> 1	1.993	3.346	0.07	0.007
	CO <sub>2</sub> <sup>E</sup> 2	2.580	2.755	0.34	<0.0001
	CO <sub>2</sub> <sup>E</sup> 3	2.986	3.363	0.55	<0.0001
	CO <sub>2</sub> <sup>E</sup> 4	2.275	3.414	0.35	<0.0001
<i>L. styraciflua</i>	CO <sub>2</sub> <sup>A</sup> 1	0.558	1.602	0.32	<0.0001
	CO <sub>2</sub> <sup>A</sup> 2	0.460	1.853	0.42	<0.0001
	CO <sub>2</sub> <sup>A</sup> 3	0.371	1.921	0.27	0.002
	CO <sub>2</sub> <sup>A</sup> 4	0.313	2.105	0.35	0.002
	CO <sub>2</sub> <sup>E</sup> 1	0.386	3.940	0.14	0.032
	CO <sub>2</sub> <sup>E</sup> 2	0.399	1.911	0.30	<0.0001
	CO <sub>2</sub> <sup>E</sup> 3	0.362	2.961	0.18	0.004
	CO <sub>2</sub> <sup>E</sup> 4	0.336	2.008	0.42	<0.0001
Canopy	CO <sub>2</sub> <sup>A</sup> 1	2.261	4.004	0.19	0.0004
	CO <sub>2</sub> <sup>A</sup> 2	3.184	1.919	0.58	<0.0001
	CO <sub>2</sub> <sup>A</sup> 3	2.309	3.087	0.34	0.002
	CO <sub>2</sub> <sup>A</sup> 4	2.221	2.176	0.19	0.003
	CO <sub>2</sub> <sup>E</sup> 1	2.602	2.772	0.60	0.002
	CO <sub>2</sub> <sup>E</sup> 2	2.962	2.799	0.33	<0.0001
	CO <sub>2</sub> <sup>E</sup> 3	3.214	4.305	0.18	0.015
	CO <sub>2</sub> <sup>E</sup> 4	2.518	3.871	0.21	0.004

**Table A2.4.2: *P* values from a Student's *t*-test.** These are the results from comparison between the ratio of stomatal conductance under elevated relative to ambient [CO<sub>2</sub>] with that obtained under the background conditions of +200 μmol mol<sup>-1</sup> [CO<sub>2</sub>] (Figure 2.3d-f, horizontal solid lines).

[CO <sub>2</sub> ] level	<i>P. taeda</i>	<i>L. styraciflua</i>	Canopy
A	0.24	0.36	0.36
A+100	0.47	0.08	1.00
A+150	0.36	0.10	0.48
A+200	0.30	0.85	0.06
A+300	0.63	0.36	0.63

**Table A2.4.3: Results from Randomized Intervention Analyses (RIA).** Values in the table represent the number of elevated-[CO<sub>2</sub>] plots (out of  $n=4$ ) affected by the 5-day changes of [CO<sub>2</sub>] relative to the long-term background of +200  $\mu\text{mol mol}^{-1}$  [CO<sub>2</sub>] tested against needed difference of  $\alpha = 0.05$  (see Figure A2.4.1). The ranges of  $P$  values among the four elevated [CO<sub>2</sub>] plots in short-term [CO<sub>2</sub>] level are also shown.

[CO <sub>2</sub> level]	<i>P. taeda</i>	<i>L. styraciflua</i>	Canopy
A	0 ( $P = 0.22-0.68$ )	0 ( $P = 0.15-0.62$ )	0 ( $P = 0.11-0.83$ )
A+100	0 ( $P = 0.10-0.70$ )	0 ( $P = 0.18-0.66$ )	0 ( $P = 0.19-0.70$ )
A+150	0 ( $P = 0.14-0.67$ )	0 ( $P = 0.10-0.70$ )	0 ( $P = 0.16-0.86$ )
A+200	0 ( $P = 0.20-0.42$ )	0 ( $P = 0.14-0.69$ )	0 ( $P = 0.07-0.69$ )
A+300	0 ( $P = 0.11-0.70$ )	0 ( $P = 0.22-0.59$ )	0 ( $P = 0.20-0.53$ )

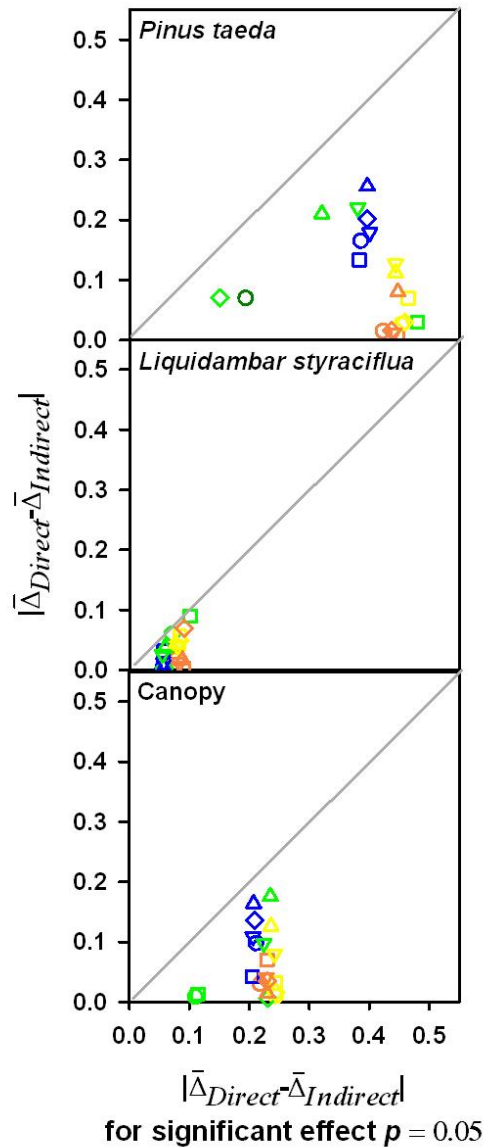


**Figure A2.4.1: Results from Randomized Intervention Analysis (RIA).** The analysis was performed to test for direct effects of elevated  $[\text{CO}_2]$ . For each plot (shown in different colors), the actual difference (y-axis) between mean treatment difference of  $G_s$  during the background experiment period of  $+200 \mu\text{mol mol}^{-1} [\text{CO}_2]$  (*Indirect*) and each level of enrichment (shown as shapes) during the  $[\text{CO}_2]$ -response period (*Direct*) is compared to the value required for significant treatment effect ( $\alpha = 0.05$ ). Differences obtained from all plots and enrichment levels were smaller than is necessary to be considered significant.

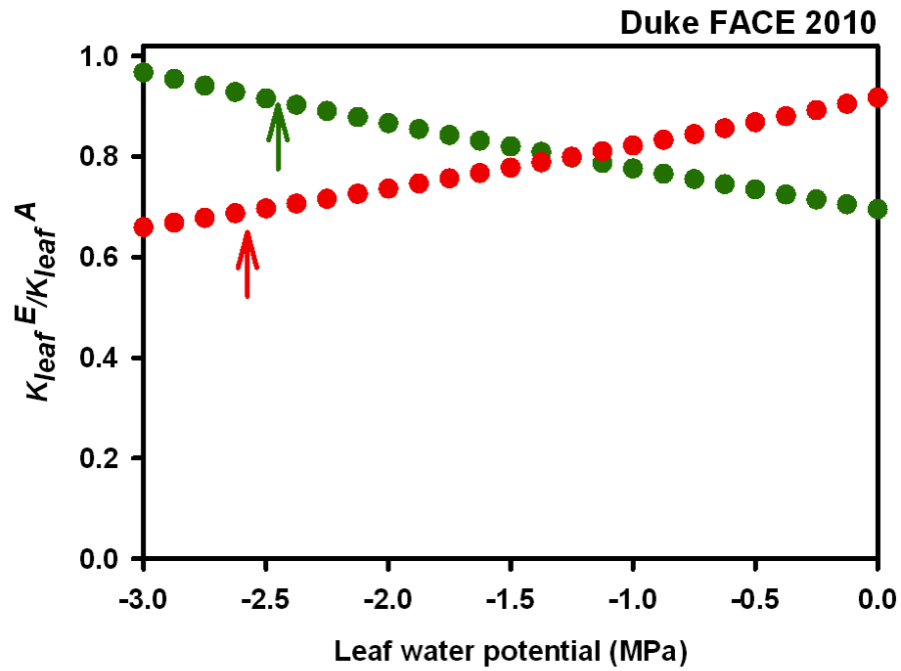


**Figure A2.4.2: Elevated-to-Ambient [CO<sub>2</sub>] ratios of  $K_{leaf}$ .** The ratio of  $K_{leaf}$  under ambient and elevated-[CO<sub>2</sub>] ( $K_{leaf}^E:K_{leaf}^A$ ) of *P. taeda* (green) and *L. styraciflua* (red) over a large range of  $\Psi_{leaf}$ . Arrows represent the minimum  $\Psi_{leaf}$  measured in each species.

### **3. Adaptation of pine crown architecture to growing season solar elevation supports low branches and prevents extra light from reaching competing subcanopy species**

#### ***3.1 Introduction***

Forests dominated by the genus *Pinus* are found over a wide range of environments, from near the Arctic Circle with cold winters and short growing seasons to the tropics with year-round growing season (Knight et al. 1994). They also include stands on soils ranging from nutrient rich to sandy, poor soils (Knight 1991, Knight et al. 1994). Many pine species range widely or have been introduced across a large latitudinal range in attempt to increase fiber yields (Elfving and Norgren 1993, Elfving et al. 2001, Engelmark et al. 2001). Although it has been observed that exotic species can maintain and even increase production relative to that at their original latitudes, and relative to native species, mechanistic explanations for these observations remain elusive, limiting the scope of inference of such findings (Hierro et al. 2005, Gurevitch et al. 2011).

Proposed mechanisms explaining higher stem wood production in species' exotic relative to native environment, and in exotic versus native species, range from less pressure from nematodes, insects and diseases (Keane and Crawley 2002) and more advantageous soil microbiota (Gundale et al. 2014), to factors affecting canopy photosynthesis and carbon (C) allocation to above- versus belowground (Wilsey and Polley 2006, Jansons et al. 2013). Although crown architecture may greatly affect light

absorption (Mäkelä 1997, Stenberg 1998, Nilson 1999, Kim et al. 2011) and, thus both gross primary production and photosynthesis per unit C investment in crowns, we are unaware of studies analyzing how variation of crown attributes interact with latitudinal locations (and thus solar elevation during the growing season) to affect light absorption in forest canopies, and the carbon cost associated with maintaining the structure of these canopies. Such analyses can help define the latitudinal limits of a species depending on its ability to vary crown attributes within the constraints of its allometry, as well as indicate latitudes where a species can absorb more light than a native species, possibly growing faster but certainly affecting subcanopy composition, production and dynamics.

Crown architecture influences canopy photosynthesis and maintenance of positive carbon gain by controlling the amount and distribution of canopy light absorption (Kim et al. 2008). Absorption of light and light-use efficiency (carbohydrate production per unit light absorbed) may vary 50 - 80% among forests of different species composition, growing on sites of different fertility and subjected to different silvicultural treatments (Binkley et al. 2013). Species- and site-specific foliage and crown aggregation influence the amount and distribution of canopy light interception (Sampson and Smith 1993, Binkley et al. 2013). In forest ecosystems, plants organize themselves by orienting foliage, grouping foliage into shoots within trees and trees in stands, and vertically adjusting the distribution of foliage, thereby creating crown and canopy architecture

that allows efficient light interception (Oker-Blom and Kellomäki 1983, Chen et al. 1994, Stenberg 1998). For example, foliage at the top of canopy may be vertically inclined and clumped and, while still receiving ample light on leaf surfaces, allow substantial amount of light transmitted to lower leaves which are more horizontally oriented and spread out (Sprugel et al. 1996, Stenberg et al. 2001). Latitude, which affects solar angle, determines the intensity and duration of incoming light, influencing light interception and photosynthesis of the leaves depending on leaf-surface orientation (Chen et al. 1994). Therefore, the crown architecture of a species should reflect the light environment prescribed by latitudinal location and stand conditions.

The cost-benefit concepts have been developed to investigate patterns of dominant plant traits and species across ranges of environments (e.g. Miller and Mooney 1974, Givnish 2002). The principle behind the calculations is that natural selection should maximize carbon gain per unit carbon invested in tissue construction (Kikuzawa 1991). Because, at the canopy level, light absorption is directly related to plant photosynthesis and growth (Bergh et al. 2005), cost-benefit analysis quantifying plant adaptation to certain environments is often performed in terms of light interception. For example, studies employing this principle examine the optimal strategies for trees to maintain leaves at different irradiance intensities (Givnish 1988) and along a height-related light gradient (Givnish 1982), to display leaves at different angles within crowns (Hikosaka and Hirose 1997), and to adjust crown depth in forests

of different latitudes (Vermeulen 2014). At the scale of individuals, Onoda et al. (2014) used this approach to study the coexistence of species within the same forest, considering competition for light based on light interception efficiency, defined as total canopy light interception per unit aboveground biomass. Such cost-benefit analysis allows separating between two possible reasons for one species to annually absorb more light than another – the annual investment of carbon in crowns versus the translation of this carbon investment into different crown architectural properties.

Considering light interception and its use efficiency as setting the *potential* for growth rate, our focus here is on how these quantities would change when a species is moved from its native environment to an exotic one. Specifically, we evaluated the impact of crown architecture (i.e. foliage organization within the crown) and solar elevation (i.e. site latitude) on canopy light absorption, and its likely implications for overstory growth and associated ecological consequences to the understory. We studied a hypothetical monospecific stand composed of three commercially important northern hemisphere species: *P. taeda* (loblolly pine; *Pt*) of North Carolina, USA, *P. contorta* (lodgepole pine; *Pc*) of British Columbia, Canada, and *P. sylvestris* (Scots pine; *Ps*) of northern Sweden. At this time, no species outperforms *Pt* on its favorite sites of its native range. However, in Sweden, the exotic *Pc* is performing as well or better than *Ps*. It has been estimated to produce 36% more wood than *Ps* (Elfving and Norgren 1993).

Consequently, *Pc* provenances from northern Canada have been planted over an area of 600,000 ha in the past 25 years (Elfving et al. 2001, Gundale et al. 2014).

In the analyses, we made several simplifying assumptions. First, light intercepted by live branches at the bottom of crowns in the native habitat represents the minimum ‘tolerable’ daily average light absorbed over the growing season by a branch of that species. This assumption can be challenged on the grounds that the crown base of trees of a given size can extend lower to the ground in rich sites than in poor sites, thus allowing higher leaf area index (*L*) to develop. However, in nutrient poor sites, lower branches must absorb more light to maintain a null carbon balance because their photosynthetic rate is nutrient limited (Linder and Lohammar 1981, Dewar et al. 2012). Second, changes in growing season length do not affect the balance between photosynthesis and respiration of lower branches, and that branches are largely autonomous units (Sprugel et al. 1991). Third, we assumed that the leaf area dynamics and growth of a species in an exotic environment over the simulation year remain as in the native environment. This assumption allows focusing on crown characteristics and, because we analyze large individuals, would change absolute quantities little without affecting the relative outcome of the analyses.

Based on the above, we posed two largely theoretical hypotheses, and one hypothesis of practical implication. It is clear that there can be many reasons why *Pt* may not perform well in SE, and similarly *Ps* in NC (Way and Montgomery 2014).

Focusing on light, however, we hypothesized that, at fully occupied sites in SE, the crown properties of *Pt* will not allow sufficient light for maintaining the function of its lower crown, and reduce light availability to subcanopy relative to a similar *Ps* stand (**H1**). The crown of *Pt* will need to undergo adjustment to light availability forcing the trees outside the range observed in the species' allometric functions. Conversely, at a fully occupied site in NC, *Ps* bottom branches will have more than sufficient light, but the canopy would still allow more light to reach the understory than the native *Pt* canopy does (**H2**), risking intense competition. Again, structural adjustments to increase canopy light absorption would require an allometric change outside the range observed in *Ps*. Our realistic hypothesis was that *Pc* genotypes from its northern latitude have crown architecture permitting more light absorption than that of *Ps* without subjecting lower branches to too low light; however, the crown would allow too little light penetration to maintain a productive understory (**H3**). In all simulations, we kept stand-scale properties the same so we can focus on the effect of changes in crown properties.

Finally, we adapted the cost-benefit analysis of Onoda et al. (2014) by considering the efficiency of the total amount of light captured in the crown relative to the amount of carbon used to produce and maintain the crown structure, i.e. the annual investment in leaves and branches. We used this modified cost-benefit concept as a proxy of carbon balance to compare species' performance in the exotic environment relative to its native conditions and to the species' counterpart. For example, an

alternative to **H3** is that *Pc* grows faster than *Ps* in SE because of a superior efficiency of light interception, allowing larger allocation of available carbohydrate to produce stem instead of crown elements.

## ***3.2 Materials and Methods***

### **3.2.1 Settings**

Our analyses relied on measured stand and crown characteristics of *Pinus taeda* (*Pt*), *Pinus sylvestris* (*Ps*), and *Pinus contorta* (*Pc*), forests in temperate and boreal zones. While most of the data on *Pt* and *Ps* were collected from two stands (Actual Stand in Table 3.1), necessary inputs for *Pc* were obtained mostly from various published sources. The *Pt* plantation in North Carolina, USA was established in 1965, thinned in 1983 and 1998, and harvested in 2006. Approximately 2% of total stand basal area was comprised of understory hardwoods (Uebelherr 2008). The terrain is relatively flat and the soil is well-drained sand with average bulk density and porosity (in the top 60 cm) of 1.5 g cm<sup>-3</sup> and 0.43, respectively. Long-term mean annual temperature and total precipitation were 15.8 °C and 1145 mm (McCarthy et al. 2007). We utilized mensuration data from 2003 to represent our *Pt* canopy structure (Table 3.1; J.M. Uebelherr and A.C. Oishi, unpublished). The *Ps* forest in Rosinedal, Sweden, was naturally regenerated in 1920 – 1925, non-commercially thinned in 1955 and thinned in 1976 and 1993. The soil is fine sand, and the profile formed is that of a weakly developed podsol with an organic morlayer ranging in thickness from 2 to 5 cm. The understory vegetation is characterized

by the dwarf shrubs *Vaccinium myrtillus* (bilberry) and *Vaccinium vitis-idaea* (lingonberry), a ground layer of mosses, *Pleurozium schreberi* and *Hylocomium splendens* and lichens, *Cladonia spp.* (Hasselquist et al. 2012). The 30-year mean annual temperature and precipitation (1981 – 2010), measured at the Svartberget field station (8 km from the study site) were 1.8 °C and 614 mm (Laudon et al. 2013). On average, the area is covered by snow from late October to early May. Tree heights and diameters at breast height (DBH) were measured annually. A total of 21 trees were harvested (15 trees in 2006 and 6 in 2011) to develop allometric equations (Lim et al., in review).

Many factors, such as differences in stand density and leaf area, may confound the effect of crown characteristics in comparison of light interception (or absorption) at different latitudes. At the stand scale, crown size and tree spatial pattern produce clumping akin to needle clumping (degree of self-shading) at the shoot scale (Nilson 1999, Kim et al. 2011). Stenberg et al. (2014) suggested that crown clumping (within-tree self-shading) is independent of tree size and that the whole-stand clumping is induced by spatial pattern of trees. Our analyses focus on plantations with a uniform arrangement of trees. Moreover, we aimed at comparing stands with identical mean tree size and the corresponding maximum density for each species and, thus assessed the maximum size-density relation of each species (Reineke 1933). We generated the relations for *Pt* using data from the region (Harrington and Edwards 1996, Scott 1997); for *Pc*, using a regional density management diagram (Farnden 1996) and for *Ps* using

data from 17 plots we established near the study site (Lim et al., in review). The three species shared the same relation between mean tree size (quadratic mean diameter at breast height; qDBH) and maximum density (Figure 3.1a), with a self-thinning slope of -0.59 ( $\log(\text{qDBH}) = -0.59 \log(\text{stand density}) + 2.58$ ;  $r^2=0.84$ ,  $p<0.001$ ). We selected a hypothetical stand with tree size and density falling between the stands in NC and SE, but on the self-thinning line (Figure 3.1a; star) and used it in all analyses.

### 3.2.2 Canopy structure

Tree height and DBH were measured on 90 trees in NC and 307 trees in SE and used to generate branch and stem surface areas and crown dimensions (i.e. crown width and crown length, assuming ellipsoidal shape). Branch surface area was estimated from a logarithmic function of DBH and crown ratio for *Pt* (Baldwin et al. 1997, McCarthy et al. unpublished). For *Ps*, branch surface area was estimated from a relation of branch dry weight to DBH (Lim et al, in review) and branch surface area versus branch dry weight (Halldin 1985, Ilvesniemi and Liu 2001). The vertical profile of branch surface area of *Pt* was taken from a nearby site (Kim et al. 2011), and of *Ps* from a similar stand (Halldin 1985). In both species, the dry mass of dead branches below the crown was ~4-6% of total branch mass, and is not likely to have an appreciable effect on light interception. Stem surface area was determined from segmented polynomial tapering equations (Sharma and Burkhardt 2003) using diameter measurements along stems from the nearby site in NC (Kim et al. 2011) and harvested trees in SE (Lim et al. in review). Crown

length was measured at each site. Crown radii were derived from equations presented in Baldwin and Peterson (1997) for *Pt* and Rautiainen and Stenberg (2005) for *Ps*.

Hemi-surface  $L$  of *Pt* was estimated from monthly measurements using a plant canopy analyzer (LAI-2000, Li-Cor BioSciences, Lincoln, NE, USA). We used a factor of 1/2 to convert the hemi-surface  $L$  to projected  $L$  (Stenberg 1996). The LAI-2000 measurements were performed at 20 locations each along two perpendicular transects. Vertical distribution of  $L$  was obtained from LAI-2000 measurement at 2-m intervals along a tower at the site. A correction factor of 0.59 (Th  r  zien et al. 2007) was applied to account for foliage clumping (Stenberg 1996). For *Ps*, we used annual  $L$  value estimated from allometric function, and annual production and litterfall in SE (Lim et al, in review). The seasonality of  $L$  was obtained from a study of *Ps* stand of similar age and site characteristics (Rautiainen et al. 2011). The vertical distribution of  $L$  was obtained from the harvested individuals (Lim et al. in review).

Shoot characteristics including needle angle distribution (NAD), shoot transmission coefficient ( $c$ ), and clumping factor (CF) of *Pt* were assumed to be similar to those measured at a nearby site (Kim et al. 2011), CF and NAD of *Ps* were obtained from measurements of shoot structure in a *Ps* stand in central Finland (Stenberg et al. 2001).  $c$  was then estimated from an empirical relation (Th  r  zien et al. 2007). For *Pc* structural attributes such as height, crown length, crown width, wood surface areas, foliar vertical distribution and biomass components were generated from published data (Gary 1978,

Pearson et al. 1984, Sampson and Smith 1993, Wonn 2001, Lambert et al. 2005, Sattler and LeMay 2011). Shoot structural parameters were estimated from measurements of shoot samples from two *Pc* trees in a nearby, young *Ps* stand in SE (with DBH of 7.8 and 12.0 cm and height of ~10 m). Because the site was more open ( $L \sim 1.4$ ) than our hypothetical site ( $L = 2$ ), we selected trees that were surrounded by others to resemble those in a closed canopy. We divided the crown into five layers and randomly selected 1 to 2 shoots from each layer. We measured needle angle of three needles per shoot using a protractor and needle and shoot length with a ruler. We also counted the number of fascicles and sampled 10 fascicles for projected leaf area measurement by analyzing the scanned images using ImageJ (Schneider et al. 2012). We calculated CF and  $c$  using the approach outlined in Th  rezien et al. (2007). We realize that these estimates may not represent a continuous *Pc* canopy, but they should provide a rough estimate of the difference of shoot characteristics between *Pc* and *Ps*.

### **3.2.3 Absorbed Photosynthetically Active Radiation (APAR)**

We used a one-dimensional multi-layer radiative transfer model (a module of Canopy Conductance Constrained Carbon Assimilation model, 4C-A; Sch  fer et al. 2003, Kim et al. 2008) to estimate canopy APAR. Details of the computation scheme are presented in Kim et al. (2011). Briefly, the model estimates light absorption and vertical distribution integrating essential elements of three models: Campbell and Norman (1998), Nilson (1999), and Stenberg (1998). Clumping of foliage into crowns (i.e. tree

clumping) and shoot-level clumping are incorporated in the computation of the proportion of sunlit area on horizontal surface at each sun angle. The transfer of direct, diffuse and scattered radiation is estimated sequentially along 1-m layers downward through the canopy. The light absorbed by each layer is determined by taking the difference between two adjacent layers and integrating over all layers to estimate total canopy APAR.

Because some model inputs, e.g., branch surface area, were not directly measured we performed a sensitivity analysis of the effects of changes in those parameters on the simulated diffuse non-intercepted radiation (DIFN) under each canopy. We compared the simulated DIFN to measurements at each site (DIFN from LAI-2000 in NC, and indirect site factor, ISF, in SE from hemispherical photographs analyzed with HemiView software, Delta-T Devices Ltd., UK). The final radiative transfer simulations were based on adjusting branch surface area such that simulated and measured DIFN were within  $< 2\%$  and branch surface area was within 5% of estimates based on measurements and literature data.

We estimated APAR for the active growing season delineated by the first day after daily mean temperature exceeded  $+5\text{ }^{\circ}\text{C}$  for five consecutive days until it dropped below  $+5\text{ }^{\circ}\text{C}$  for five consecutive days (Table 3.1; Mäkelä et al. 2006). We used 3-year average temperature measured at the NC and SE sites, and modeled climate data for BC (ClimateBC/WNA; Center for Forest Conservation and Genetics).

We used theoretical maximum photosynthetically active radiation ( $PAR_{max}$ ) as the incident radiation in our comparative analyses. Half-hourly  $PAR_{max}$  was calculated from solar zenith angle (Campbell and Norman 1998). We estimated the direct and diffuse components of incoming radiation as described by Liu and Jordan (1960). We then estimated APAR for direct and diffuse PAR separately for clear days, while all incoming radiation was assumed to be  $PAR_{Diffuse}$  on overcast days. To anchor the theoretical results in reality, we estimated daily sky conditions over an average year based on eight-year (2002-2009) measured PAR data from representative sites in both NC and SE. The number of cloudy days was similar at the two sites ( $p > 0.1$  in each of five non-overlapping intra-annual periods). Therefore, all analyses in this study were based on a single annual sequence based on the statistics of clear and overcast days during the eight years, with 48% of days designated as clear.

### **3.2.4 Cost-benefit analysis of light absorption/crown carbon investment**

To link comparisons to canopy carbon balance (i.e. photosynthesis versus respiration) as opposed to comparisons of APAR alone, we employed a simplified cost-benefit analysis to compare the performance of each species in the exotic environment, relative to its native conditions and to the native species. As the starting point, we consider the crown of each species in the hypothetical stand (Figure 3.1a; star) with canopy structure as defined in Table 3.1. We tracked growth for one year, based on mean diameter increment, along the self-thinning line (Figure 3.1a; Relative Stand

Density (RSD) = 1.00 line). Mean diameter increment for *Pt*, *Pc* and *Ps* was 0.56, 0.50 and 0.23 cm y<sup>-1</sup>, respectively ( $CV < 5\%$ , McCarthy et al. unpublished, Amponsah et al. 2005, Lim et al. in review), moving the hypothetical stands accordingly up the line. We estimated foliage and branch biomass using allometric equations described earlier, and the diameter before and after the growing season. We defined an index of performance efficiency (modified from Onoda et al. 2014) of a species as the *benefit*, in terms of growing season light absorption (APAR<sub>GS</sub>) per *cost*, in terms of annual carbon invested in building and maintaining the existing crown structure (C<sub>T</sub>). In other words, the light-capturing efficiency (LCE, MJ gC<sup>-1</sup>), during the growing season, can be expressed as

$$\text{LCE} = \frac{\text{APAR}_{\text{GS}}}{C_{\text{T}}} \quad (3.1)$$

The denominator, similar to capital accumulation in economics, was the sum of production (C<sub>P</sub>), construction (C<sub>C</sub>), and maintenance (C<sub>M</sub>) costs. Because plant respiration depends on climates and may acclimate to the new environment when plants are moved to an exotic location (Atkin and Tjoelker 2003, Smith and Dukes 2013), we bounded the value of C<sub>M</sub> by assuming un-acclimated respiration (based on the same parameters at the exotic site as the species has in its native environment) versus fully acclimated respiration (based on the parameters of the native species) in all species. (see Supplementary data Appendix 1 for details).

### 3.3 Results

Daily  $\text{PAR}_{\text{max}}$  was greater in NC than in SE with decreasing difference between the two locations towards the peak of growing season when days were much longer in SE (Figure 3.1b). Daily and diurnal radiation profiles of BC (Figure 3.1b; dotted lines) were situated between those of NC and SE. In their native latitudes,  $P_t$  received approximately 79% higher total growing season  $\text{PAR}_{\text{max}}$  than  $P_s$  due to the longer growing season period in NC. The  $P_c$  canopy in BC received only 14% more PAR compared to that on  $P_s$  canopy in SE. At summer solstice (DOY 173), day length (i.e. the number of hours when  $\text{PAR}_{\text{max}} > 0$ ) was ~5 hours shorter in NC but the total daily  $\text{PAR}_{\text{max}}$  was 3% greater than in SE (Figure 3.1b, inset). The day length was 1 hour shorter in BC than in SE with similar (<1% difference) total daily  $\text{PAR}_{\text{max}}$  at the two sites.

The canopy characteristics used to parameterize the 1-D radiative transfer model for estimating APAR in total and at each canopy layer is illustrated in Figure 3.2. APAR increased only 1-2% when dead branches were considered, so their surface area was neglected. Crown parameters including CF and NAD (Figure 3.2c-d) of each species were kept static during the entire growing season, while  $L$  was allowed to vary according to the observed dynamics in the native location (Figure 3.3a).

To illustrate the effects of solar angle (or latitude) on light absorption during the course of a growing season, we calculated spatial (depth into canopy) and temporal (daily) differences of APAR of each species in the exotic versus native site (Figure 3.3).

The simulations combined effects from  $PAR_{Direct}$  and  $PAR_{Diffuse}$  by incorporating the statistics of sky conditions over the year in the representations of the incident PAR. Growing season period of the exotic site for each species is denoted by solid lines and that of the native site by dashed lines. The vertical distribution of the sum of all canopy surfaces (from Figure 3.2a-b) are shown for context (Figure 3.3b,e,h).

When *Pt* was moved from NC to SE, it absorbed more light at the top, especially during the mid-growing season, but absorption was reduced in the lower third of the canopy throughout the growing season (Figure 3.3c; between solid lines). The effect of decreasing light absorption toward the bottom of *Pt* canopy in SE became more pronounced when the growing season was extended to match that of NC (Figure 3.3c; between dashed lines). The *Pc* canopy in SE also absorbed more light in its upper crown, but experienced only a slight decrease of APAR at the bottom canopy, compared to its native site in BC (Figure 3.3f). This effect may be slightly altered by the small difference in growing season lengths between SE and BC (Figure 3.3f; compare solid and dashed lines, respectively). As seen in the differences between the growing season length of the exotic location (represented by solid lines in Figure 3.3i) and that of the growing season length of the native location (dashed lines), if *Ps* was planted in NC, it would intercept less light at high sun angles, compared to in its native conditions in SE, but absorbed more light with decreasing solar angle. However, because the NC growing season is much longer than SE's, the average effect on daily cumulative APAR is small.

Even if tree crowns absorb more light in total, shaded leaves in the canopy may not be able to photosynthesize enough to maintain a positive carbon gain. We analyzed the illumination conditions of live branches down the canopy of each species relative to that in the native environment (normalized by number of growing season days) to assess the conditions of its lowest branches. The following analyses were based on the relative changes of daily APAR during the growing season (GS) of a species in its exotic versus native sites defined as

$$R_{\text{Daily,GS}} = \frac{\sum_{\text{GS,Exotic}} \text{APAR}_{\text{Exotic}} / N_{\text{Exotic}}}{\sum_{\text{GS,Native}} \text{APAR}_{\text{Native}} / N_{\text{Native}}} \quad (3.2)$$

where  $N$  represents the number of days during the growing season period of the exotic or native sites.

We performed the analyses of direct and diffuse radiation on clear and on cloudy days separately to identify the most distinct gradients of light down the canopy. We found that on cloudy days,  $Pt$  and  $Ps$  absorb a similar amount of light in the upper crown in both environments, but that  $Pt$  absorbs less in the lower canopy (Figure 3.3d,j; gray lines). On clear days (~half of all days), the top crown half of  $Pt$  in SE intercepted more (2 - 14%) light, leaving the bottom half crown in shade (up to 30% reduction), relative to its native site in NC (Figure 3.3d; blue line). In contrast, the top crown half of  $Ps$  in NC absorbed less light (8 - 14%) than in SE, intercepting slightly more light (1 - 2%)

in the bottom half of the crown (Figure 3.3j; blue line). Relative to its performance in BC, *Pc* in SE absorbed more light (1 - 14%) in the upper crown, causing essentially no reduction of light absorption lower in its canopy (Figure 3.3g).

On a daily basis, *Pt* canopy in SE acquired up to 7% greater light at the top half crown; whereas, the bottom half crown experienced up to 19% reduction in daily light absorption compared to its native settings (Figure 3.4a). The opposite trend was observed in *Ps* with up to 6% reduction of APAR at the top half crown and ~1% increase at the lower crown. The increases of daily growing season APAR of *Pc* in SE were persistent throughout the crown with maximum increase of 11% at the top and less than 1% reduction at the bottom crown. We assumed that a species in an exotic site requires at any level of its canopy at least the same amount of mean growing season daily APAR as the bottom layer of its canopy receives in its native habitat. Based on our analysis, the lowest branch of *Pt* crown, in its native conditions, needs at least  $0.94 \text{ mol m}^{-2} \text{ day}^{-1}$  of mean growing season daily APAR to survive. Similarly, *Pc* and *Ps* must maintain a minimum APAR of  $0.75$  and  $0.35 \text{ mol m}^{-2} \text{ day}^{-1}$  in the lowest branch during the growing seasons of their native sites. We found that *Pt* crown in SE reached the required minimum APAR at ~58% crown depth, leaving the lower crown in too shaded condition (Figure 3.4b) whereas the entire length of the *Pc* crown met the minimum APAR of its native BC latitude. The bottom branches of *Ps* crown in NC yielded 78% higher APAR than the minimum requirement.

Could *Pt* and *Ps* adjust to the exotic environments by decreasing or increasing their  $L$  (and thus leaf biomass of individuals), while remaining at the same position on the size-density relations? To investigate this, we pooled foliage-biomass-to-DBH relation from six studies of various stand conditions (e.g., age, soil type and nutrient availability) of *Pt* in the Piedmont region including NC (Van Lear et al. 1986, Ter-Mikaelian and Korzukhin 1997, Naidu et al. 1998, Rubilar et al. 2005, McCarthy et al. unpublished), and four studies of *Ps* stands in Sweden (Albrektson et al. 1984, Marklund 1988, Ulvcrona 2011, Lim et al. in review) and generated a general relation for each species bounded by two standard errors (Figure 3.4c,d; lines and bars). Our hypothetical stands fall near or on this narrow statistical range. However, for its lowest branch to maintain the average daily APAR as in NC, *Pt* growing in SE would have to lose 35% of its leaf area placing it well below the bound for the species (Figure 3.4c). In contrast, to fully take advantage of the higher light availability in NC, *Ps* would need to increase its leaf area by 52% for its lowest branch to reach the same average daily APAR as it does in SE, placing it well above the bound for the species (Figure 3.4d).

Because stand density, at a given  $L$ , affects APAR by clumping foliage in crowns within the canopy, fully occupied stands straddling the self-thinning line can experience large changes in APAR as stand density decreases. Moreover, these stand- and tree-scale changes may interact with solar angle, producing different APAR responses to latitude depending on the position of stands on the self-thinning line. Our analysis shows that,

indeed, APAR increases with stand density (Figure 3.5), suggesting that as density decrease from self-thinning with age, so does APAR, especially for *Ps* in SE. The increase in total growing season APAR between locations was primarily the result of a longer growing season (Figure 3.1b). Nevertheless, at northern latitudes, for stands along the maximum size-density relation, growing season APAR becomes similar for all species as stand density increases above 900 ha<sup>-1</sup> (compare dashed and dotted lines versus solid lines).

We assessed the performance of each exotic species relative to the native counterpart by comparing the light-capturing efficiency (LCE; Appendix 1) that serves as a proxy for carbon balance of each canopy. We made comparisons based on ratios between LCEs of exotic and native species ( $LCE_{\text{Exotic}} / LCE_{\text{Native}}$ ). Annual cost estimates for the crown of each species under native and exotic conditions are shown in Figure 3.6b (see Supplementary data Table A3.6.1 for the components of the carbon cost). In general, total costs are sensitive to environmental conditions, increasing southward (Figure 3.6b; compare black- to gray-shaded bars). The assumptions on  $C_M$  acclimation can generate up to ~38% difference in the annual cost. Nevertheless,  $C_T$  varied little in the native sites from ~300 (*Ps*) to ~400 g m<sup>-2</sup> yr<sup>-1</sup> (*Pt* and *Pc*) in all three species. Because of the narrow  $C_T$  range, the LCE of exotic relative to native species (Figure 3.6c) was mostly a reflection of the ratio of their APAR (Figure 3.6a). On average between the two regimes of acclimation, relative to *Ps* in SE, 20 and 26% higher canopy APAR and 14 and 24%

higher  $C_T$  of *Pt* and *Pc*, respectively, combined to a slightly higher LCE of *Pt* relative to the native *Ps*, and a similar LCE in *Pc* and *Ps*. In contrast, 26% lower canopy APAR of *Ps* than *Pt* in NC, yet similar  $C_T$ , resulted in a similarly lower LCE than the native *Pt*.

Lastly, we investigated the potential reason for why *Pc* is growing faster than *Ps* in SE in a more management-relevant RSD regime (C1 to C4 in Figure 3.1a). We found that moving between two management boundaries of RSD of 0.30 and 0.45 from two post-thinning positions (1320 and 660 trees ha<sup>-1</sup>) as trees increase in size, and  $L$  increases from 1.0 to 2.0, *Pc* absorbs more light down the canopy than it does in its native environment (Figure 3.7a), and more light than is required to keep its lower branch as illuminated as in its native BC (Figure 3.7b). The mean growing season daily APAR of *Pc* increased relative to that of *Ps* with tree size, as trees grew from 6 to 9 cm of DBH in the high density conditions (C1 to C2) and from 9 to 13 cm in a lower density condition (C3 to C4), averaging ~50% higher daily APAR across the 4 positions (Figure 3.7c).

### **3.4 Discussion**

We investigated the physiological and ecological consequences of virtual and actual introduction of a pine species into an exotic latitude considering *only* its crown structural attributes through their effects on absorbed PAR. Clumping of trees in stands and crown dimensions affect APAR and its vertical distribution, frustrating comparisons among stands of different structure. However, in contrast to expectations of decreasing slopes with latitude (Enquist and Niklas 2001), the three species we analyzed shared a

similar size-density relation (Figure 3.1a) despite large differences in their native environments (Figure 3.1b; Table 3.1). This allowed selecting a stand of similar density and mean tree size for the analyses of all species and locations (Table 3.1). The effect on canopy APAR of variation of shoot structural parameters (e.g., vertical profiles) diminish with increasing  $L$  and stand density (Kim et al 2011). While our two stands on poor sites, as are vast areas of pine-dominated forests, support low canopy leaf area (Vose et al. 1994), we also repeated the analysis of vertical changes of APAR in canopies with twice the  $L$  ( $L = 4 \text{ m}^2 \text{ m}^{-2}$ ), quite high for these species (Bréda 2003). We found only slightly less pronounced changes of the vertical APAR differences between exotic and native species (1 - 5% in  $Pt$ , <1% in  $Pc$  and 2 - 5% in  $Ps$ ). Over a wide range of stand density (adjusting tree size according to the self-thinning line in Figure 3.1a), APAR increases somewhat with density, yet the effect on APAR of moving to an exotic latitude is conserved (Figure 3.5). In the northernmost latitude and, at fixed  $L$  of 2, total canopy APAR reaches a similar value for all three species at a density of  $\sim 1000 \text{ trees ha}^{-1}$ . More management-relevant size-density positions are discussed later, as we use the approach to assess the better performance of  $Pc$  in SE relative to the native  $Ps$ .

The vertical profiles of surface area of the aboveground components were similar among the species (Figure 3.2a-b). Thus, the main variables affecting light absorption are the shoot-scale characteristics, the grouping of foliage (CF) and needle inclination (NAD) (Niinemets and Kull 1995, Stenberg 1998, Th  r  zien et al. 2007). Grouping of leaves

decreases APAR at fixed  $L$ ; and high clumping at the canopy top (i.e. small value of CF) allows more light penetration through the canopy, increasing APAR of less clumped lower leaves. The pattern of CF, leading to a more even APAR through the canopy (Oker-Blom et al. 1989, Stenberg et al. 2001), was apparent in all species in our data, but clumping was higher in the two more northern species  $P_s$  and  $P_c$  (Figure 3.2c) which also tended to have more vertically angled foliage than  $P_t$  (Figure 3.2d). This may reflect a necessary adaptation to the low solar incidence angles dominating northern latitudes (e.g. Sprugel 1989). The tendency of  $P_c$  to have slightly greater leaf clumping than  $P_s$  at the top of the canopy, and more horizontal distribution of needles at the bottom facilitate both better distribution and greater absorption of light, which should lead to greater canopy photosynthesis (Stenberg 1998, Bergh et al. 2005) and less unabsorbed light reaching the forest floor. In contrast, in  $P_t$  stands with the least clumped leaves and more horizontally oriented needles, light quickly diminishes with distance from the canopy top. In shallow canopies and at high solar angles of the native range of  $P_t$ , this appears to be an effective way to capture incoming light.

Ultimately, photosynthetic rate depends on the amount and distribution of light on leaf surfaces. In highly clumped leaves, much of the leaf surface of each shoot may be shaded, and the mean light on needle surfaces would decrease as the angle of leaves relative to the sun deviates from the perpendicular. With such architecture, PAR distribution in the canopy is more efficient, avoiding too high energy load which may

lead to photoinhibition on the surface of leaves at the canopy top (Björkman et al. 1988, Gamon and Pearcy 1989), while extending favorable conditions at the canopy base (Stenberg 1998). Furthermore, greater shoot-level clumping decreases the fraction of gap area within the shoot envelope (i.e. shoot transmission coefficient) and, thus, the light transfer through the shoot and the frequency of penumbra (occurrence of 'partial shade'; Stenberg 1998, Thérézien et al. 2007). Although all three species shared a similar vertical pattern of the light transmission coefficient (not shown), indicating increasing penumbral effect with depth in the canopy, this effect would be greater in the *Pt* canopy throughout. The penumbral phenomenon does not affect the mean light at any given depth or light absorption by the canopy but evens out the distribution of direct light on leaves such that the rate of canopy photosynthesis per unit  $L$  is higher (Horn 1971, Miller and Norman 1971, Palmroth et al. 1999). Taken together, *Ps* and *Pc* crown architecture facilitates a more even distribution of APAR down the canopy than the architecture of *Pt* and, between the northern species, *Pc* crowns should absorb more light. In contrast, *Pt* crown architecture may result in a higher APAR and photosynthesis, at a given amount of incident PAR.

We estimated APAR of our hypothetical stand (Table 3.1) over an average year, in the exotic and native latitudes. To allow assessing the effect of latitude-induced changes in incident PAR on APAR without the confounding effects of uncertain changes in leaf area, the  $L$  dynamics in the exotic latitude were kept the same as in the native

latitude (Figure 3.3a). Moving north, *Pt* absorbed more light in the upper canopy during growing-season clear days, and only slightly less in cloudy days, at the expense of the lower canopy and subcanopy (Figure 3.3c). The average daily pattern during the growing season (Figure 3.3d) shows a maximum effect of northward placement would subject the bottom branches of *Pt* canopy to ~10% - 35% lower APAR than in NC. Conversely, *Ps* absorbed less light on clear days at the top of the canopy and more light at the bottom upon southward placement (Figure 3.3i). On average across sky conditions, the bottom of *Ps* in NC would receive more light than in SE (Figure 3.3j). The different shoot characteristics of these two species might not serve them well when one is subjected to solar angles prevailing in the latitude of the other (Figure 3.4a). In case of *Pc*, however, the average daily pattern during the growing season (Figure 3.3g) shows that a slight northward placement would subject the bottom branches of *Pc* canopy to a similar APAR to what it is accustomed to in BC, suggesting a comfortable relocation (Figure 3.4a).

We estimated an average daily APAR for each species using the native and exotic growing season length (a mean by layer of the results in Figure 3.3c,f,i). We then normalized the vertical pattern of each species by the mean growing season APAR of its lowest crown layer in the native latitude (Figure 3.4b), and found that, although *Ps* would absorb relatively less light in the exotic relative to its native latitude at the top of the canopy (Figure 3.4a), APAR along its entire canopy should be sufficiently high to

support the crown in NC. The pattern for *Pc* in SE is similar, with only the bottom of the crown reaching the estimated APAR in BC. For *Pt*, in contrast, a large section of its crown would receive lower mean daily APAR over the growing season in the exotic latitude relative to NC (Figure 3.4b). Adjusting leaf area to match the APAR conditions at the bottom of the canopy in their native latitude would require each species to either move off the maximum size-density line, or to adjust allometry well outside the bound for the species (Figure 3.4c-d). We therefore conclude that the crown characteristics of these two species are not suitable for the exotic latitude to which we subjected them, consistent with **H1** and **H2**. On the other hand, *Pc* latitudinal change was relatively small, it absorbs more light than *Ps*, perhaps contributing to the greater stemwood production observed when *Pc* is planted in SE, consistent with **H3**.

Greater light absorption may come at a greater cost of carbon investment in the crown, reducing the efficiency with which APAR is converted to stemwood. Our analysis showed that this is not the case (Figure 3.6). Annual cost of various components was similar among the species (see Table A3.6.1; inconsistent with alternative hypotheses), with the greatest difference seen in maintenance respiration depending on whether it was estimated as acclimated or not. Overall, LCE of *Pt* was greater than that of *Ps* in SE, and the converse occurred when *Ps* was compared to *Pt* in NC (Figure 3.6c). Most importantly, however, is the finding that LCE of *Pc* was not higher than that of *Ps* in SE, meaning that the greater APAR of *Pc* was not discounted by a greater carbon cost.

Differences in growing season APAR of a species between exotic and native latitudes may be because of both differences in the length of growing season and interaction between crown architecture and solar angle. Our results suggest that the differences seen between latitudes (values in black in Figure 3.8a-c) are dominated by growing season length, and are essentially eliminated when the same period is prescribed in the native and exotic latitudes (values in blue). The ~20% differences observed between exotic and native species placed at the same latitude are the product of interaction between their crown characteristics and solar angle (values in black Fig. 8d-f). Nevertheless, 20% greater APAR is not likely to explain the observed > 30% greater growth of *Pc* than *Ps* stands (Elfving and Norgren 1993). Other factors may allow *Pc* to grow faster than *Ps*, including higher nitrogen use efficiency, leaf area ratio and specific leaf area (Norgren 1995). Furthermore, a recent study showed that soil biota in Sweden contributes to increased productivity of *Pc* compared to its origin in BC (Gundale et al. 2014).

Yet, the 20% greater APAR estimated for *Pc* stand situated on the maximum size-density line (RSD = 1.0) is not representative of managed stands where the greater growth of this species is observed. When we compared APAR of *Pc* and *Ps* bracketing common management regimes of pines (Figure 3.1a; dashed lines directly obtained from Harrington 2001), a clear advantage emerged for having a *Pc* crown structure: sufficient

light was available throughout the canopy, and APAR was sufficiently higher to explain the observed growth differences between the species (Figure 3.7a-c).

A crown architecture that does not allow light to reach lower branches would also affect the light reaching subcanopy species in the new environments. To illustrate this, we compare the effects of exotic species replacing a native one on growing season APAR in the canopy (APAR<sub>c</sub>) and below-canopy non-intercepted PAR (Figure 3.8d-f). In SE, *Pt* and *Pc* absorbed 26 and 20% more light than *Ps*, but halving the light reaching the understory (consistent with **H1** and **H3**), while, in NC, *Ps* absorbed 74% of that absorbed by *Pt*, and more than doubling the light supply below the canopy (**H2**).

Understory vegetation is an important component of boreal forests (Nilsson and Wardle 2005), affecting tree regeneration, decomposition and nutrient cycling, and thus forest productivity (e.g. Wardle et al. 1997, Turetsky 2003). The ~40% reduction of PAR reaching the understory of *Pc* stands in SE should have noticeable consequences to understory composition. Indeed, the understory of *Pc* in SE was found to have a smaller species pool, with fewer shade-intolerant species (Engelmark et al. 2001, Nilsson et al. 2008).

In contrast, a much higher light supply to understory vegetation under *Ps* than the native *Pt* canopy in NC (Figure 3.8d), would promote understory growth and competition for soil resources with the canopy species (Canham 1988, McGuire et al. 2001). Indeed, plantations of *Pinus echinata* (shortleaf pine), a southeastern US pine

species with similar needle and shoot characteristics to *Ps* (Lawson 1990, Th  r  zien et al. 2007) require careful control of competing understory to maintain acceptable growth rates (Grano 1970, Shelton and Murphy 1991). In areas within the overlapping ranges of *Pt* and *P. echinata*, *Pt* outperformed the local *Ps*-analog (Chandler et al. 1943, Meade 1951, Williston 1972). Furthermore, where both species share a stand, *Pt* annual height increment was ~40% greater, quickly overtopping *P. echinata* during the stand establishment phase (Cain 1990), suggesting a similar fate awaits *Ps* in such latitudes.

### ***3.5 Concluding remarks***

Our theoretical analyses show that, rather than large difference in cost, crown architecture interact with solar angle to result in growing season light absorption and vertical distribution that may limit the ability of certain pine species to succeed in single species stands in northern or southern latitudes in the northern hemisphere. Crown characteristics that permit light penetration deeper through the canopy and support moderate understory component in northern latitude would allow greater amount of light through the canopy in temperate regions, and thus the development of highly competitive understory, including regeneration of fast growing tree species. Crown characteristics as those of fast growing temperate species such as *P. taeda*, promote high rate of absorption while relying on stronger penumbral effect to increase light use efficiency (Long et al. 2006), and would not allow sufficient light to lower branches. Such

characteristics may limit poleward movement of certain species as the climate becomes more suitable for their biology (Woodward 1987, Hughes 2000, McCarty 2001).

In contrast, a more efficient light absorption by the exotic *P. contorta* canopy can indeed lead to a greater fiber production than the native *P. sylvestris*. We note that there are variations of crown characteristics within each species, presenting an opportunity to match characteristics to latitude, thus increasing APAR and growth (Emhart et al. 2007, Laforest-Lapointe et al. 2014). However, whether APAR in the canopy increases as a result of planting exotic instead of a native species, or selecting a native genotype of similar characteristics, the increase of canopy APAR is at the expense of the understory. Because *Pc* can readily regenerate in SE (Engelmark et al. 2001), the potential changes of understory composition and diversity should be considered in the context of increased stemwood production.

**Table 3.1: Site and stand information.** Values for the actual stands represent measurements in 2003 for *P. taeda* and in 2011 for *P. sylvestris*. Values for the hypothetical stand were calculated based on allometric relationships, assuming mean tree size as indicated on the self-thinning line (Figure 3.1a; star). See Materials and Methods for details of calculations. *H* – mean canopy height; *qDBH* – quadratic mean diameter at 1.3 m; *SD* – stand density; *RSD* – relative stand density; *L* – mean growing season leaf area index; *S* – mean growing season plant surface area index; *GS* – growing season.

Variables	Actual Stand		Hypothetical Stand		
	<i>P. taeda</i> (NC)	<i>P. sylvestris</i> (SE)	<i>P.taeda</i>	<i>P. contorta</i>	<i>P. sylvestris</i>
Location	36°20'N 79°28'W	64°10'N 19°45'E	36°N 79°W	58°N 125°W	64°N 19°E
Elevation (m asl)	212	145			
Age (year)	38	~90		-	
<i>H</i> (m)	23	19	19	19	20
<i>qDBH</i> (cm)	36	18		29	
<i>SD</i> (trees ha <sup>-1</sup> )	308	1017		660	
<i>RSD</i>	0.68	0.69		1	
<i>L</i> (m <sup>2</sup> m <sup>-2</sup> )	1.60	2.02		2.00	
<i>S</i> (m <sup>2</sup> m <sup>-2</sup> )	2.90	2.30	2.80	2.70	2.40
Native GS period			Mar 16- Dec 6	Apr 20 – Oct 11	May 1 – Sep 30
Number of GS days		-	266	175	153

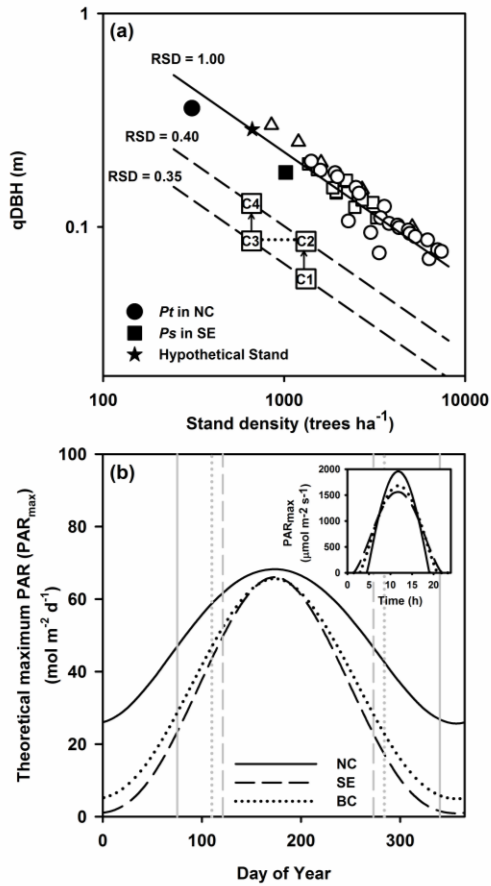


**Figure 3.1: Settings. (a) Size-density line.** The relationship between average tree size, expressed as quadratic mean diameter at breast height (qDBH), versus stand density. Open symbols show published or measured data of *P. taeda* in Piedmont region in USA (circles), *P. sylvestris* near Rosinedal, Sweden (squares) and *P. contorta* in British Columbia, Canada (triangles) used to generate the relation. Closed symbols refer to the study sites of *P. taeda* in North Carolina (closed circle) and *P. sylvestris* in Rosinedal (closed square). The hypothetical stand (star) used in all analyses of this study is also shown. Two dashed lines represent the optimum regime for operational thinning at RSD between 0.30 and 0.45. C1 – C4 denote the silvicultural conditions for the comparative analysis between *P. contorta* and *P. sylvestris* in Sweden. See Discussion for details. **(b) Theoretical maximum photosynthetically active radiation, PAR<sub>max</sub>.** Daily patterns of calculated PAR<sub>max</sub> used in the analyses in North Carolina, Rosinedal and British Columbia. Inset shows diurnal pattern of PAR<sub>max</sub> on the summer solstice (DOY 173).

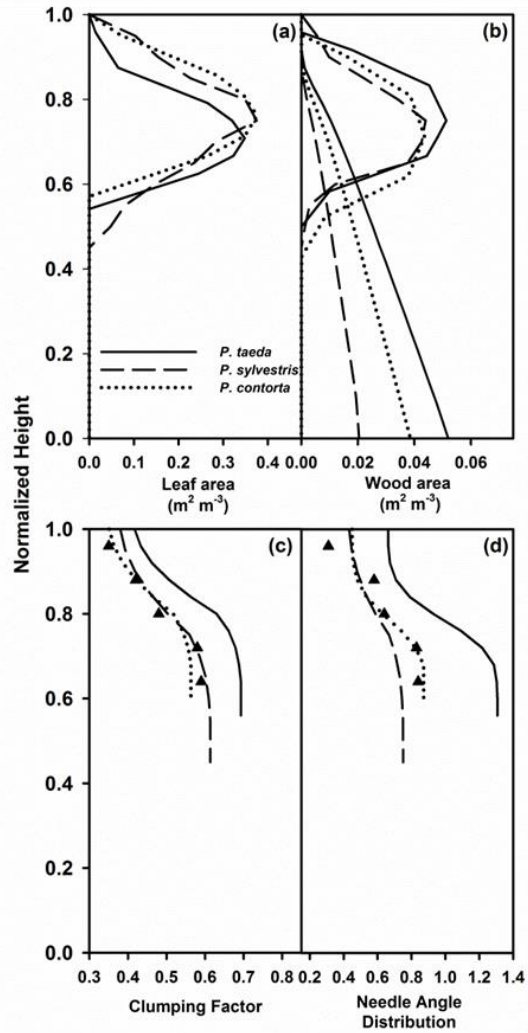


**Figure 3.2: Canopy structures.** Vertical profiles of canopy attributes as input parameters for the radiation attenuation model. The structural properties were generated from field measurements. **(a) - (b)** Plant surface area profile (the leaf area profile is during the summer solstice). Wood surface area includes that of branches and stem. **(c) - (d)** Shoot characteristic profiles. Measured shoot parameters for *Pc* are shown as triangles (see Materials and Methods). Pictorial presentations of pine shoots illustrate foliage arrangement corresponding to the ranges of each shoot characteristic.

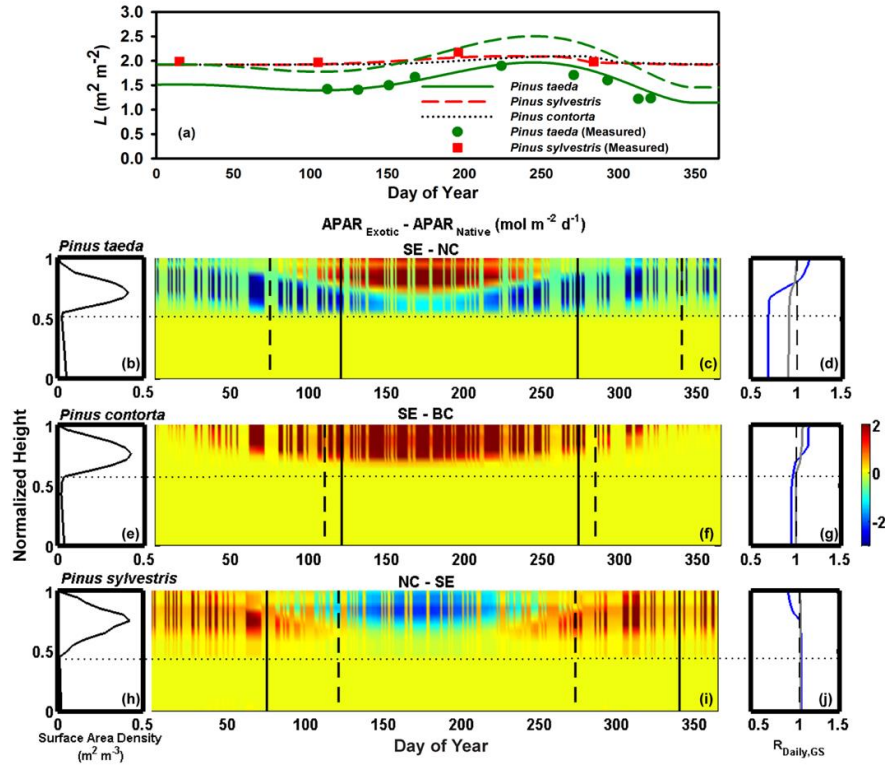


**Figure 3.3: Daily growing season average absorbed photosynthetically active radiation, APAR, profiles. (a) Projected leaf area index ( $L$ ) dynamics of each species during the year. Symbols represent field measurements from the actual sites of *Pt* and *Pc* (see Materials and Methods). The  $L$  dynamic of *Pc* was assumed to be similar to that of *Ps*, adjusted for the different growing season in the native site. **Green dashed line represents projected  $L$  of the hypothetical stand of *Pt* in the analyses.** (b), (e), and (h) Vertical profiles of plant (foliage+branch+stem) surface area density in the three pine canopies. (c), (f), and (i) Absolute difference of daily APAR between exotic and native latitude, of each species. Solid lines represent the start and the end of growing season period in the exotic location while those of the native location are denoted by dashed lines. (d), (g), and (j) Relative changes of daily growing season average APAR ( $R_{\text{Daily,GS}}$ ) calculated from equation (2). The  $R_{\text{Daily,GS}}$  values are shown separately for clear (blue lines) and cloudy (gray lines) days. Horizontal dotted lines delineate the base of the canopy.**

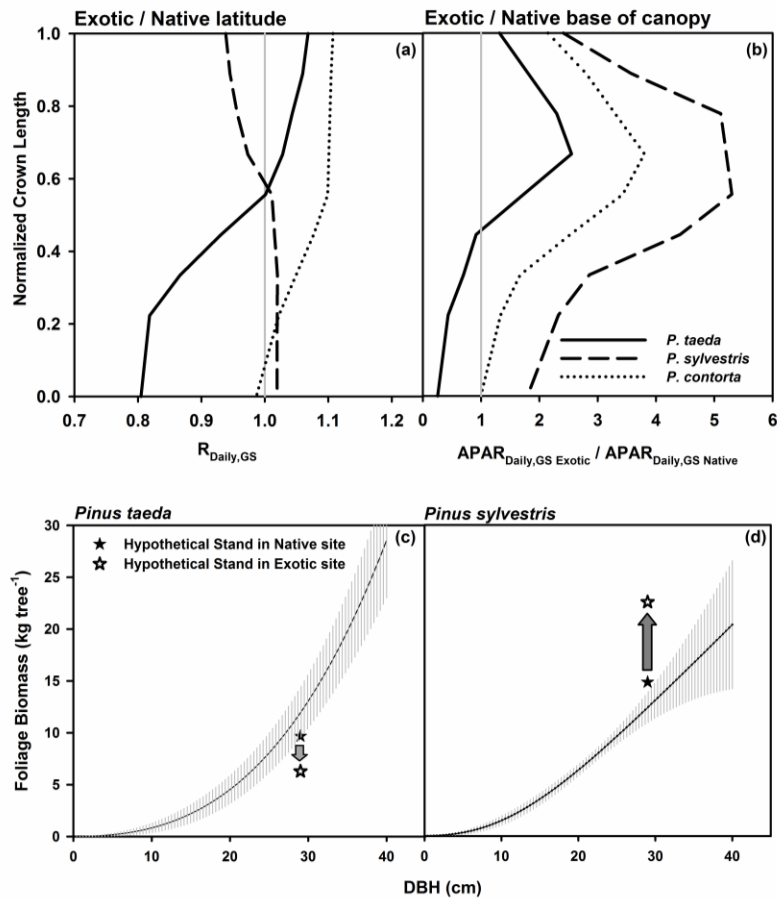


**Figure 3.4: Comparisons of vertical light distribution within crown** (a) Vertical distribution of daily growing season average absorbed photosynthetically active radiation, APAR for each species in an exotic relative to its native latitude. The results are based on representative PAR derived from theoretical PAR with varying sky conditions. Gray lines indicate no change of the daily growing season average APAR ( $R_{\text{Daily,GS}}$ ) in the exotic compared to its native latitude. (b) Vertical distribution of APAR of each species in its exotic location relative to the minimum APAR required by the bottom branches at the native site. (c) – (d) Literature-based allometric relations between foliage biomass and diameter at 1.3 m (DBH), the position of the average tree of the hypothetical *P. taeda* and *P. sylvestris* stands in their native latitude, and the requisite change of foliage biomass necessary to generate a similar APAR for bottom branches in the exotic latitude as in the native latitude.

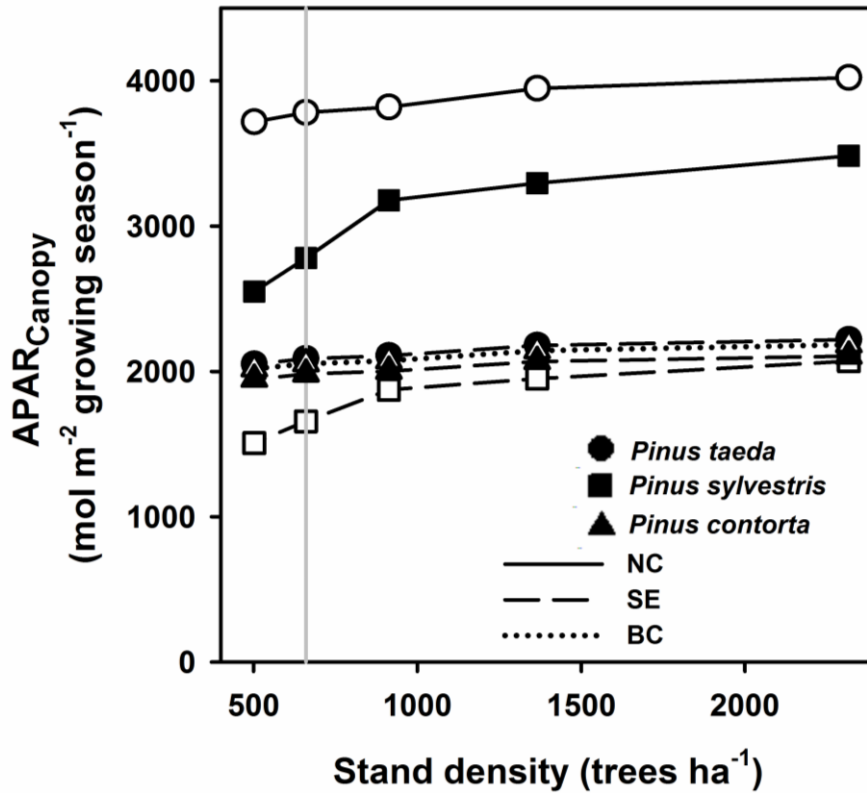


**Figure 3.5: Total absorbed photosynthetically active radiation (APAR) in the crown.** Simulated growing season sums of total crown absorption based on theoretical PAR incorporating representative sky conditions (see Materials and Methods for details) along a range of stand density. Open symbols show values of the species in their native sites whereas closed symbols represent those in the corresponding exotic latitude. The vertical gray line indicates values of the hypothetical stand (see Table 3.1).

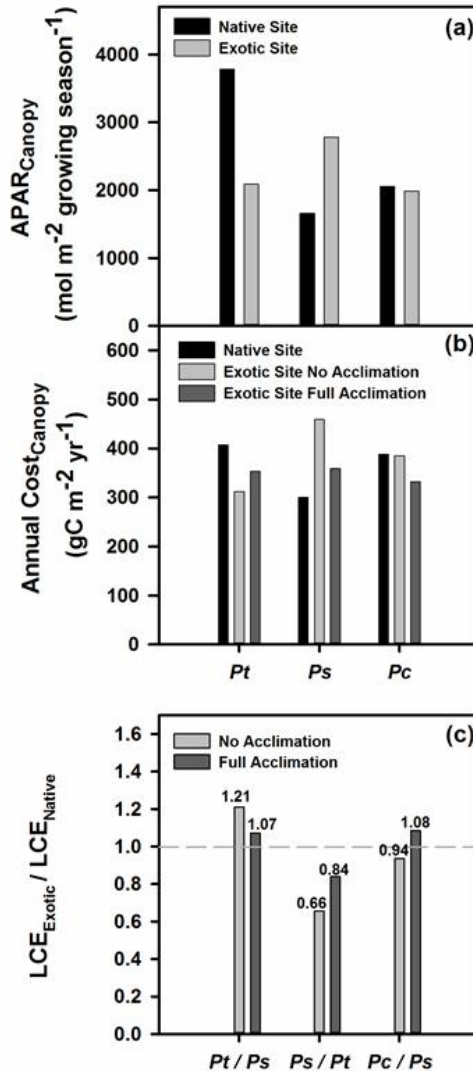


**Figure 3.6: Comparison of light-capturing efficiency (LCE) and its components between exotic and native species at a given latitude. (a)** Absorbed photosynthetically active radiation in the canopy,  $APAR_{Canopy}$ , during the growing season for each species in the native and exotic latitudes. **(b)** Annual carbon cost of maintaining the canopy light capturing capacity in the native latitude and in the exotic latitude, the latter assuming no acclimation or full acclimation of maintenance respiration. **(c)** LCE of exotic relative to native species assuming either no maintenance respiration acclimation or full acclimation of the exotic canopies.

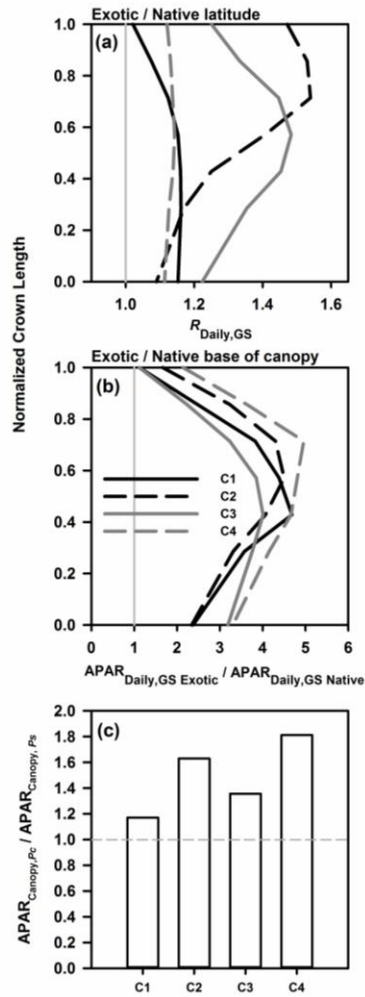


**Figure 3.7: Comparison of *P. contorta* and *P. sylvestris* in Sweden in silvicultural context. (a) – (b) show the same ratios as in Figure 3.4a-b but for the smaller trees corresponding to the silvicultural treatment scenario C1 – C4 (see text for details). (c) Relative growing season total absorption of *P. contorta* to *P. sylvestris* in Sweden under each scenario.**

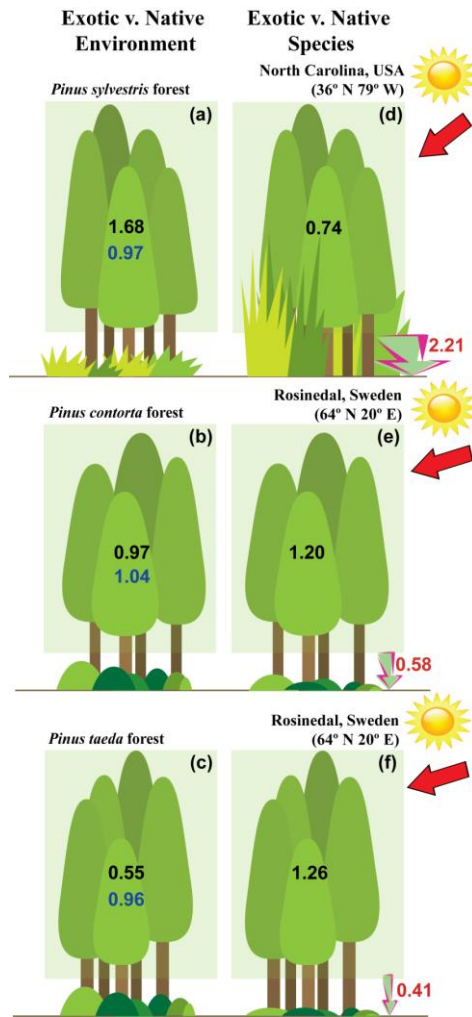


**Figure 3.8: Summary of findings.** (a) – (c) Comparison of total crown absorption by each species in the exotic versus native latitude. Ratios are the amount of APAR in the canopy at the exotic latitude normalized by that at the native latitude. Ratios in black are calculated from the respective growing season days in each location (i.e. taking into account the difference in growing season length between the two locations). Ratios in blue are computed from the growing season days of the exotic site. (d) – (f) Comparison of total crown absorption in each latitude of exotic versus native species. Ratios are the amount of APAR in the canopy of the exotic species normalized by that at the native species. Ratios in red are for non-intercepted PAR that will be available for the understory in stands of the exotic versus native species.

## 3.6 Appendix

### 3.6.1 Calculation of total carbon cost in the crown for estimating light-capturing efficiency (LCE)

Total carbon investment in the crown ( $C_T$ ) is the combination of production ( $C_P$ ), construction ( $C_C$ ), and maintenance ( $C_M$ ) costs; all fluxes are given in  $\text{gC m}^{-2} \text{yr}^{-1}$ .

Production cost,  $C_P$ , is the annual amount of carbon invested in foliage and branch biomass. It was calculated as the change in biomass between the current and previous years plus replacement of biomass lost during the same period. Both foliage and branches have costs associated with annual replacement, estimated differently. The production cost for foliage ( $C_{Pf(t)}$ ) was calculated as

$$C_{Pf(t)} = \Delta W_{f(t)} + \frac{W_{f(t-1)}}{\tau} \quad (\text{A3.1})$$

where  $\Delta W_f$  is the annual increment of foliage standing biomass ( $\text{gC m}^{-2}$ ), and  $t$  is the current year. The parameter  $\tau$  (year) was needle longevity differing among species (4.5 for  $Pc$ , Amponsah et al. 2005; 3.5 for  $Ps$ , Pensa and Jalkanen 2005; 1.5 for  $Pt$ , McCarthy et al. 2007).

Production cost for branches ( $C_{Pb}$ ) was determined by

$$C_{Pb(t)} = \Delta W_{b(t)} + b\Delta H_{c(t)} \quad (\text{A3.2})$$

where  $\Delta W_{b(t)}$  is the annual increment of live branch standing biomass,  $b$  is the rate of  $W_b$  replacement in the bottom canopy as the crown moved upward ( $\text{gC m}^{-3}$ ) and  $\Delta H_{c(t)}$  ( $\text{m y}^{-1}$ ) is the annual crown base height increase as trees grow taller. We calculated  $b$  from harvest data of branch dry weight at the bottom layer from the nearby site of *Pt* and the site of *Ps* (McCarythy et al. unpublished; Lim et al. in review) and assumed the same value as *Pt* for *Pc* because of similar mean diameter increment. We used carbon content of 0.524 and 0.507 for *Ps*'s branches and foliage (Lim et al. in review) and of 0.48 for both components of *Pt* (McCarthy et al. 2010). The carbon fraction of *Pc*'s crown biomass components was assumed 0.475 (Magnussen and Reed 2004). Combining both components of the crown, we get

$$C_{P(t)} = C_{Pf(t)} + C_{Pb(t)} \quad (\text{A3.3})$$

Construction cost,  $C_c$ , is carbon used in the support of synthesizing new foliage and branches. This cost was estimated as a constant fraction of  $C_{P(t)}$  (Ryan 1991a):

$$C_{C(t)} = 0.25C_{P(t)} \quad (\text{A3.4})$$

Maintenance cost,  $C_M$ , is carbon cost of protein synthesis, replacement and repair in plant cells (Penning de Vries 1975) of the crown elements in this study. This cost component depends on tissue temperature and its  $N$  concentration (Amthor 1984, Ryan 1991b, Ryan et al. 1994). For each species, we obtained, from published studies, the

instantaneous maintenance respiration rates, based on surface area for foliage or sapwood volume for woody tissues, at a reference temperature measured during low activity period and the associated  $Q_{10}$  values ( $Q_{10}$  which is the rate change with a 10 °C change in temperature; Ryan et al. 1995, Ryan 1995, Maier et al. 2004, Kolari et al. 2009). Then, we scaled the instantaneous rates to the annual maintenance costs of foliage ( $C_{Mf}$ ) and branches ( $C_{Mb}$ ) based on temperature distribution measured in the actual sites for NC and SE and obtained from the modeled climate data for BC. Finally, the total annual maintenance cost was calculated as

$$C_{M(t)} = C_{Mf(t)} + C_{Mb(t)} \quad (A3.5)$$

**Table A3.6.1: Components of cost estimates of the crown.** Values, in  $\text{gC m}^{-2} \text{y}^{-1}$ , are estimates of carbon costs for branch and foliage that were used to determine light-capturing efficiency (LCE; see 3.2 Materials and Methods).  $C_P$ ,  $C_C$  and  $C_M$  represent costs associated with carbon production, construction and maintenance of the materials.  $C_{M,\text{Native}}$  and  $C_{M,\text{Exotic}}$  are the maintenance cost of the species under native and exotic environments, respectively. The maintenance costs of each species in the exotic conditions are listed separately under two extremes of acclimation. Accordingly, the comparisons of annual costs between exotic and native species are presented as the ratios,  $\text{Cost}_{\text{Exotic}} / \text{Cost}_{\text{Native}}$ , under each acclimation regime.

<b>Species</b>	$C_P$	$C_C$	$C_M,$ Native	$C_{M, \text{Exotic}}$ (No Acclimation)	$C_{M,\text{Exotic}}$ (Full Acclimation)	$\text{Cost}_{\text{Exotic}} /$ $\text{Cost}_{\text{Native}}$ (No Acclimation)	$\text{Cost}_{\text{Exotic}} /$ $\text{Cost}_{\text{Native}}$ (Full Acclimation)
<i>Pt</i>	199	50	158	63	104	1.04	1.18
<i>Ps</i>	157	37	106	265	165	1.13	0.88
<i>Pc</i>	181	46	161	158	105	1.28	1.11

## **4. Daily transpiration of forests is controlled spatially by variation of canopy leaf area and soil texture and temporally by variation in atmospheric and soil humidity: Synthesis of new and published results**

### ***4.1 Introduction***

Forests, the dominant terrestrial carbon sinks (*e.g.*, Fan *et al.*, 1998; Rayner *et al.*, 1999), play a major role in biosphere-atmosphere exchange of water and energy (Bonan, 2008). In a forest ecosystem, canopy transpiration, the largest component of evapotranspiration (Roberts *et al.*, 1980; Calder, 1998), exerts great influence on the earth's surface energy balance, affecting mesoscale circulation, weather patterns, and water supply to downstream systems (Avisar *et al.*, 1985; Andre *et al.*, 1989; Oishi *et al.*, 2010). Most ecological models predicting biosphere-atmosphere exchanges of energy, carbon and water, are driven by variations in both atmospheric and soil conditions and the responses of vegetation to these variations (*e.g.*, De Kauwe *et al.*, 2013; Zaehle *et al.*, 2014). These models consider physiological processes, such as stomatal responses to soil moisture and atmospheric demand, and stand properties such as canopy leaf area, for predicting transpiration and photosynthesis (*e.g.*, Woodward *et al.*, 1995; Kowalczyk *et al.*, 2006; Oleson *et al.*, 2010). Therefore, it is not surprising that the inter-annual variation in canopy transpiration is coupled to ecosystem productivity (Stoy *et al.*, 2006).

Different considerations apply when analyzing transpiration at different spatial and temporal scales. In forests where stomata are well coupled to the atmosphere, transpiration of a leaf can be described empirically as a multiplicative set of responses reducing stomatal conductance from a maximum under favorable conditions, as light, and atmospheric and soil humidity decrease, and temperature fluctuates relative to the optimal (Jarvis, 1976; Pataki & Oren, 2003). At a daily timescale, such variation of leaf-scale stomatal conductance, and therefore transpiration, correlates well with changes of vapor pressure deficit and soil moisture during the growing season (Granier *et al.*, 2000a). This is because, during the growing season, daily stomatal conductance is not sensitive to air temperature over a relatively broad range of temperatures (Landsberg, 1986). Upscaling leaf transpiration to the canopy requires accounting for the effect of leaf area index ( $L$ ). Increasing transpiring leaf surface area decreases mean light intensity on the leaf surfaces and thus mean canopy stomatal conductance (*e.g.*, Tor-ngern *et al.*, 2015). As the reduction in mean canopy stomatal conductance is typically not proportional to the increase in  $L$ , one expects that, generally, total canopy stomatal conductance would increase with  $L$  (Kelliher *et al.*, 1995; Granier *et al.*, 2000a). Thus, in forests where the canopy is well coupled to the atmosphere (*e.g.*, Ewers & Oren, 2000; Kim *et al.*, 2014), canopy transpiration should potentially increase with  $L$ .

Despite the strong general relations between environment, physiology, and water use, canopy transpiration depends on other factors, such as location (latitude and altitude) affecting available energy (Alo & Wang, 2008; Matyssek *et al.*, 2009), precipitation and soil texture affecting soil moisture availability (Hacke *et al.*, 2000; Xu *et al.*, 2011) and species composition affecting the response to environmental drivers (Pataki & Oren, 2003; Ford *et al.*, 2011). Within a species, mean canopy stomatal conductance is conservative across a moisture gradient, and the adjustments to differences in water availability are manifested in changes in tree-scale hydraulic properties and stand-scale  $L$  (Addington *et al.*, 2006). However, where stands on poor, sandy soils are irrigated and/or fertilized, hydraulic adjustments may alter the relations between canopy transpiration and  $L$  (Ewers *et al.* 2000; Lai *et al.* 2002). Thus, only if  $L$  is shown to dominate canopy transpiration in forests, an emerging relationship of forest transpiration and  $L$  will provide a useful tool for modelling ecological processes, and assessing long-term responses to environmental changes (Betts *et al.*, 1997; Tor-ngern *et al.*, 2015).

In the forest hydrologic cycle, incoming precipitation is coarsely partitioned into evapotranspiration, outflow and additions to soil water storage. Thus, the quantity of water used as evapotranspiration influences the amount of precipitation, and ultimately contributes to groundwater and to downstream ecosystems and users. Because canopy

transpiration is the major component of evapotranspiration, the inter-annual variation of evapotranspiration reflects the sensitivity of canopy transpiration to weather changes, and thus may differ among forests types at a given location. For instance, annual evapotranspiration of a loblolly pine plantation may be more sensitive to changes in precipitation, while such sensitivity was not observed at a nearby hardwood stand (Phillips & Oren, 2001; Schäfer *et al.*, 2002; Stoy *et al.*, 2006; Oishi *et al.*, 2010). Depending on the sensitivity of evapotranspiration to environmental and climatic changes, variation of precipitation may govern outflow from forests (Oishi *et al.*, 2010), with further implication for projected climate change impacts on water cycling, such as predicted increases in annual mean precipitation in high-latitudinal regions and decreases in some mid-latitudinal and subtropical dry regions (Collins *et al.*, 2013).

Forests dominated by the genus *Pinus* are found over a wide range of environments, from the Arctic Circle with cold winters and short growing seasons to the tropics with year-round growing season (Knight *et al.*, 1994). They also include stands on soils ranging from nutrient rich to sandy, poor soils (Knight, 1991; Knight *et al.*, 1994). These forests differ in many characteristics involving leaf phenology, leaf morphology and canopy structure, which affect canopy conductance and transpiration (Roberts, 2000). Because of their extent and commercial importance, many studies have quantified sap flux in pine forests, making them ideal for evaluating how well the variation of  $L$

among these very different forests reflects their capacity to transpire. Here, we initially estimated canopy transpiration of two of the most dominant pine species worldwide with large geographical ranges: a mid-latitude *Pinus taeda* (L.) (North Carolina, USA) and a high-latitude *Pinus sylvestris* (L.) (Northern Sweden), both growing on sandy soil. The latter species included two levels of nutrient availability and three levels of developmental stage-related *L*. We used these data to determine **(1)** whether the maximum daily growing season canopy transpiration is primarily related to *L*, with the remaining variations related to soil and atmospheric humidity. We then explored **(2)** whether the patterns from **(1)** identified in these contrasting stands are consistent with those obtained from published studies on forests of various species, soil textures and locations. **(3)** Based on canopy transpiration estimates and water balance calculations from our mature stands and other published studies, we assessed the sensitivity of forest hydrologic components, including evapotranspiration and outflow, to growing season and annual precipitation.

## ***4.2 Materials and Methods***

Definitions of all abbreviation and variables in the following sections are presented in Table 4.1.

### 4.2.1 Settings

The study was conducted in pine forests of contrasting size, nutrient availability and climate zones (for detailed stand characteristics see Supporting Information Table A4.6.1). The mature *Pinus taeda* L. plantation (PT) in North Carolina, USA (36° 20'N 79° 28'W) was established in 1965, thinned in 1983, and harvested in 2006. The broadleaf understory was sparse, comprising 2% of stand basal area (Uebelherr, 2008). The soil was well-drained sand with average bulk density and porosity (in the top 60 cm) of 1500 kg m<sup>-3</sup> and 0.43, respectively. Long-term (111-year) average annual temperature and total precipitation were 15.8 °C and 1145 mm (McCarthy *et al.*, 2007).

The old *Pinus sylvestris* L. (PS) forests in Rosinedal, Sweden (64° 10'N, 19° 45'E) were regenerated with seed trees in 1920 – 1925, pre-commercially thinned in 1955 and thinned in 1976 and 1993, respectively. These forests have been used for long-term fertilization experiment with control (PS<sub>MC</sub>) and fertilized (PS<sub>MF</sub>) stands located ~2 km apart. Fertilizer of 100 kg N ha<sup>-1</sup> yr<sup>-1</sup> was applied to PS<sub>MF</sub> from 2006 to 2011 and a reduced rate of 50 kg N ha<sup>-1</sup> yr<sup>-1</sup> has been used afterwards (Lim *et al.*, in review). The *P. sylvestris* regenerating forest (PS<sub>Y</sub>) was in Åheden (~7 km from Rosinedal). The understory of both stands is characterized by a field layer of dwarf shrubs, (*Vaccinium myrtillus* and *V. vitis-idaea*), and a ground layer of mosses (*Pleurozium schreberi* and *Hylocomium splendens*) and lichens (*Cladonia spp.*) (Hasselquist *et al.*, 2012; Palmroth *et al.*,

2014). These forests share similar soil texture of well-drained, deep sandy sediment with 2 – 5 cm soil organic layer (Mellander *et al.*, 2005) and bulk density and porosity (in the top 10 cm) of 1230 kg m<sup>-3</sup> (Giesler *et al.*, 1996) and 0.49 (Lundmark & Jansson, 2009). The 30-year mean annual temperature and precipitation (1981 – 2010), measured at the Svartberget field station (8 km from PSMC and 1 km from PSV) were 1.8 °C and 614 mm, respectively (Laudon *et al.*, 2013). On average, the area is covered by snow from late October to early May.

#### **4.2.2 Environmental measurements**

A summary of instrumentation for environmental measurements in the four sites is presented in Table A4.6.2. Other assumptions associated with the presented measurements in Table A4.6.2 and additional measurements are briefly discussed as follows.

In Sweden, air temperature ( $T_A$ , °C) and relative humidity (RH, %) were measured below the forest canopies (Table A4.6.2). Nevertheless, these data were used to represent above-canopy measurements because there is a strong coupling between the canopy and the atmosphere and small gradient of vapor pressure deficit ( $D$ ) throughout the canopy depth in forests with low  $L$  (Ewers & Oren, 2000). In PSV, the global radiation was measured and converted to photosynthetic photon flux density (PPFD) using a factor of 0.47 (Papaioannou *et al.*, 1993).

In PS<sub>MC</sub> and PS<sub>MF</sub>, two sets of soil moisture probes were used for measurements at different periods. To obtain the soil moisture at 15 cm depth ( $\theta_{15}$ , m<sup>3</sup> m<sup>-3</sup>) at the plot level, we employed the relationship between the long- (near tower) and short- (around sap-flux trees) term data (see Table A4.6.2) during June - September 2013 ( $r^2 \geq 0.85$ ) to adjust values from the continuous, long-term measurement. In PS<sub>Y</sub>, we used soil moisture data from PS<sub>MC</sub> to estimate values during the unmeasured period in PS<sub>Y</sub> ( $r^2 = 0.72$ ,  $p < 0.001$  for relationship between daily mean  $\theta_{15}$  of both sites).

At all sites, the growing season was delineated beginning the day after daily mean temperature exceeded +5 °C for five consecutive days, and lasted until it dropped below +5 °C for five consecutive days (Mäkelä *et al.*, 2006). The average growing season period during three study years was approximately March - November in PT and May-September in the PS sites. To facilitate the cross-site comparison, soil moisture was represented by Relative Extractable Water (REW) calculated according to (Granier *et al.*, 2000a):

$$\text{REW} = \frac{\theta - \theta_m}{\theta_{FC} - \theta_m} \quad (4.1)$$

where  $\theta_m$  is minimum volumetric soil moisture and  $\theta_{FC}$  is soil moisture at field capacity with average value of  $0.15 \pm 0.02$  m<sup>3</sup> m<sup>-3</sup> among our study sites. Vapor pressure deficit ( $D$ ) was calculated from  $T_A$  and RH (Abtew & Melesse, 2013). Daylength-

normalized  $D$  ( $D_z$ ) was calculated as  $D_D \times (\frac{n_d}{24})$  where  $D_D$  was daytime mean  $D$  and  $n_d$  was number of daylight hours (Phillips & Oren, 2001).

### 4.2.3 Estimation of sapwood area and leaf area index

In PT, sapwood area ( $A_s$ , m<sup>2</sup>) was estimated from stem discs taken at breast height from the trees harvested in 2006. Leaf area index ( $L$ ; projected-area based) and its dynamics were derived from monthly measurement. A correction factor of 0.59 (Th  r  zien *et al.*, 2007) was applied to  $L$  to account for foliage clumping (Stenberg, 1996).

In Sweden,  $A_s$  and  $L$  were estimated using allometric equations. For  $PS_{MC}$  and  $PS_{MF}$ , maximum  $L$  was estimated based on annual foliage production derived from trees harvested in October 2011, six each in, and litterfall (Lim *et al.*, in review). For  $PS_Y$ ,  $A_s$  and maximum  $L$  were estimated based on allometric equations derived from eight trees harvested in September 2013 (P. Tor-ngern & L. Tarvainen, *unpublished*). For all stands, the  $L$  dynamics was obtained from a study of *P. sylvestris* stands of similar site characteristics (Rautiainen *et al.*, 2011).

### 4.2.4 Sap flux measurements and scaling to the canopies

In the *P. taeda* stand (PT), sap flux density ( $J_s$ , g<sub>H2O</sub> m<sup>-2</sup> sapwood s<sup>-1</sup>) was measured at breast height in 24 trees with thermal dissipation probes, converting voltage-difference output to sap flux after Granier (1987). Radial (Ford *et al.*, 2004; Oishi *et al.*, 2008) and

azimuthal (Lu *et al.*, 2000; James *et al.*, 2002; Tateishi *et al.*, 2008) variations of  $J_s$  may, however, produce considerable errors when scaling up from tree measurement to stand. To capture such variations, seventy-two sensors were distributed in the north, southeast and southwest sides of stems and at five 20-mm interval depths from the inner bark (*i.e.*, 0 - 20 mm, 20 - 40 mm, 40 - 60 mm, 60 - 80 mm and 80 - 100 mm), operating from May 2003 to August 2005.

In Sweden, the similar Granier-type sensors were installed at breast height on six mature *P. sylvestris* trees each in PS<sub>MC</sub> and PS<sub>MF</sub>. In each site, we distributed 14 sensors at four depths and four azimuthal directions (north, south, east and west), measuring  $J_s$  from July 2011. Additionally, we incorporated  $J_s$  measurements from other experiments in PS<sub>MC</sub> and PS<sub>MF</sub>. In one experiment, from August to September 2011, eight sensors were installed at the outer 20-mm sapwood layer of eight trees in each site. In another short-term experiment, from August to September 2012, fifteen sensors were distributed among five trees in PS<sub>MF</sub> to measure  $J_s$  at three sapwood depths. Excluding the treatment days in these other experiments, we combined  $J_s$  data of the outermost layers from the additional experiments by performing a weighted average. Therefore, we used a total of 22 and 37 sensors to estimate canopy-average sap flux density for PS<sub>MC</sub> and PS<sub>MF</sub>, respectively. Similarly, twenty sensors were distributed among 12 *P. sylvestris* trees at PS<sub>Y</sub>. The sensors were installed at either one or two sapwood depths at breast height and

data were collected from June 2012 to June 2014. In all sites, half-hourly average data were recorded on the same type of data logger (CR1000, Campbell Scientific, Logan, UT, USA).

To calculate daily canopy transpiration ( $E_{CD}$ , mm d<sup>-1</sup>), we employed the following approach to scale the point-measurement of  $J_s$  to the entire forest. Daily sum  $J_s$  ( $J_{SD}$ , g<sub>H<sub>2</sub>O</sub> cm<sup>-2</sup><sub>sapwood</sub> d<sup>-1</sup>) was considered in the analysis to avoid issues related to tree water storage and measurement errors (Phillips & Oren, 1998). The daily sum sap flux density ( $J_{SD}$ ) in the outer 20-mm xylem ( $J_{SD,Out}$ ) was scaled to a mean daily sap flux density over the entire xylem area ( $\bar{J}_{SD}$ ). For all sites, there was no significant variation of  $J_{SD,Out}$  with tree size ( $p \geq 0.10$ ,  $r^2 \leq 0.16$ ,  $n \geq 12$ ) nor circumferentially ( $p \geq 0.46$ ). However, the radial variation of  $J_{SD}$  was significant ( $p \leq 0.0001$ ) and independent of azimuth ( $p \geq 0.31$ ). We developed a scaling function to account for the radial variation of  $J_{SD}$  to allow simple gapfilling of missing values, after finding that using the average ratios of measured inner-to-outer  $J_{SD}$  generated only < 2% difference of  $\bar{J}_{SD}$  compared to using a continuous function. Within the studied species, we observed maximum  $J_{SD}$  within 10 - 30 mm xylem depth, decreasing non-linearly towards the stem center (Čermák *et al.*, 1992; Ford *et al.*, 2004; Oishi *et al.*, 2008). Therefore, for each canopy, we generated a scaling function, describing the decline of  $J_{SD}$  beyond a critical xylem depth ( $c$ ) by a Gaussian function, as

$$\frac{J_{SD,i}}{J_{SD,Out}} = 1 \quad ; X_R \leq c$$

$$\frac{J_{SD,i}}{J_{SD,Out}} = 1 \times e^{-0.5 \left( \frac{X_R - 1}{\beta} \right)^2} \quad ; X_R > c \quad (4.2)$$

where  $J_{SD,i}$  is  $J_{SD}$  at inner xylem depths (e.g.,  $i = 1$  at 20 - 40 mm layer),  $X_R$  is the ratio between sensor depth relative to xylem radius,  $c$  is the  $X_R$  at which  $J_{SD}$  starts decreasing with sapwood depth and  $\beta$  is the fitting parameter. We employed an average function to derive  $\bar{J}_{SD}$  of each forest for the entire study period as no daily variation of the function was observed ( $p \geq 0.3$ ; see Table A4.6.3). Sapwood thickness exceeded probe length, such that 1 - 6% of sapwood areas were not captured by the sensors in all sample trees, and thus no correction method (e.g., Clearwater *et al.*, 1999) to account for non-conductive sapwood in  $\bar{J}_{SD}$  estimation was needed.

Despite careful considerations of spatial and temporal variability in scaling procedures, we did not calibrate the  $J_s$  sensors specifically for the two pine species studied here, which may cause potential errors in the estimates of canopy transpiration (Steppe *et al.*, 2010; Sun *et al.*, 2012; Vergeynst *et al.*, 2014). Sap flux density measured with this method has, however, been examined in both species in previous studies (e.g., Ford *et al.*, 2004; Lundblad *et al.*, 2001; Oliveras & Llorens, 2001) with results in

agreement with local water balance and eddy covariance estimates (Granier *et al.*, 1996a; Schäfer *et al.*, 2002; Domec *et al.*, 2012).

Finally,  $E_{CD}$ , given the units of variables as defined in Table 4.1, was calculated as

$$E_{CD} = 10 \times \bar{J}_{SD} \frac{A_S}{A_G} \quad (4.3)$$

where  $\bar{J}_{SD}$  was calculated from the above scaling approach and  $\frac{A_S}{A_G}$  ( $\text{m}^2_{\text{sapwood}} \text{m}^{-2}_{\text{ground}}$ ) represented the total sapwood area of all trees ( $A_S$ ) per unit ground area of the stand ( $A_G$ ).

We performed a boundary line analysis (Schäfer *et al.*, 2000; Ewers *et al.*, 2001) to obtain the response of  $E_{CD}$  under the optimal conditions (Martin *et al.*, 1997). The canopy transpiration varies with  $D_z$ , PPFD and soil water availability (Jarvis, 1976; Phillips & Oren, 2001). Because  $D_z$  and PPFD were correlated in our study sites ( $r^2 \geq 0.69$ ,  $p < 0.001$ ), we focused on  $D_z$  and REW as the physiologically driving variables. First, we determined REW ranges in which  $E_{CD}$  was best explained by  $D_z$ , *i.e.*, well-watered conditions, and obtained the maximum daily canopy transpiration ( $E_{Cm}$ ). Then, for each study site, we pooled these data over the REW range in which soil moisture does not affect transpiration, and performed the boundary line analysis by binning  $E_{Cm}$  based on  $D_z$  data (see Schäfer *et al.*, 2000; Ewers *et al.*, 2001 for details). Finally,  $E_{Cm}$  was described by the function (Ewers *et al.*, 2001),

$$E_{Cm} = a(1 - e^{-bDz}) \quad (4.4)$$

where  $a$  is asymptotic  $E_{Cm}$  value at high  $Dz$  and  $b$  is the initial increasing rate of  $E_{Cm}$  with  $Dz$ . Taking into account the soil drying effect on  $E_{Cm}$ , we performed another boundary line analysis on  $E_{CD}$  values obtained from  $E_{CD}$  versus  $Dz$  curves under a range of soil moisture conditions (*i.e.*, REW), relative to the  $E_{CD}$  in wet soil (*i.e.*,  $E_{Cm}$  obtained from the response in Eq. 4).

#### 4.2.5 Hydrologic balance

We estimated hydrologic components of PT, PSMC and PSMF sites. For a growing season, the local water balance was used to estimate the residual component ( $R$ ) that was not directly measured (Schäfer *et al.*, 2002) based on the mass balance equation:

$$P = I_C + E_C + E_U + Q + \Delta S + R \quad (4.5)$$

where  $P$  is precipitation,  $I_C$  is evaporation from canopy interception,  $E_C$  is canopy transpiration,  $E_U$  is below-canopy evapotranspiration that included evaporation from soil and litter and transpiration from the understory vegetation,  $Q$  is drainage below rooting zone (2 m depth in PT; Ewers *et al.*, 2000, and 0.4 m depth in the PS sites; Mellander *et al.*, 2004) and  $\Delta S$  is the change in soil moisture storage which was measured at 0.3 m depth ( $\theta_{30}$ ) in PT and 0.15 m depth ( $\theta_{15}$ ) in the PS stands. All components are in mm per growing season. Overland flow was assumed negligible due to flat topography and high infiltration rate of the soil (*cf.* Abrahamson *et al.*, 1998).

The evaporation from canopy interception ( $I_c$ ) was calculated as the difference between  $P$  and throughfall ( $P_T$ ). To estimate growing season  $P_T$  values, a linear relationship between biweekly sum of  $P$  and  $P_T$  was developed for each site (slopes were  $0.88 \pm 0.02$  (SE) for PT and  $0.79 \pm 0.03$  for  $PS_{MC}$  and  $PS_{MF}$ ;  $r^2 \geq 0.94$ ,  $p < 0.0001$  for the relationships and  $p = 0.64$  for the difference between  $PS_{MC}$  and  $PS_{MF}$ ). The  $E_c$  was scaled from continuous  $E_{CD}$  obtained by gapfilling missing values of  $J_{SD,Out}$  (ranging 19 - 36% of total growing season days) with a function dependent on daily average PPFD and  $D_z$  (see Appendix S1 & Table A4.6.3). We computed  $E_u$  using the relationship between the non-transpiration component of evapotranspiration ( $LE - E_c$ ) and below-canopy non-intercepted PPFD on days without precipitation during the non-growing season period (Stoy *et al.*, 2006; when daily average  $T_A < 5$  °C). We calculated non-intercepted PPFD by subtracting total canopy PPFD absorption from the above-canopy incidence. Total PPFD absorption was determined using a one-dimensional radiative transfer scheme (Schäfer *et al.*, 2003; Kim *et al.*, 2011). The  $r^2$  values for the relationships were low (ranging 0.2 - 0.5 for all sites) but significant ( $p \leq 0.02$ ). Therefore, we applied these relationships to estimate  $E_u$  for the entire growing season. This quantity, representing on average 14 - 20% of  $E_T$  and 7 - 16% of  $P$  is the least certain among the hydrologic balance components of our sites. Stemflow was neglected in the analysis because of its typically small amount in coniferous forests (Delfs, 1967; Viville *et al.*, 1993; Uebelherr, 2008). Drainage ( $Q$ ) was

modeled from a plane at the bottom of rooting zones (Schäfer *et al.*, 2002; Oishi *et al.*, 2010). The model was parameterized using physical properties of sand (Clapp & Hornberger, 1978; Katul *et al.*, 1997). Root profiles were obtained from nearby sites of the same species and soil characteristics (Ewers *et al.*, 2000, Hacke *et al.*, 2000 for PT; Mellander *et al.*, 2004 for PS sites). For acceptable local water balance, the residual component ( $R$ ) should be small and the sum of all measured and estimated components should not be significantly different from  $P$  (Oren *et al.*, 1998a).

#### **4.2.6 Statistical analyses**

All regression analyses were performed in SigmaPlot version 12.0, from Systat Software, Inc., San Jose, CA USA. We used an  $F$ -test to compare fitting results on different datasets with the same function (*e.g.*, the analysis of transpiration response to vapor pressure deficit and soil drying effect of the four stands and comparisons of scaling and gapfilling functions between control and fertilized PS sites). Two-factor ANOVA with interaction term was applied to analyze the effect of radial and azimuthal variation on  $J_{SD}$ .  $T$ -test was utilized to compare means of growing season values. All computations, including calculations of variables and drainage, were conducted in MATLAB 7.6.0 R2008a (Natick, Massachusetts: The MathWorks Inc., 2008).

## 4.3 Results

### 4.3.1 Environmental conditions

PT experienced a variable inter-annual weather pattern with a wet growing season ( $P = 850$  mm) in 2003 and a relatively dry growing season (449 mm) in 2005 (Fig. 4.1d bars). The PPF<sub>D</sub> and  $D_z$  were low in 2003 compared to other years (Fig. 4.1a). Growing season REW was high in 2003 (averaged REW =  $0.56 \pm 0.08$  standard deviation (SD) or  $\sim 0.45 \pm 0.05$  m<sup>3</sup> m<sup>-3</sup> of  $\theta_{30}$ ), moderate in 2004 (averaged REW =  $0.47 \pm 0.06$  or  $\sim 0.32 \pm 0.04$  m<sup>3</sup> m<sup>-3</sup> of  $\theta_{30}$ ) and decreased to an average of  $0.32 \pm 0.14$  ( $\sim 0.22 \pm 0.04$  m<sup>3</sup> m<sup>-3</sup> of  $\theta_{30}$ ) during the 2005 growing season (Fig. 4.1d line). In contrast, growing season weather was similar among the study years in Sweden with average  $P$  and PPF<sub>D</sub> of  $400 \pm 30$  mm and  $29 \pm 2$  mol m<sup>-2</sup> d<sup>-1</sup> (Fig. 4.1e,f bars for  $P$ ; 1b,c black lines for PPF<sub>D</sub>). However,  $D_z$  was slightly lower in 2012 relative to other years (Fig. 4.1b,c gray lines). Generally, REW values were higher in PS<sub>MF</sub> (gray dashed line in Fig. 4.1e) with the seasonality similar to the other PS sites (*i.e.*, gray solid lines in Fig. 4.1e,f). Within each of the forests in Sweden, REW was of similar range in 2011 and 2012 but reached the minimum REW of 0.03-0.26 ( $\sim 0.01$ - $0.08$  m<sup>3</sup> m<sup>-3</sup>  $\theta_{15}$ ) in 2013. Therefore, these study periods cover a wide range of environmental conditions for pine forests on sandy soil.

### 4.3.2 Daily sap flux density and transpiration

In general, growing season  $J_{SD,Out}$  in mature trees was lower than in young trees (Fig. 4.2, compare solid lines). Among the mature stands, total sapwood area per unit ground area ( $A_s/A_G$ ,  $m^2 ha^{-1}$ ) of PT was lower, averaging  $17 \pm 0.23$  (SD)  $m^2 ha^{-1}$  across three growing seasons, contributing to its higher  $J_{SD,Out}$  (averaging  $72 \pm 33$   $g_{H_2O} cm^{-2} sapwood d^{-1}$ ) than those of PS sites. Comparing the two mature PS stands,  $J_{SD,Out}$  was similar ( $p = 0.39$ ) with mean growing season values of  $44 \pm 25$  and  $48 \pm 26$   $g_{H_2O} cm^{-2} sapwood d^{-1}$  for  $PS_{MC}$  and  $PS_{MF}$ , respectively. The slightly higher mean  $J_{SD,Out}$  value in  $PS_{MF}$  was due to slightly lower  $A_s/A_G$  ( $22 \pm 0.38$  versus  $25 \pm 0.09$   $m^2 ha^{-1}$  in  $PS_{MC}$ ) because of sparser canopy compared to  $PS_{MC}$  (see Table A4.6.1). Young trees in  $PS_Y$  had the lowest  $A_s/A_G$  ( $5 \pm 0.42$   $m^2 ha^{-1}$ ) and the highest  $J_{SD,Out}$  ( $98 \pm 28$   $g_{H_2O} cm^{-2} sapwood d^{-1}$ ) of all stands. As a result,  $J_{SD,Out}$  decreased linearly with  $A_s/A_G$  among the four sites ( $r^2 = 0.96$ ;  $p < 0.001$ ).

Scaled to the canopies,  $E_{CD}$  was of similar values at the mature stands, averaging  $0.94 \pm 0.71$ ,  $0.94 \pm 0.52$  and  $0.89 \pm 0.49$   $mm d^{-1}$  for PT,  $PS_{MC}$  and  $PS_{MF}$ , over three growing seasons (data not shown). For the young stand  $PS_Y$ ,  $E_{CD}$  was  $0.56 \pm 0.33$   $mm d^{-1}$ . Growing season  $L$  was higher at the mature stands than at  $PS_Y$  (Fig. 4.2, compare dashed lines). Over the three growing seasons, the mature, unfertilized  $PS_{MC}$  stand had higher  $L$  ( $2.5 \pm 0.36$   $m^2 m^{-2}$ ) than the PT stand ( $1.6 \pm 0.32$   $m^2 m^{-2}$ ; Fig. 4.2a,b dashed lines). The fertilized

stand PS<sub>MF</sub> had the highest  $L$  ( $3.1 \pm 0.32 \text{ m}^2 \text{ m}^{-2}$ ; Fig. 4.2c), while the young stand PS<sub>Y</sub> had the lowest ( $1.5 \pm 0.17 \text{ m}^2 \text{ m}^{-2}$ ; Fig. 4.2d).

### 4.3.3 Canopy transpiration in relation to atmospheric, soil and stand conditions

We found a similar response of  $E_{Cm}$  to  $Dz$  among the mature canopies of PT, PS<sub>MC</sub> and PS<sub>MF</sub> ( $p = 0.9$ ), initially increasing faster with  $Dz$  and reaching higher saturating  $E_{Cm}$  value than the young forest (Fig. 4.3a). Our  $E_{Cm}$  versus  $Dz$  responses shared similar pattern to the results from our analysis of 17 other studies on pine forests (Fig. 4.3b). We then examined the parameters regulating  $E_{Cm}$  versus  $Dz$  responses in Fig. 4.3b. In the following analyses, all linear regression was forced through the origin as there is no transpiration when leaf area is zero. First, we defined a reference  $E_{Cm}$  value at 1 kPa  $Dz$ , analogous to parameter  $a$  in the  $E_{Cm}$  versus  $Dz$  response function (Eq. 4), as  $E_{Cm-ref}$ .  $E_{Cm-ref}$  was linearly related to  $L$ , showing  $0.57 \pm 0.03$  (SE)  $\text{mm d}^{-1}$  increase of  $E_{Cm-ref}$  with a unit increase of  $L$  (Fig. 4.4a). The increasing rate was not significantly different between sandy and non-sandy soils (orange and dark red symbols, respectively, in Fig. 4a;  $p = 0.23$ ). The sensitivity of  $E_{Cm}$  to  $Dz$  (*i.e.*, the  $b$  parameter; Eq. 4.4) was linearly and similarly related to  $E_{Cm-ref}$  across soil types ( $p = 0.43$ ; Fig. 4.4b). Using the relationships in Fig. 4.4a,b, we can derive the  $E_{Cm}$  versus  $Dz$  response under non-limiting soil moisture

condition similar to those in Fig. 4.3b with only 3% bias ( $r^2 = 0.63$ ) compared to the original curves in Fig. 4.3b.

To test for the generality of this approach, we evaluated published dataset of forests of various species, locations and soil types (Table A4.6.1). Based on 45 studies across latitudes of the northern hemisphere,  $E_{Cm-ref}$  linearly increased with  $L$  similarly among forest ( $p = 0.43$ ) and soil ( $p = 0.71$ ) types (regression statistics presented in Table A4.6.4). Nevertheless, the slope of the response of  $E_{Cm-ref}$  versus  $L$  in other conifer combined with broadleaved species was 20% steeper than in the pines, and thus the separate slopes were shown for pines and other, non-pine, species (*i.e.*, Fig. 4.4c, Table A4.6.4). The same linearly increasing trend was also found for the  $b$  versus  $E_{Cm-ref}$  relationship. Again, the relationship was similar among soil types ( $p = 0.7$ ) but different for pines and non-pine species ( $p < 0.0001$  for comparison of pines and non-pine species, Fig. 4.4d).

For the soil drying effect, our new data revealed only 10% reduction of  $E_{Cm}$  as REW declined to 0.11 across the four stands ( $p = 0.8$ , Fig. 4.5a, Table A4.6.4). We found only four more conifers that included two new pine species, one broadleaved and one mixed-species stand with data needed for this analysis (see Appendix S1 & Table A4.6.5). The decrease of  $E_{Cm}$  with  $REW < 0.11$  of our sites was more abrupt than we find in other studies on sandy soils. Overall, sandy sites were less sensitive to changes in

REW than other sites until a critical threshold (ranging 0.06 – 0.39 REW for sandy soils) was reached and  $E_{Cm}$  declined more rapidly (Fig. 4.5b solid lines, representing three pine species and one other conifer from eight studies) than in non-sandy soils (REW threshold ranging 0.37 – 0.66, Fig. 4.5b dashed lines, representing seven studies). Thus, the soil drying effect on  $E_{Cm}$  was strongly controlled by soil type ( $p < 0.0001$ ; Fig. 4.5c).

Combining fitted curves from Fig. 4.4a,b and 4.5c,  $E_{CD}$  of pine forests can be estimated from  $L$ ,  $T_A$  and RH (to calculate  $D$ ), radiation (to determine day length) and soil moisture and properties such as field capacity and non-extractable soil moisture (for estimating REW). Under non-limiting soil water condition, regardless of soil type (Fig. 4.4a,b),  $E_{Cm-ref} = (0.57 \pm 0.03)L$  and  $b = (1.53 \pm 0.06)E_{Cm-ref}$ , where “ $\pm$ ” is followed by SE of the estimate. Correcting for soil drying effect (Fig. 4.5c) results in

$$\frac{E_{CD}}{E_{Cm}} = 1 - e^{-(18.59 \pm 5.33) \times REW}$$

for sandy soils. For non-sandy soils, the exponent is –

$8.09 \pm 0.98 REW$ . While these equations can be combined to calculate  $E_{CD}$ , we note, that this approach is not applicable to a particular stand but may be used for estimating the average  $E_{CD}$  of multiple pine stands over a large area after finding less bias between results estimated from the above approach and data from our combined four stands than when testing the approach separately with data from an individual stand.

#### 4.3.4 Hydrologic balance across study sites

For three sites (*i.e.*, PT, P<sub>SMC</sub> & P<sub>SMF</sub>) with data for complete hydrologic balance calculations, the residuals ( $R$ ) of the hydrologic budget were relatively small, ranging 1% to 7% of  $P$ , and were not significantly different from zero among years at a given site ( $p \geq 0.3$ , Table A4.6.6). Because growing season  $\Delta S$  was estimated from shallow soil depth while  $Q$  was calculated at a greater depth representing the root zone,  $\Delta S$  would be underestimated resulting in overestimation of  $R$ . During the growing seasons,  $E_c$  and  $E_u$  were  $50 \pm 1\%$  and  $18 \pm 2\%$  of  $E_T$ , respectively, while  $I_c$  was  $22 \pm 2\%$  of  $P$ . Overall,  $E_T$  was  $68 \pm 3\%$  of  $P$ , allowing  $\sim 30 \pm 3\%$  as  $Q$  below the rooting depth. Considering inter-annual growing season estimates,  $I_c$  was largely explained by incoming  $P$  in all sites (Fig. 4.6,  $p < 0.001$ ) whereas  $E_c$  was insensitive to variation in  $P$  over three growing seasons of each site ( $p \geq 0.71$ ). Considering the inter-annual variability within each site,  $E_T$  was less sensitive than  $Q$  to  $P$  with increases of  $E_T$  ranging from 18 to 27 mm for a 100 mm increase of  $P$ , about a third of the increases of  $Q$  ranging from 64 to 83 mm.

A synthesis of hydrologic components of forests (Table A4.6.7), representing a large gradient in growing season and annual  $P$ , suggests differences in their sensitivity to  $P$ . First, during the growing season,  $I_c$  significantly increased with the regional  $P$  (Fig. 4.7a, inverted triangles; Table A4.6.4); but became insensitive to  $P$  when considering estimates of the entire year (inverted triangles in Fig. 4.7b, dashed line not significant).

With increasing integration period to a whole year, the proportion of  $I_c$  to  $P$  decreased appreciably (from roughly 33% of  $P$  during the growing season to 17% of  $P$  annually) averaging  $172 \pm 91$  mm over a twofold range of  $P$ .

Considering the evaporative budget, evaporation from below the dominant tree canopy (*i.e.*, that from understory species, soil and litter) contributed more to  $E_T$  in regions of low growing season  $P$  (Fig. 4.7a, dark gray region). This behavior reflects decreasing canopy  $L$  with regional  $P$ , allowing more radiation to reach the understory. We found weak but significant relationship between  $L$  and annual  $P$  in the literature-based dataset ( $r^2 = 0.21$ ,  $p = 0.01$ ). However, annually, below canopy contribution to  $E_T$  was a much smaller proportion of  $E_T$  (8% *versus* 20% during the growing season; Fig. 4.7b, compare the top two regression lines), meaning that the majority of annual  $E_T$  in forests representing a wide range of  $P$  was contributed by evaporation from canopy interception and transpiration from canopy.

When growing season  $P$  was ample, excess water was readily available for drainage (Fig. 4.7a, light gray region). However, under dry conditions,  $E_T$  exceeded  $P$  and the forest depended on extraction of stored water (*e.g.*,  $P \leq \sim 370$  mm growing season<sup>-1</sup>; Fig. 4.7a, light gray diagonal shaded region). However, annually, these forests, representing a large gradient of  $P$ , utilized similar proportion of the water delivered.

Overall, water annually draining from these forests represented about a third of  $P$  ( $36 \pm 24\%$  SD).

#### **4.4 Discussion**

The data from the four pine stands on sandy soils showed that transpiration during periods in which soil moisture was not limiting ( $E_{Cm}$ ) saturated with increasing  $D_z$  at a lower value in the young ( $PS_y$ ) than in the mature stands, which was consistent with its lower  $L$  (Fig. 4.3a). However, the mature PT and PS stands transpired similarly in response to atmospheric demand, even when the nutrient availability was enhanced as in  $PS_{MF}$ . This suggests that the higher  $L$ , introduced by fertilization, decreased light intensity on leaf surfaces, reducing mean stomatal conductance (Oren *et al.*, 1986; Zimmermann *et al.*, 1988; Ewers *et al.*, 2001), thus contributing to similar canopy transpiration in  $PS_{MC}$  and  $PS_{MF}$ . Many factors, including differential sensitivities to shading among species, may contribute to the ~40% unexplained variation of  $E_{Cm-ref}$  with respect to  $L$  among pine stands (Fig. 4.4a), and to the 28% unexplained variation among stands of other species (Fig. 4.4c). Nevertheless,  $L$  explained most of the variation of  $E_{Cm-ref}$  (Fig. 4.4a) and  $E_{Cm} - D_z$  response in 12 pine species (Fig. 4.3b), regardless of various treatments including fertilization, irrigation, and elevated atmospheric  $CO_2$  concentration. The same approach also applied well to a combination of five other conifer and 15 broadleaved species (Fig. 4.4c). Increases of  $E_{Cm}$  with  $L$  were observed in

crops and an oak stand (Ritchie & Burnett, 1971; Bréda & Granier, 1996), but had not been previously shown among the diverse forest species, climates and stand conditions presented here.

Although, statistically, the sensitivity of  $E_{Cm-ref}$  to  $L$  of pines was similar to that of other species (*i.e.*, other conifer and broadleaved species), the magnitude of difference was not small, with ~20% less sensitivity to increasing  $L$  in pines than in other, non-pine species. Furthermore, the sensitivity of  $E_{Cm}$  to  $Dz$  increased linearly with  $E_{Cm-ref}$  at a higher rate for pines than other conifers combined with broadleaved species (Fig. 4.4b,d). Thus, under non-limiting soil moisture, the maximum canopy transpiration correlated well with  $L$ , regardless of latitude, stand conditions and forest type. However, faster initial increasing rate with increasing leaf area was found in pines than in other, non-pine species.

Based on a smaller number of studies with available data, we accounted for soil drying effects on the variation of daily canopy transpiration. The results demonstrated a clear difference in the response of diverse forests to soil moisture between sandy and non-sandy soils (Fig. 4.5b,c). A decline in transpiration with decreasing soil moisture beginning at a lower soil moisture (*e.g.*, on sandy soil) has been attributed to rapid water depletion of stands with shallower roots (Bréda *et al.*, 1993; Oren *et al.*, 1998b; Granier *et*

*al.*, 2007). Shallow rooting and sandy texture (even with deep rooting) represent situations of low moisture availability for plants, apparently eliciting a similar response.

The sap flux density ( $J_s$ ) of our stands decreased with increasing competition as reflected by the areal density of sapwood ( $A_s/A_G$ ) as has been shown previously (Oren *et al.*, 1998a; Zhang *et al.*, 2011). The lower maximum  $J_s$  at low competition, and faster decrease with increasing competition observed across our four sandy sites relative to those at the clayey site (Oren *et al.*, 1998a) are likely reflecting differences in both soil and plant hydraulic properties (Hacke *et al.*, 2000; Ewers *et al.*, 2000). Scaling  $J_s$  to  $E_{CD}$  estimates (0.56 – 0.94 mm d<sup>-1</sup> with  $L \sim 1.5-3.1$ ), produced values which were within the range found in other studies of pine forests on sandy soil (0.45 – 1.6 mm d<sup>-1</sup> with  $L \sim 0.8 - 3$ ; Čermák *et al.*, 1995; Loustau *et al.*, 1996; Saugier *et al.*, 1997; Ewers *et al.*, 1999; Zimmermann *et al.*, 2000; Irvine *et al.*, 2004; Mellander *et al.*, 2006). Nevertheless, many of these studies, including ours, did not calibrate the sensors specifically for the stand and site conditions in which they were employed, potentially contributing to the unexplained variation presented in Fig. 4.4 (Steppe *et al.*, 2010; Sun *et al.*, 2012; Vergeynst *et al.*, 2014). Indeed, eight of 63 values in Fig. 4.4 were estimated from heat-pulse, heat-balance or heat-ratio methods, showing  $34 \pm 27$  % greater flux ( $p = 0.24$ ) than would be expected based on a fit for the constant heat dissipation approach used by most studies.

These methodological differences and variation in plant-soil hydraulic properties (*i.e.*, by species, Wullschleger *et al.*, 1998; or via growing conditions, Margolis *et al.*, 1995; Ryan *et al.*, 2000; Novick *et al.*, 2009) contributed to variation in transpiration per unit  $L$  (Fig. 4.4c), making it rather remarkable that  $L$  was so useful explaining the variation in daily canopy transpiration.

#### **4.4.1 Sensitivity of forest hydrologic components to climate**

Within each of the three mature pine forests studied (*i.e.*, PT, PSMC, PSMF), for which data included three growing seasons, the sensitivity of growing season  $E_T$  to  $P$  was relatively weak (Fig. 4.6, Table A4.6.4), mostly because  $E_C$  was insensitive to inter-annual variation of  $P$ . Similarly weak relationships between inter-annual  $E_T$  and  $P$  have been shown before in a water balance study on a temperate broadleaved deciduous forest (Oishi *et al.*, 2010), a watershed covered with a mosaic of land-cover types, mostly broadleaved species and PT in North Carolina (Palmroth *et al.*, 2010), as well as in a boreal PS forest, and a mixed PS and *Picea abies* stand in Sweden (Berg Hasper *et al.*, in review). In our study, the growing season  $E_C$  fraction of  $E_T$  was within the range of 35 - 92% of annual  $E_T$  found in coniferous forests of various age, soil type and latitudes with  $L \sim 1 - 5.5$  (Whitehead & Kelliher, 1991; Grelle *et al.*, 1997; Schäfer *et al.*, 2002; Stoy *et al.*, 2006; Ilvesniemi *et al.*, 2010; Domec *et al.*, 2012). Below-canopy evaporation ( $E_u$ ) was similar to previous observations in low  $L$  and relatively sparse forests (up to 45% of  $E_T$ ;

Roberts *et al.*, 1982; Granier *et al.*, 1990; Whitehead & Kelliher, 1991; Domec *et al.*, 2012). The  $I_c$  fraction of  $P$  was similar to a Scots pine-dominated stand in central Sweden (20%, Grelle *et al.*, 1997) but lower than other pine forests with higher  $L$  (32% with  $L \sim 5 - 7$  Gash & Stewart, 1977; 31% with  $L \sim 4$  Benyon & Doody, 2014). Altogether, most of the inter-annual variability of  $P$  was absorbed by  $Q$ , making this the most sensitive hydrologic component to future changes in  $P$ .

Based on the new data and the synthesis with published information,  $E_T$  varied widely among forests (*e.g.*, Fig. 4.7), yet, within a given forest, inter-annual invariability of  $E_T$  with  $P$  (mostly reflecting the invariability of  $E_C$ , Fig. 4.6), could cause a drastic reduction of water flow to downstream ecosystems and users in dry years. Furthermore, when focusing on the growing season,  $E_T$  in regions of low  $P$  may consume more water than is delivered to forests, which would result in little to no water yield from these forests during that period. Nevertheless, forests were in equilibrium with the prevailing precipitation, annually returning to the atmosphere as  $E_T$  a conservative proportion of the annual precipitation.

#### ***4.5 Concluding remarks***

We showed that, based on a few variables (*i.e.*, leaf area index, air temperature, relative humidity and solar radiation), maximum daily canopy transpiration rates during the growing season can be estimated among many forests types and latitudinal

locations. The potential, maximum rates can be adjusted to actual transpiration rates if soil type and soil moisture are known. This approach facilitates the estimation of daily canopy transpiration, particularly at scales where remotely sensed data may be used to extract leaf area index (Zheng & Moskal, 2009) in combination with meteorological data. However, we note that the distribution of stands between the two soil types presented in this study was far from optimal, with potential effects on the extracted parameters. An effort to systematically assemble a worldwide sap flux data would allow further evaluation of the generality of the derived approach.

**Table 4.1: Definitions.** A summary of abbreviations and variables used in the study.

Variable	Definition	Unit
$A_s$	Sapwood area	m <sup>2</sup>
$A_G$	Ground area	m <sup>2</sup>
$A_s/A_G$	Total sapwood area per unit ground area	m <sup>2</sup> m <sup>-2</sup> or m <sup>2</sup> ha <sup>-1</sup>
$a$	Asymptotic value of the maximum daily canopy transpiration	mm d <sup>-1</sup>
$b$	The initial increasing rate of the maximum daily canopy transpiration with day-length normalized vapor pressure deficit	kPa <sup>-1</sup>
$D$	Vapor pressure deficit	kPa
$c$	The critical relative xylem depth at which sap flux density starts decreasing	-
$D_D$	Daytime average vapor pressure deficit	kPa
$D_z$	Day-length normalized vapor pressure deficit	kPa
$E_c$	Growing season or annual canopy transpiration	mm
$E_{CD}$	Daily canopy transpiration	mm d <sup>-1</sup>
$E_{Cm}$	Maximum daily canopy transpiration under non-limiting soil water condition	mm d <sup>-1</sup>
$E_{Cm-ref}$	Reference maximum daily canopy transpiration at day-length normalized vapor pressure deficit of 1 kPa	mm d <sup>-1</sup>
$E_T$	Growing season or annual evapotranspiration	mm
$E_u$	Growing season or annual evaporation from below canopy	mm
$I_c$	Growing season or annual canopy interception	mm
$J_s$	Sap flux density	g m <sup>-2</sup> s <sup>-1</sup>
$J_{SD}$	Daily sum sap flux density	g cm <sup>-2</sup> d <sup>-1</sup>
$J_{SD,i}$	Daily sum sap flux density at inner sapwood depths	g cm <sup>-2</sup> d <sup>-1</sup>
$J_{SD,Out}$	Daily sum sap flux density in the outer 20-mm xylem	g cm <sup>-2</sup> d <sup>-1</sup>
$\bar{J}_{SD}$	Mean daily sap flux density over the entire xylem area	g cm <sup>-2</sup> d <sup>-1</sup>
$L$	Leaf area index	m <sup>2</sup> m <sup>-2</sup>
$LE$	Latent heat flux	W m <sup>-2</sup>
$LE - E_c$	Non-canopy transpiration component of the evapotranspiration	mm
$na$	Number of daylight hours	-
$P$	Growing season or annual precipitation	mm
PPFD	Photosynthetic Photon Flux Density	μmol m <sup>-2</sup> s <sup>-1</sup> or mol m <sup>-2</sup> d <sup>-1</sup>
PS	Refers to all <i>Pinus sylvestris</i> sites in this study	-
PS <sub>MC</sub>	Mature <i>Pinus sylvestris</i> site in northern Sweden under non-fertilized condition	-
PS <sub>MF</sub>	Mature <i>Pinus sylvestris</i> site in northern Sweden under fertilized condition	-
PS <sub>Y</sub>	Young <i>Pinus sylvestris</i> site in northern Sweden	-
PT	<i>Pinus taeda</i> site in North Carolina, USA	-
$P_T$	Growing season or annual throughfall	mm
$Q$	Growing season or annual drainage below rooting zone	mm
$R$	Residual term of the water balance calculation (i.e., calculated as $P - I_c - E_c - E_u - Q - \Delta S$ )	mm
REW	Relative Extractable Water	-
RH	Relative humidity	%
$\Delta S$	Change in soil water storage	mm
$T_A$	Air temperature	°C
$X_R$	The ratio between sensor depth relative to sapwood radius	-
$\beta$	Fitting parameter of the Gaussian function for scaling	-
$\theta_{FC}$	Soil moisture at field capacity	m <sup>3</sup> m <sup>-3</sup>

---

$\theta_m$	Minimum volumetric soil moisture	$\text{m}^3 \text{m}^{-3}$
$\theta_{15}$	Volumetric soil moisture at 15 cm depth	$\text{m}^3 \text{m}^{-3}$
$\theta_{30}$	Volumetric soil moisture at 30 cm depth	$\text{m}^3 \text{m}^{-3}$

---

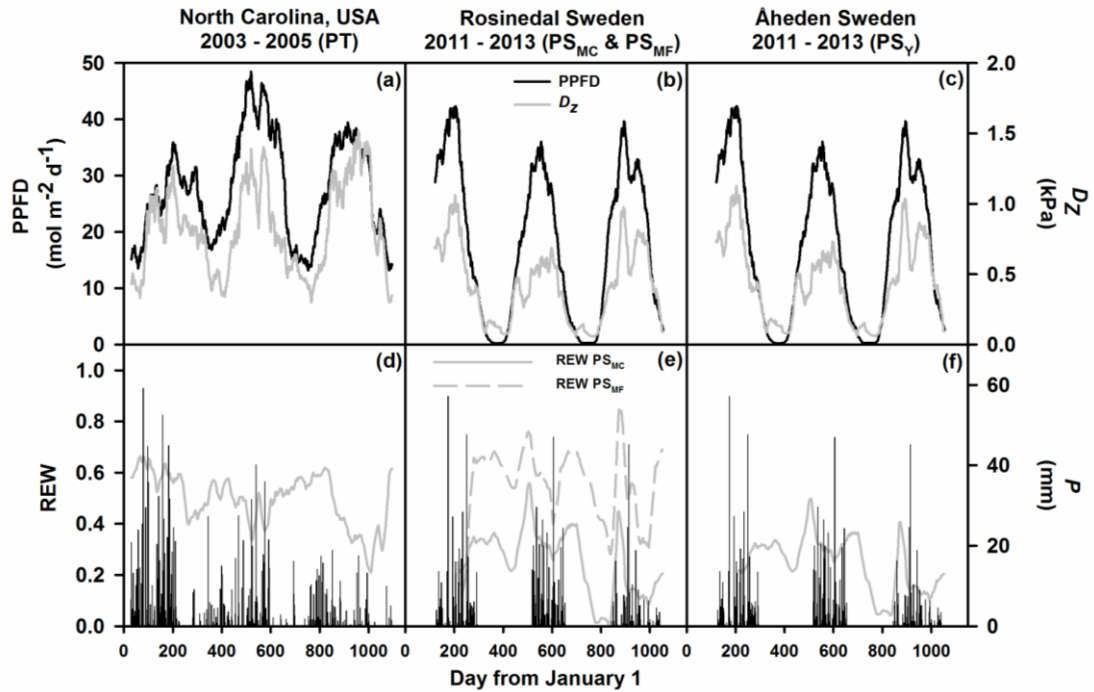


**Figure 4.1: Environmental conditions.** (a)-(c) Daily sum of photosynthetic photon flux density (PPFD, mol m<sup>-2</sup> d<sup>-1</sup>, black lines) and daylength-normalized daytime average vapor pressure deficit ( $D_z$ , kPa, gray lines) (d)-(f) Soil moisture expressed as Relative Extractable Water (REW, gray lines) and precipitation (bars). Data are presented as 30-day running mean. See Table 1 and text for explanations of each environmental variable.

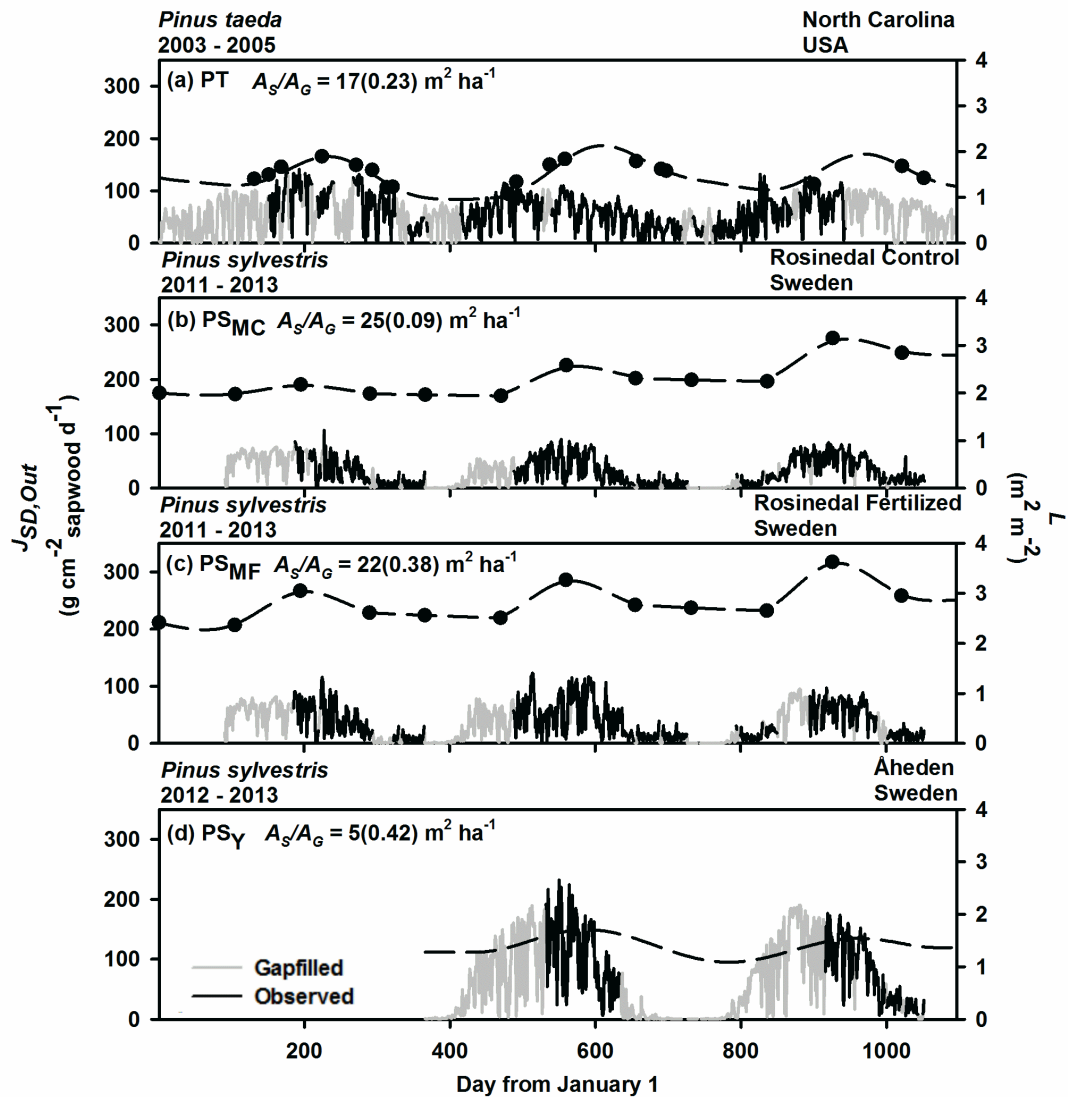


**Figure 4.2: Variables for scaling to the canopy.** For each panel, daily sum sap flux density in the outermost xylem layer (*i.e.*, at 0-20 mm depth from inner bark;  $J_{SD,Out}$  in  $\text{g cm}^{-2}\text{sapwood d}^{-1}$ ) is presented as solid lines with both measured (black lines) and estimated (gray lines) values (see text for gapfilling approach and Table A4.6.3 for gapfilling functions). Estimates of leaf area index ( $L$ ) are shown in dashed lines, together with measured values (circles). Total sapwood area per unit ground area ( $A_s/A_G$ ;  $\text{m}^2 \text{ha}^{-1}$ ) value is shown as legend in each panel.

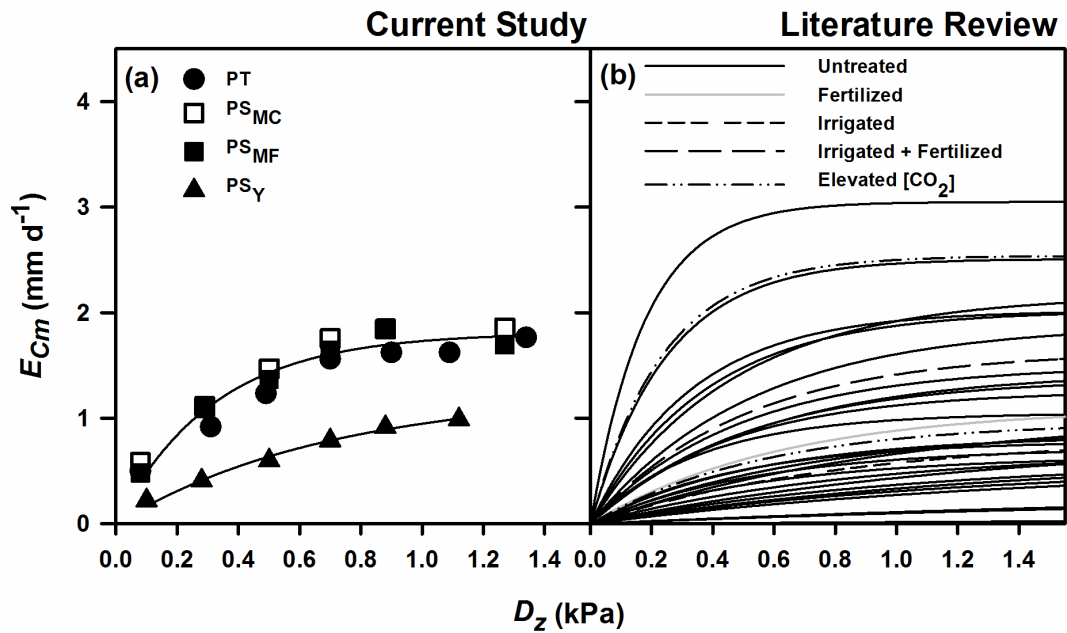


**Figure 4.3: Responses of canopy transpiration to environmental conditions. (a)** Daily canopy transpiration under non-limiting soil moisture ( $E_{cm}$ ;  $\text{mm d}^{-1}$ ) in response to daylength-normalized vapor pressure deficit ( $D_z$ ,  $\text{kPa}$ ) for the forests in this study and **(b)** from other *Pinus* forests as listed in Table S1. Regression statistics for **(a)** is presented in Table A4.6.4.

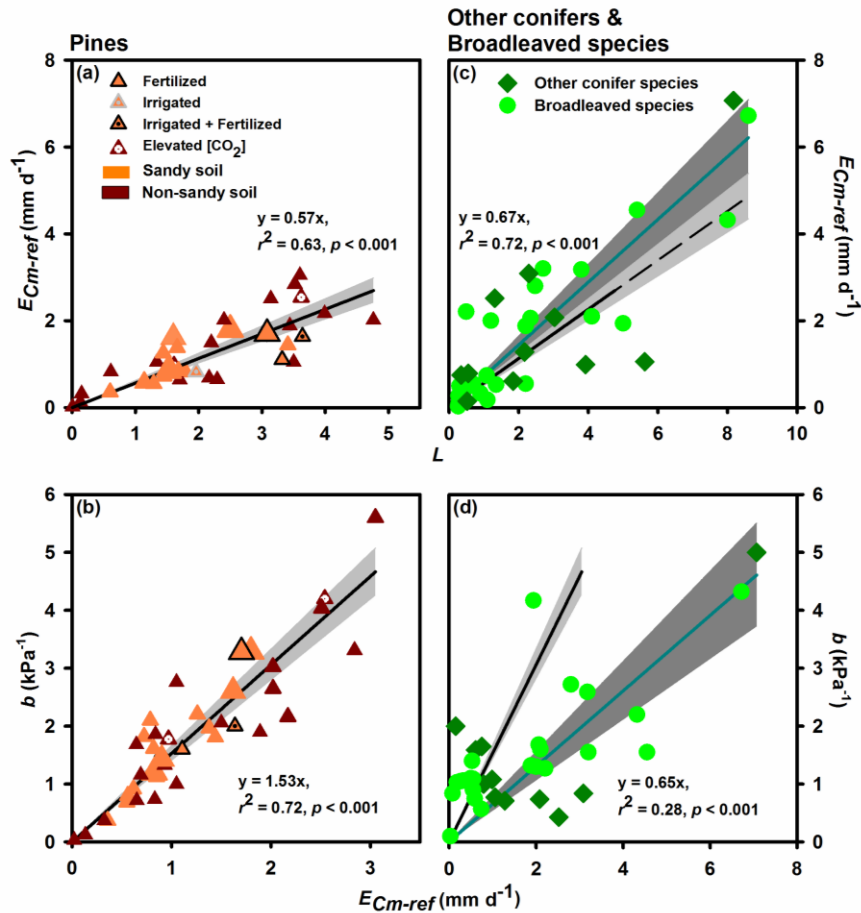


**Figure 4.4: Functions to estimate daily canopy transpiration of forests.** (a) Synthesis response of reference canopy transpiration under well-watered condition ( $E_{Cm-ref}$ ) to leaf area index ( $L$ ) in pine forests. (b) The sensitivity of canopy transpiration of pine forests to changes in vapor pressure deficit as a function of  $E_{Cm-ref}$  from (a). Yellow (dark red) color represents sites on sandy (non-sandy) soil. Enlarged symbols refer to our four study stands. (c), (d) Similar relationships to (a), (b) but for other conifers combined with broadleaved species. Dark cyan lines are linear regression results for other conifer combined with broadleaved species. Regression results from (a), (b) are duplicated in (c), (d) for reference. See Table A4.6.1 for site information and Table A4.6.4 for results of regression analyses and statistical tests. Shaded regions show 95% significant interval of the regression lines.

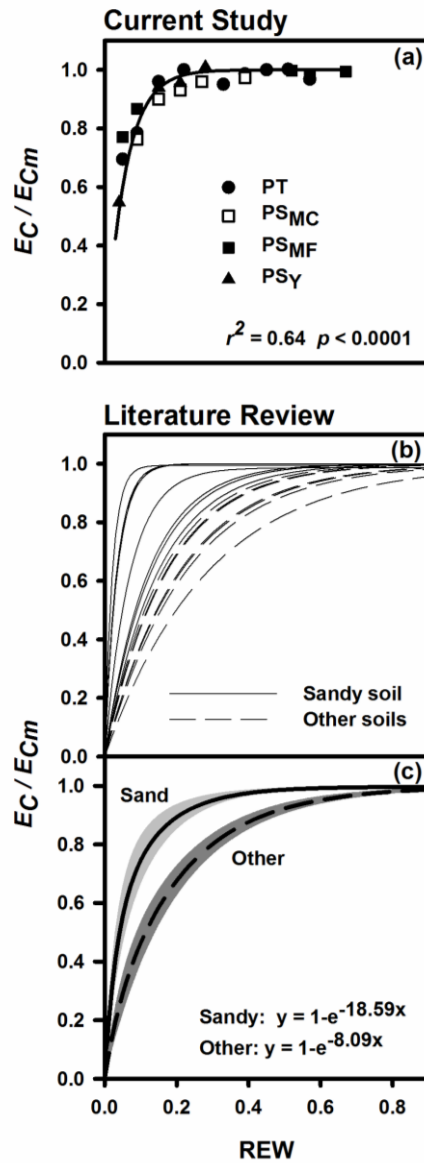


**Figure 4.5: Incorporating soil drying effect.** (a) Soil drying effect on canopy transpiration under favorable conditions ( $E_{Cm}$ ) as observed in forests in this study and (b) other studies as presented in Table S5. (c) Functions accounting for soil drying effect for sandy and other soil types with one standard error shown as shaded regions (see Appendix S1 for method). These functions combined with those in Fig. 4 are used to estimate daily canopy transpiration. All regression statistics are presented in Table A4.6.4.

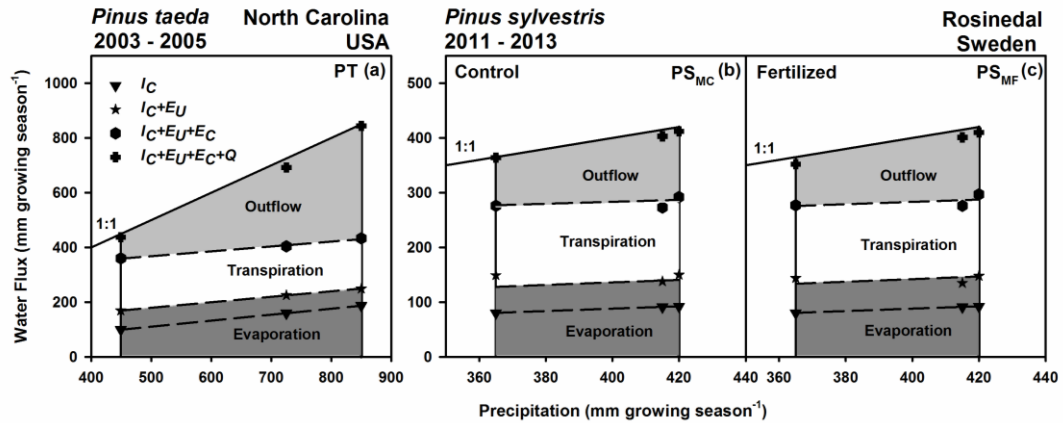


**Figure 4.6: Water balance of the mature pine forests in the present study.** Each hydrologic component is shown in total growing season values ( $\text{mm growing season}^{-1}$ ) as a function of incoming growing season precipitation. Definitions of abbreviations are listed in Table 1. Dashed lines are linear regression of the inter-annual growing season quantities with respect to precipitation. Solid lines represent the one-to-one line of the relationship between  $I_c+Eu+Ec+Q$  and precipitation. Note different scales for the water flux in North Carolina and in Sweden. All regression statistics are presented in Table A4.6.4.

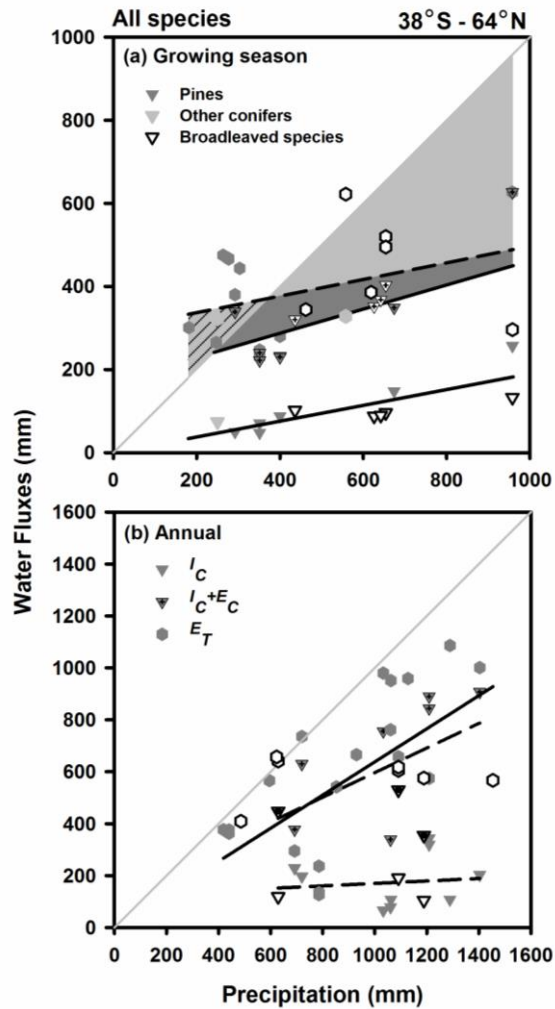


**Figure 4.7:** Synthetic analysis of hydrologic components of forests. **(a)** Sensitivity of hydrologic components to precipitation averaged over multiple growing season periods and **(b)** over annual timescales for forests at various latitudes. See Table A4.6.7 for site information and Table A4.6.4 for summary of regression statistics. Species types are identified by different colors; black, gray and white represent pines, other conifers and broadleaved species, respectively. Solid lines show statistically significant and dashed lines insignificant results.

## 4.6 Supplementary Data

### 4.6.1 Appendix S1

#### 4.6.1.1 Derivation of gapfilling functions for $J_{SD,Out}$

First, we partitioned the  $J_{SD,Out}$  ( $\text{g cm}^{-2} \text{ sapwood d}^{-1}$ ) data into five groups based on different ranges of vapor pressure deficit. Next, we divided data in each of the five groups into two categories; one for model derivation and the other for model validation. Light (PPFD), daylength-normalized vapor pressure deficit ( $D_z$ ) and soil moisture (REW) influence  $J_{SD,Out}$  variation. First, we evaluated soil moisture effect by selecting data at high PPFD (and therefore high  $D_z$ ) and found that REW did not explain  $J_{SD,Out}$  variation ( $r^2 \leq 0.10$ ,  $p \geq 0.37$ ). Therefore, we performed regression analysis on the data for model derivation using the following function.

$$J_{SD,Out} = \alpha \left( 1 - e^{-\beta D_z} \right) \left( 1 - e^{-\gamma PPFD} \right) \quad (\text{A4.1})$$

where  $\alpha$ ,  $\beta$  and  $\gamma$  are fitting parameters. Then, we checked if the residuals varied with each independent variable (*i.e.*,  $D_z$  and PPFD) using linear regression and no significant variation was found ( $p \geq 0.23$ ). We used the resulting functions (summarized in Table A4.6.3) to estimate  $J_{SD,Out}$  values during missing periods and the scaling functions to derive mean  $J_{SD}$  ( $\bar{J}_{SD}$ ) for the entire sapwood area and hence obtaining  $E_c$ .

#### 4.6.1.2 Literature review for $E_c$ versus $D_z$ response and hydrologic components

For cross-site comparison, we searched for published studies on transpiration in forests of various species and site conditions as listed in Table A4.6.1. We selected studies that reported daily canopy transpiration estimates or sap flux density and  $D_z$  or daytime vapor pressure deficit ( $D$ ; average for PPFD > 0). In some studies where the response was not shown, daily  $E_c$  data were digitized and regressed against  $D_z$  using the saturating exponential function  $y = a(1 - e^{-bx})$  as in Fig. 4.3a,b, focusing on the upper boundary of data to represent non-limiting soil water condition. We estimated  $D_z$  by calculating daylight hours based on day of year and latitude in degrees (Forsythe *et al.*, 1995) and averaged for the growing season days. Then,  $E_{Cm-ref}$  was determined from the fitting result as the value at  $D_z = 1$  kPa and the initial increasing rate of  $E_{Cm}$  with  $D_z$  was obtained as parameter  $b$  as described in Materials and Methods. Mean growing season leaf area index ( $L$ ) obtained from the literature was converted to projected values following the approach to standardize  $L$  presented in a global analysis (Iio *et al.*, 2014). Briefly, the half total surface area was converted to projected value by a factor of 0.71 for pines, 0.87 for other conifers and 1 for broadleaf species. When optical measurement was used to measure  $L$ , a global mean value of total clumping index (0.56; Iio *et al.*, 2014) was employed to correct for clumping effect, particularly in conifers. From each water budget study, we recorded growing season and annual estimates of water fluxes for

each year. For the sensitivity analysis of the hydrologic components to precipitation, we focused on the average over study years in each study.

#### 4.6.1.3 Literature review for soil moisture effect

We obtained the relationships of reduction of transpiration, stomatal conductance or CO<sub>2</sub> assimilation with soil moisture content ( $\theta$ ) from other published studies. These relationships showed no consistent pattern of CO<sub>2</sub> assimilation rate reducing more slowly than transpiration with drying soil as might be a concern when vapor pressure deficit increases accompanying drought, making transpiration less variable (Oishi *et al.*, 2010). Therefore, all curves, obtained from different variables of transpiration, stomatal conductance or photosynthesis rate, were used to describe the soil drying effect on transpiration. Based on the information of soil texture presented in each study, we converted  $\theta$  to REW using equation (4.1) together with the soil moisture at field capacity ( $\theta_{FC}$ ) and that at wilting point ( $\theta_w$ ) as the minimum soil moisture from Kätterer *et al.* (2006). The data from each study were regressed with the function  $y = a(1 - e^{-bx})$  and presented as in Fig. 4.6a,b. Having only 15 responses, we categorized the fitting results into two soil type, sand ( $n = 7$ ) and other soils ( $n = 8$ ), and averaged the parameters within each population as shown in Fig. 4.6c with one standard error.

**Table A4.6.1:** Site characteristics of surveyed forests used to derive the functions for estimating daily canopy transpiration (Fig. 4.4)

Species	Location	Soil type	$N_s$ (trees ha <sup>-1</sup> )	H (m)	DBH (cm)	B (m <sup>2</sup> ha <sup>-1</sup> )	$S_A$ (m <sup>2</sup> ha <sup>-1</sup> )	L (m <sup>2</sup> m <sup>-2</sup> )	$E_{Cm-ref}$ (mm d <sup>-1</sup> )	b (kPa <sup>-1</sup> )	Reference
<i>Pinus taeda</i>	36°N 79°W	Sand	308	23	36	35	32	1.60	1.78	2.61	This study
<i>Pinus sylvestris</i>	64°N 20°E (Control)	Sand	1020	17	19	27	25	2.50	1.91	3.29	
	64°N 20°E (Fertilized)	Sand	870	16	18	24	22	3.08	1.81	3.28	
<i>Pinus sylvestris</i>	64°N 19°E (13-30-year-old)	Sand	3565	4	5	11	6	1.53	1.25	1.43	
<i>Pinus sylvestris</i>	64°N 19°E	Sand	3400	7	n/a	4.7	n/a	1.43	0.82	1.62	Mellander <i>et al.</i> , 2004
<i>Pinus taeda</i>	35°N 79°W (Control)	Sand	1260	8.8	12.2	11.2	9	1.79	0.83	1.20	Ewers <i>et al.</i> , 1999
	35°N 79°W (Irrigated)	Sand	1260	8.8	12.1	11.6	9	1.96	0.83	1.20	
	35°N 79°W (Fertilized)	Sand	1260	11.9	15.6	19.6	15.2	3.32	1.11	1.60	
	35°N 79°W (Irrigated + Fertilized)	Sand	1260	12.5	18	25.9	21.9	3.64	1.64	2.00	
<i>Pinus taeda</i>	36°N 79°W (6-year-old)	Clayey loam	3530	4.9	n/a	19.71	16.75	1.34	1.36	1.66	Phillips & Oren, 2001
	36°N 79°W (9-year-old)	Clayey loam	3930	7.1	n/a	20.01	17.01	1.61	1.35	1.16	
	36°N 79°W (11-year-old)	Clayey loam	1540	9.2	n/a	23.52	16.17	1.70	0.97	0.91	
	36°N 79°W (Elevated CO <sub>2</sub> )	Clayey loam	1260	8.5	n/a	19.6	17.66	1.61	1.46	1.33	
<i>Pinus contorta</i>	41°N 106°W	Inceptisol	3200	n/a	16.8	59.87	31.72	6.80	2.02	2.65	Pataki <i>et al.</i> , 2000
<i>Pinus taeda</i>	36°N 79°W	Sandy loam	n/a	n/a	n/a	1.12	n/a	4.4	3.04	1.95	Pataki <i>et al.</i> , 1998b
<i>Pinus resinosa</i>	46°N 90°W	Loamy sand	5140	15.1	14	51.6	39.3	3.50	2.90	2.25	Ewers <i>et al.</i> , 2007
<i>Pinus sylvestris</i>	60°N 89°E (67-year-old)	Sand	2800	10.5	10	n/a	1141	1.66	1.38	1.97	Zimmermann <i>et al.</i> , 2000
	60°N 89°E (138-year-old)	Sand	1100	15.2	18	n/a	572	1.29	0.55	0.69	
	60°N 89°E (204-year-old)	Sand	800	16.3	22	n/a	769	1.45	0.72	1.82	

	60°N 89°E (243-year-old)	Sand	500	19.5	33	n/a	680	0.60	0.36	0.37	
	60°N 89°E (383-year-old)	Sand	200	14.6	26	n/a	372	1.60	0.79	2.10	
<i>Pinus taeda</i>	36°N 79°W (Control)	Clayey loam	886	20.2	21.4	48.4	40.4	3.14	2.51	4.04	Tor-ngern <i>et al.</i> , 2014
	36°N 79°W (Elevated CO <sub>2</sub> )	Clayey loam	868	23.9	21.8	56.7	47.3	3.62	2.54	4.2	
<i>Pinus canariensis</i>	28°N 16°W	Leptosol	291	10.3	25.4	16.7	n/a	2.57	0.65	0.72	Brito <i>et al.</i> , 2014
<i>Pinus canariensis</i>	28°N 27°W	Andosol	825	20	n/a	53.8	n/a	2.43	0.69	1.16	Luis <i>et al.</i> , 2005
<i>Pinus ponderosa</i>	38°N 120°W	Cohasset series	~600	5-6	14.1	n/a	n/a	1.57	1.50	2.06	Kurpius <i>et al.</i> , 2003
<i>Pinus strobus</i>	35°N 83°W	Mixed fine loam	556	30.9	40.5	66.5	n/a	3.86	1.89	1.90	Ford <i>et al.</i> , 2010
<i>Pinus radiata</i>	35°S 147°E	Sandy loam	1667	10	17	n/a	n/a	9.10	7.30	1.04	Myers <i>et al.</i> , 1998
<i>Pinus banksiana</i>	56°N 98°W (18-year-old)	Well-drained	1039	~12	~7.8	n/a	0.077	0.007	0.08	0.33	Angstmann <i>et al.</i> , 2012
	56°N 98°W (43-year-old)	Well-drained	2801	~12	~7.8	n/a	3.66	0.61	0.88	0.89	
	56°N 98°W (18-year-old)	Poorly- drained	520	~7	~2.8	n/a	0.25	0.13	0.24	0.36	
	56°N 98°W (43-year-old)	Poorly- drained	469	~7	~2.8	n/a	0.931	0.15	0.35	1.18	
<i>Pinus palustris</i>	29°N 82°W	Sand	237	23.9	32.35	12.34	9.50	1.68	0.85	1.12	Gonzales-Benecke <i>et al.</i> , 2011
<i>Pinus elliotii</i>	29°N 82°W	Sand	55	27.3	34.18	4.56	2.88	3.41	1.44	1.81	
<i>Pinus pinaster</i> Ait.	44°N 0°W (32-year-old)	Sand	513	20	31	36.1	21	2.00	1.26	2.21	Delzon & Loustau, 2005
	44°N 0°W (54-year-old)	Sand	254	27	44	38	21	1.29	0.62	0.91	
	44°N 0°W (91-year-old)	Sand	156	29	52	33	20	1.27	0.56	0.80	
<i>Populus trichocarpa</i> Torr. * <i>P. deltoids</i> Bartr. & Marsh.	46°N 118°W (Irrigated)	Sand	3175	>8	~8	n/a	n/a	8.00	4.32	2.22	Kim <i>et al.</i> , 2008
Tropical forest	5°N 53°W	Sand	220	30	58	n/a	n/a	8.60	6.72	4.32	Granier <i>et al.</i> , 1996b
<i>Taxodium</i> <i>distichum</i>	35°N 79°W	Artificial impoundment	722	27	36	73.6	31.7	2.20	1.88	1.32	Oren <i>et al.</i> , 1999a

<i>Abies amabilis</i> / <i>Tsuga heterophylla</i>	47°N 122°W	Sandy loam	1121	16	23	47.4	n/a	8.17	7.07	5.00	Martin <i>et al.</i> , 1997
<i>Populus tremuloides</i>	41°N 106°W	Inceptisol	17100	5-20	13.4	43	28.9	3.80	3.18	2.59	Pataki <i>et al.</i> , 2000
<i>Abies lasiocarpa</i>	41°N 106°W	Inceptisol	3200	5-20	4.2	23	12.1	1.84	0.61	1.59	Pataki <i>et al.</i> , 2000
<i>Carya tomentosa</i>	36°N 79°W	Loam	n/a	~30	35.4	n/a	n/a	1.35	0.53	1.40	Pataki & Oren, 2003
<i>Quercus alba</i>	36°N 79°W	Loam	n/a	~30	26.1	n/a	n/a	0.26	0.03	0.10	Pataki & Oren, 2003
<i>Quercus rubra</i>	36°N 79°W	Loam	n/a	~30	39.5	n/a	n/a	0.27	0.08	0.84	Pataki & Oren, 2003
<i>Liquidambar styraciflua</i>	36°N 79°W	Loam	n/a	~30	26.5	n/a	n/a	0.44	0.59	0.75	Pataki & Oren, 2003
<i>Liquidambar tulipifera</i>	36°N 79°W	Loam	n/a	~30	37.6	n/a	n/a	0.62	0.55	0.90	Pataki & Oren, 2003
<i>Quercus alba</i> / <i>Acer rubrum</i>	36°N 79°W	Silt loam	1325	n/a	n/a	23	n/a	5.00	1.94	4.17	Oren & Pataki, 2001
<i>Picea mariana</i> (Mill.)	56°N 98°W (43-year-old)	Well-drained	29285	n/a	n/a	n/a	6.93	3.03	2.08	0.74	Angstmann <i>et al.</i> , 2012
	56°N 98°W (77-year-old)	Well-drained	36429	n/a	n/a	n/a	17.5	5.62	1.06	0.77	
	56°N 98°W (157-year-old)	Well-drained	25337	n/a	n/a	n/a	11.3	3.92	0.99	1.08	
	56°N 98°W (18-year-old)	Poorly-drained	27803	n/a	n/a	n/a	1.62	0.55	0.79	1.00	
	56°N 98°W (43-year-old)	Poorly-drained	48888	n/a	n/a	n/a	7.32	2.29	3.09	0.84	
	56°N 98°W (77-year-old)	Poorly-drained	12223	n/a	n/a	n/a	8.16	2.17	1.28	0.71	
	56°N 98°W (157-year-old)	Poorly-drained	21574	n/a	n/a	n/a	7.40	1.31	2.52	0.43	
<i>Populus tremuloides</i> Michx.	56°N 98°W (18-year-old)	Well-drained	38457	n/a	n/a	n/a	3.96	0.49	2.21	1.27	Angstmann <i>et al.</i> , 2012
	56°N 98°W (43-year-old)	Well-drained	2801	n/a	n/a	n/a	2.30	1.08	0.74	0.57	
	56°N 98°W (18-year-old)	Poorly-drained	28323	n/a	n/a	n/a	0.947	0.27	0.27	1.05	
<i>Acer saccharum</i>	46°N 90°W	Loamy sand	370	18.6	22.4	18.8	12.6	4.10	2.10	1.60	Ewers <i>et al.</i> , 2007
<i>Tilia americana</i>	46°N 90°W	Loamy sand	145	18.2	25.4	9.7	4.2	0.30	0.50	1.10	Ewers <i>et al.</i> , 2007
<i>Populus tremuloides</i>	46°N 90°W	Loamy sand	2930	14.7	11	30	15.8	2.70	3.20	1.55	Ewers <i>et al.</i> , 2007

<i>Abies balsamea</i>	46°N 90°W	Loamy sand	890	4.2	6.6	3.7	2.5	0.52	0.15	2.00	Ewers <i>et al.</i> , 2007
<i>Thuja occidentalis</i>	46°N 90°W	Loamy sand	796	10.1	19.3	24.4	6.1	0.35	0.75	1.65	Ewers <i>et al.</i> , 2007
<i>Alnus regosa</i>	46°N 90°W	Loamy sand	42500	5.6	n/a	n/a	16.1	1.20	2.00	1.30	Ewers <i>et al.</i> , 2007
<i>Eucalyptus grandis</i>	35°S 147°E	Sandy loam	1667	18	17	n/a	n/a	5.40	4.55	1.55	Myers <i>et al.</i> , 1998
<i>Carya spp.</i>	35°N 83°W	Fine loam	50	28.7	38.6	5.5	n/a	0.90	0.33	1.06	Ford <i>et al.</i> , 2010
<i>Liquidambar tulipifera</i>	35°N 83°W	Fine loam	53	36.6	45.4	4	n/a	0.60	0.50	1.02	Ford <i>et al.</i> , 2010
<i>Quercus prinus</i> L.	35°N 83°W	Fine loam	81	27.9	51.2	13.5	n/a	2.20	0.55	1.09	Ford <i>et al.</i> , 2010
<i>Quercus rubra</i> L.	35°N 83°W	Fine loam	19	30.2	59.4	6.5	n/a	1.10	0.18	1.03	Ford <i>et al.</i> , 2010
<i>Liquidambar styraciflua</i>	36°N 79°W	Sandy loam	n/a	n/a	n/a	0.36	n/a	2.47	2.80	2.72	Pataki <i>et al.</i> , 1998b
<i>Quercus phellos</i>	36°N 79°W	Sandy loam	n/a	n/a	n/a	0.31	n/a	2.34	2.06	1.68	Pataki <i>et al.</i> , 1998b
<i>Pinus taeda</i>	35°N 76°W (early rotation)	Organic matter / sandy loam	1040	3.5	14	14.5	n/a	1.55	0.93	1.33	Domec <i>et al.</i> , 2012
	35°N 76°W (mid rotation)	Organic matter / sandy loam	635	18.7	35	56.2	n/a	3.52	2.84	3.31	

$N_s$  = stand density,  $H$  = mean canopy height,  $DBH$  = mean diameter at breast height,  $B$  = basal area index,  $S_A$  = sapwood area index,  $L$  = mean growing season projected leaf area index,  $E_{Cm-ref}$  = daily canopy transpiration at 1 kPa vapor pressure deficit under non-limiting soil water,  $b$  = sensitivity of canopy transpiration to changes in vapor pressure deficit.

**Table A4.6.2: Summary of instrumentation for environmental measurements at the study sites**

Site	Variable	Number of instruments	Instrument position	Measurement Period	Measurement interval	Instrument	Manufacturer
PT	Air temperature ( $T_A$ , °C)	1	Above forest canopy	January 2003 – December 2005	30 minutes	HMP35C probes	Campbell Scientific, Logan, UT, USA
	Relative humidity (RH)						
	Photosynthetic photon flux density (PPFD, $\mu\text{mol m}^{-2} \text{s}^{-1}$ )	1	Above forest canopy		30 minutes	LI-190	Li-Cor BioSciences, Lincoln, NE, USA
	Latent heat flux (LE, $\text{W m}^{-2}$ )	1	Above forest canopy		30 minutes	Eddy covariance system, CSAT3 IRGA, LI-7500	Campbell Scientific, Logan, UT, USA Li-Cor BioSciences, Lincoln, NE, USA
	Precipitation ( $P$ , mm)	1	Above forest canopy		30 minutes	TE-525M	Texas Electronics, Dallas, TX, USA
	Volumetric soil moisture ( $\theta_{30}$ , $\text{m}^3 \text{m}^{-3}$ )	4	30 cm soil depth		30 minutes	CS615	Campbell Scientific, Logan, UT, USA
	$T_A$ , RH, PPFD, LE, $P$ , $\theta_{30}$	1			30 minutes	Datalogger CR23X	Campbell Scientific, Logan, UT, USA
	Throughfall ( $P_T$ , mm)	10	Ground		Biweekly	Rain gauges (collection diameter of 0.1 m)	Productive Alternatives, Fergus Falls, MN, USA

	Leaf area index ( $\text{m}^2 \text{m}^{-2}$ )	20	Two perpendicular transects		Monthly	LAI-2000	Li-Cor BioSciences, Lincoln, NE, USA
<b>PS<sub>MC</sub></b>	Air temperature ( $T_A$ , °C)	1	1.5 m above ground	April 2011 – November 2013	30 minutes	HC2-S3 & MP-101A	Rotonic AG, Switzerland
<b>&amp; PS<sub>MF</sub></b>	Relative humidity (RH)	1	Above forest canopy		30 minutes	LI-190SA	Li-Cor BioSciences, Lincoln, NE, USA
	Photosynthetic photon flux density (PPFD, $\mu\text{mol m}^{-2} \text{s}^{-1}$ )	1	Above forest canopy		30 minutes	Eddy covariance system, R3 LI-7200	Gill Instruments Ltd., Lymington, UK
	Latent heat flux (LE, $\text{W m}^{-2}$ )	1	Above forest canopy		30 minutes		Li-Cor BioSciences, Lincoln, NE, USA
	Volumetric soil moisture ( $\theta_{15}$ , $\text{m}^3 \text{m}^{-3}$ )	1	15 cm soil depth; near the flux tower	July 2011 – November 2013	30 minutes	SM300	Delta-T devices Ltd., Cambridge, UK
		6	15 cm soil depth; around sap flux trees	June – September 2013			
	$T_A$ , RH, PPFD, LE, $P$ , $\theta_{30}$	1		April 2011 – November 2013	30 minutes	Datalogger CR10X	Campbell Scientific, Logan, UT, USA
	Throughfall ( $P_T$ , mm)	9	Ground		Monthly	Biwee Collector (collection area of $0.5 \text{m}^2$ )	n/a
<b>PS<sub>MF</sub></b>	Precipitation ( $P$ , mm)	1	Above forest canopy		30 minutes	Tipping bucket,	Campbell Scientific, Logan,

---

<b>PS<sub>Y</sub></b>	Air temperature ( $T_A$ , °C)	1	1.7 m above ground		30 minutes	ARG100	UT, USA
	Relative humidity (RH)					HC2-S3 & MP-101A	Rotonic AG, Switzerland
	Global radiation ( $\mu\text{mol m}^{-2} \text{s}^{-1}$ )	1	1.7 m above ground		30 minutes	CM3	Kipp & Zonen, Delft, Holland
	Volumetric soil moisture ( $\theta_{15}$ , $\text{m}^3 \text{m}^{-3}$ )	4	15 cm soil depth	July 2013 – June 2014	30 minutes	CS615	Campbell Scientific, Logan, UT, USA
		1				Datalogger CR1000	Campbell Scientific, Logan, UT, USA

---

**Table A4.6.3: Summary of empirical functions.** Functions used for scaling the point-measured sap flux density to the mean sapwood area for calculating canopy transpiration and those for estimating missing values of the daily sum sap flux density in the outermost xylem layer ( $J_{SD,Out}$ ;  $\text{g cm}^{-2} \text{d}^{-1}$ ) from daylength-normalized daytime vapor pressure deficit ( $D_z$ ; kPa) and daily sum photosynthetically active radiation (PPFD;  $\text{mol m}^{-2} \text{d}^{-1}$ ). In the scaling functions,  $J_{SD,i}$  refers to daily sum sap flux density at inner depth into sapwood.  $J_{SD,Out}$  is the daily sum sap flux density in the outermost xylem layer.  $X_R$  represents the relative sapwood depth of the measured point to the outermost xylem layer.  $c$  is the  $X_R$  value at which the sap flux density begins to decline.

Code	Scaling function	$r^2$	Gapfilling function	$r^2$
PT	$\frac{J_{SD,i}}{J_{SD,Out}} = e^{-0.5\left(\frac{X_R - 0.0058}{0.4172}\right)^2}$ ; $c = 0.13$	0.42 $p < 0.001$	$J_{SD,Out} = 126.10\left(1 - e^{-1.16D_z}\right)\left(1 - e^{-0.05Q_p}\right)$	0.58 $p < 0.001$
PS <sub>MC</sub> , PS <sub>MF</sub> *	$\frac{J_{SD,i}}{J_{SD,Out}} = e^{-0.5\left(\frac{X_R - 0.0017}{0.2601}\right)^2}$ ; $c = 0.30$	0.65 $p < 0.001$	$J_{SD,Out} = 79.37\left(1 - e^{-2.39D_z}\right)\left(1 - e^{-0.11Q_p}\right)$	0.61 $p < 0.001$
PS <sub>Y</sub>	$\frac{J_{SD,i}}{J_{SD,Out}} = e^{-0.5\left(\frac{X_R - 0.2930}{0.4435}\right)^2}$ ; $c = 0.28$	0.84 $p < 0.001$	$J_{SD,Out} = 219.20\left(1 - e^{-4.99D_z}\right)\left(1 - e^{-0.04Q_p}\right)$	0.69 $p < 0.001$

\*Functions for PS<sub>MC</sub> and PS<sub>MF</sub> were not significantly different ( $p = 0.72$  for scaling function and  $p = 0.56$  for gapfilling function).

Table A4.6.4: Summary of regression statistics

Figure	Variables	Species	Soil type	<i>n</i> / <i>N</i>	Relationship	<i>r</i> <sup>2</sup>	<i>p</i>	Test for difference ( $\alpha = 0.05$ )
3a	<i>E<sub>Cm</sub></i> vs <i>Dz</i>	<i>Pt</i> , <i>PsC</i> , <i>PsF</i>	Sandy	n/a	$y = 1.81(1 - e^{-3.12x})$	0.93	<0.0001	Among the three sites, $p = 0.9$
		<i>PsY</i>	Sandy	n/a	$y = 1.25(1 - e^{-1.43x})$	0.99	<0.0001	
4a	<i>E<sub>Cm-ref</sub></i> vs <i>L</i>	Pines	All	37/18	$y = 0.57x$	0.63	<0.0001	Among soil types, $p = 0.23$
4c	<i>E<sub>Cm-ref</sub></i> vs <i>L</i>	Other conifers & Broadleaved species	All	35/27	$y = 0.67x$	0.72	<0.0001	Among soil types, $p = 0.71$ Between the two species groups, $p = 0.32$
4b	<i>b</i> vs <i>E<sub>Cm-ref</sub></i>	Pines	All	37/18	$y = 1.53x$	0.72	<0.0001	Among soil types, $p = 0.43$
4d	<i>b</i> vs <i>E<sub>Cm-ref</sub></i>	Other conifers & Broadleaved species	All	35/27	$y = 0.47x + 0.7$	0.57	<0.0001	Among soil types, $p = 0.7$ Between the two species groups, $p = 0.31$
6a	<i>Ec</i> / <i>E<sub>Cm</sub></i>	<i>Pt</i> , <i>PsC</i> , <i>PsF</i> , <i>PsY</i>	Sandy	n/a	$y = 1 - e^{-18.34x}$	0.64	<0.0001	Among the four sites, $p = 0.8$
7	<i>Ic</i> vs <i>P</i>	<i>Pt</i>	Sandy	n/a	$y = 0.2x$	0.99	<0.001	
		<i>PsC</i> & <i>PsF</i>	Sandy	n/a	$y = 0.22x$	0.99	<0.001	
		<i>Pt</i>	Sandy	n/a	$y = 0.2x + 79.36$	0.99	0.008	
	<i>Ic+Eu</i> vs <i>P</i>	<i>PsC</i>	Sandy	n/a	$y = 0.23x + 43.86$	0.69	0.26	
		<i>PsF</i>	Sandy	n/a	$y = 0.24x + 45.86$	0.64	0.28	
		<i>Pt</i>	Sandy	n/a	$y = 0.18x + 278.7$	0.98	0.06	
	<i>Ic+Eu+Ec</i> vs <i>P</i>	<i>PsC</i>	Sandy	n/a	$y = 0.15x + 220.87$	0.20	0.71	
		<i>PsF</i>	Sandy	n/a	$y = 0.21x + 200.09$	0.29	0.64	
		<i>Pt</i>	Sandy	n/a	$y = 0.98x$	0.99	0.0002	
	<i>Ic+Eu+Ec+Q</i> vs <i>P</i>	<i>PsC</i>	Sandy	n/a	$y = 0.98x$	0.84	0.003	
		<i>PsF</i>	Sandy	n/a	$y = 0.97x$	0.92	0.001	
		<i>Pt</i>	Sandy	n/a	$y = 0.97x$	0.92	0.001	
8a	<i>Ic</i> vs <i>P</i>	All	All	13/9	$y = 0.19x$	0.63	<0.0001	
		All	All	13/9	$y = 0.29x + 171.6$	0.36	0.02	
		All	All	15/7	$y = 0.2x + 297.4$	0.11	0.07	
8b	<i>Ic</i> vs <i>P</i>	All	All	12/8	$y = 0.05x + 122.7$	0.08	0.69	
		All	All	12/8	$y = 0.47x + 122.2$	0.20	0.11	
		All	All	27/19	$y = 0.64x$	0.29	<0.001	

*n* is the number of data and *N* is the number of studies involved in the analyses (see Table A4.6.1-A4.6.3 for the information of each study). All soil types refer to both sandy and other soils in this study.

**Table A4.6.5:** Site characteristics of forests used to determine soil drying effect on canopy transpiration (Fig. 4.5c)

No	Species	Location	Soil type	Age (year)	N (trees ha <sup>-1</sup> )	H (m)	DBH (cm)	L (m <sup>2</sup> m <sup>-2</sup> )	REW <sub>c</sub>	Reference
1	<i>Pinus taeda</i> & <i>Pinus sylvestris</i>	36°N 79°W & 64°N 20°E	Sand	~40 & 13-70	308 & 870- 3565	23 & 4-19	35 & 11-27	2 & 1.5-3.1	0.11	This study
2	<i>Pseudotsuga menziesii</i> (Mirb.) Franco	45°N 121°W	Sandy loam	450	427	19	111	9	0.39	Warren <i>et al.</i> , 2005
	<i>Pinus ponderosa</i>	44°N 121°W	Sand	250	72	35	63	2.1	0.08	
3	<i>Pseudotsuga menziesii</i> (Mirb.) Franco	50°N 125°W	Sandy loam	23	1840	8-10	10.6	7.5-8	0.48	Black, 1979
4	<i>Pseudotsuga menziesii</i> (Mirb.) Franco	48°N 6°E	Loam	24	2545	17.5	14.6	n/a	0.37	Granier, 1987
5	<i>Pinus sylvestris</i>	60°N 17°E	Sand	~50	872	17	20	~5.73	0.28	Lagergren & Lindroth, 2002
	<i>Picea abies</i>								0.30	
6	<i>Pinus sylvestris</i>	42°N 1°E	Sandy loam	60	2165	11	15.2	1.71*	0.06	Poyatos <i>et al.</i> , 2005
7	<i>Pinus strobus</i>	42°N 80°W	Sand	70	421	22	36	4	0.39	MacKay <i>et al.</i> , 2012
8 <sup>v</sup>	<i>Pinus sylvestris</i>	47°N 10°E	Sand	125	1690	18	26.5	n/a	0.06	Leo <i>et al.</i> , 2014
9 <sup>c</sup>	Various coniferous and broadleaved species (Pines include <i>Pinus sylvestris</i> , <i>Pinus pinaster</i> , <i>Pinus banksiana</i> )	4-52°N 100°W-13°E	Loam	5-120	215- 3873	4.7-29	5.7-58	2.2- 10.8	0.66	Granier <i>et al.</i> , 2000a
10 <sup>c</sup>	<i>Pseudotsuga menziesii</i> (Mirb.) Franco	52°N 6°E	Sand	~30	780	21.6	n/a	7.8- 10.5	0.08	Wijk <i>et al.</i> , 2000
11 <sup>c</sup>	<i>Quercus ilex</i>	43°N 3°E	Silty clay loam	n/a	7149	5.5	<4 (12% of total) >10 (12.5% of total)	2.9	0.52	Rambal <i>et al.</i> , 2003
12 <sup>c</sup>	<i>Pinus taeda</i>	35°N 79°W	Sand	10	1260	6	10	1.3-1.5	0.34	Ewers <i>et al.</i> , 2001
13 <sup>c</sup>	<i>Pinus sylvestris</i>	56°N 3°W	Sandy loam	41	836	15	20.1	1.92	0.49	Perks <i>et al.</i> , 2002
14 <sup>c</sup>	<i>Pinus taeda</i>	35°N 79°W	Clayey loam	13	5240	7.1	5.5	3	0.40	Oren <i>et al.</i> , 1998b
15 <sup>n</sup>	<i>Pinus sylvestris</i>	61°N 89°E	Sand	215	290	16	28	1.5	0.16	Kelliher <i>et al.</i> , 1998

$N$  = stand density,  $H$  = mean canopy height,  $DBH$  = mean diameter at breast height,  $L$  = mean growing season projected leaf area index,  $REW_c$  =  $REW$  value at which canopy transpiration reaches 90% of its maximum value, \* denotes maximum leaf area index,  $\gamma^{\zeta\eta}$  refer to different variables used to determine the soil drying effects including sap flux density, canopy stomatal conductance and canopy photosynthesis, respectively.

**Table A4.6.6: Growing season water balance of the study sites.** Total growing season estimates (in mm of water) of hydrologic components in the mature forests in this study.

<b>Code</b>	<b>Growing season year</b>	<b><i>P</i></b>	<b><i>P<sub>r</sub></i></b>	<b><i>I<sub>c</sub></i></b>	<b><i>E<sub>c</sub></i></b>	<b><i>E<sub>u</sub></i></b>	<b><i>E<sub>r</sub></i></b>	<b><i>Q</i></b>	<b><math>\Delta S</math></b>	<b><i>R</i></b>
<i>Pt</i>	2003	850	663	187	205	62	433	390	-4	10
	2004	725	566	159	187	66	404	280	12	21
	2005	449	350	99	211	70	360	57	-3	15
<i>P<sub>s</sub>C</i>	2011	420	328	92	150	50	292	120	6	2
	2012	415	324	91	138	44	273	130	-8	20
	2013	365	285	80	149	47	276	88	-8	9
<i>P<sub>s</sub>F</i>	2011	420	328	92	148	57	297	113	19	-24
	2012	415	324	91	135	50	276	125	5	23
	2013	365	285	80	144	53	277	75	11	2

**Table A4.6.7:** Site characteristics of forests used for the analysis of hydrologic components (Fig. 4.7)

Species	Location	Soil type	Year	<i>L</i>	<i>P</i>		<i>I<sub>c</sub></i>		<i>E<sub>c</sub></i>		<i>E<sub>r</sub></i>		<i>Q</i>		Reference
					(mm)		(mm)		(mm)		(mm)		(mm)		
					GS	Y	GS	Y	GS	Y	GS	Y	GS	Y	
<i>Pinus taeda</i>	36°N 79°W	Sand	2003-2005	1.60	674 (205)	n/a	148 (45)	n/a	201 (12)	n/a	399 (37)	n/a	242 (170)	n/a	This study
<i>Pinus sylvestris</i>	64°N 20°E (Control)	Sand	2011-2013	2.50	400 (40)	n/a	88 (7)	n/a	146 (7)	n/a	280 (10)	n/a	113 (22)	n/a	
	64°N 20°E (Fertilized)	Sand	2011-2013	3.08	400 (40)	n/a	88 (7)	n/a	142 (7)	n/a	283 (12)	n/a	104 (26)	n/a	
<i>Pinus radiata</i>	38°S 176°E	Sandy loam	1986-1987	5.54	292	1403	50	203	289	704	380	1001	7	349	Whitehead & Kelliher, 1991
<i>Pinus pinaster</i> Ait.	44°N 0°W	Sand	1997-1998	1.07	n/a	930	n/a	n/a	n/a	n/a	n/a	666 (93)	n/a	n/a	Berbigier <i>et al.</i> , 2001
<i>Pinus radiata</i>	38°S 141°E	Limestone	Varied from 1978 - 2007	4.36	n/a	720	n/a	197	n/a	433	n/a	736	n/a	n/a	Benyon & Doody, 2014
<i>Pinus taeda</i>	35°N 76°W (Early rotation)	Typical Umbraquilt	2007-2009	1.50	n/a	1061 (253)	n/a	79 (31)	n/a	260 (96)	n/a	762 (176)	n/a	223 (14)	Domec <i>et al.</i> , 2012
	35°N 76°W (Mid-rotation)	Historical mineral	2007-2009	3.60	n/a	1033 (216)	n/a	66 (9)	n/a	690 (76)	n/a	980 (46)	n/a	171 (99)	
<i>Pinus sylvestris</i>	52°N 0°E	Sand	1975	3.30	224	595	n/a	n/a	n/a	353	n/a	566	n/a	n/a	Gash & Stewart, 1977
<i>Pinus sylvestris</i>	61°N 24°E	Sand	1998-2006	n/a	n/a	692 (82)	n/a	229 (45)	n/a	149 (17)	n/a	295 (46)	n/a	196 (58)	Ilvesniemi <i>et al.</i> , 2010
<i>Pinus ponderosa</i>	44°N 121°W (Young)	Sandy loam	1999-2002	0.59	n/a	440	n/a	n/a	100	n/a	229	363	n/a	n/a	Irvine <i>et al.</i> , 2004
	44°N 121°W (Mature)	Sandy loam	2002	1.97	n/a	440	n/a	n/a	113	n/a	254	376	n/a	n/a	
	44°N 121°W (Old)	Sandy loam	2002	1.20	n/a	419	n/a	n/a	108	n/a	231	377	n/a	n/a	
<i>Pinus taeda</i>	36°N 79°W	Clayey loam	2001-2004	3.30	654 (183)	1091 (182)	n/a	n/a	403 (59)	490 (66)	495 (60)	658 (74)	n/a	n/a	Stoy <i>et al.</i> , 2006
<i>Pinus elliotii</i>	29°N 83°W	Sand	1998-	0.71	n/a	1128	n/a	n/a	n/a	n/a	n/a	959	n/a	n/a	Gholz & Clark, 2002

	(Clear-cut)		1999			(169)						(127)			
	29°N 83°W	Sand	1998-1999	1.46	n/a	1062	n/a	108	n/a	n/a	n/a	951	n/a	n/a	
	(Mid-rotation)					(262)		(1)				(90)			
	29°N 83°W	Sand	1998-1999	1.88	n/a	1289	n/a	108	n/a	n/a	n/a	1086	n/a	n/a	
	(Full-rotation)					(145)		(8)				(120)			
<i>Pinus taeda/Liquidambar styraciflua</i>	36°N 79°W	Clayey loam	1998-2000	3.70*	n/a	1209	n/a	320	n/a	524	n/a	575	n/a	355	Schäfer <i>et al.</i> , 2002
	(Ambient CO <sub>2</sub> )					(201)		(53)		(8)		(39)		(142)	
	36°N 79°W	Clayey loam	1998-2000	3.70*	n/a	1209	n/a	344	n/a	546	n/a	575	n/a	236	
	(Elevated CO <sub>2</sub> )					(201)		(65)		(20)		(39)		(155)	
<i>Pinus taeda/Liquidambar styraciflua</i>	36°N 79°W	Clayey loam	1994	3.00	351	n/a	71	n/a	169	n/a	230	n/a	35	n/a	Oren <i>et al.</i> , 1998b
	(Ambient CO <sub>2</sub> )														
	36°N 79°W	Clayey loam	1994	2.40	351	n/a	48	n/a	174	n/a	247	n/a	23	n/a	
	(Elevated CO <sub>2</sub> )														
<i>Pinus pinaster</i> Ait.	44°N 0°W	Sand	2010	0.82	181	853	n/a	n/a	65	128	301	542	n/a	n/a	Moreaux <i>et al.</i> , 2013
<i>Pinus contorta</i>	41°N 106°W	Loam	1979-1981	2.61	277	553	n/a	n/a	232	n/a	466	n/a	42	n/a	Knight <i>et al.</i> , 1985
	(Dry Park I)				(15)	(108)			(67)		(62)		(34)		
	41°N 106°W	Loam	1979-1981	2.54	277	587	n/a	n/a	237	n/a	468	n/a	72	n/a	
	(Dry Park II)				(15)	(140)			(70)		(67)		(67)		
	41°N 106°W	Loam	1979-1981	1.39	247	600	n/a	n/a	141	n/a	265	n/a	327	n/a	
	(Albany)				(15)	(137)			(19)		(44)		(128)		
	41°N 106°W	Loam	1979-1981	3.54	263	643	n/a	n/a	232	n/a	475	n/a	138	n/a	
	(Nash Fork)				(21)	(76)			(29)		(26)		(52)		
	41°N 106°W	Loam	1979-1981	1.61	303	733	n/a	n/a	217	n/a	444	n/a	205	n/a	
	(French Creek)				(6)	(107)			(3)		(20)		(94)		
<i>Pinus strobus</i>	35°N 83°W	Mixed fine loam	2004-2006	3.85	958	2057	257	n/a	370	n/a	627	n/a	n/a	n/a	Ford <i>et al.</i> , 2010
					(385)	(327)	(83)		(47)		(118)				
<i>Pinus pinaster</i> Ait.	44°N 0°W	Sand	2001-2002	2.00	n/a	785	n/a	n/a	n/a	n/a	n/a	237	n/a	n/a	Delzon & Loustau, 2005
	(32-year-					(33)						(84)			

	old)														
	44°N 0°W (54-year-old)	Sand	2001-2002	1.29	n/a	785 (33)	n/a	n/a	n/a	n/a	n/a	134 (14)	n/a	n/a	
	44°N 0°W (91-year-old)	Sand	2001-2002	1.27	n/a	785 (33)	n/a	n/a	n/a	n/a	n/a	127 (0)	n/a	n/a	
<i>Picea abies</i> / <i>Pinus sylvestris</i>	60°N 17°E	Sand	1995	3.90	250	n/a	74	n/a	243	n/a	322	n/a	n/a	n/a	Grelle <i>et al.</i> , 1997
<i>Picea abies</i>	51°N 12°E	Cambisol	2007	n/a	558	n/a	n/a	n/a	n/a	n/a	328	n/a	n/a	n/a	Petzold <i>et al.</i> , 2011
<i>Fagus sylvatica</i>	48°N 7°E	Luvisol	1995	n/a	462	n/a	n/a	n/a	255	n/a	345	n/a	n/a	n/a	Granier <i>et al.</i> , 2000b
<i>Fagus sylvatica</i>	48°N 7°E	Sand	1995	n/a	436	n/a	102	n/a	218	n/a	n/a	n/a	n/a	n/a	Granier <i>et al.</i> , 2000b
<i>Populus tremuloides</i> Michx.	54°N 106°W	Silt clay	2001-2003	2.38	n/a	485	n/a	n/a	n/a	n/a	340	409	n/a	n/a	Krishnan <i>et al.</i> , 2006
<i>Eucalyptus globulus</i>	38°S 141°W	Limestone	Varied	3.50	n/a	629	n/a	119	n/a	329	n/a	641	n/a	n/a	Benyon & Doody, 2014
<i>Carya tomentosa</i> (Poir.) Nutt / <i>Carya glabra</i> (P. Mill). Sweet. / <i>Liriodendron tulipifera</i> L. / <i>Liquidambar styraciflua</i> L. / <i>Quercus alba</i> L. / <i>Quercus michauxii</i> Nutt. / <i>Quercus phellos</i> L. <i>Carya</i>	36°N 79°W (Sap-flux based transpiration)	Clay loam	2002-2005	3.74	654	1091	96	191	307	339	520	605	201	482	Oishi <i>et al.</i> , 2010
	36°N 79°W	Clay	2002-	3.74	654	1091	n/a	n/a	410	443	495	618	n/a	n/a	Stoy <i>et al.</i> , 2006

<i>tomentosa</i> (Poir.) Nutt / <i>Carya glabra</i> (P. Mill). Sweet. / <i>Liriodendron</i> <i>tulipifera</i> L. / <i>Liquidambar</i> <i>styraciflua</i> L. / <i>Quercus alba</i> L. / <i>Quercus</i> <i>michauxii</i> Nutt. / <i>Quercus</i> <i>phellos</i> L.	(Modeled transpiration)	loam	2005													
Mixed hardwoods	36°N 79°W	Loam	1997	3.30	626	n/a	88	n/a	264	n/a	n/a	n/a	n/a	n/a	Pataki & Oren, 2003	
<i>Quercus alba</i> / <i>Acer rubrum</i>	35°N 79°W	Silt loam	1993	5.00	642	n/a			278	n/a	n/a	n/a	n/a	n/a	Oren & Pataki, 2001	
Oak/ Maple/ Hickory	35°N 84°W	Well- drained, typic Paleud ult	1995- 1997	n/a	n/a	1454	n/a	n/a	n/a	n/a	n/a	567	n/a	n/a	Wilson & Baldocchi, 2000	
Chesnut oak/ White oak/ Black gum/ Red maple	35°N 84°W	Well- drained, typic Paleud ult	1998- 1999	n/a	n/a	1189	n/a	105	n/a	250	n/a	576	n/a	n/a	Wilson <i>et al.</i> , 2001	
Mixed hardwoods	35°N 83°W	Mixed fine loam	2004- 2006	6.20	958	2057	133	n/a	163	n/a	296	n/a	n/a	n/a	Ford <i>et al.</i> , 2010	
<i>Populus</i> <i>maximowiczii</i> x <i>P. nigra</i>	51°N 12°E	Luviso l	2007	4.33	558	n/a	n/a	n/a	n/a	n/a	622	n/a	n/a	n/a	Petzold <i>et al.</i> , 2011	
<i>Fagus</i>	51°N 12°E	Cambi	2007	n/a	619	n/a	n/a	n/a	n/a		386	n/a	n/a	n/a	Petzold <i>et al.</i> , 2011	

<i>syloatica</i>		sol								/a					
<i>Eucalyptus</i>	43°N 1°E	Silt	2010-	4.50	n/a	623	n/a	n/a	n/a	419	362	657	n/a	n/a	Moreaux <i>et al.</i> , 2013
<i>gumii x</i>		loam	2011												
<i>dalrympleana</i>															

$L$  = mean growing season projected leaf area index,  $P$  = Precipitation,  $I_c$  = Canopy interception,  $E_c$  = canopy transpiration,  $E_T$  = Evapotranspiration,  $Q$  = drainage, GS = Growing Season estimates, Y = Yearly estimates. Values in parentheses represent one standard deviation of the mean.

## **5. Estimates of gross primary productivity (GPP) and resource-use efficiencies of *Pinus taeda* and *Pinus sylvestris* forests in temperate and boreal zones**

### ***5.1 Introduction***

Terrestrial ecosystems sequester ~27% of anthropogenic CO<sub>2</sub> emissions according to global carbon budgets (Le Quéré et al. 2014). Forest ecosystems are the most significant carbon sink among terrestrial ecosystems because of their long-term carbon storage in stem wood (Pan et al. 2011) and soil (Malhi et al. 1999, Amundson 2001, Grace et al. 2006). Nowadays, global environmental changes, such as increasing atmospheric CO<sub>2</sub> concentration and temperature, land-use changes and nitrogen deposition, raise concerns about the fate of carbon in forests as related declines in global forest sink strength could potentially exacerbate the climate change impacts on the Earth (Lawrence and Vandecar 2015). Accurate quantification of carbon pools and fluxes in global forests and their responses to climate and environmental conditions are essential for understanding, predicting and managing the global carbon cycle (Frank and Dugas 2002).

Continuous measurements of carbon exchange between forests and atmosphere using the eddy covariance system (Baldocchi et al. 2001) have been conducted in many locations across biomes, contributing to the knowledge of ecosystem response to

environmental gradients (e.g. Law et al. 2002, Yi et al. 2010). Environmental gradients, for example variations across latitudes, may affect photosynthesis (carbon inflow) and respiration (carbon outflow) of forests differently. For instance, gross primary productivity (GPP), representing forest carbon uptake, was shown to be strongly driven by water balance in European sites (Beer et al. 2007). In the warmer and relatively water-limited southern Europe, water availability significantly controlled GPP while mean annual air temperature was responsible for variation in GPP in the colder northern Europe (Reichstein et al. 2007). Another Euro-flux research showed that annual ecosystem respiration increased with increasing latitudes (Valentini et al. 2000). However, eddy covariance cannot measure GPP directly. During daytime, it measures the net ecosystem productivity (the difference between photosynthesis and ecosystem respiration), and, at nighttime, it measures ecosystem respiration. By scaling nighttime measurements to estimates of their daytime equivalent and adding this to daytime values, it is possible to estimate gross ecosystem productivity (Vickers et al. 2009), but not GPP of the autotrophs alone. One possible solution lies in the studies of quantities and responses at the canopy scale for use in combination with the eddy covariance measurement, thus avoiding spurious correlations in flux partitioning (Lasslop et al. 2009), and for application in large-scale modelling analyses based on the canopy-scale response functions (Law et al. 2002).

Ecosystem models employ various approaches in calculating GPP and net primary productivity (NPP, the difference between GPP and autotrophic respiration). Using absorbed photosynthetically active radiation (APAR) and light-use efficiency (LUE, the ratio of GPP or NPP to radiation absorbed by forest), some models calculate these carbon fluxes from a fixed LUE value (CASA; Potter et al. 1993), from values depending on environmental variables (GLO-PEM; Prince and Goward 1995), from biome-specific maximum conversion efficiencies with a multiplier taking into account environmental effects (3-PG; Landsberg and Waring 1997), or from biome-specific values combined with biometric characteristics of forests (MODIS algorithms; Running et al. 1999, 2000). Some models estimate GPP based on APAR and LUE, and estimate NPP based on a constant NPP/GPP ratio (i.e. the carbon-use efficiency, CUE), thus accounting for the cost of plant maintenance and construction respiration (CASA; Potter et al. 1993, MBL/SPA; Williams et al. 1997). The ratio used is based on several studies that reported CUE to be conserved among ecosystem types (Gifford 1994, Ryan et al. 1994, Landsberg and Gower 1997, Landsberg and Waring 1997, Dewar et al. 1998, Waring et al. 1998). Later studies, however, questioned the use of a constant CUE, as the range found varied widely among forest types (Chapin et al. 2002, Xiao et al. 2003, DeLucia et al. 2007). Recently, a synthesis of carbon flux studies in ~50 forests around the globe, suggested that nutrient availability may be the main regulator of CUE, increasing the conversion

rate of photosynthetic carbon to growth biomass (Vicca et al. 2012). This is consistent with studies under elevated CO<sub>2</sub>, showing that once canopy leaf area index (*L*) reached a certain amount, further increases where nutrients are not limiting did not produce increases of GPP (Palmroth et al. 2006). The increase of NPP with a further increase of *L* was due to changes in partitioning from below- to aboveground, significantly affecting net ecosystem production, or NPP, rather than GPP as is commonly assumed in ecosystem modelling (Fernández-Martinez et al. 2014).

To better evaluate the responses of forest carbon balance to environmental changes, the responses of LUE and CUE should be assessed against inter-annual variation in weather along a wide range of climate regimes (e.g. as characterized by latitudinal locations), different stages of stand development, and spatial variation caused by soil characteristics which affect water and nutrient supplies. Field-based studies considering these factors and focusing on canopy scale will expand the database of carbon fluxes of global forests, facilitating understanding of the responses of these fluxes to environmental changes and informing ecosystem model employed in predicting the future status of the global terrestrial carbon cycle.

Forests dominated by the genus *Pinus* are found over a wide range of environments, from near the Arctic Circle with cold winters and short growing seasons to the tropics with a year-round growing season (Knight et al. 1994). They also include

stands on soils ranging from nutrient rich to sandy, poor soils (Knight 1991, Knight et al. 1994). These forests also differ in many characteristics involving phenology, leaf life span and canopy structure which affect canopy conductance and transpiration (Roberts 2000). Because of their extent and commercial importance, many studies have quantified sap flux in pine forests, making them ideal for evaluating how well the variation of  $L$  among these very different forests reflects their capacity to fix carbon. Thus, we study both temporal and spatial variations of carbon fluxes of two pine species with large ranges, a mid-latitude species *Pinus taeda* (North Carolina, USA) and a high-latitude species *Pinus sylvestris* (northern Sweden), both on sandy soil. The *P. sylvestris* forests had two levels of nutrient availability and three levels of stage-related  $L$ . We hypothesized that **(1)** the high frequency response of mean canopy photosynthesis per unit leaf area ( $A_{netc}$ ,  $\mu\text{mol C m}^{-2}\text{leaf s}^{-1}$ ) to environmental variables will be similar across these ecosystems because of the similar edaphic properties which influence plant water availability and nutrient. Consequently, due to inter-annual climatic variations within each site, **(2)**  $A_{netc}$  and thus half-hourly GPP, averaged over the growing season, will vary among years. **(3)** Among the four forests, there will be no difference in the mean growing season half-hourly GPP because of the compensatory effect between  $L$  and  $A_{netc}$ . Spatially, **(4)** GPP, integrated over the growing season, will mostly be governed by differences in growing season length and solar elevation of these sites. Despite the

spatial variability of  $L$ , latitudes which influence growing season length and solar elevation, and clumping of the species, (5) growing season or annual GPP is linearly related to canopy light absorption among forests. Nevertheless, the allocation of GPP for growth (i.e. NPP) will largely be determined by soil nutrient as suggested by a previous study on global forests.

## ***5.2 Materials and Methods***

Definitions of all abbreviation and variables in the following sections are presented in Table 5.1.

### **5.2.1 Settings**

The study was conducted in pine forests of contrasting size, nutrient availability and climate zones. Stand characteristics of each site are summarized in Table 5.2. The *Pinus taeda* plantation (PT) in North Carolina, USA (36° 20'N 79° 28'W) was established in 1965, thinned in 1983, and harvested in 2006. The soil was well-drained sand with average bulk density and porosity (in the top 60 cm) of 1500 kg m<sup>-3</sup> and 0.43, respectively. Long-term (111-year) average annual temperature and total precipitation were 15.8 °C and 1145 mm (McCarthy et al. 2007). The broadleaf understory was sparse, comprising 2% of total stand basal area (Uebelherr 2008).

The mature *Pinus sylvestris* (PS) forests in Rosinedal, Sweden (64° 10'N, 19° 45'E) were regenerated with seed trees in 1920 – 1925, pre-commercially thinned in 1955 and

thinned in 1976 and 1993, respectively. These forests have been used for long-term fertilization experiment with control (PS<sub>MC</sub>) and fertilized (PS<sub>MF</sub>) stands located ~2 km apart. Fertilizer of 100 kg N ha<sup>-1</sup> yr<sup>-1</sup> was applied to PS<sub>MF</sub> from 2006 to 2011 and a reduced rate of 50 kg N ha<sup>-1</sup> yr<sup>-1</sup> has been used afterwards (Lim et al. in review). The *P. sylvestris* regenerating forest (PS<sub>Y</sub>) was in Åheden (~7 km from Rosinedal). These forests share similar soil texture of well-drained, deep sandy sediment with 2 – 5 cm soil organic layer (Mellander et al. 2005) and bulk density and porosity (in the top 10 cm) of 1230 kg m<sup>-3</sup> (Giesler et al. 1996) and 0.49 (Lundmark and Jansson 2009).

The 30-year mean annual temperature and precipitation (1981 – 2010), measured at the Svartberget field station (8 km from PS<sub>MC</sub> and 1 km from PS<sub>Y</sub>) were 1.8 °C and 614 mm, respectively (Laudon et al. 2013). On average, the area is covered by snow from late October to early May. The understory is characterized by the dwarf shrubs, *Vaccinium myrtillus* (bilberry) and *Vaccinium vitis-idaea* (lingonberry), a ground layer of mosses, *Pleurozium schreberi* and *Hylocomium splendens*, and lichens, *Cladonia* spp. (Hasselquist et al. 2012, Palmroth et al. 2014).

### 5.2.2 Biometric measurements

Tree height, diameter at breast height (DBH) and crown length were measured in 90, 307, 260 and 140 trees in PT, PS<sub>MC</sub>, PS<sub>MF</sub> and PS<sub>Y</sub>, respectively. In PT and PS<sub>Y</sub> the measurements were conducted once in 2003 and 2013, respectively. Values for other

years were determined from the relationship between diameter growth and DBH derived from tree cores for PT and ring widths measured from harvested stem discs taken at breast height for PS<sub>Y</sub>. In PS<sub>MC</sub> and PS<sub>MF</sub>, annual mensuration measurements have been performed since 2005. Sapwood area was estimated from the stem discs collected at breast height in the 2006 harvest in PT, from the 2011 harvest in PS<sub>MC</sub> & PS<sub>MF</sub> and from the 2013 harvest in PS<sub>Y</sub>. For PT canopy, projected  $L$  and its dynamic were derived from monthly measurements (LAI-2000, Li-Cor BioSciences, Lincoln, NE, USA) performed at 20 locations each along two perpendicular transects. A correction factor of 0.59 (Th  r  zien et al. 2007) was applied to  $L$  to account for foliage clumping (Stenberg 1996). For PS<sub>MC</sub> & PS<sub>MF</sub> sites,  $L$  was estimated from allometric equations with annual production and litterfall (Lim et al. in review). The  $L$  dynamic was obtained from a study of *P. sylvestris* stand of similar age and site characteristics (Rautiainen et al. 2011). For PS<sub>Y</sub>,  $L$  was determined from an allometric equation derived from the harvest trees, assuming the same dynamic as in the other PS forests.

### **5.2.3 Environmental measurements**

A summary of instrumentation for environmental measurements in the four sites are presented in Table A5.6.1 in the Supplementary Data. Other assumptions associated with the presented measurements in Table A5.6.1 and additional measurements are briefly discussed as follows.

In Sweden, air temperature ( $T_A$ , °C) and relative humidity (RH, %) were measured below the forest canopies (Table A5.6.1). Nevertheless, these data were used to represent above-canopy measurements because there is a strong coupling between the canopy and the atmosphere and small gradient of vapor pressure deficit ( $D$ ) throughout the canopy depth in forests with low  $L$  (Ewers and Oren 2000). In  $PS_Y$ , the global radiation was measured and converted to photosynthetically active radiation (PAR) using a factor of 0.47 (Papaioannou et al. 1993).

In  $PS_{MC}$  and  $PS_{MF}$ , two sets of soil moisture probes were used for measurements at different periods. To obtain the soil moisture at 15 cm depth ( $\theta_{15}$ ,  $m^3 m^{-3}$ ) at the plot level, we employed the relationship between the long- (near tower) and short- (around sap-flux trees) term data (Table A5.6.1) during June - September 2013 ( $r^2 \geq 0.85$ ) to adjust values from the continuous, long-term measurement. In  $PS_Y$ , we used soil moisture data from  $PS_{MC}$  to estimate values during the unmeasured period in  $PS_Y$  ( $r^2 = 0.72$ ,  $p < 0.001$  for relationship between daily mean  $\theta_{15}$  of both sites).

At all sites, the growing season was delineated beginning the day after daily mean temperature exceeded +5 °C for five consecutive days, and lasted until it dropped below +5 °C for five consecutive days (Mäkelä et al. 2006). The average growing season period during three study years was approximately March - November in PT and May-September in the PS sites. To facilitate the cross-site comparison, soil moisture was

represented by Relative Extractable Water (REW) calculated according to (Granier et al. 2000a):

$$\text{REW} = \frac{\theta - \theta_m}{\theta_{FC} - \theta_m} \quad (5.1)$$

where  $\theta_m$  is minimum volumetric soil moisture and  $\theta_{FC}$  is soil moisture at field capacity with average value of  $0.15 \pm 0.02 \text{ m}^3 \text{ m}^{-3}$  among our study sites. Vapor pressure deficit ( $D$ ) was calculated from  $T_A$  and RH (Abteu and Melesse 2013).

#### 5.2.4 Calculating mean canopy stomatal conductance ( $G_s$ )

Measurements of half-hourly sap flux density ( $J_s$ ,  $\text{g m}^{-2}_{\text{sapwood}} \text{ s}^{-1}$ ) in these forests were previously presented in details (Torngern et al. in review (a)). For each site, we employed a scaling approach to determine canopy transpiration by using a locally derived function accounting for the decline of  $J_s$  with increasing sapwood depth (Torngern et al. in review (a)). Because water stored within tree trunks may largely contribute to transpiration (Waring et al. 1979), we evaluated time lags between water uptake (i.e.  $J_s$ ) and transpiration by performing the cross-correlation analysis between  $J_s$  and  $D$  (Ewers and Oren 2000; Phillips et al. 2001). The results showed maximum correlation at zero lag in *P. taeda* and the young *P. sylvestris* trees, and one lag in *P. sylvestris* trees under both control and fertilized conditions ( $r^2 \geq 0.70$ ). Therefore, we incorporated a 30-minute lag of  $J_s$  to calculate canopy transpiration of  $\text{PS}_{\text{MC}}$  and  $\text{PS}_{\text{MF}}$

sites. In pine forests with no vertical gradient of  $D$  within the canopy, leaf-level stomatal conductance scaled with vertical leaf area distribution was correlated, without bias, to sap-flux based mean canopy stomatal conductance ( $G_s$ ,  $\text{mmol m}^{-2}\text{leaf s}^{-1}$ ; Ewers and Oren 2000), suggesting the well-coupling of forests to the atmosphere and allowing us to calculate  $G_s$  using the simplified Penman-Monteith equation (Ewers et al. 2001, Torgern et al. 2015) as follows.

$$G_s = \frac{K_G(T_a)E_c}{LD} \quad (5.2)$$

where  $K_G(T_a) = 115.8 + 0.4236T_a$  was the conductance coefficient in  $\text{kPa m}^3 \text{kg}^{-1}$  which was derived from a function including air temperature ( $T_a$ ) effects on the psychrometric constant, latent heat of vaporization, specific heat of air at constant pressure and air density (Phillips and Oren 1998) and  $E_c$  was canopy transpiration in  $\text{kg m}^{-2} \text{s}^{-1}$ .

### 5.2.5 Estimating gross primary productivity (GPP)

Gross primary productivity (GPP) was estimated based on canopy photosynthesis ( $A_{netc}$ ) which was calculated by the Canopy Conductance Constrained Carbon Assimilation (4C-A) model. Detailed descriptions of the 4C-A scheme are presented elsewhere (Schäfer et al. 2003, Kim et al. 2008). Briefly, the model, comprising light and photosynthesis modules, determines  $A_{netc}$  in one-dimensional multi-layer canopy at 30-minute time step. First, canopy dimension (e.g. height, crown length and width) and crown architecture (e.g. the distribution of leaf surface area, clumping and

angle along the canopy height) are characterized as inputs for the model. For conifers, shoot and tree clumping can also be incorporated in the calculation by defining clumping factors, needle angle distribution, shoot transmission coefficient and stand density. The light module calculates canopy light absorption, based on the measured incoming PAR and the prescribed canopy structure. In the computation,  $G_s$  is used to constrain estimates of stomatal conductance scaled from porometric measurement and leaf area distribution. The resulting constrained conductance is then coupled to a Farquhar-type photosynthesis model (Farquhar and von Caemmerer 1982). GPP is calculated as the sum of  $A_{netc}$  and daytime respiration ( $R_{day}$ ) which is assumed to be 0.015 times the maximum carboxylation capacity or  $V_{cmax}$  (Casella and Ceulemans 2002). The unique feature of this approach is that it accounts for the responses of stomatal conductance, as estimated through  $J_s$ , to environmental conditions and thus yielding the instantaneous estimates of  $A_{netc}$  and GPP.

We characterized canopy structure based on measurements of crown and stand characteristics and data from published sources when measurements were not available. Detailed canopy characterization for PT and PS<sub>MC</sub> sites was described in a previous study (Tor-ngern et al. in review (b)) and the similar approach was used for PS<sub>MF</sub> and PS<sub>Y</sub> canopies. Photosynthetic parameters (projected leaf area basis), including  $V_{cmax}$  and the maximum capacity for electron transport rate ( $J_{max}$ ) at 25°C ( $V_{cmax25}$  and  $J_{max25}$ ,

respectively), and leaf-level stomatal conductance ( $g_s$ ) response to light were obtained from gas-exchange measurements. In PT, response curves of photosynthesis to intercellular CO<sub>2</sub> concentration ( $A-C_i$ ) and the light response of leaf stomatal conductance were measured on four sun and shade one-year-old needles (total is eight needles) using the open gas exchange system Li-6400 (LI-COR Inc., Lincoln, NE, USA) with an integrated fluorescence chamber head (Li-6400-40; LI-COR Inc.) in April 2007 (K. Novick unpublished). The  $V_{cmax25}$  and  $J_{max25}$  values were then derived from the  $A-C_i$  curves (Farquhar et al. 1980, Sharkey et al. 2007). The  $V_{cmax25}$  ( $67 \pm 19 \mu\text{mol m}^{-2} \text{s}^{-1}$ ) and  $J_{max25}$  ( $117 \pm 16 \mu\text{mol m}^{-2} \text{s}^{-1}$ ) values of one-year-old needle were higher than those measured in SETRES (Maier et al. 2002) but lower than those found in another site with higher  $L$  (Ward 2012).

For  $PS_{MC}$  and  $PS_{MF}$ , the  $A-C_i$  curves were measured from current-year, one-year-old and two-year-old needles at the top canopy, and only current- and one-year-old needles in the middle and low canopy levels using a LI-6400 Portable Photosynthesis System with the standard 2x3 cm chamber with a light source (6400-02B LED Light Source, Li-Cor Biosciences, Lincoln, NE, USA). The parameters of photosynthetic capacity were derived from the measured  $A-C_i$  curves using Farquhar model (Farquhar et al. 1980) as described in Tarvainen et al. (2013). The  $V_{cmax25}$  value was significantly higher in fertilized treatment (averaged  $92 \pm 5 \mu\text{mol m}^{-2} \text{s}^{-1}$  in  $PS_{MC}$  and  $108 \pm 12 \mu\text{mol m}^{-2}$

$s^{-1}$  in  $PS_{MF}$ ,  $p = 0.03$ ) but  $J_{max25}$  was similar ( $p = 0.18$ , averaged  $171 \pm 11 \mu\text{mol m}^{-2} \text{s}^{-1}$ ). Both values did not vary with height in either PS stand ( $p \geq 0.25$ ), reflecting no acclimation of biochemical machinery along the canopy light gradient (Palmroth and Hari 2001). We assumed the same photosynthetic parameters as those of  $PS_{MC}$  for  $PS_Y$ , after finding similar nitrogen content of the current-year needles from these two sites ( $p = 0.92$ ; N. Hasselquist, unpublished for  $PS_Y$  and Lim et al., in review for  $PS_{MC}$ ) because  $V_{cmax}$  and  $J_{max}$  have been found to correlate well with needle nitrogen content (Casella and Ceulemans 2002).

### 5.2.6 Estimating net primary productivity (NPP)

Standing biomass of each component was obtained from local allometric equations derived from harvest data of each site. For PT, foliage NPP was calculated as the difference between current- to previous-year standing biomass combined with needle replacement computed from previous-year foliage biomass times needle turnover rate (0.67 with needle longevity of 1.5 years; McCarthy et al. 2007). NPP of branches was computed from the difference of current- to previous-year standing biomass augmented with bottom branch replacement with vertical growth of the crown (Tor-ngern et al. in review (b)). Stem biomass was determined from stem volume equation and wood specific gravity obtained from a nearby loblolly pine site (McCarthy et al. unpublished). Plot-level biomass of coarse roots was calculated as a function of

aboveground-biomass (Johnsen et al. 2004). Then, NPP values of stem and coarse roots were calculated as the difference between current- to previous-year standing biomass. Conversions of biomass to carbon were performed using carbon fractions of 0.48 for foliage, branches and stem, and 0.44 for coarse roots (Oren et al. 2001, Schäfer et al. 2003). Fine root (< 2 mm in diameter) biomass was computed from the ratio of fine root-to-foliage biomass of a nearby loblolly pine forest on sandy soil (Maier et al. 2004) and the production was subsequently determined using a turnover rate of 0.58 (Pritchard et al. 2008). A carbon content of 0.41 was used to convert biomass to carbon of fine root (Matamala and Schlesinger 2000).

Detailed methods for calculating biomass components for  $PS_{MC}$  and  $PS_{MF}$  are presented in Lim et al. (in review) and the NPP for the study years were directly obtained from that study. However, the NPP of fine roots was measured for 2012 only; therefore, assuming no significant changes across the study years (H. Lim, personal communication), we used the ratio of fine root-to-foliage biomass in 2012 to estimate fine-root NPP for other years. For  $PS_Y$ , we derived allometric and biomass equations from eight trees harvested in September 2013. The same procedures for estimating NPP as those for  $PS_{MC}$  (Lim et al. in review) were applied to  $PS_Y$  site, including the carbon content of tree components and fine root-to-foliage biomass ratio.

## 5.2.7 Statistical Analyses

All regression analyses were performed in SigmaPlot version 12.0, from Systat Software, Inc., San Jose, CA USA. We used an *F*-test to compare fitting results on different datasets with the same function. Analysis of Variance was performed in JMP statistical software (ver. 10.0.0, SAS Institute Inc., Cary, NC) to analyze fertilization and canopy height effects of photosynthetic parameters. Computations of variable, boundary line and cross correlation analyses were conducted in MATLAB 7.6.0 R2008a (Natick, Massachusetts: The MathWorks Inc., 2008).

## 5.3 Results

### 5.3.1 Environmental conditions and variable estimates

PT experienced a variable inter-annual weather pattern with wet growing season (850 mm *P*) in 2003 and relatively dry growing season (449 mm *P*) in 2005 (Figure 5.1d; bar). The PAR and *D* were low in 2003 compared to other years (Figure 5.1a). Growing season REW was high in 2003 (averaged REW =  $0.56 \pm 0.08$  standard deviation (SD) or  $\sim 0.45 \pm 0.05 \text{ m}^3 \text{ m}^{-3}$  of  $\theta_{30}$ ), moderate in 2004 (averaged REW =  $0.47 \pm 0.06$  or  $\sim 0.32 \pm 0.04 \text{ m}^3 \text{ m}^{-3}$  of  $\theta_{30}$ ) and decreased to an average of  $0.32 \pm 0.14$  ( $\sim 0.22 \pm 0.04 \text{ m}^3 \text{ m}^{-3}$  of  $\theta_{30}$ ) during the 2005 growing season (Figure 5.1d; line). In contrast, growing season weather was similar among the study years in Sweden with average *P* and PAR of  $400 \pm 30$  mm and  $29 \pm 2 \text{ mol m}^{-2} \text{ d}^{-1}$  (Figure 5.1e,f; bars for *P*; 1b,c black lines for PAR). However, *D* was

slightly lower in 2012 relative to other years (Fig. 1b,c gray lines). Generally, REW values were high in PS<sub>MF</sub> (Figure 5.1e; gray dashed line) with the seasonality similar to the other PS sites (i.e. Figure 5.1e,f; gray solid lines). Among the forests in Sweden, REW was of similar range in 2011 and 2012 but reached the minimum REW of 0.03-0.26 (~0.01-0.08 m<sup>3</sup> m<sup>-3</sup>  $\theta_{15}$ ) in 2013. Therefore, these study periods facilitate useful analyses covering a wide range of environmental conditions for pine forests on sandy soil.

The zero time lag in PT canopy was similar to the finding from a nearby loblolly pine canopy on sandy soil (SETRES site; Ewers and Oren 2000) but different from that found in another forest with ~30-minute time lag (Phillips et al. 1997). For the Scots pine forests, the zero time lag of the young trees was similar to an older Scots pine stand with insignificant time lags between water flow in stem and transpiration measured in a cuvette (Perämäki et al. 2001). The similarity of time lag in PS<sub>MC</sub> and PS<sub>MF</sub> agreed with the lack of treatment effect in a *Picea abies* forest nearby (Phillips et al. 2001). Therefore, intra- and inter-specific differences in time lags exist and a local time lag needs to be determined specifically for each site. Moreover, we included spatial variation of  $J_s$  within the cross-sectional sapwood area when scaling to canopy (Tor-ngern et al. in review (a)). These procedures were conducted to minimize errors in the scaling of point-measured  $J_s$  to canopy  $G_s$  (Ewers and Oren 2000). For 4C-A model validation, we compared the  $C_i/C_a$  output to independent measurements available for PT, PS<sub>MC</sub> and PS<sub>MF</sub> sites (Table 5.3).

Overall, the modeled  $C_i/C_a$  agreed relatively well ( $\leq 7\%$ ) with observations although the values are lower than the assumed constant ratio of 0.7 across a wide range of species (Wong et al. 1979; Norman 1982). Nevertheless, the small difference between measured and modeled estimates provided confidence in our estimates of canopy photosynthesis and GPP.

Figure 5.2 shows final estimates of variables used in the analyses including canopy transpiration ( $E_c$ ), canopy absorbed photosynthetically active radiation (APAR) and GPP, together with daily variation of  $L$  over the study years. Overall, the seasonality of these variables was in phase with one another and with changes of PAR and  $D$  (Figure 5.1a-c). Across the four sites, daily  $E_c$  during the growing season ranged from  $0.56 \pm 0.33$  mm d<sup>-1</sup> in PS<sub>Y</sub> to  $0.94 \pm 0.52$  mm d<sup>-1</sup> in PS<sub>MF</sub>, reflecting the difference in  $L$  ( $1.5 \pm 0.17$  in PS<sub>Y</sub> and  $3.1 \pm 0.32$  in PS<sub>MF</sub>). Daily APAR was ~19% lower in Sweden compared to North Carolina with much larger difference (~50%) when integrating over the growing season because of the long growing season period in the latter (Table 5.4). Daily GPP ranged from  $4.5 \pm 1.4$  gC m<sup>-2</sup> d<sup>-1</sup> in PS<sub>Y</sub> to  $8.5 \pm 2.2$  gC m<sup>-2</sup> d<sup>-1</sup> in PS<sub>MF</sub> and was unaffected by fertilization ( $p = 0.27$ , compare PS<sub>MC</sub> and PS<sub>MF</sub>). Mean growing season GPP ranged from  $593 \pm 33$  gC m<sup>-2</sup> y<sup>-1</sup> in the young PS<sub>Y</sub> forest to  $1324 \pm 127$  gC m<sup>-2</sup> y<sup>-1</sup> in the PS<sub>MF</sub> site. In general, NPP was higher in mature stands (PT, PS<sub>MC</sub> and PS<sub>MF</sub>) than in the young forest (Table 5.4). The component estimates of NPP were summarized in Table A5.6.2. Mean

NPP estimates ranged from  $203 \pm 15 \text{ gC m}^{-2} \text{ y}^{-1}$  for the young trees in PS<sub>Y</sub> to  $538 \pm 12 \text{ gC m}^{-2} \text{ y}^{-1}$  in PT. In general, aboveground NPP contributed 47 - 89% of total NPP, with higher degree of contribution in PS<sub>Y</sub> (Table A5.6.2). Fertilization had no effect on growing season GPP (Table 5.4, compare PS<sub>MC</sub> and PS<sub>MF</sub>,  $p = 0.44$ ) but significantly increased NPP in the PS stands ( $p = 0.007$ ).

### 5.3.2 Temporal responses of photosynthesis to environmental variation

To isolate the contributors to temporal changes of GPP intra- and inter-annually, we considered the environmental responses of  $A_{netc}$  ( $\mu\text{molC m}^{-2}\text{leaf s}^{-1}$ ) and its associated variables according to Fick's law (Katul et al. 2000):

$$A_{netc} = G_c (C_a - C_i) = G_c C_a \left(1 - \frac{C_i}{C_a}\right) \quad (5.3)$$

where  $G_c$  is canopy conductance to CO<sub>2</sub> ( $= G_s/1.6$ ; Jarvis 1971),  $C_a$  and  $C_i$  are atmospheric and leaf-intercellular CO<sub>2</sub> concentrations, respectively.

First, we examined half-hourly variation of  $A_{netc}$  with  $D$ , light (PAR) and soil moisture (REW) as the main physiological drivers. The boundary-line analysis has been used to interpret plant responses to a single variable when others are not limiting (Chambers et al. 1985). We employed the same approach outlined in Schäfer et al. (2000) to perform this analysis investigating the responses of  $A_{netc}$  to each variable while the other two were non-limiting (REW, PAR) or under standard condition ( $D$  at 1 kPa). All

variables were normalized to the maximum to allow assessing the relative contribution of  $G_s$  and  $(1-C_i/C_a)$  to  $A_{netc}$ .

Similar patterns of responses to the environments among the sites were observed (Figure 5.3). Both  $A_{netc}$  and  $G_s$  decreased with increasing atmospheric demand in a logarithmic fashion while increasing exponentially to a saturating value with soil moisture and light (see Table A5.6.3 for summary of regression statistics of the responses). The opposite trends were found for  $(1-C_i/C_a)$ . Figure 5.3 shows the responses to  $D$  and REW only because the sensitivity to PAR was very similar across the four sites and mostly driven by the model. The sensitivity of  $(1-C_i/C_a)$  was much weaker than that of  $G_s$  (Figure 5.3e,f), signifying the dominant control of stomata over photosynthesis. Overall, these forests responded similarly to REW but more variably with  $D$  (compare curves in Figure 5.3a,c versus 5.3b,d). These responses contributed to the inter-annual variation of half-hourly GPP (as implied by  $A_{netc}$ ) for all sites. The mean growing season GPP ( $\mu\text{molC m}^{-2}_{\text{ground}} \text{s}^{-1}$ ) declined with increasing mean growing season  $D$  and increased with increasing mean growing season REW (not shown).

Next, we assessed the spatial variation of photosynthesis among the four sites considering mean growing season  $G_s$  and  $A_{netc}$  with respect to mean growing season averaged  $L$  (Figure 5.4). We considered  $G_s$  and the main controlling factor influencing  $A_{netc}$  (Figure 5.3). The mean growing season  $G_s$  decreased with increasing  $L$  (Figure 5.4a)

and contributing to the same variation of  $A_{netc}$  with  $L$  (Figure 5.4b). The combined effect of  $A_{netc}$  and  $L$  seemed to compensate for each other but the effect was not complete, resulting in a weak (not significant,  $p = 0.18$ ) increase of mean growing season half-hourly GPP with  $L$  (Figure 5.4c).

Moving to the longer timescale of growing season, we evaluated the temporal and spatial variations of total growing season GPP ( $\text{gC m}^{-2}_{\text{ground}} \text{y}^{-1}$ , Table 5.4). Based on the half-hourly analyses above, the inter-annual variation of mean growing season GPP was correlated with weather patterns among the years. However, the integrated growing season GPP within each site reflected inter-annual difference in growing season length, rather than the climates (Table 5.4). For spatial variation, we found that growing season GPP increased with  $L$ , reaching saturation at high  $L$  values. The relationship of growing season GPP versus  $L$  was different between the two canopies at different latitudes, being in higher GPP range for lower latitude and vice versa (Figure 5.5, lines are regressions of simulated estimates of GPP for PT and PS canopies at various  $L$ ). The discrepancy between the two curves for PT and PS canopies seemed to be related to the difference in growing season length, solar elevation as characterized by latitudes and clumping nature of each species. These effects are illustrated by simulations of each scenario switching one of these factors, independently from others, between the two canopies (Figure 5, patterned symbols). PT canopy that experienced shorter growing

season, lower solar elevation (i.e. higher latitude) or PS-like clumping characteristics had lower GPP than in its normal condition (Figure 5.5, patterned circles with downward arrow). In contrast, PS canopy that experienced longer growing season, higher solar elevation (i.e. lower latitude) or PT-like clumping showed higher GPP than in its native environment (Figure 5.5, patterned squares with upward arrow). Therefore, growing season GPP of forests with the same  $L$  was mostly controlled by characteristics of the sites, including growing season length, latitudinal location and clumping of the canopy.

### 5.3.3 Resource-use efficiencies

We investigated the efficiencies of utilizing resources including water, light and photosynthesized carbon for growth. The average growing season water-use efficiency (WUE), defined as the ratio of GPP to  $E_c$ , of our forests were 6.5 gC mm<sup>-1</sup> for PT and 8.6-9.7 gC mm<sup>-1</sup> for the Scots pine stands. Within each site, there was little inter-annual variation of WUE during the study period and no significant changes with inter-annual growing season climates were observed ( $p \geq 0.3$ ). Nevertheless, among the four study sites, WUE decreased with the growing season mean vapor pressure deficit and total precipitation; ( $p \leq 0.01$ ). Both growing season LUE and CUE of each site were relatively constrained during the study years. LUE ranged from 0.18 gC mol<sup>-1</sup> in PS<sub>Y</sub> to 0.41 gC mol<sup>-1</sup> in PS<sub>MF</sub>, reflecting spatial variation of  $L$  ( $p < 0.001$ ) among the four sites. In contrast,

CUE, ranging 0.33-0.42 across the four stands, did not show a clear pattern with spatially different characteristics of these sites, such as  $L$ , latitudes and climates.

## **5.4 Discussion**

### **5.4.1 Spatio-temporal variations of GPP at half-hourly timescale**

Based on Fickian diffusion, stomatal regulation was the dominant factor influencing canopy photosynthesis in our stands (Figure 5.3). The responses of  $G_s$  to environmental variables, including  $D$ , REW and PAR followed the same patterns across the four sites and resembled the Jarvis-type multiplicative function (Jarvis 1976) of stomatal conductance. Consequently, the half-hourly mean canopy photosynthesis ( $A_{netc}$ ) was sensitive to environmental factors in the similar manner to  $G_s$  with some compensatory effect from the difference between leaf-internal and atmospheric CO<sub>2</sub> concentration ( $1 - C_i/C_a$ ). These trends affected the inter-annual variation of  $A_{netc}$ , and thus GPP, within each site. In the dry year, with relatively high  $D$  and low REW, mean growing season half-hourly GPP was low compared to the wet year, with relatively low  $D$  and high REW. Therefore, our results showed that the high-frequency responses of  $A_{netc}$  were similar across these forests (1) and such environmental responses caused inter-annual variation of the mean growing season half-hourly GPP (2). Considering half-hourly variables and relating them to  $L$  of these sites,  $A_{netc}$  decreased with increasing  $L$  (Figure 5.4b) because of the reduced  $G_s$  induced by increasing mutual shading of high  $L$

canopy (Figure 5.4a, Sellin and Kupper 2005; Tor-ngern et al. 2015). However, the counter-effect of  $A_{netc}$  and  $L$  did not fully compensate for each other, resulting in a slight increase in mean growing season half-hourly GPP with  $L$  (Figure 5.4c) which rejected hypothesis (3). The lack of such compensatory effect, especially in the low  $L$  range, may reflect the less mutual shading of leaves in the stands with lower  $L$  (e.g. Yamamura et al. 1993).

Regarding the nitrogen treatment in the Scots pine forests, fertilization increased  $L$  in  $PS_{MF}$  resulted in increased mutual shading which further reduced  $G_s$  as discussed previously (compare open and closed squares in Figure 5.4a). The fertilization effect on enhancing canopy leaf area has been demonstrated previously in both species (Linder and Axelsson 1982; Albaugh et al. 1998). The decreased  $G_s$  of the fertilized canopy was previously observed in SETRES which was attributed to lower saturated hydraulic conductivity in the newly produced fine roots (Ewers et al. 2001). In addition, preferential allocation of carbon to support growth of lower branches in treated Scots pine was previously demonstrated in a site following long-term nitrogen fertilization (Mälkönen and Kukkola 1991) which may be related to increased sapwood permeability of these lower branches, causing lower leaf stomatal conductance in the upper branches of the fertilized trees (Amponsah et al. 2004).

## 5.4.2 Total growing season GPP

Temporally, growing season sum of GPP did not vary with inter-annual climatic variation within each site. Rather, it increased with longer growing season length. Spatially, our combined simulated and experimental estimates of GPP versus  $L$  (Figure 5.5) suggested that growing season GPP followed an increasing logarithmic function with  $L$  for both loblolly (PT) and Scots (PS) pine canopies. Moving PT from lower to higher latitude (i.e. PT canopy moved from North Carolina to Sweden, Figure 5.5, patterned circles and downward arrow) decreased GPP to the extent that it performed worse than the native PS canopy (Figure 5.5, plus circle) because of the low solar elevation in Sweden associated with PT crown architecture with more horizontally oriented needles and lower clumping than PS (Tor-ngern et al. in review (b)). In contrast, moving PS canopy from northern Sweden down to North Carolina would increase GPP (Figure 5.5, patterned squares and upward arrow). These analyses reflect the influence of latitude (i.e. growing season length and solar elevation) and crown architecture (i.e. needle arrangement within crown and clumping within the canopy) on forest productivity which is the result of their impact on canopy light absorption (Tor-ngern et al. in review (b)). Thus, our results supported **(4)** in that total growing season GPP is mostly dictated by latitudinal difference influencing growing season length and solar elevation.

### 5.4.3 Analyses of the resource-use efficiencies

Within our study sites, the Scots pine in boreal forests used water more conservatively (i.e. higher WUE) than the loblolly pine in a temperate forest. The boreal climate with low precipitation and low temperature and short growing season limit growth of the trees in boreal forests by allowing low  $L$  (Woodward 1987, Waring and Running 1998) and therefore low canopy stomatal conductance (Kelliher et al. 1995). Despite the short growing season, boreal forests experience long summer days which facilitate high light absorption for photosynthesis (Stenberg et al. 1995) and adapt the photosynthetic capacity to overcome cold stress and utilize warm spells for maximum photosynthesis (Kolari et al. 2014). The combined effect of low transpiration (i.e. low canopy stomatal conductance) and optimal photosynthesis resulted in higher plant WUE of the Scots pine compared to that of the loblolly pine in the temperate zone. Although direct comparisons of our WUE estimates to those from other studies were impeded by different definitions of WUE, our values were within the wide range of estimates from forests across the northern hemisphere ( $\sim 2.35 - 11 \text{ gC mm}^{-1}$ ; see Table A5.6.4 for a summary of WUE estimates of 33 studies including six pine, six other conifers, five broadleaved species and five mixed forests) which were mostly determined from GPP divided by evapotranspiration. Combining our estimates with the surveyed values, no clear response of WUE to precipitation gradient was observed but

there seemed to be an increasing trend with latitude up to ~50 °N and then declined towards the high latitude (data not shown). This pattern agrees with a recent study showing a consistent latitudinal trend in WUE (based on evapotranspiration), increasing from the subtropics to the northern latitudes with peaks at around 51 °N and decreasing afterward (Tang et al. 2014).

Based on the analysis in Figure 5.5, because APAR usually increases with  $L$  (Binkley et al. 2011), we further explored how APAR influenced GPP of forests, implying the light-use efficiency. We analyzed the relationship between GPP and APAR using data from our four forests combined with others from literature. The synthesis data consisted of estimates from 11 studies (total 51 data points) with seven pine, seven other conifer, four broadleaved species, 15 forest types and three non-forest ecosystems (Table A5.6.5). The GPP estimates from these studies were either obtained various approaches including process-based models, remote-sensing calculation (MODIS), synthesized global database, and the NPP/GPP ratio based on a global study presented in Vicca et al. (2012). Here, we only considered plant GPP and therefore excluded estimates from eddy covariance measurement which included heterotrophic respiration. Our analysis showed that GPP was linearly related to APAR with the slope or light-use efficiency of  $0.33 \text{ gC mol}^{-1}$  regardless of soil nutrient status ( $p = 0.42$ , Figure 5.6a), thus supporting (5). For comparison, the derived slope fell within the LUE range found in

forests under managed and natural conditions (ranged 0.22 – 0.55 gC mol<sup>-1</sup>, Figure 5.6a gray-shaded region, estimated from LUE for NPP presented in Ruimy et al. 1994, assuming NPP/GPP = 0.47, Waring et al. 1998). The spread of data along the APAR range reflects the variability of GPP at fixed  $L$  (as observed in Figure 5.5) of forests subjected to different latitudinal locations (i.e. growing season length and solar elevation) and species-specific clumping characteristics.

According to data from Vicca et al. (2012) and a few additional studies (total 65 studies of seven pine, 10 other conifer, 16 broadleaved species and seven mixed forests; Table A5.6.6), forests with low nutrient availability converted 23% less carbon for growth than those under non-limiting nutrient conditions (combined medium- and high-nutrient in Vicca et al. (2012),  $p < 0.0001$  for the difference between soil nutrient status, Figure 5.6b). Our estimates for non-fertilized stands (i.e. PT, PS<sub>MC</sub> and PS<sub>Y</sub>) were close to the relationship for low-nutrient soil while that of PS<sub>MF</sub> was relatively lower than the relationship for high-nutrient soil (Figure 5.6b, symbols). The small deviation of PS<sub>MF</sub> estimate may be attributed to the non-measured belowground carbon which is known to be highly variable (Linder and Axelsson 1982; Helmisaari et al 2002; Xiao et al 2003). However, comparing the paired sites for the fertilization experiment, PS<sub>MF</sub> did have higher CUE (0.4) than the non-treated PS<sub>MC</sub> (0.33). Overall, our synthetic analyses revealed that forests across latitudes conservatively utilized energy for photosynthesis;

however, those subjected to limited nutrient availability will convert photosynthetic carbon less efficiently than those growing on rich soils.

## **5.5 Conclusion**

We found that the sensitivity of half-hourly canopy photosynthesis to environments was similarly dominated by stomatal conductance based on Fickian diffusion in our *P. taeda* and *P. sylvestris* forests in temperate and boreal zones. Consequently, such environmental responses affected inter-annual variation of carbon fluxes, averaged over the growing season at the high-temporal resolution. The spatial analysis of the four sites indicated that the increased mutual shading, induced by high leaf area index ( $L$ ), caused reduction in mean canopy stomatal conductance and photosynthesis. However, the compensation between increasing  $L$  and decreasing canopy photosynthesis was not complete, resulting in a slight increase in mean growing season GPP with  $L$  across the study sites. At the growing season timescale, inter-annual variation of GPP reflected changing growing season length within each site, rather than climates. Spatially, total growing season GPP increased with  $L$ , reaching saturation at high range of  $L$ . In forests with the same  $L$ , however, GPP varied with growing season length, latitudinal location (i.e. solar elevation) and clumping characteristics of the canopy. Nevertheless, GPP estimated from this study and various approaches from others was linearly related to canopy light absorption with some variability potentially

contributed to the difference in the aforementioned factors. Our synthetic analyses showed that forests of various types and latitudes utilized similar proportion of energy for photosynthesis but converting the acquired carbon for growth more efficiently under non-limiting nutrient conditions.

**Table 5.1: Definitions.** A summary of abbreviations and variables used in the study with their full definitions.

Variable	Definition	Unit
$A$	Photosynthetic rate	$\mu\text{molC m}^{-2}\text{leaf s}^{-1}$
$A_{netc}$	Net canopy photosynthesis	$\mu\text{molC m}^{-2}\text{leaf s}^{-1}$
$A_{netc,PARm}$	Net canopy photosynthesis under non-limiting light condition	$\mu\text{molC m}^{-2}\text{leaf s}^{-1}$
APAR	Absorbed photosynthetic photon flux density	$\mu\text{mol m}^{-2}\text{ s}^{-1}$ or $\text{mol m}^{-2}\text{ d}^{-1}$ or $\text{mol m}^{-2}\text{ y}^{-1}$
$C_a$	Atmospheric carbon dioxide concentration	$\mu\text{mol mol}^{-1}$
$C_i$	Leaf intercellular carbon dioxide concentration	$\mu\text{mol mol}^{-1}$
CUE	Carbon-Use Efficiency	-
$D$	Vapor pressure deficit	kPa
$E_c$	Canopy transpiration	$\text{kg m}^{-2}\text{ s}^{-1}$ or $\text{mm d}^{-1}$
GPP	Gross primary productivity	$\text{gC m}^{-2}\text{ y}^{-1}$
$G_s$	Mean canopy stomatal conductance	$\text{mmol m}^{-2}\text{leaf s}^{-1}$
$G_{sref}$	Mean canopy stomatal conductance at 1kPa D	$\text{mmol m}^{-2}\text{leaf s}^{-1}$
$G_{sref,PARm}$	Mean canopy stomatal conductance at 1kPa D under maximum light condition	$\text{mmol m}^{-2}\text{leaf s}^{-1}$
$g_s$	Leaf stomatal conductance	$\text{mmol m}^{-2}\text{leaf s}^{-1}$
$J_{max}$	Light saturated electron transport rate	$\mu\text{molC m}^{-2}\text{leaf s}^{-1}$
$J_{max25}$	Light saturated electron transport rate at 25 °C	$\mu\text{molC m}^{-2}\text{leaf s}^{-1}$
$J_s$	Sap flux density	$\text{g m}^{-2}\text{ s}^{-1}$
$L$	Leaf area index	$\text{m}^2\text{ m}^{-2}$
LUE	Light-Use Efficiency	$\text{gC mol}^{-1}$
$m$	Stomatal sensitivity to vapor pressure deficit	$\text{mmol m}^{-2}\text{ s}^{-1}\text{ ln(kPa)}^{-1}$
NPP	Net primary productivity	$\text{gC m}^{-2}\text{ y}^{-1}$
$P$	Growing season precipitation	mm
PAR	Photosynthetically active radiation	$\mu\text{mol m}^{-2}\text{ s}^{-1}$ or $\text{mol m}^{-2}\text{ d}^{-1}$ or $\text{mol m}^{-2}\text{ y}^{-1}$
PS	Refers to all <i>Pinus sylvestris</i> sites in this study	-
PS <sub>MC</sub>	Mature <i>Pinus sylvestris</i> site in northern Sweden under non-fertilized condition	-
PS <sub>MF</sub>	Mature <i>Pinus sylvestris</i> site in northern Sweden under fertilized condition	-
PS <sub>Y</sub>	Young <i>Pinus sylvestris</i> site in northern Sweden	-
PT	<i>Pinus taeda</i> site in North Carolina, USA	-
$R_{day}$	Daytime respiration rate	$\mu\text{molC m}^{-2}\text{leaf s}^{-1}$
REW	Relative Extractable Water	-

RH	Relative humidity	%
$T_A$	Air temperature	°C
$V_{cmax}$	Maximum Rubisco capacity	$\mu\text{molC m}^{-2}\text{leaf s}^{-1}$
$V_{cmax25}$	Maximum Rubisco capacity at 25 °C	$\mu\text{molC m}^{-2}\text{leaf s}^{-1}$
WUE	Water-Use Efficiency	$\text{gC mm}^{-1}$
$\theta_{FC}$	Soil moisture at field capacity	$\text{m}^3 \text{m}^{-3}$
$\theta_m$	Minimum volumetric soil moisture	$\text{m}^3 \text{m}^{-3}$
$\theta_{15}$	Volumetric soil moisture at 15 cm depth	$\text{m}^3 \text{m}^{-3}$
$\theta_{30}$	Volumetric soil moisture at 30 cm depth	$\text{m}^3 \text{m}^{-3}$

**Table 5.2: Summary of characteristics of the study forests.** *H* is mean canopy height (m), *DBH* is the diameter at breast height (cm), *L* is leaf area index averaged over the growing season (m<sup>2</sup> m<sup>-2</sup>).

Species	Location	Code name	Treatment	Growing season years	Stand density (trees ha <sup>-1</sup> )	Age (Year)	<i>H</i> (m)	<i>DBH</i> (cm)	Basal Area (m <sup>2</sup> ha <sup>-1</sup> )	Sapwood Area (m <sup>2</sup> ha <sup>-1</sup> )	<i>L</i> (m <sup>2</sup> m <sup>-2</sup> )
<i>Pinus taeda</i>	36 N 79 W	<i>Pt</i>	n/a	2003-2005	308	38	23	36	35	32	1.6
<i>Pinus sylvestris</i>	64 N 20 E	<i>PsC</i>	Control	2011-2013	1020	70	17	19	27	25	2.5
		<i>PsF</i>	Fertilized		870	70	16	18	24	22	3.1
<i>Pinus sylvestris</i>	64 N 20 E	<i>PsY</i>	n/a	2012-2013	3565	13-30	4	5	11	6	1.5

**Table 5.3:  $C_i/C_a$  ratios.** Comparisons of the ratios of intercellular and atmospheric CO<sub>2</sub> concentration ( $C_i/C_a$ ) obtained from gas exchange measurements at different heights in the canopy and estimated from the 4C-A model.

Site	Canopy position	Ci/Ca Gas-exchange measurement		Ci/Ca 4C-A	
		Mean	Standard Deviation	Mean	Standard Deviation
<b>PT</b>	Top	0.63	0.04	0.61	0.07
<b>PS<sub>MC</sub></b>	Top	0.59	0.08	0.58	0.06
	Middle	0.61	0.07	0.6	0.05
	Bottom	0.79	0.04	0.74	0.07
	<b>Total</b>	<b>0.66</b>	<b>0.11</b>	<b>0.64</b>	<b>0.10</b>
<b>PS<sub>MF</sub></b>	Top	0.64	0.08	0.61	0.07
	Middle	0.66	0.01	0.62	0.08
	Bottom	0.78	0.05	0.75	0.04
	<b>Total</b>	<b>0.69</b>	<b>0.09</b>	<b>0.66</b>	<b>0.11</b>

**Table 5.4: Summary of growing season estimates of variables used in the analyses.** DOY denotes Day of Year. Numbers in parentheses are one standard error of the three replicated plots.  $\mu$  is the average value over the study years with SD as standard deviation.

Site	Year	APAR (mol m <sup>-2</sup> gs <sup>-1</sup> ) 1)	$E_c$ (mm gs <sup>-1</sup> )	NPP (gC m <sup>-2</sup> gs <sup>-1</sup> ) 1)	GPP (gC m <sup>-2</sup> gs <sup>-1</sup> )	Growing season dates (DOY)	Growing season length (days)
<i>Pt</i>	2003	5560	205	528	1114	55 – 313	259
	2004	7036	187	536	1392	75 – 314	240
	2005	6000	211	551	1375	83 – 320	238
	$\mu \pm \text{SD}$	<b>6199±758</b>	<b>201±12</b>	<b>538±12</b>	<b>1294±156</b>		<b>246±12</b>
<i>PsC</i>	2011	3765	150	294 (26)	1295	111 – 279	169
	2012	2789	138	421 (36)	1175	136 – 281	146
	2013	3339	149	529 (56)	1289	132 – 286	155
	$\mu \pm \text{SD}$	<b>3297±490</b>	<b>146±7</b>	<b>415±24</b>	<b>1253±68</b>		<b>157±12</b>
<i>PsF</i>	2011	3718	148	560 (42)	1425	111 – 279	169
	2012	2779	125	465 (46)	1182	136 – 281	146
	2013	3228	132	552 (56)	1366	132 – 286	155
	$\mu \pm \text{SD}$	<b>3242±470</b>	<b>135±12</b>	<b>526±28</b>	<b>1324±127</b>		<b>157±12</b>
<i>PsY</i>	2012	2643	56	192	569	136 – 281	146
	2013	2945	49	213	616	132 – 286	155
	$\mu \pm \text{SD}$	<b>2794±213</b>	<b>53±5</b>	<b>203±15</b>	<b>593±33</b>		<b>151±6</b>

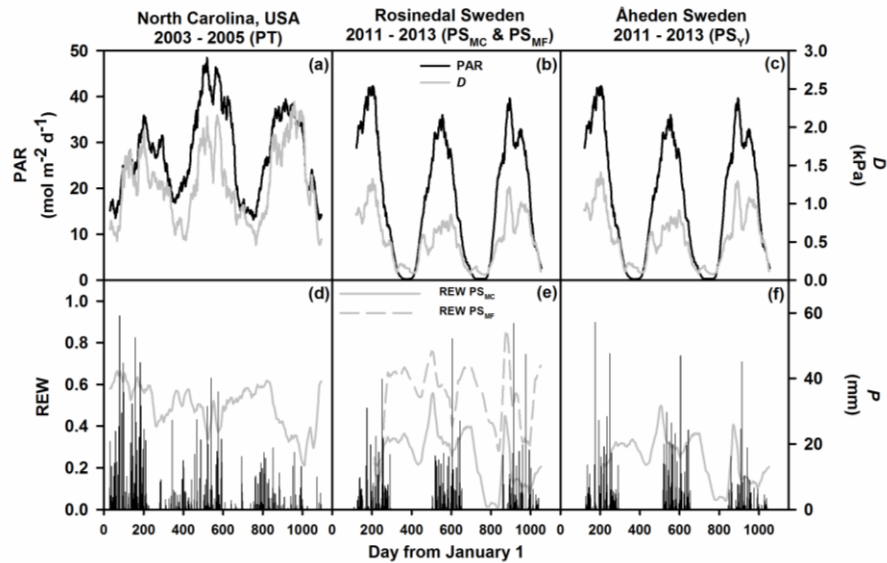


**Figure 5.1: Environmental conditions.** (a)-(c) daily sum of photosynthetically active radiation (PAR; mol m<sup>-2</sup> d<sup>-1</sup>, black lines) and daytime average vapor pressure deficit ( $D$ ; kPa, gray lines) (d)-(f) Soil moisture expressed as Relative Extractable Water (REW, gray lines) and precipitation ( $P$ , black bars). Data were presented as 30-day running mean.

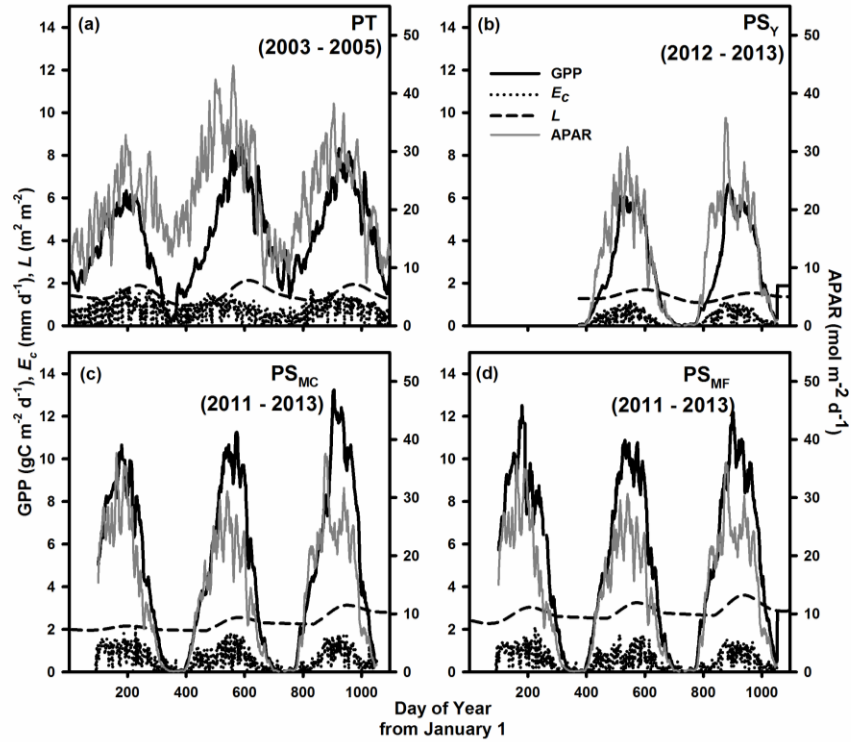


**Figure 5.2: Estimates of the variables.** Ten-day running mean of daily estimates of canopy transpiration ( $E_c$ ,  $\text{mm d}^{-1}$ , dotted lines), canopy absorbed photosynthetically active radiation (APAR,  $\text{mol m}^{-2} \text{d}^{-1}$ , gray lines), gross primary productivity (GPP,  $\text{gC m}^{-2} \text{d}^{-1}$ , black lines) and leaf area index ( $L$ ,  $\text{m}^2 \text{m}^{-2}$ , dashed lines) for all study sites.

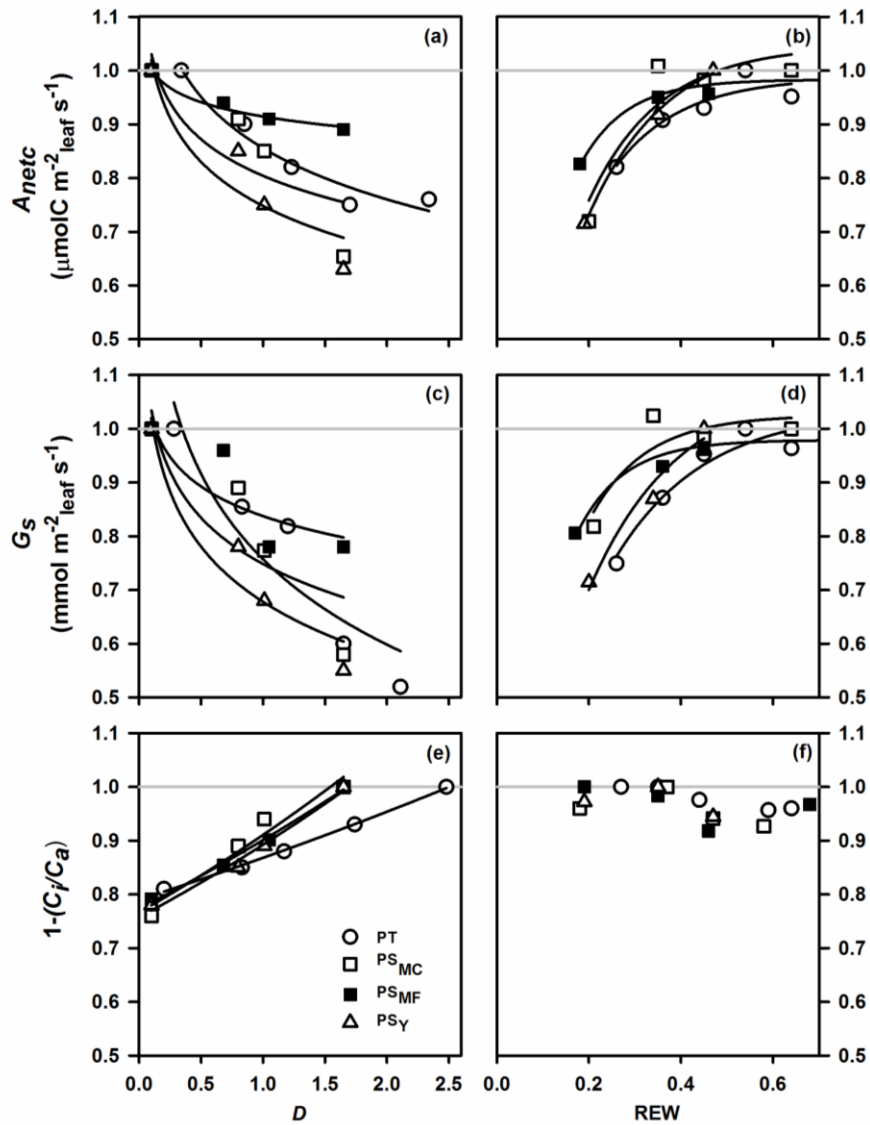


**Figure 5.3: Environmental responses of half-hourly variables.** Sensitivity of half-hourly mean canopy photosynthesis per unit leaf area ( $A_{netc}$ ), mean canopy stomatal conductance ( $G_s$ ) and the residual of intercellular- to atmospheric- $\text{CO}_2$  concentration ratio ( $1- C_i/C_a$ ) based on Fick's Law (Equation (5.3)) to vapor pressure deficit **(a),(c),(e)** and soil moisture expressed as Relative Extractable Water **(b),(d),(f)**. Values are from the boundary-line analysis (see text) and normalized by the maximum of each variable. Regression statistics are summarized in Table A5.6.3.

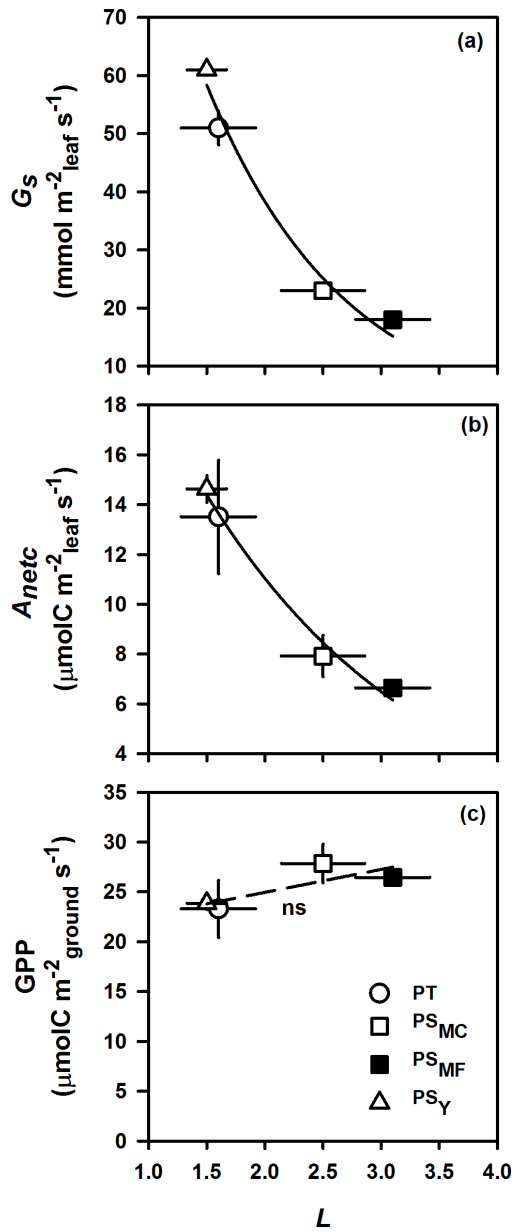


**Figure 5.4: Spatial variation of the half-hourly variables.** The relationship between (a)  $G_s$ , (b)  $A_{netC}$  and (c) GPP with leaf area index ( $L$ ) of the four sites, averaged over the growing season.

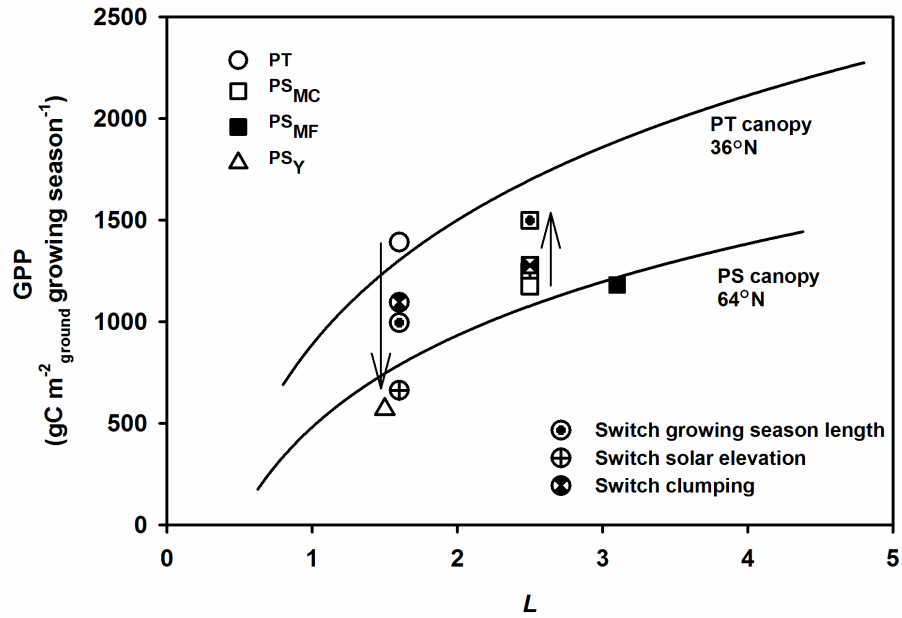


**Figure 5.5: Total growing season GPP.** The relationship between growing season GPP and  $L$  of two studied species with curves regressed from simulated GPP with various  $L$  of each species and data estimated from the four study sites (symbols with no pattern). Patterned circles (squares) indicate independently changing characteristics in the simulation to test the effects of growing season length, solar elevation associated with site latitude and clumping factors for loblolly (Scots) pine canopy.

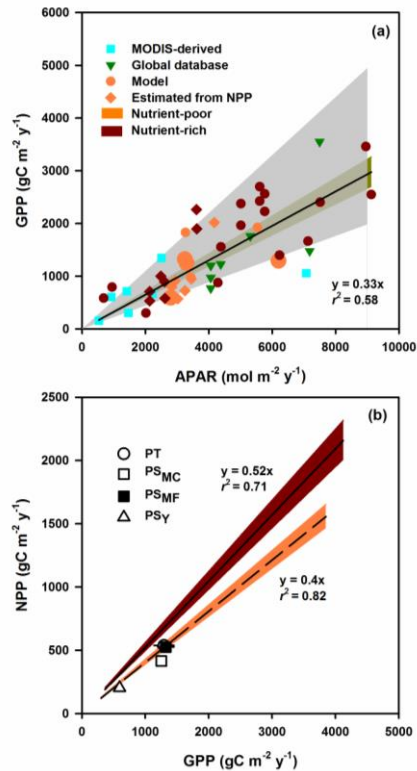


**Figure 5.6: The synthetic analyses of light- and carbon-use efficiencies. (a) The relationship of gross primary productivity (GPP) versus canopy light absorption (APAR) implies the light-use efficiency (LUE) of forests. Symbols signify different methods for estimating GPP. Orange (dark red) color represents forest on nutrient-poor (nutrient-rich) soil. The narrow, green shaded region is 95% confidence interval of the linear regression. See Table S5 for site information. Gray shaded region shows LUE estimated from the reported LUE for NPP of forests in Ruimy et al. 1994. (b) The relationship of NPP versus GPP indicates the carbon-use efficiency of forests. The linear relationships were derived from data directly obtained from Vicca et al. (2012) and other recent published studies (see Table S6). The relationship for nutrient-rich sites is the combination of medium- and rich-level of nutrients presented in Vicca et al. (2012). Symbols are the estimates from this study. Shaded regions are 95% confidence intervals of the linear fits.**

## 5.6 Supplementary Data

**Table A5.6.1: Summary of instrumentation for environmental measurements at the study sites**

Site	Variable	Number of instruments	Instrument position	Measurement Period	Measurement interval	Instrument	Manufacturer
PT	Air temperature ( $T_A$ , °C)	1	Above forest canopy	January 2003 – December	30 minutes	HMP35C probes	Campbell Scientific, Logan, UT, USA
	Relative humidity (RH)	1		2005			
	Photosynthetic photon flux density (PPFD, $\mu\text{mol m}^{-2} \text{s}^{-1}$ )	1	Above forest canopy		30 minutes	LI-190	Li-Cor BioSciences, Lincoln, NE, USA
	Latent heat flux (LE, $\text{W m}^{-2}$ )	1	Above forest canopy		30 minutes	Eddy covariance system, CSAT3 IRGA, LI-7500	Campbell Scientific, Logan, UT, USA
	Precipitation ( $P$ , mm)	1	Above forest canopy		30 minutes	TE-525M	Li-Cor BioSciences, Lincoln, NE, USA
	Volumetric soil moisture ( $\theta_{30}$ , $\text{m}^3 \text{m}^{-3}$ )	4	30 cm soil depth		30 minutes	CS615	Texas Electronics, Dallas, TX, USA
	$T_A$ , RH, PPFD, LE, $P$ , $\theta_{30}$	1			30 minutes	Datalogger CR23X	Campbell Scientific, Logan, UT, USA
Throughfall ( $P_T$ , mm)	10	Ground		Biweekly	Rain gauges (collection diameter of 0.1 m)	Productive Alternatives, Fergus Falls, MN, USA	
Leaf area index ( $\text{m}^2 \text{m}^{-2}$ )	20	Two perpendicular transects		Monthly	LAI-2000	Li-Cor BioSciences, Lincoln, NE, USA	
PS <sub>MC</sub> &	Air temperature ( $T_A$ , °C)	1	1.5 m above ground	April 2011 – November	30 minutes	HC2-S3 & MP-101A	Rotonic AG, Switzerland

<b>PS<sub>MF</sub></b>	Photosynthetic photon flux density (PPFD, $\mu\text{mol m}^{-2} \text{s}^{-1}$ )	1	Above forest canopy	2013	30 minutes	LI-190SA	Li-Cor BioSciences, Lincoln, NE, USA
	Latent heat flux (LE, $\text{W m}^{-2}$ )	1	Above forest canopy		30 minutes	Eddy covariance system, R3 LI-7200	Gill Instruments Ltd., Lymington, UK Li-Cor BioSciences, Lincoln, NE, USA
	Volumetric soil moisture ( $\theta_{15}$ , $\text{m}^3 \text{m}^{-3}$ )	1	15 cm soil depth; near the flux tower	July 2011 – November 2013	30 minutes	SM300	Delta-T devices Ltd., Cambridge, UK
		6	15 cm soil depth; around sap flux trees	June – September 2013			
	$T_A$ , RH, PPFD, LE, $P$ , $\theta_{30}$	1		April 2011 – November 2013	30 minutes	Datalogger CR10X	Campbell Scientific, Logan, UT, USA
	Throughfall ( $P_T$ , mm)	9	Ground	2013	Biwee kly	Collector (collection area of $0.5 \text{ m}^2$ )	n/a
<b>PS<sub>MF</sub></b>	Precipitation ( $P$ , mm)	1	Above forest canopy		30 minutes	Tipping bucket, ARG100	Campbell Scientific, Logan, UT, USA
<b>PS<sub>Y</sub></b>	Air temperature ( $T_A$ , °C)	1	1.7 m above ground		30 minutes	HC2-S3 & MP-101A	Rotonic AG, Switzerland
	Relative humidity (RH)	1	1.7 m above ground		30 minutes	CM3	Kipp & Zonen, Delft, Holland
	Global radiation ( $\mu\text{mol m}^{-2} \text{s}^{-1}$ )	1	1.7 m above ground		30 minutes	CM3	Kipp & Zonen, Delft, Holland
	Volumetric soil moisture ( $\theta_{15}$ , $\text{m}^3 \text{m}^{-3}$ )	4	15 cm soil depth	July 2013 – June 2014	30 minutes	CS615	Campbell Scientific, Logan, UT, USA
		1				Datalogger CR1000	Campbell Scientific, Logan, UT, USA

**Table A5.6.2:** Summary of components of the net primary productivity (NPP). Units are in gC m<sup>-2</sup> y<sup>-1</sup>. Values in parentheses represent one standard errors for the replicated plots.

Site	Year	NPP	NPP	NPP	NPP	NPP	NPP	NPP
		stem	branch	foliage	coarse roots	fine roots	cones & miscella neous litterfall	total
PT	2003	158	37	194	47	92	n/a	528
	2004	160	38	197	48	93	n/a	536
	2005	166	39	201	50	95	n/a	551
PS <sub>MC</sub>	2011	146	29	35	27	48	9	294
		(18)	(11)	(9)	(4)	(12)	(0)	(26)
	2012	114	39	99	21	138	10	421
		(13)	(25)	(22)	(3)	(6)	(0)	(36)
	2013	131	24	137	24	191	22	529
		(14)	(7)	(31)	(3)	(44)	(0)	(56)
PS <sub>MF</sub>	2011	250	48	106	54	83	19	560
		(15)	(1)	(31)	(4)	(24)	(0.1)	(42)
	2012	156	47	118	34	92	18	465
		(10)	(20)	(39)	(2)	(7)	(0.1)	(46)
	2013	166	38	153	35	119	41	552
		(11)	(7)	(43)	(3)	(33)	(0.1)	(56)
PS <sub>Y</sub>	2012	43	30	63	21	35	n/a	192
	2013	46	34	71	23	39	n/a	213

**Table A5.6.3:** Summary of regression statistics of the sensitivity of half-hourly variables to the environments (Figure 5.3).

<b>Relationship</b>	<b>Site</b>	<b>Function</b>	<b><math>r^2</math></b>	<b><math>p</math></b>
<i>A<sub>netc</sub></i> versus <i>D</i>	PT	$y = -0.14\ln(x)+0.86$	0.94	0.004
	PS <sub>MC</sub>	$y = -0.10\ln(x)+0.80$	0.53	0.17
	PS <sub>MF</sub>	$y = -0.04\ln(x)+0.91$	0.97	0.01
	PS <sub>Y</sub>	$y = -0.12\ln(x)+0.75$	0.80	0.07
<i>A<sub>netc</sub></i> versus REW	PT	$y = 0.99(1-e^{-6.01x})$	0.84	0.02
	PS <sub>MC</sub>	$y = 1.05(1-e^{-6.44x})$	0.80	0.07
	PS <sub>MF</sub>	$y = 0.98(1-e^{-10.07x})$	0.94	0.02
	PS <sub>Y</sub>	$y = 1.06(1-e^{-5.81x})$	0.99	0.03
<i>G<sub>s</sub></i> versus <i>D</i>	PT	$y = -0.23\ln(x)+0.76$	0.81	0.02
	PS <sub>MC</sub>	$y = -0.12\ln(x)+0.75$	0.59	0.15
	PS <sub>MF</sub>	$y = -0.08\ln(x)+0.84$	0.56	0.16
	PS <sub>Y</sub>	$y = -0.15\ln(x)+0.68$	0.89	0.04
<i>G<sub>s</sub></i> versus REW	PT	$y = 1.04(1-e^{-5.12x})$	0.92	0.007
	PS <sub>MC</sub>	$y = 1.03(1-e^{-8.28x})$	0.72	0.09
	PS <sub>MF</sub>	$y = 0.98(1-e^{-9.94x})$	0.93	0.02
	PS <sub>Y</sub>	$y = 1.09(1-e^{-5.15x})$	0.93	0.12
$(1-C_i/C_a)$ versus <i>D</i>	PT	$y = 0.79e^{0.09x}$	0.99	<0.001
	PS <sub>MC</sub>	$y = 0.77e^{0.17x}$	0.92	0.03
	PS <sub>MF</sub>	$y = 0.77e^{0.15x}$	0.99	0.002
	PS <sub>Y</sub>	$y = 0.76e^{0.16x}$	0.98	0.007

**Table A5.6.4:** Literature survey of water-use efficiency (WUE) in  $\text{gC mm}^{-1}$ . GPP, E and E refer to Gross Primary Productivity of forest canopy or ecosystem ( $\text{gC m}^{-2}$  growing season<sup>-1</sup>,  $\text{gC m}^{-2} \text{y}^{-1}$ ), canopy transpiration ( $\text{mm growing season}^{-1}$ ,  $\text{mm y}^{-1}$ ) and evapotranspiration ( $\text{mm y}^{-1}$ ), respectively.

Species / Forest type	Location	Definition	WUE	Reference
<i>Pinus taeda</i>	36 N 79 W	GPP / $E_c$	6.46	This study
<i>Pinus sylvestris</i> (Control)	64 N 20 E	GPP / $E_c$	8.60	
<i>Pinus sylvestris</i> (Fertilized)	64 N 20 E	GPP / $E_c$	9.81	
<i>Pinus sylvestris</i> (13-30 years old)	64 N 20 E	GPP / $E_c$	9.66	Ward 2012
<i>Pinus taeda</i> (Ambient CO <sub>2</sub> )	36 N 79 W	GPP / $E_c$	7.66	
<i>Pinus taeda</i> (Elevated CO <sub>2</sub> )	36 N 79 W	GPP / $E_c$	10.03	
<i>Liquidambar styraciflua</i> (Ambient CO <sub>2</sub> )	36 N 79 W	GPP / $E_c$	6.08	10.22
<i>Liquidambar styraciflua</i> (Elevated CO <sub>2</sub> )	36 N 79 W	GPP / $E_c$	10.22	
<i>Pinus sylvestris</i>	51 N 4 E	GPP / $E_T$	3.99	Carrara et al. 2004
Mixed conifers	50 N 6 E	GPP / $E_T$	5.08	Aubinet et al. 2002
Evergreen broadleaved forest	3 S 60 W	GPP / $E_T$	2.82	Beer et al. 2009

<i>Pseudotsuga menziesii</i>	50 N 125 W	GPP / E <sub>T</sub>	3.06	Humphreys et al. 2005
<i>Pseudotsuga menziesii</i>	50 N 124 W	GPP / E <sub>T</sub>	3.53	Jassal et al. 2008
<i>Populus tremuloides</i>	54 N 106 W	GPP / E <sub>T</sub>	3.41	Krishnan et al. 2006
<i>Picea mariana</i>	54 N 105 W	GPP / E <sub>T</sub>	3.05	Krishnan et al. 2008
<i>Fagus sylvatica</i>	51 N 10 E	GPP / E <sub>T</sub>	5.31	Knohl et al. 2003
<i>Picea abies</i>	51 N 14 E	GPP / E <sub>T</sub>	4.55	Grünwald and Bernhofer 2007
<i>Fagus sylvatica</i>	50 N 11 E	GPP / E <sub>T</sub>	5.42	Anthoni et al. 2004
Evergreen coniferous forest	39 N 0 W	GPP / E <sub>T</sub>	2.77	Sanz et al. 2004
<i>Pinus sylvestris</i>	62 N 24 E	GPP / E <sub>T</sub>	3.61	Suni et al. 2003
<i>Pinus sylvestris</i>	67 N 27 E	GPP / E <sub>T</sub>	2.82	Thum et al. 2007
<i>Fagus sylvatica</i>	49 N 7 E	GPP / E <sub>T</sub>	4.51	Granier et al. 2000c
<i>Pinus pinaster</i> Ait.	45 N 0 W	GPP / E <sub>T</sub>	2.63	Berbigier et al. 2001
<i>Quercus ilex</i>	44 N 4 E	GPP / E <sub>T</sub>	3.14	Rambal et al. 2003
<i>Fagus sylvatica</i>	42 N 14 E	GPP / E <sub>T</sub>	6.07	Valentini et al. 1996
Evergreen broadleaved forest	42 N 12 E	GPP / E <sub>T</sub>	3.51	Tirone et al. 2003
Deciduous broadleaved forest	45 N 11 E	GPP / E <sub>T</sub>	3.15	Beer et al. 2009
Deciduous broadleaved forest	45 N 9 E	GPP / E <sub>T</sub>	2.98	Beer et al. 2009

---

forest				
<i>Quercus cerris</i> L.	42 N 12 E	GPP / E <sub>T</sub>	3.54	Tedeschi et al. 2006
<i>Picea abies</i>	64 N 19 E	GPP / E <sub>T</sub>	2.66	Lindroth et al. 2007
<i>Picea rubens</i>	45 N 69 W	GPP / E <sub>T</sub>	3.98	Hollinger et al. 2004
<i>Pinus elliottii</i>	30 N 82 W	GPP / E <sub>T</sub>	2.35	Clark et al. 2004
<i>Cocos nucifera</i>	15 S 167 E	GPP / E <sub>T</sub>	3.17	Roupsard et al. 2006
<i>Pinus ponderosa</i>	44 N 121 W	GPP / E <sub>T</sub>	10.89	Law et al. 2000
Evergreen coniferous forest	2-65 N; 20 W – 25 E	GPP / E <sub>T</sub>	2.4	Law et al. 2002
Deciduous broadleaved forest	2-65 N; 20 W – 25 E	GPP / E <sub>T</sub>	3.4	
<i>Pinus banksiana</i>	54 N 104 W	GPP / E <sub>T</sub>	3.8	Mahrt and Vickers 2002
Aspen	56 N 98 W	GPP / E <sub>T</sub>	8.3	
<i>Picea engelmannii</i> / <i>Abies lasiocarpa</i>	41 N 106 W	GPP / E <sub>T</sub>	2.8	Zeller and Nikolov 2000
Aspen	53 N 106 W	GPP / E <sub>T</sub>	13.2	Ponton et al. 2006
<i>Pseudotsuga menziesii</i>	50 N 125 W	GPP / E <sub>T</sub>	19.8	
Deciduous forest	42 N 129 E	GPP / E <sub>T</sub>	9.43	Yu et al. 2007
Conifers	26 N 115 E	GPP / E <sub>T</sub>	9.27	
Evergreen broadleaved forest	23 N 112 E	GPP / E <sub>T</sub>	6.9	

---

**Table A5.6.5:** Literature survey of growing season or annual absorbed photosynthetically active radiation (APAR, mol m<sup>-2</sup> y<sup>-1</sup> or mol m<sup>-2</sup> growing season<sup>-1</sup>) and Gross Primary Productivity (GPP, gC m<sup>-2</sup> y<sup>-1</sup>) used for the analysis in Figure 5.5. We used to the same approach presented in Vicca et al. (2012) for classification of the soil; however, we only focus on poor (P) versus non-poor (NP) soils. The latter refers to either moderate or high levels of nutrient availability. The indicators for nutrient availability were based on soil type, soil nitrogen content, availability of other nutrients, cation exchange capacity, pH and water status. For the ‘Estimated from NPP’ method for estimating GPP, we used relationship of NPP versus GPP from Vicca et al. (2012) for different soil nutrient status to calculate GPP from NPP.

Species / Forest type	Latitude	L	Nutrient status	APAR (mol m <sup>-2</sup> y <sup>-1</sup> or mol m <sup>-2</sup> growing season <sup>-1</sup> )	GPP (mol m <sup>-2</sup> y <sup>-1</sup> or mol m <sup>-2</sup> growing season <sup>-1</sup> )	Method for GPP estimation	Reference
<i>Pinus sylvestris</i> (Control)	64	2.5	P	3297	1253	Model (4C-A)	This study
<i>Pinus sylvestris</i> (Fertilized)	64	3.1	P	3242	1324		
<i>Pinus sylvestris</i>	64	1.5	P	2794	593		
<i>Pinus sylvestris</i>	67	1.7	P	2352	609	Eddy Covariance	Mäkelä et al., 2008
<i>Pinus sylvestris</i>	61	2.9	P	3474	967	Eddy Covariance	Mäkelä et al., 2008
<i>Pinus sylvestris</i> / <i>Picea abies</i>	60	4.5	P	4168	2021	Estimated from NPP	Lagergren et al., 2005
<i>Pinus taeda</i>	36	1.6	P	6199	1294	Model (4C-A)	This study
<i>Pinus taeda</i> (Ambient CO <sub>2</sub> )	36	2.9	NP	9126	2550	Model (4C-A)	Ward 2012
<i>Pinus taeda</i> (Elevated CO <sub>2</sub> )	36	3.4	NP	8957	3461		
<i>Pinus alba</i> (Ambient CO <sub>2</sub> )	42	3.2	NP	5764	2230	Model (Empirical)	Gielen et al., 2001, 2005
<i>Pinus alba</i> (Elevated CO <sub>2</sub> )	42	3.4	NP	5764	2563		
<i>Pinus nigra</i> (Ambient CO <sub>2</sub> )	42	3.6	NP	5608	2424		
<i>Pinus nigra</i> (Elevated CO <sub>2</sub> )	42	4.1	NP	5608	2699		
<i>Pinus pinaster</i>	44	2.9	P	5535	1926	Model (MAESTRA)	Medlyn et al., 2005
<i>Pinus pinaster</i>	44	1.7	P	5850	1464	Eddy Covariance	Mäkelä et al., 2008
<i>Pinus ponderosa</i>	44	3	NP	3437	1404	Eddy Covariance	Mäkelä et al., 2008

<i>Pinus ponderosa</i>	44	0.8	NP	2614	581	Estimated from NPP	Runyon et al., 1994
<i>Pinus resinosa</i>	46	4.2	P	3446	953	Estimated from NPP	Ahl et al., 2004
<i>Alnus rubra</i>	44	3.9	NP	4378	1558	Model (MBL/SPA)	Runyon et al., 1994; Williams et al., 1997
<i>Juniperus occidentalis</i>	44	0.4	NP	602	302	Model (MBL/SPA)	Runyon et al., 1994; Williams et al., 1997
<i>Picea abies</i>	64	2.2	P	3429	979	Model (MAESTRA)	Medlyn et al., 2005
<i>Picea abies</i>	51	7.6	NP	5088	1695	Eddy Covariance	Mäkelä et al., 2008
<i>Picea abies</i> / <i>Pinus sylvestris</i>	60	4.3	P	4602	1076	Eddy Covariance	Mäkelä et al., 2008
<i>Picea abies</i>	64	2	P	2109	1000	Eddy Covariance	Bergh et al., 1999; Valentini et al. 2000; Law et al., 2002
<i>Picea mariana</i>	55	4.2	P	3698	682	Eddy Covariance	Mäkelä et al., 2008
<i>Picea sitchensis</i>	56	6.5	P	3262	1831	Model (MAESTRA)	Medlyn et al., 2005
<i>Picea sitchensis</i> / <i>Tsuga heterophylla</i>	44	7.2	NP	6230	1400	Model (MBL/SPA)	Runyon et al., 1994; Williams et al., 1997
<i>Pseudotsuga menziesii</i>	44	6.3	NP	7129	1665	Model (MBL/SPA)	Runyon et al., 1994; Williams et al., 1997
<i>Tsuga heterophylla</i> / <i>Pseudotsuga menziesii</i>	44	8.5	NP	7514	2404	Model (MBL/SPA)	Runyon et al., 1994; Williams et al., 1997
<i>Tsuga mertensiana</i>	44	3	NP	4285	879	Model (MBL/SPA)	Runyon et al., 1994; Williams et al., 1997
<i>Liquidambar styraciflua</i> (Ambient CO <sub>2</sub> )	36	2	NP	679	586	Model (4C-A)	Ward 2012
<i>Liquidambar styraciflua</i> (Elevated CO <sub>2</sub> )	36	2.3	NP	943	795		
<i>Liquidambar styraciflua</i> (Ambient CO <sub>2</sub> )	36	5.5	NP	3616	1900	Estimated from NPP	Norby et al., 2005
<i>Liquidambar styraciflua</i> (Elevated CO <sub>2</sub> )	36	5.5	NP	3607	2267		
<i>Populus x euamericana</i> (Ambient CO <sub>2</sub> )	42	2.3	NP	5014	1966	Model (Empirical)	Gielen et al., 2001, 2005
<i>Populus x euamericana</i> (Elevated CO <sub>2</sub> )	42	2.7	NP	5014	2377		
<i>Populus tremuloides</i> (Ambient CO <sub>2</sub> )	45	2.7	NP	2129	710	Estimated from NPP	Norby et al., 2005
<i>Populus tremuloides</i>	45	3.4	NP	2483	1004		

(Elevated CO <sub>2</sub> )							
<i>Populus tremuloides</i> / <i>Betula papyrifera</i> (Ambient CO <sub>2</sub> )	45	2.7	NP	2129	534	Estimated from NPP	Norby et al., 2005
<i>Populus tremuloides</i> / <i>Betula papyrifera</i> (Elevated CO <sub>2</sub> )	45	3.4	NP	2603	898		
<i>Populus tremuloides</i>	46	3.3	P	2828	797	Estimated from NPP	Ahl et al., 2004
Arctic tundra	71	n/a	n/a	529	158	MODIS	Turner et al., 2003, 2006
Boreal forest	55	4	n/a	2218	664	MODIS	Turner et al., 2003, 2006
Boreal humid evergreen	58	4.1	n/a	4060	973	Global database	Luyssaert et al., 2007
Boreal semiarid evergreen	59	3.4	n/a	4060	773	Global database	Luyssaert et al., 2007
Boreal semiarid deciduous	61	3.5	n/a	4060	1201	Global database	Luyssaert et al., 2007
Conifer forest	44	2.1	n/a	7073	1058	MODIS	Turner et al., 2003, 2006
Corn / soybean	40	5	n/a	921	607	MODIS	Turner et al., 2003, 2006
Desert grassland	34	4	n/a	1459	306	MODIS	Turner et al., 2003, 2006
Forested wetland	46	3.7	P	3243	728	Estimated from NPP	Ahl et al., 2004
Hardwood forest	42	3	n/a	2501	1347	MODIS	Turner et al., 2003, 2006
Mediterranean warm evergreen	40	3.5	n/a	7183	1478	Global database	Luyssaert et al., 2007
Northern hardwood	46	3.5	P	2933	911	Estimated from NPP	Ahl et al., 2004
Tallgrass prairie	39	1.6	n/a	1408	716	MODIS	Turner et al., 2003, 2006
Temperate humid evergreen	44	7	n/a	5308	1762	Global database	Luyssaert et al., 2007
Temperate humid deciduous	44	6.1	n/a	6245	1375	Global database	Luyssaert et al., 2007
Temperate semiarid evergreen	44	1.8	n/a	4372	1228	Global database	Luyssaert et al., 2007
Tropical humid evergreen	14	5.2	n/a	7495	3551	Global database	Luyssaert et al., 2007
Upland conifer	46	3.1	P	3021	573	Estimated from NPP	Ahl et al., 2004

**Table A5.6.6: Literature survey of NPP and GPP estimates used in the analysis in Figure 5.5. Units are in gC m<sup>-2</sup> y<sup>-1</sup>.** We used to the same approach presented in Vicca et al. (2012) for classification of the soil; however, we only focus on poor versus non-poor soils. The latter refers to either moderate or high levels of nutrient availability. The indicators for nutrient availability were based on soil type, soil nitrogen content, availability of other nutrients, cation exchange capacity, pH and water status.

Species	Location	Forest type	Climatic zone	Treatment	Soil type/ Nutrient condition	NPP	GPP	NPP: GPP	Reference
<i>Pinus sylvestris</i>	64 N 20 E	Conifer	Boreal	Control	Sand/Poor	415	1253	0.42	This study
	64 N 20 E	Conifer	Boreal	Fertilized	Sand/Non -poor	526	1324	0.42	
<i>Pinus sylvestris</i>	64 N 20 E	Conifer	Boreal	n/a	Sand/Poor	203	508	0.40	This study
<i>Picea mariana</i>	56 N 98 W	Conifer	Boreal	n/a	Silt clay/Poor	252	1080	0.23	Ryan et al., 1997
<i>Pinus banksiana</i>	56 N 98 W	Conifer	Boreal	n/a	Silt clay/Poor	229	880	0.26	Ryan et al., 1997
<i>Picea mariana</i>	54 N 105 W	Conifer	Boreal	n/a	Dark earth/Poor	307	1090	0.28	Ryan et al., 1997
<i>Pinus banksiana</i>	54 N 105 W	Conifer	Boreal	n/a	Dark earth/Poor	237	772	0.31	Ryan et al., 1997
<i>Picea mariana</i>	54 N 105 W	Conifer	Boreal	n/a	Peat/Poor	517	963	0.54	Malhi et al., 1999
<i>Picea mariana</i>	56 N 98 W	Conifer	Boreal	n/a	Poorly- drained/ Poor	181	812	0.22	Turner et al., 2003
<i>Pinus sylvestris</i>	63 N 30 E	Conifer	Boreal	n/a	Sand/Poor	550	1023	0.54	Zha et al., 2007
<i>Picea abies</i>	64 N 19 E	Conifer	Boreal	n/a	Sand/Poor	540	1000	0.54	Bergh et al., 1999; Valentini et al., 2000; Law et al., 2002
<i>Abies amabilis / Pinus contorta</i>	39 N 105 W	Conifer	Boreal	n/a	Sand/Poor	254	977	0.26	Ryan et al., 1991; Murty et al., 1996
<i>Populus tremuloides</i>	56 N 98 W	Broadleaf	Boreal	n/a	Silt	416	1160	0.36	Ryan et al., 1997

<i>Populus tremuloides</i>	55 N 106 W	Broadleaf	Boreal	n/a	clay/Poor	440	1350	0.33	Ryan et al., 1997
<i>Picea mariana / Pinus banksiana</i>	56 N 98 W	Mixed	Boreal	n/a	Sand/Poor	276	633	0.44	Goulden et al., 2011
<i>Pinus taeda / Liquidamber styraciflua</i>	36 N 79 W	Conifer	Temperate	Ambient CO <sub>2</sub>	Mixed/ Poor	891	2381	0.37	Schäfer et al., 2003
	36 N 79 W	Conifer	Temperate	Elevated CO <sub>2</sub>	Clayey loam/ Non-poor	1112	2769	0.40	
<i>Picea sitchensis / Tsuga heterophylla</i>	45 N 124 W	Conifer	Temperate	n/a	Sandy loam/ Non-poor	681	1400	0.49	Runyon et al., 1994; Williams et al., 1997
<i>Pseudotsuga menziesii / Quercus garryana</i>	44 N 123 W	Conifer	Temperate	n/a	Sandy loam/ Non-poor	770	1665	0.46	Runyon et al., 1994; Williams et al., 1997
<i>Tsuga heterophylla / Pseudotsuga menziesii</i>	44 N 122 W	Conifer	Temperate	n/a	Sandy loam/ Non-poor	1122	2403	0.47	Runyon et al., 1994; Williams et al., 1997
<i>Tsuga mertensiana / Abies lasiocarpa / Picea engelmannii</i>	44 N 121 W	Conifer	Temperate	n/a	Sandy loam/ Poor	373	879	0.42	Runyon et al., 1994; Williams et al., 1997
<i>Pinus ponderosa</i>	44 N 121 W	Conifer	Temperate	n/a	Sandy loam/high	159	363	0.44	Runyon et al., 1994; Williams et al., 1997
<i>Juniperus occidentalis</i>	44 N 121 W	Conifer	Temperate	n/a	Sandy loam/ Non-poor	122	302	0.40	Runyon et al., 1994; Williams et al., 1997
<i>Pinus taeda</i>	36 N 79 W	Conifer	Temperate	n/a	Sand/Poor	538	1294	0.48	This study
<i>Pinus sylvestris</i>	51 N 4 E	Conifer	Temperate	n/a	Sand/Poor	1230	3850	0.32	Xiao et al., 2003
<i>Pinus taeda</i>	34 N 79 W	Conifer	Temperate	Control	Sand/Poor	556	1313	0.42	Maier et al., 2004

	34 N 79 W	Conifer	Temperate	Irrigated	Sand/Non -poor	680	1584	0.43	
	34 N 79 W	Conifer	Temperate	Fertilized	Sand/Non -poor	1032	2550	0.40	
	34 N 79 W	Conifer	Temperate	Irrigate+ Fertilized	Sand/Non -poor	1124	2664	0.42	
<i>Pinus taeda</i>	36 N 79 W	Conifer	Temperate	n/a	Sandy loam/ Non-poor	2056	4124	0.50	Kinerson et al., 1977
<i>Pinus taeda</i>	34 N 79 W	Conifer	Temperate	Control	Sand/Poor	781	1220	0.64	Lai et al., 2002
	34 N 79 W	Conifer	Temperate	Fertilized	Sand/Non -poor	1185	1795	0.66	
<i>Pinus radiata</i>	35 S 149 E	Conifer	Temperate	Control	Sand/Poor	904	2950	0.31	Ryan et al., 1996
	35 S 149 E	Conifer	Temperate	Irrigated	Sand/Non -poor	1142	2690	0.42	
	35 S 149 E	Conifer	Temperate	Irrigated+ Fertilized	Sand/Non -poor	1720	3690	0.47	
<i>Pinus radiata</i>	42 S 172 E	Conifer	Temperate	n/a	Sandy loam/ Non-poor	960	1780	0.54	Arneth et al., 1998
<i>Pinus ponderosa</i>	44 N 121 W	Conifer	Temperate	n/a	Sandy loam/ Poor	412	1204	0.34	Law et al., 1999, 2000, 2001
<i>Pseudotsuga menziesii</i>	45 N 122 W	Conifer	Temperate	n/a	Clay loam/ Poor	597	1906	0.31	Harmon et al., 2004
<i>Picea sitchensis</i>	52 N 7 W	Conifer	Temperate	n/a	Wet mineral/ Non-poor	1381	2001	0.69	Black et al., 2004, 2007
<i>Picea abies</i>	51 N 11 E	Conifer	Temperate	n/a	Silt clay	836	1857	0.45	Anthoni et al., 2004

<i>Quercus rubra</i> / <i>Acer rubrum</i>	42 N 72 W	Broadleaf	Temperate	n/a	loam/ Non-poor Sandy	659	1246	0.53	Aber et al., 1993
<i>Nothofagus truncate</i>	41 S 172 E	Broadleaf	Temperate	n/a	loam/ Non-poor Sand/Poor	1010	2470	0.41	Benecke and Evans, 1987
<i>Alnus rubra</i>	45 N 124 W	Broadleaf	Temperate	n/a	Sandy loam/ Non-poor	813	1557	0.52	Runyon et al., 1994; Williams et al., 1997
<i>Populus trichocarpa</i> Torr. X <i>Populus deltoids</i> Barth. & Marsh.	46 N 118 W	Broadleaf	Temperate	Irrigated	Sand/Non -poor	1008	2357	0.43	Kim et al., 2008
<i>Liquidambar styraciflua</i>	35 N 84 W	Broadleaf	Temperate	Ambient CO <sub>2</sub>	Silty clay loam/ Non-poor	1032	2002	0.52	Norby et al., 2002; DeLucia et al., 2005
	35 N 84 W	Broadleaf	Temperate	Elevated CO <sub>2</sub>	Silty clay loam/ Non-poor	1198	2438	0.49	
<i>Betula ermanii</i> / <i>Betula platyphylla</i> / <i>Quercus mongolia</i>	36 N 137 E	Broadleaf	Temperate	n/a	Non-poor	817	1146	0.71	Saigusa et al., 2005
<i>Quercus alba</i> / <i>Quercus pinus</i> / <i>Carya ovate</i>	36 N 84 W	Broadleaf	Temperate	n/a	Silt loam/ Poor	944	1725	0.55	Malhi et al., 1999
<i>Populus alba</i>	42 N 11 E	Broadleaf	Temperate	Ambient CO <sub>2</sub>	Loam/ Non-poor	1493	2585	0.58	Gielen et al., 2005
	42 N 11 E	Broadleaf	Temperate	Elevated CO <sub>2</sub>	Loam/ Non-poor	2029	2829	0.72	
<i>Populus nigra</i>	42 N 11 E	Broadleaf	Temperate	Ambient CO <sub>2</sub>	Loam/ Non-poor	1983	2773	0.72	Gielen et al., 2005

	42 N 11 E	Broadleaf	Temperate	Elevated CO <sub>2</sub>	Loam/ Non-poor	2413	2921	0.83	
<i>Populus x euramericana</i>	42 N 11 E	Broadleaf	Temperate	Ambient CO <sub>2</sub>	Loam/ Non-poor	1532	2150	0.71	Gielen et al., 2005
	42 N 11 E	Broadleaf	Temperate	Elevated CO <sub>2</sub>	Loam/ Non-poor	1853	2550	0.73	
<i>Fagus sylvatica</i>	48 N 7 E	Broadleaf	Temperate	n/a	Luvisol/ Poor	622	1584	0.39	Granier et al., 2000c; Campioli et al., 2011
<i>Alnus glutinosa</i>	54 N 10 E	Broadleaf	Temperate	n/a	Sand/Poor	895	2420	0.37	Dilly et al., 2000; Kutsch et al., 2001
<i>Fagus sylvatica</i>	55 N 10 E	Broadleaf	Temperate	n/a	Sand/Poor	702	1324	0.53	Dilly et al., 2000; Kutsch et al., 2001
Broadleaf forest	44 N 71 W	Broadleaf	Temperate	n/a	Spodosols /Non-poor	548	1053	0.52	Ollinger and Smith, 2005
<i>Fagus sylvatica</i>	51 N 10 E	Broadleaf	Temperate	n/a	Cambisols /Non-poor	669	1594	0.42	Knohl et al., 2003
Mixed species	35-45 N 84- 90 W	Broadleaf	Temperate	n/a	Poor	550	1279	0.43	Curtis et al., 2002; Law et al., 2002
<i>Fagus sylvatica</i>	48 N 7 E	Broadleaf	Temperate	n/a	Luvisol/ Non-poor	1004	1434	0.70	Valentini et al., 2000; Granier et al., 2008
<i>Alnus glutinosa / Fraxinus excelsior</i>	53 N 10 E	Broadleaf	Temperate	n/a	Non-poor	685	1594	0.43	Kutsch et al., 2005
<i>Fagus sylvatica</i>	54 N 10 E	Broadleaf	Temperate	n/a	Non-poor	720	1470	0.49	Kutsch et al., 2005
<i>Quercus robur</i>	55 N 10 E	Broadleaf	Temperate	n/a	Non-poor	1130	1794	0.63	Kutsch et al., 2005
<i>Acer pseudoplatanus / Fraxinus excelsior</i>	51 N 1 W	Broadleaf	Temperate	n/a	Cambisols / Non- poor	802	2110	0.38	Fenn et al., 2010
<i>Populus grandidentata / Populus tremuloides</i>	45 N 84 W	Broadleaf	Temperate	n/a	Spodosols / Poor	675	1350	0.50	Schmid et al., 2003; Gough et al., 2007
<i>Pinus strobus / Acer</i>	45 N 84 W	Mixed	Temperate	n/a	Sand/Poor	661	1221	0.54	Curtis et al., 2005

<i>rubrum</i>										
<i>Quercus alba</i> / <i>Quercus coccinea</i>	41 N 73 W	Mixed	Temperate	n/a	Sand/Poor	598	1324	0.45	Whittaker and Woodwell, 1969	
<i>Quercus rubra</i> / <i>Acer rubrum</i> / <i>Taxus Canadensis</i>	43 N 72 W	Mixed	Temperate	n/a	Glacial till/ Non-poor	637	1639	0.39	Turner et al., 2003	
<i>Pinus halepensis</i> Mill.	31 N 35 E	Conifer	Semi-arid	n/a	Rendzina/ Poor	344	899	0.38	Maseyk et al., 2008	
Mixed species	26 N 115 E	Conifer	Tropical	n/a	Red earth/ Poor	1010	1870	0.54	Ma et al., 2008	
<i>Eucalyptus saligna</i>	20 N 156 W	Broadleaf	Tropical	Control	Typic hydrudan d/ Non-poor	1485	2950	0.50	Giardina et al., 2003	
				Fertilized	Typic hydrudan d/ Non-poor	2100	3950	0.53		
Mixed species	2 S 60 W	Broadleaf	Tropical	n/a	Clay/Poor	1064	3040	0.35	Chambers et al., 2004; Malhi et al, 2009	
<i>Dipterocarp</i> ( <i>Shorea siamensis</i> , <i>Vitex peduncularis</i> , <i>Xylia xylocarpa</i> )	14 N 98 E	Broadleaf	Tropical	n/a	Ultisol/ Poor	1518	3230	0.47	Clark et al., 2001; Hirata et al., 2008	
Mixed species	3 S 54 W	Broadleaf	Tropical	n/a	Poor	900	3000	0.30	Goulden et al., 2004	
>200 species per ha	2 S 50 W	Mixed	Tropical	n/a	Oxisols / Poor	1560	3040	0.51	Malhi et al., 1999	
Mixed species	1 S 51 W	Mixed	Tropical	n/a	Latosol/ Poor	1234	3630	0.34	Carswell et al., 2002; Aragao et al., 2009	

## 6. Concluding Remarks

Through a series of research studies on forest ecosystems, I quantified and analyzed the temporal and spatial variabilities of water and carbon fluxes using a widely-used technique of sap-flux measurement and a process-based modelling approach. In the comparative studies, I extracted data from a number of published studies to expand the database used for my analyses. Although the methods of data extraction and estimation were based on known principles and previous findings, there could be errors involved that may generate some bias. Therefore, the general relationships found in this dissertation should be regarded as implications for further development of ecosystem modelling which will benefit global climate prediction, rather than being directly applied to the models. Nevertheless, I believe that my studies have demonstrated the need for careful considerations of ecosystem modelling approaches that are currently applied in the global climate models and for further investigation in the water and carbon studies of global forests based on field-based measurements at the canopy scale.

## References

- Aber JD, Magill A, Boone R, Melille JM, Steudler P, Bowden R (1993) Plant and soil responses to chronic nitrogen additions at the Harvard Forest, Massachusetts. *Ecol Appl* 3: 156 – 166.
- Abrahamson DA, Dougherty PM, Zarnoch SJ (1998) Hydrological components of a young loblolly pine plantation on a sandy soil with estimates of water use and loss. *Water Resources Research*, **34**, 3503 - 3513.
- Abtew W, Melesse A (2013) *Evaporation and Evapotranspiration Measurement and Estimations*. Springer Netherlands.
- Addington RN, Donovan LA, Mitchell RJ *et al.* (2006) Adjustments in hydraulic architecture of *Pinus palustris* maintain similar stomatal conductance in xeric and mesic habitats. *Plant, Cell & Environment*, **29**, 535 – 545.
- Ågren GI (1983) Nitrogen productivity of some conifers. *Canadian Journal of Forest Research*, **14**, 494 - 500.
- Ahl DE, Gower ST, Mackay DS, Burrows SN, Norman JM, Diak GR (2004) Heterogeneity of light use efficiency in a northern Wisconsin forest: implications for modelling net primary production with remote sensing. *Remote Sense Environ* 93: 168 – 178.
- Ainsworth EA, Long SP (2005) What have we learned from 15 years of free-air CO<sub>2</sub> enrichment (FACE)? A meta-analytic review of the responses of photosynthesis, canopy properties and plant production to rising CO<sub>2</sub>. *New Phytologist*, **165**, 351 - 372.
- Ainsworth EA, Rogers A (2007) The response of photosynthesis and stomatal conductance to rising [CO<sub>2</sub>]: mechanisms and environmental interactions. *Plant, Cell & Environment*, **30**, 258 - 270.
- Albrektson A, Valinger E, Johnson C (1984) Några funktioner för bestämning av tallars biomassa i södra Norrland. *SST* **82**, 5 - 12.

- Alder NN, Sperry JS, Pockman WT (1996) Root and stem xylem embolism, stomatal conductance, and leaf turgor in *Acer grandidentatum* populations along a soil moisture gradient. *Oecologia*, **105**, 293 – 301.
- Alo CA, Wang G (2008) Potential future changes of the terrestrial ecosystem based on climate projections by eight general circulation models. *Journal of Geophysical Research*, **113**, G01004, doi:10.1029/2007JG000528.
- Amponsah IG, Lieffers VJ, Comeau PG, Brockley RP (2004) Growth response and sapwood hydraulic properties of young lodgepole pine following repeated fertilization. *Tree Physiology*, **24**, 1099 – 1108.
- Amponsah IG, Comeau PG, Brockley RP, Lieffers VJ (2005) Effects of repeated fertilization on needle longevity, foliar nutrition, effective leaf area index, and growth characteristics of lodgepole pine in interior British Columbia, Canada. *Canadian Journal of Forest Research*, **35**, 440 - 451.
- Amthor JS (1984) The role of maintenance respiration in plant growth. *Plant, Cell and Environment*, **7**, 561 - 569.
- Amundson R (2001) The carbon budget in soils. *Ann Rev Earth Plan Sci* 29: 535-562.
- Andre J-C, Bougeault P, Mahfouf J-F, Mascart P, Noilham J, Pinty J-C (1989) Impacts of forests on mesoscale meteorology. *Philosophical Transactions of The Royal Society B*, **324**, 407 - 422.
- Angstmann JL, Ewers BE, Kwon H (2012) Size-mediated tree transpiration along soil drainage gradients in a boreal black spruce forest wildfire chronosequence. *Tree Physiology*, **32**, 599 - 611.
- Anthoni PM, Knohl A, Rebmann C, Freibauer A, Mund M, Ziegler W et al. (2004) Forest and agricultural land-use-dependent CO<sub>2</sub> exchange in Thuringia, Germany. *Global Change Biol* 10: 2005-2019.
- Apps MJ, Kurz WA, Luxmoore RJ et al. (1993) Boreal forests and tundra. *Water, Air, and Soil Pollution*, **70**, 39 - 53.
- Aragao L, Malhi Y, Metcalfe DB, Silva-Espejo JE, Jimenez E, Navarrete D et al.

- (2009) Above- and below-ground net primary productivity across ten Amazonian forests on contrasting soils. *Biogeosci* 6: 2759-2778.
- Arneeth A, Kelliher FM, McSeveny TM, Byers JN (1998) Net ecosystem productivity, net primary productivity and ecosystem carbon sequestration in a *Pinus radiata* plantation subject to soil water deficit. *Tree Physiol* 18: 785 – 793.
- Atkin OK, Tjoelker MG (2003) Thermal acclimation and the dynamic response of plant respiration to temperature. *Trends in Plant Science*, 8, 343 - 351.
- Aubinet M, Heinesch B, Longdoz B (2002) Estimation of the carbon sequestration by a heterogeneous forest: Night flux corrections, heterogeneity of the site and inter-annual variability. *Global Change Biol* 8: 1053 – 1072.
- Avissar R, Avissar P, Mahrer Y, Bravdo BA (1985) A model to simulate response of plant stomata to environmental conditions. *Agricultural and Forest Meteorology*, 34, 21 – 29.
- Baldocchi DD, Falge E, Gu L et al. (2001) FLUXNET: A new tool to study the temporal and spatial variability of ecosystem-scale carbon dioxide, water vapor and energy flux densities. *Bull Am Meteorol Soc* 82: 2415 – 2434.
- Baldwin VC, Peterson KD (1997) Predicting the crown shape of loblolly pine trees. *Canadian Journal of Forest Research*, 27, 102 - 107.
- Baldwin VC, Peterson KD, Burkhatt HE, Amateis RL, Dougherty PM (1997) Equations for estimating loblolly pine branch and foliage weight and surface area distributions. *Canadian Journal of Forest Research*, 27, 918 - 927.
- Ball JT, Woodrow IE, Berry JA (1987) A model predicting stomatal conductance and its contribution to the control of photosynthesis under different environmental conditions. In: Biggins J, ed. *Progress in Photosynthesis Research*. Springer Netherlands, 221 - 224.
- Barclay H (2001) Distribution of leaf orientations in six conifer species. *Botany*, 79, 389 – 397.
- Barr AG, Black TA, Hogg EH et al. (2007) Climatic controls on the carbon and water balances of a boreal aspen forest, 1994-2003. *Global Change Biology*, 13, 561 – 576.

- Bates BC, Kundzewicz ZW, Wu S, Palutikof JP, eds. (2008) Climate change and water. Technical Paper. Geneva: Intergovernmental Panel on Climate Change (IPCC) Secretariat. 210 p.
- Beer C, Reichstein M, Ciais P, Farquhar GD, Papale D (2007) Mean annual GPP of Europe derived from its water balance. *Geophys Res Lett* 34: L05401, doi: 10.1029/2006GL029006.
- Beer C, Ciais P, Reichstein M, Baldocchi D, Law BE, Papale D, Soussana J-F, Ammann C, Buchmann N, Frank D, Gianelle D, Janssens IA, Knohl A, Köstner B, Moors E, Rouspard O, Verbeeck H, Vesala T, Williams CA, Wohlfahrt G (2009) Temporal and among-site variability of inherent water use efficiency at the ecosystem level. *Global Biogeochem Cycle* 23: GB2018, doi:10.1029/2008GB003233.
- Benecke U, Evans G (1987) Growth and water use in *Nothofagus truncata* (hard beech) in temperate hill country, Nelson, New Zealand. In *The Temperate Forest Ecosystem*. Eds. Y. Hanxi, W. Zhan, J.N.R. Jeffers and P.A. Ward. ITE Symposium No. 20., Institute of Terrestrial Ecology, Grange over Sands, Cumbria, U.K. pp 131-140.
- Benyon RG, Doody TM (2014) Comparison of interception, forest floor evaporation and transpiration in *Pinus radiata* and *Eucalyptus globulus* plantations. *Hydrological Processes* DOI: 10.1002/hyp.10237.
- Berbigier P, Bonnefond J-M, Mellmann P (2001) CO<sub>2</sub> and water vapour fluxes for 2 years above Euroflux forest site. *Agricultural and Forest Meteorology*, **108**, 183 – 197.
- Berg B, Berg MP, Box E *et al.* (1993) Litter mass loss in pine forests of Europe: relationship with climate and litter quality. In: Breymeyer A, Krawczyk B, Kulikowski R, Solon J, Rosciszewski M, Jaworska B, eds. *Geography of Organic Matter Production and Decay*. Polish Academy of Sciences, Warsaw, Poland, 81 - 109.
- Bergh J, Linder S, Bergström J (2005) Potential production of Norway spruce in Sweden. *Forest Ecology and Management*, **204**, 1 – 10
- Berg Hasper T, Wallin G, Lamba S *et al.* (in review) Water use by Swedish boreal forests in a changing climate.

- Betts R, Cox PM, Lee SE, Woodward FI (1997) Contrasting physiological and structural vegetation feedbacks in climate change simulations. *Nature*, **387**, 796 – 799.
- Betts RA, Boucher O, Collins M *et al.* (2007) Projected increase in continental runoff due to plant responses to increasing carbon dioxide. *Nature*, **448**, 1037-U5.
- Binkley D, Campoe OC, Gspalti M, Forrester DI (2013) Light absorption and use efficiency in forests: Why patterns differ for trees and stands. *Forest Ecology and Management*, **288**, 5 - 13.
- Björkman O, Demmig B, Andrew TJ (1988) Mangrove photosynthesis: response to high-irradiance stress. *Australian Journal of Plant Physiology*, **15**, 43 - 61.
- Black TA (1979) Evapotranspiration from Douglas fir stands exposed to soil water deficits. *Water Resources Research*, **15**, 164 - 170.
- Black K, Tobin B, Saiz G, Byrne KA, Osborne B (2004) Improved estimates of biomass expansion factors for Sitka spruce. *Irish For* 61: 50-65.
- Black K, Bolger T, Davis P, Nieuwenhuis M, Reidy B, Saiz G *et al.* (2007) Inventory and eddy covariance-based estimates of annual carbon sequestration in a Sitka spruce (*Picea sitchensis* (Bong.) Carr.) forest ecosystem. *Eur J For Res* 126: 167-178.
- Boisvenue C, Running SW (2006) Impacts of climate change on natural forest productivity – evidence since the middle of the 20<sup>th</sup> century. *Global Change Biology*, **12**, 862 – 882.
- Bonan GB (2008) Forests and climate change: forcings, feedbacks, and the climate benefits of forests. *Science*, **320**, 1444 – 1449.
- Bosveld FC, Bouten W (2001) Evaluation of transpiration models with observations over a Douglas-fir forest. *Agricultural and Forest Meteorology*, **108**, 247 – 264.
- Bounoua L, Hall FG, Sellers PJ, Kumar A, Collatz GJ, Tucker CJ, Imhoff ML (2010) Quantifying the negative feedback of vegetation to greenhouse warming: A modeling approach. *Geophysical Research Letters*, **37**, L23701.
- Bradshaw CJA, Warkentin IG (2015) Global estimates of boreal forest carbon stocks and flux. *Global and Planetary Change*, **128**, 24 – 30.

- Bréda N, Cochard H, Dreyer E, Granier A (1993) Water transfer in a mature oak stand (*Quercus petraea*): seasonal evolution and effects of a severe drought. *Canadian Journal of Forest Research*, **3**, 1136–1143.
- Bréda N, Granier A (1996) Intra- and interannual variations of transpiration, leaf area index and radial growth of a sessile oak stand (*Quercus petraea*). *Annals of Forest Science*, **53**, 521 - 536.
- Bréda NJJ (2003) Ground-based measurements of leaf area index: a review of methods, instruments and current controversies. *J Exp Bot* 54: 2403-2417.
- Brito P, Lorenzo JR, González-Rodríguez ÁM, Morales D, Wieser G, Jimenez MS (2014) Canopy transpiration of a *Pinus canariensis* forest at the tree line: implications for its distribution under predicted climate warming. *European Journal of Forest Research*, **133**, 491 - 500.
- Brodribb TJ, Feild TS (2010) Leaf hydraulic evolution led a surge in leaf photosynthetic capacity during early angiosperm diversification. *Ecology Letters*, **13**, 175 – 183.
- Brodribb TJ, Holbrook NM (2003) Stomatal closure during leaf dehydration, correlation with other leaf physiological traits. *Plant Physiology*, **132**, 2166 – 2173.
- Buckley TN, Robert DW (2005) How should leaf area, sapwood area and stomatal conductance vary with tree height to maximize growth? *Tree Physiology*, **26**, 145.
- Cain MD (1990) Incidental observations on the growth and survival of loblolly and shortleaf pines in an even-aged natural stand. *Southern Journal of Applied Forestry*, **14**, 81 - 84.
- Campbell GS, Norman JM (1998) An introduction to environmental biophysics. Springer-Verlag, New York.
- Campioli M, Gielen B, Göckede M, Papale D, Bouriaud O, Granier A (2011) Temporal variability of the NPP-GPP ratio at seasonal and interannual time scales in a temperate beech forest. *Biogeosci* 8: 2481 – 2492.
- Canham CD (1988) Growth and canopy architecture of shade-tolerant trees: response to canopy gaps. *Ecology*, **69**, 786 - 795.

- Cao L, Bala G, Caldeira K, Nemani R, Ban-Weiss G (2010) Importance of carbon dioxide physiological forcing to future climate change. *Proceedings of the National Academy of Sciences USA*, **107**, 9513 - 9518.
- Carpenter SR, Frost TM, Heisey D, Kratz TK (1989) Randomized Intervention Analysis and the interpretation of whole-ecosystem experiments. *Ecology*, **70**, 1142 - 1152.
- Carrara A, Janssens IA, Curiel Yuste J, Ceulemans R (2004) Seasonal changes in photosynthesis, respiration and NEE of a mixed temperate forest. *Agric For Meteorol* 126: 15 – 31.
- Carswell FE, Costa AL, Palheta M, Malhi Y, Meir P, Costa DR et al. (2002) Seasonality in CO<sub>2</sub> and H<sub>2</sub>O flux at an eastern Amazonian rain forest. *J Geophys Res* 107: 8076.
- Casella E, Ceulemans R (2002) Spatial distribution of leaf morphological and physiological characteristics in relation to local radiation regime within the canopies of 3-year-old *Populus* clones in coppice culture. *Tree Physiology*, **22**, 1277 – 1288.
- Čermák J, Cienciala E, Kučera J, Hallgren JE (1992) Radial velocity profiles of water flow in trunks of Norway spruce and oak and the response of spruce to severing. *Tree Physiology*, **10**, 367-380.
- Čermák J, Cienciala E, Kučera J, Lindroth A, Bednářová E (1995) Individual variation of sap-flow rate in large pine and spruce trees and stand transpiration: a pilot study at the central NOPEX site. *Journal of Hydrology*, **168**, 17 - 27.
- Chambers JL, Hinckley TM, Cox GS, Metcalf CL, Aslin RG (1985) Boundary-line analysis and models of leaf conductance for four oak-hickory forest species. *Forest Science*, **31**, 437 – 450.
- Chambers JQ, Tribuzy ES, Toledo LC, Crispim BF, Higuchi N, dos Santos J et al. (2004) Respiration from a tropical forest ecosystem: Partitioning of sources and low carbon use efficiency. *Ecol Appl* 14: S72-S88.
- Chandler RF, Jr., Schoen PW, Anderson DA (1943) Relation between soil types and the growth of loblolly pine and shortleaf pine in east Texas. *Journal of Forestry*, **41**, 505 - 506.

- Chapin FS, Matson PA, Mooney HA, Chapin MC (2002) Principles of terrestrial ecosystem ecology. Springer-Verlag, New York, NY.
- Chen SG, Shao BY, Impens I, Ceulemans R (1994) Effects of plant canopy structure on light interception and photosynthesis. *Journal of Quantitative Spectroscopy and Radiative Transfer*, **52**, 115 - 123.
- Clapp RB, Hornberger GM (1978) Empirical equations for some hydraulic properties. *Water Resource Research*, **14**, 601 – 604.
- Clark DA, Brown S, Kicklighter DW, Chambers JQ, Thomlinson JR, Ni J et al. (2001) Net primary production in tropical forests: An evaluation and synthesis of existing field data. *Ecol Appl* 11: 371-384.
- Clark K, Gholz H, Castro M (2004) Carbon dynamics along a chronosequence of slash pine plantations in north Florida. *Ecol Appl* 14: 1154 – 1171.
- Clearwater MJ, Meinzer FC, Andrade JL, Goldstein G, Holbrook M (1999) Potential errors in measurement of nonuniform sap flow using heat dissipation probes. *Tree Physiology*, **19**, 681 – 687.
- ClimateBC\_Map – An interactive platform for visualization and data access.  
<http://climatemodels.forestry.ubc.ca/climatebc/> (28 July 2014, date last accessed).
- Cochard H, Breda N, Granier A (1996) Whole tree hydraulic conductance and water loss regulation in *Quercus* during drought: evidence for stomatal control of embolism? *Annals of Forest Science*, **53**, 197 – 206.
- Collins M, Knutti R, Arblaster J *et al.* (2013) Long-term Climate Change : Projections, Commitments and Irreversibility. In: Stocker TF, Qin D, Plattner G-K, Tignor M, Allen SK, Boschung J, Nauels A, Xia Y, Bex V, Midgley PM, eds. *Climate Change 2013 : The Physical Science Basis. Contribution of Working Group I to the Fifth Assessment Report of the Intergovernmental Panel on Climate Change*, Cambridge University Press, Cambridge, UK and New York, NY, USA.
- Curtis PS, Hanson PJ, Bolstad P, Barford C, Randolph JC, Schmid HP et al. (2002) Biometric and eddy-covariance based estimates of annual carbon storage in five eastern North American deciduous forests. *Agric For Meteorol* 113: 3-19.

- Curtis PS, Vogel CS, Gough CM, Schmid HP, Su H-B, Bovard BD (2005) Respiratory carbon losses and the carbon-use efficiency of a northern hardwood forest, 1999-2003. *New Phytol* 167: 437 – 456.
- De Boer HJ, Lammertsma EI, Wagner-Cremer F, Dilcher DL, Wassen MJ, Dekker SC. (2011) Climate forcing due to optimization of maximal leaf conductance in subtropical vegetation under rising CO<sub>2</sub>. *Proceedings of the National Academy of Sciences USA*, **108**, 4041 - 4046.
- De Kauwe MG, Medlyn BE, Zaehle S *et al.* (2013) Forest water use and water use efficiency at elevated CO<sub>2</sub>: a model-data intercomparison at two contrasting temperate forest FACE sites. *Global Change Biology*, **19**, 1759 – 1779.
- DeLucia EH, Drake JE, Thomas RB, Gozales-Meler M (2007) Forest carbon use efficiency: is respiration a constant fraction of gross primary production? *Glob Change Biol* 13: 1157 – 1167.
- Delzon S, Loustau D (2005) Age-related decline in stand water use : sap flow and transpiration in a pine forest chronosequence. *Agricultural and Forest Meteorology*, **129**, 105 - 119.
- Dewar RC, Medlyn BE, McMurtrie RE (1998) A mechanistic analysis of light and carbon use efficiencies. *Plant Cell Environ* 21: 573 – 588.
- Dewar RC, Tarvainen L, Parker K, Wallin G, McMurtrie RE (2012) Why does leaf nitrogen decline within tree canopies less rapidly than light? An explanation from optimization subject to a lower bound on leaf mass per area. *Tree Physiology*, **32**, 520 - 534.
- Dilly O, Bach HJ, Buscot F, Eschenbach C, Kutsch WL, Middelhoff U *et al.* (2000) Characteristics and energetic strategies of the rhizosphere in ecosystems of the Bornhoved Lake district. *Appl Soil Ecol* 15: 201-210.
- Dixon RK, Andrasko KJ, Sussman FG, Lavinson MA, Trexler MC, Vinson TS (1993) Forest sector carbon offset projects: near-term opportunities to mitigate greenhouse gas emissions. *Water, Air, and Soil Pollution*, **70**, 561 – 577.
- Dixon RK, Brown S, Houghton RA, Solomon AM, Trexler MC, Wisniewski J (1994) Carbon pools and flux of global forest ecosystems. *Science*, **263**, 185 - 190.

- Domec J-C, Palmroth S, Ward EJ, Maier CA, Th  r  zienne M, Oren R (2009) Acclimation of leaf hydraulic conductance and stomatal conductance of *Pinus taeda* (loblolly pine) to long-term growth in elevated CO<sub>2</sub> (free-air CO<sub>2</sub> enrichment) and N-fertilization. *Plant, Cell & Environment*, **32**, 1500 - 1512.
- Domec J-C, Sch  fer KVR, Oren R, Kim H-S, McCarthy HR (2010) Variable conductivity and embolism in roots and branches of four contrasting tree species and their impacts on whole-plant hydraulic performance under future atmospheric CO<sub>2</sub> concentration. *Tree Physiology*, **30**, 1001 - 1015.
- Domec J-C, Sun G, Noormets A *et al.* (2012) A comparison of three methods to estimate evapotranspiration in two contrasting loblolly pine plantations: age-related changes in water use and drought sensitivity of evapotranspiration components. *Forest Science*, **58**, 497 - 512.
- Douville H, Planton S, Royer J-F *et al.* (2000) Importance of vegetation feedbacks in doubled-CO<sub>2</sub> climate experiments. *Journal of Geophysical Research*, **105**, 14841 - 14861.
- Eamus D, Jarvis PG (1989) The direct effects of increase in the global atmospheric CO<sub>2</sub> concentration on natural and commercial temperate trees and forests. In: Begon A, MacFadyen A, eds. *Advances in ecological research*. London, UK: Academic Press, 1 - 55.
- Elfving B, Norgren O (1993) Volume yield superiority of lodgepole pine compared to Scots pine in Sweden. In: Lindgren D, ed. *Pinus contorta from untamed forests to domesticated crop*. Proceedings of the IUFRO meeting and Frans Kempe Symposium 1992 on *Pinus contorta* provenances and breeding. Dept of Forest Genetics and Plant Physiology, Swed Univ Agril Sci, Ume  , Report 11, 69 - 80.
- Elfving B, Ericsson T, Rosvall O (2001) The introduction of lodgepole pine for wood production in Sweden – a review. *Forest Ecology and Management*, **141**, 15 - 29.
- Emhart VI, Martin TA, White TL, Huber DA (2007) Clonal variation in crown structure absorbed photosynthetically active radiation and growth of loblolly pine and slash pine. *Tree Physiology*, **27**, 412 – 430.
- Engelmark O, Sj  berg K, Andersson B *et al.* (2001) Ecological effects and management aspects of an exotic tree species: the case of lodgepole pine in Sweden. *Forest Ecology and Management*, **141**, 3 - 13.

- Enquist BJ, Niklas KJ (2001) Invariant scaling relations across tree-dominated communities. *Nature*, **410**, 655 - 660.
- Ewers BE, Oren R (2000) Analyses of assumptions and errors in the calculation of stomatal conductance from sap flux measurements. *Tree Physiology*, **20**, 579 - 589.
- Ewers BE, Oren R, Albaugh TJ, Dougherty PM (1999) Carry-over effects of water and nutrient supply on water use of *Pinus taeda*. *Ecological Applications*, **9**, 513 – 525.
- Ewers BE, Oren R, Sperry JS (2000) Influence of nutrient versus water supply on hydraulic architecture and water balance in *Pinus taeda*. *Plant, Cell & Environment*, **23**, 1055–1066.
- Ewers BE, Oren R, Phillips N, Strömgren M, Linder S (2001) Mean canopy stomatal conductance responses to water and nutrient availabilities in *Picea abies* and *Pinus taeda*. *Tree Physiology*, **21**, 841 – 850.
- Ewers BE, Mackay DS, Samanta S (2007) Interannual consistency in canopy stomatal conductance control of leaf water potential across seven tree species. *Tree Physiology*, **27**, 11-24.
- Fan S, Gloor M, Mahlman J, Pacala S, Sarmiento J, Takahashi T, Tans P (1998) A large terrestrial carbon sink in North America implied by atmospheric and oceanic carbon dioxide data and models. *Science*, **282**, 442-446.
- Farnden C (1996) Stand density management diagrams for lodgepole pine, white spruce and interior Douglas-fir. Pacific Forestry Centre. Information Report BC-X-360. Canadian Forest Service. Victoria, British Columbia.
- Farquhar GD, von Caemmerer S, Berry JA (1980) A Biochemical Model of Photosynthetic CO<sub>2</sub> assimilation in leaves of C<sub>3</sub> species. *Planta*, **149**, 78 – 89.
- Farquhar GD, von Caemmerer S (1982) Modeling of photosynthetic response to environmental conditions. In: Lange OL, Nobel PS, Osmond CB, Ziegler H, eds. *Physiological Plant Ecology. II Water Relations and Carbon Assimilation*. Springer-Verlag, Berlin, 549 – 588.
- Fenn K, Malhi Y, Morecroft M, Lloyd C, Thomas M (2010) Comprehensive description of the carbon cycle of an ancient temperate broadleaved woodland. *Biogeosci Disc* **7**: 3735-3763.

- Ford CR, McGuire MA, Mitchell RJ, Teskey RO (2004) Assessing variation in the radial profile of sap flux density in Pinus species and its effect on daily water use. *Tree physiology*, **24**, 241 - 249.
- Ford CR, Hubbard RM, Vose JM (2011) Quantifying structural and physiological controls on variation in canopy transpiration among planted pine and hardwood species in the southern Appalachians. *Ecohydrology*, DOI : 10.1002/eco.136
- Forster P, Ramaswamy V, Artaxo P *et al.* (2007) Changes in Atmospheric Constituents and in Radiative Forcing. In: Solomon, S., D. Qin, M. Manning, Z. Chen, M. Marquis, K.B. Averyt, M.Tignor and H.L. Miller, eds. *Climate Change 2007: The Physical Science Basis. Contribution of Working Group I to the Fourth Assessment Report of the Intergovernmental Panel on Climate Change*. Cambridge University Press, Cambridge, United Kingdom and New York, NY, USA.
- Forsythe WC, Rykiel EJ Jr., Stahl RS, Wu H-I, Schoolfield RM (1995) A model comparison for daylength as a function of latitude and day of year. *Ecological Modelling*, **80**, 87 - 95.
- Fox TR, Jokela EJ, Allen HL (2004) The evolution of pine plantation silviculture in the Southern United States. In: Rauscher HM, Johnsen K eds. *Southern Forest Science: Past, Present, and Future*. Gen. Tech. Rep. SRS-75, Asheville, NC, U.S. Department of Agriculture, Forest Service, Southern Research Station, (Chapter 8), 63 – 82.
- Frank AB, Dugas WA (2002) Carbon dioxide fluxes over a northern semiarid, mixed-grass prairie. *Agric For Meteorol* 108: 317 – 326.
- Gamon JA, Pearcy RW (1989) Leaf movement stress avoidance and photosynthesis in *Vitis californica*. *Oecologia*, **79**, 475 - 481.
- Gary HL (1978) The vertical distribution of needles and branchwood in thinned and unthinned 80-year-old lodgepole pine. *Northwest Science*, **52**, 303 - 309.
- Gash JHC, Stewart JB (1977) The evaporation from Thetford Forest during 1975. *Journal of Hydrology*, **35**, 285 - 396.

- Gedney N, Cox PM, Betts RA, Boucher O, Huntingford C, Stott PA (2006) Detection of a direct carbon dioxide effect in continental river runoff records. *Nature*, **439**, 835 - 838.
- Gholz HL, Clark KL (2002) Energy exchange across a chronosequence of slash pine forests in Florida. *Agricultural and Forest Meteorology*, **112**, 87 - 102.
- Giardina CP, Ryan MG, Binkley D, Fownes JH (2003) Primary production and carbon allocation in relation to nutrient supply in a tropical experimental forest. *Global Change Biol* 9: 1438 - 1450.
- Gielen B, Calfapietra C, Sabatti, Ceulemans R (2001) Leaf area dynamics in a closed poplar plantation under free-air carbon dioxide enrichment. *Tree Physiol* 21: 1245 - 1255.
- Gielen BC, Calfapietra C, Lukac M, Wittg VE, De Angelis P, Janssens IA, Moscatel MC et al. (2005) Net carbon storage in a poplar plantation (POPFACE) after three years of free-air CO<sub>2</sub> enrichment. *Tree Physiol* 25: 1399 - 1408.
- Giesler R, Lundström US, Grip H (1996) Comparison of soil solution chemistry assessment using zero-tension lysimeters or centrifugation. *Eur J Soil Sci* 47: 395 - 405.
- Gifford RM (1994) The global carbon cycle: a viewpoint on the missing sink. *Aus J Plant Physiol* 21: 1 - 15.
- Givnish TJ (1982) On the adaptive significance of leaf height in forest herbs. *The American Naturalist*, **120**, 353 - 381.
- Givnish TJ (1988) Adaptation to sun and shade: a whole-plant perspective. *Australian Journal of Plant Physiology*, **15**, 63 - 92.
- Givnish TJ (2002) Adaptive significance of evergreen vs. deciduous leaves: solving the triple paradox. *Silva Fennica*, **36**, 703 - 743.
- Gough CM, Vogel CS, Kazanski C, Nagel L, Flower CE, Curtis PS (2007) Coarse woody debris and the carbon balance of a north temperate forest. *For Ecol Manage* 244: 60-67.

- Goulden ML, Miller SD, da Rocha HR, Menton MC, de Freitas HC, Figueira A et al. (2004) Diel and seasonal patterns of tropical forest CO<sub>2</sub> exchange. *Ecol Appl* 14: S42-S54.
- Goulden ML, McMillan AMS, Winston GC, Rocha AV, Manies KL, Harden JW, Bond-lamberty BP (2011) Patterns of NPP, GPP, respiration, and NEP during boreal forest succession. *Global Change Biol* 17: 855 – 871.
- Grace J, San José J, Meir P, Miranda HS, Montes RA (2006) Productivity and carbon fluxes of tropical savannas. *J Biogeogr* 33: 387-400.
- Granier A (1987) Evaluation of transpiration in a Douglas-fir stand by means of sap flow measurements. *Tree Physiology*, 3, 309 - 320.
- Granier A, Bobay V, Gash JHC, Gelpe J, Saugier B, Shuttleworth WJ (1990) Vapour flux density and transpiration rate comparisons in a stand of Maritime pine (*Pinus pinaster* Ait.) in Les Landes forest. *Agricultural and Forest Meteorology*, 51, 309 – 319.
- Granier A, Biron P, Köstner B, Gay LW, Najjar G (1996a) Comparisons of xylem sap flow and water vapour flux at the stand level and derivation of canopy conductance for Scots pine. *Theoretical and Applied Climatology*, 53, 115–122.
- Granier A, Huc R, Barigah ST (1996b) Transpiration of natural rain forest and its dependence on climatic factors. *Agricultural and Forest Meteorology*, 78, 19 – 29.
- Granier A, Loustau D, Bréda N (2000a) A generic model of forest canopy conductance dependent on climate, soil water availability and leaf area index. *Annals of Forest Science*, 57, 755-765.
- Granier A, Biron P, Lemoine D (2000b) Water balance, transpiration and canopy conductance in two beech stands. *Agricultural and Forest Meteorology*, 100, 291–308.
- Granier A, Ceschia E, Damesin C, Dufrêne E, Epron D, Gross P, Lebaube S, Le Dantec V, Le Goff N et al. (2000c) The carbon balance of a young Beech forest. *Funct Ecol* 14: 312 – 325.

- Granier A, Reichstein M, Bréda N *et al.* (2007) Evidence for soil water control on carbon and water dynamics in European forests during the extremely dry year: 2003. *Agricultural and Forest Meteorology*, **143**, 123–145.
- Granier A, Breda N, Longdoz B, Gross P, Ngao J (2008) Ten years of fluxes and stand growth in a young beech forest at Hesse, North-eastern France. *Ann For Sci* 65: 704.
- Grano CX (1970) Small hardwoods reduce growth of pine overstory. USDA For Serv So Res Pap SO-55, 9p.
- Grelle A, Lundberg A, Lindroth A, Morén A-S, Cienciala E (1997) Evaporation components of a boreal forest: variations during the growing season. *Journal of Hydrology*, **197**, 70-87.
- Grünwald T, Bernhofer C (2007) A decade of carbon, water and energy flux measurements of an old spruce forest at the Anchor Station Tharandt. *Tellus Ser B* 59: 387 – 396.
- Gundale MJ, Kardol P, Nilsson MC, Nilsson U, Lucas RW, Wardle DA (2014) Interactions with soil biota shift from negative to positive when a tree species is moved outside its native range. *New Phytologist*, DOI: 10.1111/nph.12699
- Gunderson CA, Wullschleger SD (1994) Photosynthetic acclimation in trees to rising atmospheric CO<sub>2</sub>: a broader perspective. *Photosynthesis Research*, **39**, 369-388.
- Gurevitch J, Fox GA, Wardle GM, Inderjit TaubD (2011) Emergent insights from the synthesis of conceptual frameworks for biological invasions. *Ecology Letters*, **14**, 407 - 418.
- Hacke UG, Sperry JS, Ewers BE, Ellsworth DS, Schäfer KVR, Oren R (2000) Influence of soil porosity on water use in *Pinus taeda*. *Oecologia*, **124**, 495 – 505.
- Halldin S (1985) Leaf and bark area distribution in a pine forest. In: Hutchinson BA, Hicks BB (eds). *The forest atmosphere interaction*. Springer Netherlands, 39 - 58.
- Harmon ME, Bible K, Ryan MG, Shaw DC, Chen H, Klopatek J, Li X (2004) Production, respiration, and overall carbon balance of an old-growth *Pseudotsuga-Tsuga* forest ecosystem. *Ecosystems* 7: 498 – 512.

- Harrington TB, Edwards MB (1996) Structure of mixed pine and hardwood stands 12 years after various methods and intensities of site preparation in the Georgia Piedmont. *Canadian Journal of Forest Research*, **26**, 1490 - 1500.
- Harrington TB (2001) Silvicultural approaches for thinning southern pines: method, intensity, and timing. Georgia Forestry Commission, Publication #FSP002. 17 p.
- Hasselquist NJ, Högberg P, Metcalfe DB (2012) Contrasting effects of low and high nitrogen additions on soil CO<sub>2</sub> flux components and ectomycorrhizal fungal sporocarp production in a boreal forest. *Global Change Biology*, **18**, 3596 – 3605.
- Heath LS, Kauppi PE, Burschel P *et al.* (1993) Contribution of temperate forests to the world's carbon budget. *Water, Air, and Soil Pollution*, **70**, 55 – 69.
- Helmisaari HS, Makkonen K, Kellomäki S, Valtonen E, Mälkönen E (2002) Below- and above-ground biomass, production and nitrogen use in Scots pine stands in eastern Finland. *For Ecol Manage* 165: 317 – 326.
- Hendrey GR, Ellsworth DS, Lewin KF, Nagy J (1999) A free-air enrichment system for exposing tall forest vegetation to elevated atmospheric CO<sub>2</sub>. *Global Change Biology*, **5**, 293 - 309.
- Hierro JL, Maron JL, Callaway RM (2005) A biogeographical approach to plant invasions: the importance of studying exotics in their introduced and native range. *Journal of Ecology*, **93**, 5 - 15.
- Hikosaka K, Hirose T (1997) Leaf angle as a strategy for light competition: optimal and evolutionarily stable light-extinction coefficient within a canopy. *Ecoscience*, **4**, 501 – 507.
- Hirata R, Saigusa N, Yamamoto S, Ohtani Y, Ide R, Asanuma J *et al.* (2008) Spatial distribution of carbon balance in forest ecosystems across East Asia. *Agric For Meteorol* 148: 761-775.
- Hollinger DY, Aber J, Dail B, Davidson EA, Goltz SM, Hughes H, Leclerc MY, Lee JT, Richardson AD, Rodrigues C, Scott NA, Achuatavariar D, Walsh J (2004) Spatial and temporal variability in forest-atmosphere CO<sub>2</sub> exchange. *Global Change Biol* 10: 1689 – 1706.

- Horn HS (1971) The adaptive geometry of trees. Princeton University Press, Princeton, NJ.
- Hughes L (2000) Biological consequences of global warming: is the signal already apparent? *Trends in Ecology & Evolution*, **15**, 56 – 61.
- Iio A, Hikosaka K, Anten NPR, Nakagawa Y, Ito A (2014) Global dependence of field-observed leaf area index in woody species on climate: a systematic review. *Global Ecology and Biogeography*, **23**, 274–285.
- Ilvesniemi H, Liu C (2001) Biomass distribution in a young Scots pine stand. *Boreal Environment Research*, **6**, 3 - 8.
- Ilvesniemi H, Pumpanen J, Duursma R *et al.* (2010) Water balance of a boreal Scots pine forest. *Boreal Environment Research*, **15**, 375-396.
- IPCC 2014: Climate Change 2014: Impacts, Adaptation, and Vulnerability. Part A: Global and Sectoral Aspects. Contribution of Working Group II to the Fifth Assessment Report of the Intergovernmental Panel on Climate Change [Field, C.B., V.R. Barros, D.J. Dokken, K.J. Mach, M.D. Mastrandrea, T.E. Bilir, M. Chatterjee, K.L. Ebi, Y.O. Estrada, R.C. Genova, B. Girma, E.S. Kissel, A.N. Levy, S. MacCracken, P.R. Mastrandrea, and L.L. White (eds.)] Cambridge University Press, Cambridge, United Kingdom and New York, NY, USA, 1132 pp.
- Irvine J, Law BE, Kurpius MR, Anthoni PM, Moore D, Schwarz PA (2004) Age-related changes in ecosystem structure and function and effects on water and carbon exchange in ponderosa pine. *Tree Physiology*, **24**, 753 – 763.
- James SA, Clearwater MJ, Meinzer FC, Goldstein G (2002) Heat dissipation sensors of variable length for the measurement of sap flow in trees with deep sapwood. *Tree Physiology*, **22**, 277-283.
- Jansons A, Sisenis L, Neimane U, Rieksts-Riekstins J (2013) Biomass production of young lodgepole pine (*Pinus contorta* var. *latifolia*) stands in Latvia. *iForest*, **6**, 10-14.
- Jarvis PG (1971) The estimation of resistances to carbon dioxide transfer. In *Plant Photosynthetic Production Manual of Methods*. In: Šesták Z, Čatský J, Jarvis PG, eds. *The Hague: Junk*. 566 – 631.

- Jarvis PG (1976) The interpretation of the variations in leaf water potential and stomatal conductance found in canopies in the field. *Philosophical Transactions of the Royal Society of London B*, **273**, 593-610.
- Jarvis PG, Linder S (2000) Constraints to growth of boreal forests. *Nature*, **405**, 904 – 905.
- Jarvis PG, McNaughton KG (1986) Stomatal control of transpiration: Scaling up from leaf to region. *Advanced Ecological Research*, **15**, 1 - 49.
- Jassal RS, Black TA, Novak MD, Gaumont-Guay D, Nesic Z (2008) Effect of soil water stress on soil respiration and its temperature sensitivity in an 18-year-old temperate Douglas-fir stand. *Global Change Biol.* **14**: 1 – 14.
- Johnsen KH, Teskey B, Samuelson L *et al.* (2004) Carbon sequestration in loblolly pine plantations: methods, limitations and research needs for estimating storage pools. In: Rauscher MH, Johnsen KH, eds. *Southern Forest Science: past, present, and future* GTR-SRS-75., Asheville, NC, USA: USDS Forest Service, Southern Research Station, pp 394.
- Kätterer T, Bolinder MA, Andrén O, Kirchmann H, Menichetti L (2011) Roots contribute more to refractory soil organic matter than above-ground crop residue, as revealed by a long-term field experiment. *Agric Ecos Env* **141**: 184 – 192.
- Katul GG, Todd P, Pataki D, Kabala ZJ, Oren R (1997) Soil water depletion by oak trees and the influence of root water uptake on the moisture content spatial statistics. *Water Resource Research*, **33**, 611-623.
- Katul GG, Ellsworth DS, Lai C-T (2000) Modelling assimilation and intercellular CO<sub>2</sub> from measured conductance: a synthesis of approaches. *Plant, Cell & Environment*, **23**, 1313 – 1328.
- Katul GG, Oren R, Manzoni S, Higgins C, Parlange MB (2012) Evapotranspiration: A process driving mass transport and energy exchange in the soil-plant-atmosphere-climate system. *Reviews of Geophysics*, **50**, RG3002.
- Kauppi, PE, Mielikaeinen, K, Kuusela K (1992) Biomass and carbon budget of European forests, 1971 to 1990. *Science*, **256**, 70 – 74.

- Keane RM, Crawley MJ (2002) Exotic plant invasions and the enemy release hypothesis. *Trends in Ecology & Evolution*, **17**, 164 - 170.
- Keenan TF, Hollinger DY, Bohrer G, Dragoni D, Munger JW, Schmid HP, Richardson AD (2013) Increase in forest water-use efficiency as atmospheric carbon dioxide concentrations rise. *Nature*, **499**, 324 - 327.
- Kelliher FM, Leuning R, Raupach MR, Schulze E-D (1995) Maximum conductances for evaporation from global vegetation types. *Agricultural and Forest Meteorology*, **73**, 1 - 16.
- Kelliher FM, Lloyd J, Arneeth A *et al.* (1998) Evaporation from a central Siberian pine forest. *Journal of Hydrology*, **205**, 279-296.
- Kikuzawa K (1991) A cost-benefit analysis of leaf habit and leaf longevity of trees and their geographical pattern. *The American Naturalist*, **138**, 1250 - 1263.
- Kim D, Oren R, Oishi AC, Hsieh C-I, Phillips N, Novick KA, Stoy PC (2014) Sensitivity of stand transpiration to wind velocity in a mixed broadleaved deciduous forest. *Agricultural and Forest Meteorology*, **187**, 62 - 71.
- Kim H-S, Oren R, Hinckley TM (2008) Actual and potential transpiration and carbon assimilation in an irrigated poplar plantation. *Tree Physiology*, **28**, 559 - 577.
- Kim H-S, Palmroth S, Thérézien M, Stenberg P, Oren R (2011) Analysis of the sensitivity of absorbed light and incident light profile to various canopy architecture and stand conditions. *Tree Physiology*, **31**, 30 - 47.
- Kinerson RS, Ralston CW, Wells CG (1977) Carbon cycling in a loblolly pine plantation. *Oecologia* 29: 1 - 10.
- Knight DH, Fahey TJ, Running SW (1985) Water and Nutrient Outflow from contrasting lodgepole pine forests in Wyoming. *Ecological Monographs*, **55**, 29 - 48.
- Knight DH (1991) Pine forests: a comparative overview of ecosystem structure and function. In: *Coniferous forest ecology from an international perspective* (eds Nakagoshi N, Golley FB), pp. 121-135, SPB Acad. Publ. bv, The Hague, The Netherlands.

- Knight DH, Vose JM, Baldwin VC, Ewel KC, Grodzinska K (1994) Contrasting patterns in pine forest ecosystems. In: *Ecological Bulletins* (eds Gholz HL, Linder S, McMurtie RE), pp. 9-19.
- Knohl A, Schulze ED, Kolle O, Buchmann N (2003) Large carbon uptake by an unmanaged 250-year-old deciduous forest in Central Germany. *Agric For Meteorol* 118: 151-167.
- Kobak K, Kondrasheva N (1993) Residence time of carbon in soils of the boreal zone. In: Vinson TS, Kolchugina TP, eds. *Carbon Cycling in Boreal Forest and Sub-Arctic Ecosystems*. EPA, Corvallis, OR, 51-58.
- Kohlmaier GH, Häger C, Würth G *et al.* (1995) Effects of the age class distribution of the temperate and boreal forests on the global CO<sub>2</sub> source-sink function. *Tellus*, **47B**, 212 – 231.
- Kolari P, Kulmala L, Pumpanen J, Launiainen S, Ilvesniemi H, Hari P, Nikinmaa E (2009) CO<sub>2</sub> exchange and component CO<sub>2</sub> fluxes of a boreal Scots pine forest. *Boreal Environment Research*, **14**, 761 - 783.
- Kolari P, Chan T, Porcar-Castell A, Bäch J, Nikinmaa E, Juurola E (2014) Field and controlled environment measurements show strong seasonal acclimation in photosynthesis and respiration potential in boreal Scots pine. *Frontier in Plant Science*, **5**, 1 – 12. DOI: 10.3389/fpls.2014.00717.
- Krishnan P, Black TA, Grant NJ, Barr AG, Hogg EH, Jassal RS, Morgenstern K (2006) Impact of changing soil moisture distribution on net ecosystem productivity of a boreal aspen forest during and following drought. *Agricultural and Forest Meteorology*, **139**, 208–223.
- Krishnan P, Black TA, Barr AG, Grant NJ, Gaumont-Guay D, Nesic Z (2008) Factors controlling the interannual variability in the carbon balance of a southern boreal black spruce forest. *J Geophys Res.* 113: D09109, doi:10.1029/2007JD008965.
- Kurpius MR, Panek JA, Nikolov NT, McKay M, Goldstein AH (2003) Partitioning of water flux in a Sierra Nevada ponderosa pine plantation. *Agricultural and Forest Meteorology*, **117**, 173- 192.

- Kutsch W, Essenbach C, Dilly O, Middelhoff U, Steinborn W, Vanselow R et al. (2001) The carbon cycle of contrasting landscape elements of the Bornhöved Lake district. In *Ecosystem Properties and Landscape Function in Central Europe*. Eds. R. Lenz, R.E. Hantschel and J.D. Tenhunen, Springer Berlin, Berlin, pp. 75-95.
- Kutsch WL, Liu CJ, Hormann G, Herbst M (2005) Spatial heterogeneity of ecosystem carbon fluxes in a broadleaved forest in Northern Germany. *Global Change Biol* 11: 70-88.
- Laforest-Lapointe I, Martínez-Vilalta J, Retana J (2014) Intraspecific variability in functional traits matters: case study of Scots pine. *Oecologia*, **175**, 1337 - 1348.
- Lagergren F, Lindroth A (2002) Transpiration response to soil moisture in pine and spruce trees in Sweden. *Agricultural and Forest Meteorology*, **112**, 67 - 85.
- Lagergren F, Eklundh L, Grelle A, Lundblad M, Mölder M, Lankreijer H, Lindroth A (2005) Net primary production and light use efficiency in a mixed coniferous forest in Sweden. *Plant Cell Environ* 28: 412 – 423.
- Lai C-T, Katul G, Butnor J *et al.* (2002) Modelling the limits on the response of net carbon exchange to fertilization in a south-eastern pine forest. *Plant, Cell & Environment*, **25**, 1095 – 1119.
- Landsberg JJ, Gower ST (1997) Applications of physiological ecology to forest management. Academic Press, San Diego, CA.
- Landsberg JJ, Waring RH (1997) A generalised model of forest productivity using simplified concepts of radiation-use efficiency, carbon balance and partitioning. *For Ecol Manage* 95: 209–228.
- Lasslop G, Reichstein M, Detto M, Richardson AD, Baldocchi DD (2009) Comments on Vickers et al.: Self-correlation between assimilation and respiration resulting from flux partitioning of eddy-covariance CO<sub>2</sub> fluxes. *Agric For Meteorol*, doi: 10.1016/j.agrformet.2009.11.003.
- Laudon H, Taberman I, Ågren A, Futter M, Ottoson Lövvenius M, Bishop K (2013) The Krycklan catchment study – a flagship infrastructure for hydrological,

- biogeochemistry, and climate research in the boreal landscape. *Water Resources Research*, **49**, 7154 - 7158.
- Law BE, Ryan MG, Anthoni M (1999) Seasonal and annual respiration of a ponderosa pine ecosystem. *Global Change Biology*, **5**, 169 – 182.
- Law BE, Waring RH, Anthoni PM, Abers JD (2000) Measurements of gross and net ecosystem productivity and water vapour exchange of a *Pinus ponderosa* ecosystem, and an evaluation of two generalized models. *Global Change Biol* 6: 155 – 168.
- Law BE, Thornton PE, Irvine J, Anthoni PM, Van Tuyl S (2001) Carbon storage and fluxes in ponderosa pine forests at different developmental stages. *Global Change Biol* 7: 755 – 777.
- Law BE, Falge E, Gu L *et al.* (2002) Environmental controls over carbon dioxide and water vapor exchange of terrestrial vegetation. *Agricultural and Forest Meteorology*, **113**, 97 – 120.
- Lawrence DM, Thornton PE, Oleson KW, Bonan GB (2007) The Partitioning of Evapotranspiration into Transpiration, Soil Evaporation, and Canopy Evaporation in a GCM: Impacts on Land–Atmosphere Interaction. *Journal of Hydrometeorology*, **8**, 862 – 880.
- Lawrence D, Vandecar K (2015) Effects of tropical deforestation on climate and agriculture. *Nature Clim Change* 5: 27 – 36.
- Lawson ER (1990) Shortleaf pine. In: *Silvics of North America. Volume 1*. Burns RM, Honkala BH (eds). US Department of Agriculture, Forest Service, Agriculture Handbook 654, Washington, D.C.
- Leo M, Oberhuber W, Schuster R, Thorsten EEG, Matyssek R, Wieser G (2014) Evaluating the effect of plant water availability on inner alpine coniferous trees based on sap flow measurements. *European Journal of Forest Research*, **133**, 691 – 698.
- Le Quéré C, Moriarty R, Andrew RM *et al.* (2014) Global carbon budget 2014. *Earth System Science Data Discussion*, **7**, 521 – 610.

- Li J-H, Dugas WA, Hymus GJ, Johnson DP, Hinkle CR, Drake BG, Hungate BA (2003) Direct and indirect effects of elevated CO<sub>2</sub> on transpiration from *Quercus myrtifolia* in a scrub-oak ecosystem. *Global Change Biology*, **9**, 96 - 105.
- Lim H, Oren R, Palmroth S *et al.* (in review) Inter-annual variability of precipitation constrains the production response of boreal *Pinus sylvestris* stand to nitrogen fertilization.
- Linder S, Lohammar T (1981) Amount and quantity of information on CO<sub>2</sub>-exchange required for estimating annual carbon balance of coniferous trees. *Stud For Suec*, **160**, 73 – 87.
- Lindroth A, Klemedtsson L, Grelle A, Weslien P, Langvall O (2007) Measurement of net ecosystem exchange, productivity and respiration in three spruce forests in Sweden shows unexpectedly large soil carbon losses. *Biogeochemistry* **89**: 43 – 60, doi:10.1007/s10533-007- 9137-8.
- Liu BY, Jordan RC (1960) The interrelationship and characteristic distribution of direct, diffuse and total solar radiation. *Solar Energy*, **4**, 1 - 19.
- Long SP, Zhu X-G, Naidu SL, Ort SR (2006) Can improvement in photosynthesis increase crop yields? *Plant, Cell & Environment*, **29**, 315 – 330.
- Loustau D, Berbigier P, Roumagnac P *et al.* (1996) Transpiration of a 64-year-old maritime pine stand in Portugal. *Oecologia*, **107**, 33-42.
- Lu P, Müller WJ, Chacko EK (2000) Spatial variations in xylem sap flux density in the trunk of orchard-grown, mature mango trees under changing soil water conditions. *Tree Physiology*, **20**, 683–692.
- Luis VC, Jiménez MS, Morales D, Kucera J, Wieser G (2005) Canopy transpiration of a Canary Islands pine forest. *Agricultural and Forest Meteorology*, **135**, 117-123.
- Lundblad M, Lagergren F, Lindroth A (2001) Evaluation of heat balance and heat dissipation methods for sapflow measurements in pine and spruce. *Annals of Forest Science*, **58**, 625–638.

- Lundmark A, Jansson P-E (2009) Generic soil descriptions for modelling water and chloride dynamics in the unsaturated zone based on Swedish soils. *Geoderma* 150: 85 – 95.
- Luyssaert S, Inglima I, Jung M et al. (2007) CO<sub>2</sub> balance of boreal, temperate, and tropical forests derived from a global database. *Global Change Biology* 13: 2509 – 2537.
- Ma Z, Liu Q, Wang H, Li X, Zeng H, Xu W (2008) Observation and modeling of NPP for *Pinus elliottii* plantation in subtropical China *Sci China Ser D: Earth Sci*: 955-965.
- MacKay SL, Arain MA, Khomik M, Brodeur JJ, Schumacher J, Hartmann H, Peichl M (2012) The impact of induced drought on transpiration and growth in a temperate pine plantation forest. *Hydrological Processes*, **26**, 1779–1791.
- Magnussen S, Reed D (2004) Modelling for estimation and monitoring (FAO-IUFRO).
- Mahrt L, Vickers D (2002) Relationship of area-averaged carbon dioxide and water vapour fluxes to atmospheric variables. *Agri For Meteorol* 112: 195–202.
- Maier CA, Johnsen KH, Butnor J, Kress LW, Anderson PH (2002) Branch growth and gas exchange in 13-year-old loblolly pine (*Pinus taeda*) trees in response to elevated carbon dioxide concentration and fertilization. *Tree Physiology*, **22**, 1093 – 1106.
- Maier CA, Albaugh TJ, Allen HL, Dougherty PM (2004) Respiratory carbon use and carbon storage in mid-rotation loblolly pine (*Pinus taeda* L.) plantations: the effect of site resources on the stand carbon balance. *Global Change Biology*, **10**, 1335-1350.
- Mäkelä A (1997) A carbon balance model of growth and self-pruning in trees based on structural relationships. *For Sci* 43: 7-24.
- Mäkelä A, Kolari P, Karimäki J, Nikinmaa E, Perämäki M, Hari P (2006) Modelling five years of weather-driven variation of GPP in a boreal forest. *Agricultural and Forest Meteorology*, **139**, 382-398.
- Mäkelä A, Pulkkinen M, Kolari P et al. (2008) Developing an empirical model of stand GPP with the LUE approach: analysis of eddy covariance data at five contrasting conifer sites in Europe. *Global Change Biology* 14: 92 – 108.

- Malhi Y, Baldocchi DD, Jarvis PG (1999) The carbon balance of tropical, temperate and boreal forests. *Plant Cell Environ* 22: 715–740.
- Malhi Y, Aragao L, Metcalfe DB, Paiva R, Quesada CA, Almeida S et al. (2009) Comprehensive assessment of carbon productivity, allocation and storage in three Amazonian forests. *Global Change Biol* 15: 1255-1274.
- Mälkönen E, Kukkola M (1991) Effect of long-term fertilization on the biomass production and nutrient status of Scots pine stands. *Fertilizer Research*, 27, 113 – 127.
- Margolis H, Oren R, Whitehead D, Kaufmann MR (1995) Leaf area dynamics of conifer forests. In: *Ecophysiology of Coniferous Forests*. (eds Smith WK & Hinckley TM), Academic Press, San Diego, pp 181–223.
- Marklund LG (1988) Biomassfunktioner för tall, gran och björk i Sverige. Sveriges lantbruksuniversitet, Institutionen för skogstaxering, *Rapport*, 45, 1 - 73.
- Marland G, Schlamadinger B (1999) The Kyoto Protocol could make a difference for the optimal forest-based CO<sub>2</sub> mitigation strategy: some results from GORCAM. *Environmental Science & Policy*, 2, 111 – 124.
- Martin TA, Brown KJ, Čermák J et al. (1997) Crown conductance and tree and stand transpiration in a second growth *Abies amabilis* forest. *Canadian Journal of Forest Research*, 27, 797 - 808.
- Maseyk K, Grünzweig JM, Rotenberg E, Yakir D (2008) Respiration acclimation contributes to high carbon-use efficiency in a seasonally dry pine forest. *Global Change Biol* 14: 1553 – 1567.
- Matamala R, Schlesinger WH (2000) Effects of elevated CO<sub>2</sub> on fine root production and activity in an intact temperate forest ecosystem. *Global Change Biology*, 6, 967 – 980.
- Matyssek R, Wieser G, Patzner K, Blaschke H, Häberle K-H (2009) Transpiration of forest trees and stands at different altitude: consistencies rather than contrasts? *European Journal of Forest Research*, 128, 579 – 596.

- McCarthy HR, Oren R, Finzi AC, Ellsworth DS, Kim H-S, Johnsen KH, Millar B (2007) Temporal dynamics and spatial variability in the enhancement of canopy leaf area under elevated atmospheric CO<sub>2</sub>. *Global Change Biology*, **13**, 2479 - 2497.
- McCarthy HR, Oren R, Johnsen KH *et al.* (2010) Re-assessment of plant carbon dynamics at the Duke free-air CO<sub>2</sub> enrichment site: interactions of atmospheric [CO<sub>2</sub>] with nitrogen and water availability over stand development. *New Phytologist*, **185**, 514 – 528.
- McCarty JP (2001) Ecological consequences of recent climate change. *Conservation Biology*, **15**, 320 – 331.
- McDowell N, Barnard H, Bond B *et al.* (2002) The relationship between tree height and leaf area: sapwood area ratio. *Oecologia*, **132**, 12 - 20.
- McGuire JP, Mitchell RJ, Moser EB, Pecot SD, Gjerstad DH, Hedman CW (2001) Gaps in a gappy forest: plant resources, longleaf pine regeneration, and understory response to tree removal in longleaf pine savannas. *Canadian Journal of Forest Research*, **31**, 765 - 778.
- Meade FM (1951) Forest plantations in Arkansas – plantations in the Arkansas Ozarks and experimental planting on a Coastal Plain site in southwest Arkansas. *Arkansas Agricultural Experiment Station Bulletin*, **512**, 50p.
- Medlyn BE, Barton CVM, Broadmeadow MSJ *et al.* (2001) Stomatal conductance of forest species after long-term exposure to elevated CO<sub>2</sub> concentration: a synthesis. *New Phytologist*, **49**, 247-264.
- Medlyn BE, Berbigier P, Clement R *et al.* (2005) Carbon balance of coniferous forests growing in contrasting climates: Model-based analysis. *Agricultural and Forest Meteorology* **131**: 97 – 124.
- Mellander P-E, Bishop K, Lundmark T (2004) The influence of soil temperature on transpiration: a plot scale manipulation in a young Scots pine stand. *Forest Ecology and Management*, **195**, 15 – 28.
- Mellander P-E, Laudon H, Bishop K (2005) Modelling variability of snow depths and soil temperatures in Scots pine stands. *Agricultural and Forest Meteorology*, **133**, 109 - 118.

- Mellander P-E, Stähli M, Gustafsson D, Bishop K (2006) Modelling the effect of low soil temperatures on transpiration by Scots pine. *Hydrological Processes*, **20**, 1929 - 1944.
- Miller EE, Norman JM (1971) A sunfleck theory for plant canopies. I. Lengths of sunlit segments along a transect. *Agronomy Journal*, **63**, 735 - 738.
- Miller PC, Mooney HA (1974) The origin and structure of American arid-zone ecosystems. The producers: interactions between environment, form, and function. In: Proceedings of the First International Congress in Ecology. The Hague, the Netherlands, pp. 201-209.
- Milly PCD, Dunne KA, Vecchia AV (2005) Global pattern of trends in streamflow and water availability in a changing climate. *Nature*, **438**, 347 - 350.
- Moreaux V, O'Grady AP, Nguyen-The N, Loustau D (2013) Water use of young maritime pine and Eucalyptus stands in response to climatic drying in southwestern France. *Plant Ecology and Diversity*, **6**, 57 - 71.
- Mousseau M, Saugier B (1992) The direct effect of increased CO<sub>2</sub> on gas exchange and growth of forest tree species. *Journal of Experimental Botany*, **43**, 1121 - 1130.
- Murty D, McMurtrie RE, Ryan MG (1996) Declining forest productivity in aging forest stands: A modeling analysis of alternative hypotheses. *Tree Physiol* **16**: 187-200.
- Myers BJ, Benyon RG, Theiveyanathan S, Criddle RS, Smith CJ, Falkiner RA (1998) Response of effluent-irrigated *Eucalyptus grandis* and *Pinus radiata* to salinity and vapor pressure deficits. *Tree Physiology*, **18**, 565 - 573.
- Naidu SL, DeLucia EH, Thomas RB (1998) Contrasting patterns of biomass allocation in dominant and suppressed loblolly pine. *Canadian Journal of Forest Research*, **28**, 1116 - 1124.
- Nicholls NN, Gniza GV, Jouzel J, Karl TR, Ogallo LA, Parker DE (1996) Observed climate variability and change. In: Houghton JT, Meira Filho LG, Callander BA, Harris N, Kattenberg N, Maskell K eds. *Climate change 1995: the science of climate change*. Cambridge, United Kingdom: Cambridge University Press: 135 - 192.

- Niinemets Ü, Kull O (1995) Effects of light availability and tree size on the architecture of assimilative surface in the canopy of *Picea abies*: variation in shoot structure. *Tree Physiology*, **15**, 791 – 798.
- Nilson T (1999) Inversion of gap frequency data in forest stands. *Agricultural and Forest Meteorology*, **98-99**, 437 - 448.
- Nilsson MC, Wardle DA (2005) Understory vegetation as a forest ecosystem driver: evidence from the northern Swedish boreal forest. *Frontier in Ecology and the Environment*, **3**, 421 - 428.
- Nilsson C, Engelmark O, Cory J, Forsslund A, Carlborg E (2008) Differences in litter cover and understory flora between stands of introduced logpole pine and native Scots pine in Sweden. *Forest Ecology and Management*, **255**, 1900 - 1905.
- Norby RJ, Hanson PJ, O'Neill EG, Tschaplinski TJ, Weltzin JF, Hansen RA, Cheng W, Wullschleger SD et al. (2002) Net primary productivity of a CO<sub>2</sub>-enriched deciduous forest and the implications for carbon storage. *Ecol Appl* 12: 1261 – 1266.
- Norby RJ, DeLucia EH, Gielen B, Carlo C, Giardina CP, King JS, Ledford J, McCarthy HR, Moore DJP, Ceulemans R, Angelis PD, Finzi AC, Karnosky DF, Kubiske ME, Lukac M, Pregitzer KS, Scarascia-Mugnozza GE, Schlesinger WH, Oren R (2005) Forest response to elevated CO<sub>2</sub> is conserved across a broad range of productivity. *Proc Natl Acad Sci USA* 102: 18052 – 18056.
- Novick K, Oren R, Stoy P, Juang J-Y, Siqueira M, Katul G (2009) The relationship between reference canopy conductance and simplified hydraulic architecture. *Advances in Water Resources*, **32**, 809–819.
- Ohamura A, Wild M (2002) Is the hydrological cycle accelerating? *Science*, **293**, 1345 – 1346.
- Oishi AC, Oren R, Stoy PC (2008) Estimating components of forest evapotranspiration: a footprint approach for scaling sap flux measurements. *Agricultural Forest Meteorology*, **148**, 1719 - 1732.
- Oishi AC, Oren R, Novick KA, Palmroth S, Katul GG (2010) Interannual invariability of forest evapotranspiration and its consequence to water flow downstream. *Ecosystems*. DOI: 10.1007/s10021-010-9328-3.

- Oker-Blom P, Kellomäki S (1983) Effect of grouping of foliage on the within-stand and within-crown light regime: comparison of random and grouping canopy models. *Agricultural Meteorology*, **28**, 143 - 155.
- Oker-Blom P, Pukkala T, Kuuluvainen T (1989) Relationship between radiation interception and photosynthesis in forest canopies: effect of stand structure and latitude. *Ecological Modelling*, **49**, 73 - 87.
- Oleson KW, Lawrence DM, Bonan GB *et al.* (2010) *Technical Description of Version 4.0 of the Community Land Model (CLM) NCAR Tech. Note NCAR/TN-461 + STR*. National Centre for Atmospheric Research, Boulder, Colorado.
- Oliveras I, Llorens P (2001) Medium-term sap flux monitoring in a Scots pine stand: analysis of the operability of the heat dissipation method for hydrological purposes. *Tree Physiology*, **21**, 473–480.
- Ollinger SV, Smith ML (2005) Net primary production and canopy nitrogen in a temperate forest landscape: An analysis using imaging spectroscopy, modeling and field data. *Ecosystems* 8: 760-778.
- Onoda Y, Saluñga JB, Akutsu K, Aiba S-I, Yahara T, Anten NPR (2014) Trade-off between light interception efficiency and light use efficiency: implications for species coexistence in one-sided light competition. *Journal of Ecology*, **102**, 167 - 175.
- Oren R, Pataki DE (2001) Transpiration in response to variation in microclimate and soil moisture in southeastern deciduous forests. *Oecologia*, **127**, 549 – 559.
- Oren R, Schulze E-D, Matyssek R, Zimmermann R (1986) Estimating photosynthetic rate and annual carbon gain in conifers from specific leaf weight and leaf biomass. *Oecologia*, **70**, 187 - 193.
- Oren R, Phillips N, Katul G, Ewers BE, Pataki DE (1998a) Scaling xylem sap flux and soil water balance and calculating variance: a method for partitioning water flux in forests. *Annals of Forest Science*, **55**, 191 - 216.
- Oren R, Ewers BE, Todd P, Phillips N, Katul GG (1998b) Water balance delineates the

- soil layer in which moisture affects canopy conductance. *Ecological Applications*, **8**, 990 - 1002.
- Oren R, Phillips N, Ewers BE, Pataki DE, Megonigal JP (1999) Sap-flux-scaled transpiration responses to light, vapor pressure deficit, and leaf area reduction in a flooded *Taxodium distichum* forest. *Tree Physiology*, **19**, 337 – 347.
- Oren R, Ellsworth DS, Johnsen KH *et al.* (2001) Soil fertility limits carbon sequestration by forest ecosystems in a CO<sub>2</sub>-enriched atmosphere. *Nature*, **411**, 469 - 472.
- Palmroth S, Hari P (2001) Evaluation of the importance of acclimation of needle structure, photosynthesis, and respiration to available photosynthetically active radiation in a Scots pine canopy. *Canadian Journal of Forest Research*, **31**, 1235 – 1243.
- Palmroth S, Palva L, Stenberg P, Kotisaari A (1999) Fine scale measurement and simulation of penumbral radiation formed by a pine shoot. *Agricultural and Forest Meteorology*, **95**, 15 – 25.
- Palmroth S, Oren R, McCarthy HR *et al.* (2006) Aboveground sink strength in forests controls the allocation of carbon belowground and its CO<sub>2</sub>-induced enhancement. *Proceedings of the National Academy of Sciences, USA*, **103**, 19362 – 19367.
- Palmroth S, Katul GG, Hui D, McCarthy HR, Jackson RB, Oren R (2010) Estimation of long-term basin scale evapotranspiration from streamflow time series. *Water Resources Research*, **46**, W10512, DOI: 10.1029/2009WR008838.
- Palmroth S, Bach LH, Nordin A, Palmqvist K (2014) Nitrogen-addition effects on leaf traits and photosynthetic carbon gain of boreal forest understory shrubs. *Oecologia*, **175**, 457 - 470.
- Pan Y, Birdsey RA, Fang J *et al.* (2011) A large and persistent carbon sink in the world's forests. *Science*, **333**, 988 – 993.
- Papaioannou G, Papanikolaou N, Retails D (1993) Relationships of photosynthetically active radiation and shortwave irradiance. *Theoretical and Applied Climatology*, **48**, 23 - 27.

- Parmesan C, Yohe G (2003) A globally coherent fingerprint of climate change impacts across natural systems. *Nature*, **421**, 37 - 42.
- Pataki DE, Oren R (2003) Species differences in stomatal control of water loss at the canopy scale in a mature bottomland deciduous forest. *Advances in Water Resources*, **26**, 1267 – 1278.
- Pataki DE, Oren R, Tissue DT (1998a) Elevated carbon dioxide does not affect average canopy stomatal conductance of *Pinus taeda* L. *Oecologia*, **117**, 47 - 52.
- Pataki DE, Oren R, Katul GG, Sigmon J (1998b) Canopy conductance of *Pinus taeda*, *Liquidambar styraciflua* and *Quercus phellos* under varying atmospheric and soil water conditions. *Tree Physiology*, **18**, 307 - 315.
- Pataki DE, Oren R, Smith WK (2000) Sap flux of co-occurring species in a western subalpine forest during seasonal soil drought. *Ecology*, **81**, 2557 - 2566.
- Pearson JA, Fahey TJ, Knight DH (1984) Biomass and leaf area in contrasting lodgepole pine forests. *Canadian Journal of Forest Research*, **14**, 259 - 265.
- Penning de Vries FWT (1975) The cost of maintenance processes in plant cells. *Annals of Botany*, **39**, 77 - 92.
- Pensa M, Jalkanen R (2005) Variation in needle longevity is related to needle-fascicle production rate in *Pinus sylvestris*. *Tree Physiology*, **25**, 1265 - 1271.
- Perämäki M, Nikinmaa E, Sevanto S, Ilvesniemi H, Siivola E, Hari P, Vesala T (2001) Tree stem diameter variations and transpiration in Scots pine: an analysis using a dynamic sap flow model. *Tree Physiology*, **21**, 889 – 897.
- Perks MP, Irvine J, Grace J (2002) Canopy stomatal conductance and xylem sap abscisic acid (ABA) in mature Scots pine during a gradually imposed drought. *Tree Physiology*, **22**, 877 - 883.
- Petzold R, Schwärzel K, Feger K-H (2011) Transpiration of a hybrid poplar plantation in Saxony (Germany) in response to climate and soil conditions. *European Journal of Forest Research*, **130**, 695–706.

- Phillips N, Oren R (1998) A comparison of daily representations of canopy conductance based on two conditional time-averaging methods and the dependence of daily conductance on environmental factors. *Annals of Forest Science*, **55**, 217 - 235.
- Phillips N, Oren R (2001) Intra- and inter-annual variation in transpiration of a pine forest. *Ecological Applications*, **11**, 385 - 396.
- Phillips N, Nagchaudhuri A, Oren R, Katul G (1997) Time constant for water transport in loblolly pine trees estimated from time series of evaporative demand and stem sapflow. *Trees*, **11**, 412 - 419.
- Phillips N, Bergh J, Oren R, Linder S (2001) Effects of nutrition and soil water availability on water use in a Norway spruce stand. *Tree Physiology*, **21**, 851 - 860.
- Ponton S, Flanagan LB, Alstad KP, Johnson BG, Morgenstern K, Kljun N, Black TA, Barr AG (2006) Comparison of ecosystem water-use efficiency among Douglas-fir forest, aspen forest and grassland using eddy covariance and carbon isotope techniques. *Glob Change Biol* 12: 294–310.
- Potter CS, Randerson JT, Field CB, Matson PA, Vitousek PM, Mooney HA, Klooster SA (1993) Terrestrial ecosystem production: a process model based on global satellite and surface data. *Global Biogeochemistry Cycles*, **7**, 811 - 841.
- Poyatos R, Llorens P, Gallart F (2005) Transpiration of montane *Pinus sylvestris* L. and *Quercus pubescens* Willd. forest stands measured with sap flow sensors in NE Spain. *Hydrology and Earth System Sciences Discussions*, **2**, 1011 - 1046.
- Prince SD, Goward SN (1995) Global primary production: a remote sensing approach. *J Biogeogr* 22: 815–835.
- Pritchard SG, Strand AE, McCormack ML *et al.* (2008) Fine root dynamics in a loblolly pine forest are influenced by free-air-CO<sub>2</sub>-enrichment: a six year-minirhizotron study. *Global Change Biology*, **14**, 588 - 602.
- Rambal S, Ourcival J-M, Joffre R, Mouillot F, Nouvellon Y, Reichstein M, Rocheteau A (2003) Drought controls over conductance and assimilation of a Mediterranean evergreen ecosystem: scaling from leaf to canopy. *Global Change Biology*, **9**, 1813 - 1824.

- Rautiainen M, Stenberg P (2005) Simplified tree crown model using stand forest mensuration data for Scots pine. *Agricultural and Forest Meteorology*, **128**, 123 – 129.
- Rautiainen M, Heiskanen J, Korhonen L (2011) Seasonal changes in canopy leaf area index and MODIS vegetation products for a boreal forest site in central Finland. *Boreal Environment Research*, **17**, 72 - 84.
- Rayner PJ, Enting IG, Francey RJ, Langenfelds R (1999) Reconstructing the recent carbon cycle from the atmospheric CO<sub>2</sub>, delta <sup>13</sup>C and O<sub>2</sub>/N<sub>2</sub> observations. *Tellus B*, **51**, 213-232.
- Reichstein M, Papale D, Valentini R et al. (2007) Determinants of terrestrial ecosystem carbon balance inferred from European eddy covariance flux sites. *Geophys Res Lett* 34: L01402, doi:10.1029/2006GL027880.
- Reineke LH (1933) Perfecting a stand density index for even-aged forests. *Journal of Agricultural Research*, **46**, 627 - 638.
- Ritchie JT, Burnett E (1971) Dryland evaporative flux in subhumid climate II. Plant influences. *Agronomy Journal*, **63**, 56 - 62.
- Roberts J, Pymar CF, Wallace JS, Pitman RM (1980) Seasonal changes in leaf area, stomatal and canopy conductances and transpiration from bracken below a forest canopy. *Journal of Applied Ecology*, **17**, 409 - 422.
- Roberts J, Pitman RM, Wallace JS (1982) A comparison of evaporation from stands of Scots pine and Corsican pine in Thetford Chase, East Anglia. *Journal of Applied Ecology*, **19**, 859 - 872.
- Roberts J (2000) The influence of physical and physiological characteristics of vegetation on their hydrological response. *Hydrological Processes*, **14**, 2885 - 2901.
- Roupsard O, Bonnefond J-M, Irvine M, Berbigier P, Nouvellon Y, Dauzat J, Taga S, Hamel O, Jourdan C, Saint-André L, Mialet-Serra I, Labouisse J-P, Epron D, Joffre R, Braconnier S, Rouzière A, Navarro M, Bouillet J-P (2006) Partitioning energy and evapo-transpiration above and below a tropical palm canopy *Agric For Meteorol* 139: 252 – 268.

- Rubilar RA, Allen HL, Kelting DL (2005) Comparison of biomass and nutrient content equations for successive rotations of loblolly pine plantations on an Upper Coastal Plain site. *Biomass & Bioenergy*, **28**, 548 - 564.
- Ruimy A, Saugier B, Dedieu G (1994) Methodology for the estimation of terrestrial net primary production from remotely sensed data. *Journal of Geophysical Research*, **99**, 5263 - 5283.
- Running SW, Nemani R, Glassy JM, Thornton PE (1999) MODIS daily photosynthesis (PSN) and annual net primary production (NPP) product (MOD17), algorithm theoretical basis document, version 3.0. In: <http://modis.gsfc.nasa.gov/>.
- Running SW, Thornton PE, Nemani R, Glassy JM (2000) Global terrestrial gross and net primary productivity from the earth observing system. In: Sala, O.E., Jackson, R.B., Mooney, H.A. (Eds.), *Methods in Ecosystem Science*. Springer-Verlag, New York, pp. 44-57.
- Runyon J, Waring RH, Goward SN, Welles JM (1994) Environmental limits on net primary production and light-use efficiency across the Oregon transect. *Ecol Appl* 4: 226-237.
- Ryan MG (1991a) A simple method for estimating gross carbon budgets for vegetation in forest ecosystems. *Tree Physiology*, **9**, 255 - 266.
- Ryan MG (1991b) Effects of climate change on plant respiration. *Ecological Applications*, **1**, 157 - 167.
- Ryan MG (1995) Foliar maintenance respiration of subalpine and boreal trees and shrubs in relation to nitrogen content. *Plant, Cell & Environment*, **18**, 765 - 772.
- Ryan MG, Linder S, Vose JM, Hubbard RM (1994) Dark respiration of pines. *Ecological Bulletins (Copenhagen)*, **43**, 50 - 63.
- Ryan MG, Gower ST, Hubbard RM, Waring RH, Gholz HL, Cropper WP, Running SW (1995) Woody tissue maintenance respiration of four conifers in contrasting climates. *Oecologia*, **101**, 133 - 140.
- Ryan MG, Lavigne MB, Gower ST (1997) Annual carbon cost of autotrophic respiration

in boreal forest ecosystems in relation to species and climate. *J Geophys Res* 102: 28871 – 28883.

Ryan M, Bond BJ, Law BE, Hubbard RM, Woodruff D, Cienciala E, Kucera J (2000) Transpiration and whole-tree conductance in ponderosa pine trees of different heights. *Oecologia*, **124**, 553–560.

Sack L, Holbrook NM (2006) Leaf hydraulics. *Annual Review of Plant Biology*, **57**, 361 - 381.

Saigusa N, Yamamoto S, Murayama S, Kondo H (2005) Inter-annual variability of carbon budget components in an AsiaFlux forest site estimated by long-term flux measurements. *Agric For Meteorol* 134: 4-16.

Sampson RN, Sedjo RA (1997) Economics of carbon sequestration in forestry: an overview. *Critical Reviews in Environmental Science and Technology*, **27**, S1 – S8.

Sampson DA, Smith FW (1993) Influence of canopy architecture on light penetration in lodgepole pine forests. *Agricultural and Forest Meteorology*, **64**, 63 - 79.

Sanz MJ, Carrara A, Gimeno G, Bucher A, Lopez R (2004) Effects of a dry and warm summer conditions on CO<sub>2</sub> and energy fluxes from three mediterranean ecosystems. *Geophys Res Abstr* 6: 3239.

Sattler DF, LeMay V (2011) A system of nonlinear simultaneous equations for crown length and crown radius for the forest dynamics model SORTIE-ND. *Canadian Journal of Forest Research*, **41**, 1567 - 1576.

Saugier B, Granier A, Pontailier JY, Dufrêne E, Baldocchi DD (1997) Transpiration of a boreal pine forest measured by branch bag, sap flow and micrometeorological methods. *Tree Physiology*, **17**, 511 - 519.

Schäfer KVR, Oren R, Tenhunen JD (2000) The effect of tree height on crown level stomatal conductance. *Plant, Cell & Environment*, **23**, 365 - 375.

- Schäfer KVR, Oren R, Lai C-T, Katul GG (2002) Hydrologic balance in an intact temperate forest ecosystem under ambient and elevated atmospheric CO<sub>2</sub> concentration. *Global Change Biology*, **8**, 895 - 911.
- Schäfer KVR, Oren R, Ellsworth DS *et al.* (2003) Exposure to an enriched CO<sub>2</sub> atmosphere alters carbon assimilation and allocation in a pine forest ecosystem. *Global Change Biology*, **9**, 1378 - 1400.
- Schmid HP, Su HB, Vogel CS, Curtis PS (2003) Ecosystem-atmosphere exchange of carbon dioxide over a mixed hardwood forest in northern lower Michigan. *J Geophys Res* 108: 4417.
- Schneider CA, Rasband WS, Eliceiri KW (2012) NIH Image to ImageJ: 25 years of image analysis. *Nature Methods*, **9**, 671 - 675.
- Scott JS (1997) An examination of crown characteristics, growth efficiency, and bole wood maturation in loblolly pine of various stand densities grown in the absence of interspecific competition. MS thesis. School of Forest Resources, University of Georgia, Athens.
- Sedjo R, Macauley M (2011) Forest carbon offsets: possibilities and limitations. *Journal of Forestry*, **109**, 470 - 476.
- Sellers PJ, Bounoua L, Collatz GJ *et al.* (1996) Comparison of radiative and physiological effects of doubled atmospheric CO<sub>2</sub> on climate. *Science*, **271**, 1402 - 1406.
- Sellin A, Kupper P (2005) Effects of light availability versus hydraulic constraints on stomatal responses within a crown of silver birch. *Oecologia*, **142**, 388 - 397.
- Sharkey TD, Bernacchi CJ, Farquhar GD, Singaas EL (2007) Fitting photosynthetic carbon dioxide response curves for C<sub>3</sub> leaves. *Plant, Cell & Environment*, **9**, 1035 - 1040.
- Sharma M, Burkhart HE (2003) Selecting a level of conditioning for the segmented polynomial taper equation. *Forest Science*, **49**, 324 - 330.
- Shaver GR, Billings WD, Chapin III FS, Giblin AE, Nadelhoffer KJ, Oechel WC, Rastetter EB (1992) Global change and the carbon balance of arctic ecosystems. *Bioscience*, **42**, 433 - 441.

- Shelton MG, Murphy PA (1991) Age and size structure of a shortleaf pine-oak stand in the Ouachita Mountains – implications for uneven aged management. In: Coleman SS, Neary DG (eds). *Proceedings 6<sup>th</sup> biennial southern silvicultural research conference; October 30 – November 1, 1990; Memphis, TN. Vol 2. Gen Tech Rep SE-70 Asheville, NC: US Department of Agriculture, Forest Service, Southeastern Forest Experiment Station.* 852 - 857.
- Smith NG, Dukes JS (2013) Plant respiration and photosynthesis in global-scale models: incorporating acclimation to temperature and CO<sub>2</sub>. *Global Change Biology*, **19**, 45 - 63.
- Soja AJ, Tchebakova NM, French NHF *et al.* (2007) Climate-induced boreal forest change: Predictions versus current observations. *Global and Planetary Change*, **56**, 274 – 296.
- Solomon S, Qin D, Manning M, Chen Z, Marquis M, Averyt KB, Tignor M, Miller HL eds. (2007) *Climate Change 2007-the physical science basis. Contribution of working group I to the fourth assessment report of the Intergovernmental Panel on Climate Change.* Cambridge, United Kingdom and New York: Cambridge University Press. 996 p.
- Sperry JS, Adler FR, Campbell GS, Comstock JP (1998) Limitation of plant water use by rhizosphere and xylem conductance: results from a model. *Plant, Cell & Environment*, **21**, 347 – 359.
- Sprugel DG (1989) The relationship of evergreenness, crown architecture, and leaf size. *Am Nat* 133: 465-479.
- Sprugel DG, Hinckley TM, Schaap W (1991) The theory and practice of branch autonomy. *Annual Review of Ecology, Evolution and Systematics*, **22**, 309 - 334.
- Sprugel DG, Brooks JR, Hinckley TM (1996) Effects of light on shoot geometry and needle morphology in *Abies amabilis*. *Tree Physiology*, **16**, 91 - 98.
- Stenberg P (1996) Correcting LAI-2000 estimates for the clumping of needles in shoots of conifers. *Agricultural and Forest Meteorology*, **79**, 1 - 8.
- Stenberg P (1998) Implications of shoot structure on the rate of photosynthesis at different levels in a coniferous canopy using a model incorporating grouping and penumbra. *Functional Ecology*, **12**, 82 - 91.

- Stenberg P, DeLucia EH, Schoettle AW, Smolander H (1995) Photosynthetic light capture and processing from cell to canopy. In: Smith W, Hinckley T eds. *Resource Physiology of Conifers*. 3 – 38. Academic Press, New York.
- Stenberg P, Palmroth S, Bong BJ, Sprugel DG, Smolander H (2001) Shoot structure and photosynthetic efficiency along the light gradient in a Scots pine canopy. *Tree Physiology*, **21**, 805 - 814.
- Stenberg P, Möttus M, Rautiainen M, Sievänen R (2014) Quantitative characterization of clumping in Scots pine crowns. *Annals of Botany*, DOI: 10.1093/aob/mct310.
- Steppe K, De Pauw DJW, Doody TM, Teskey RO (2010) A comparison of sap flux density using thermal dissipation, heat pulse velocity and heat field deformation methods. *Agricultural and Forest Meteorology*, **150**, 1046 – 1056.
- Stoy PC, Katul GG, Siqueira MBS *et al.* (2006) Separating the effects of climate and vegetation on evapotranspiration along a successional chronosequence in the southeastern US. *Global Change Biology*, **12**, 1 - 21.
- Sun H, Aubrey DP, Teskey RO (2012) A simple calibration improved the accuracy of the thermal dissipation technique for sap flow measurements in juvenile trees of six species. *Trees*, **26**, 631 – 640.
- Suni T, Rinne J, Reissel A, Altimi N, Keronen P, Rannik U, Maso MD, Kulmala M, Vesala T (2003) Long-term measurements of surface fluxes above a Scots pine forest in Hyytiälä, southern Finland, 1996 – 2001. *Boreal Environ Res* 4: 287 – 301.
- Tang X, Li H, Desai AR *et al.* (2014) How is water-use efficiency of terrestrial ecosystems distributed and changing on Earth? *Scientific Reports*, **4**, 7483. DOI: 10.1038/srep07483.
- Tarvainen L, Wallin G, Rantfors M, Uddling J (2013) Weak vertical canopy gradients of photosynthetic capacities and stomatal responses in a fertile Norway spruce stand. *Oecologia*, **173**, 1179 – 1189.
- Tateishi M, Kumagai T, Utsumi Y *et al.* (2008) Spatial variations in xylem sap flux density in evergreen oak trees with radial-porous wood: comparisons with anatomical observations. *Trees*, **23**, 23-30.

- Tedeschi V, Rey ANA, Manca G, Valentini R, Jarvis PG, Borghetti M (2006) Soil respiration in a mediterranean oak forest at different developmental stages after coppicing. *Global Change Biol* 12: 110 – 121.
- Ter-Mikaelian MT, Korzukhin MD (1997) Biomass equations for sixty-five North American tree species. *Forest Ecology and Management*, **97**, 1 - 24.
- Thérézien M, Palmroth S, Brady R, Oren R (2007) Estimation of light interception properties of conifer shoots by an improved photographic method and a 3D model of shoot structure. *Tree Physiology*, **27**, 1375 - 1387.
- Thum T, Aalto T, Laurila T, Aurela M, Kolari P, Hari P (2007) Parametrization of two photosynthesis models at the canopy scale in a northern boreal Scots pine forest. *Tellus Ser B* 59: 874 – 890.
- Tirone G, Dore S, Matteucci G, Greco S, Valentini R (2003) Evergreen mediterranean forests: Carbon and water fluxes, balances, ecological and ecophysiological determinants, in *Fluxes of Carbon, Water and Energy of European Forests*. *Ecol Stud Ser* vol. 163, edited by R. Valentini, pp. 125 – 149, Springer, Berlin.
- Tor-ngern P, Oren R, Ward EJ, Palmroth S, McCarthy HR, Domec J-C (2015) Increases in atmospheric CO<sub>2</sub> have little influence on transpiration of a temperate forest canopy. *New Phytologist*, **205**, 518 - 525.
- Tor-ngern P, Oren R, Oishi AC *et al.* (in review (a)) Daily canopy transpiration of forests controlled by spatial variation of soil texture and canopy leaf area and temporal variation in atmospheric and soil humidity: Synthesis of new and published results.
- Tor-ngern P, Oren R, Palmroth S, Lim H, Ottosson-Löfvenius M, Linder S, Näsholm T (in review (b)) Adaptation of pine crown architecture to growing season solar elevation supports low branches and prevents extra light from reaching competing subcanopy species.
- Trenberth, K.E., P.D. Jones, P. Ambenje, R. Bojariu, D. Easterling, A. Klein Tank, D. Parker, F. Rahimzadeh, J.A. Renwick, M. Rusticucci, B. Soden and P. Zhai, 2007: Observations: Surface and Atmospheric Climate Change. In: *Climate Change 2007: The Physical Science Basis*. Contribution of Working Group I to the Fourth

Assessment Report of the Intergovernmental Panel on Climate Change [Solomon, S., D. Qin, M. Manning, Z. Chen, M. Marquis, K.B. Averyt, M. Tignor and H.L. Miller (eds.)]. Cambridge University Press, Cambridge, United Kingdom and New York, NY, USA.

- Turetsky MR (2003) The role of bryophytes in carbon and nitrogen cycling. *Bryologist*, **106**, 395 - 409.
- Turner DP, Ritts WD, Cohen WB, Gower ST, Zhao M, Running SW, Wofsy SC, Urbanski S, Dunn AL, Munger JW (2003) Scaling gross primary production (GPP) over boreal and deciduous forest landscapes in support of MODIS GPP product validation. *Remote Sens Environ* 88: 256 – 270.
- Turner DP, Urbanski S, Wofsy SC, Bremer DJ, Gower ST, Gregory M (2003) A cross-biome comparison of light use efficiency of gross primary production. *Global Change Biology* 9: 383 – 395.
- Turner DP, Ritts WD, Cohen WB et al. (2006) Evaluation of MODIS NPP and GPP products across multiple biomes. *Remote Sensing of Environment* 102: 282 – 292.
- Tyree MT, Hammel HT (1972) The measurement of the turgor pressure and the water relations of plants by the pressure-bomb technique. *Journal of Experimental Botany*, **23**, 267 – 282.
- Tyree MT, Ewers FW (1991) Tansley Review No. 34. The hydraulic architecture of trees and other woody plants. *New Phytologist*, **119**, 345 - 360.
- Uebelherr JM (2008) The effects of plant-area index on precipitation throughfall and its spatiotemporal variation among deciduous and evergreen forests. MS thesis. University Program in Ecology. Duke University, Durham, North Carolina USA.
- Ulvcrona KA (2011) Effects of silvicultural treatments in young Scots pine-dominated stands on the potential for early biofuel harvests. Doctor's dissertation. Acta Universitatis agriculturae Sueciae 79, 64 pp ISBN 978-91-576-7623-8
- UNFCCC (1997) Kyoto Protocol to the United Nations Framework on Climate Change, United Nations Framework Convention on Climate Change, Document FCCC/CP/1997/L.7?Add.1.

- Valentini R, De Angelis P, Matteucci G, Monaco R, Dore S, Scarascia Mucnozza GE (1996) Seasonal net carbon dioxide exchange of a beech forest with the atmosphere, *Global Change Biol* 2: 199 – 207.
- Valentini R, Matteucci G, Dolman AJ et al. (2000) Respiration as the main determinant of carbon balance in European forests. *Nature* 404: 861 – 864.
- Van Cleve K, Dyrness CT, Viereck LA, Fox J, Chapin FS, Oechel W (1983) Taiga ecosystems in interior Alaska. *Bioscience*, **33**, 39 - 44
- Van Cleve K, Yarie J (1986) Interaction of temperature, moisture, and soil chemistry in controlling nutrient cycling and ecosystem development in the taiga of Alaska. See Ref. 150a, pp. 160-89
- Van Lear DH, Taras MA, Waide JB, Augspurger MK (1986) Comparison of biomass equations for planted vs. natural loblolly pine stands of sawtimber size. *Forest Ecology and Management*, **14**, 205 - 210.
- Vergeynst LL, Vandegehuchte MW, McGuire MA, Teskey RO, Steppe K (2014) Changes in stem water content influence sap flux density measurements with thermal dissipation probes. *Trees*, **28**, 949 – 955.
- Vermeulen PJ (2014) Crown depth as a result of evolutionary games: decreasing solar angle should lead to shallower, not deeper crowns. *New Phytologist*, **202**, 1249 - 1256.
- Vicca S, Luyssaert S, Penuelas J *et al.* (2012) Fertile forests produce biomass more efficiently. *Ecology Letters*, **15**, 520 – 526.
- Vickers D, Thomas CK, Martin JG, Law B (2009) Self-correlation between assimilation and respiration resulting from flux partitioning of eddy-covariance CO<sub>2</sub> fluxes. *Agric For Meteorol* 149: 1552 – 1555.
- Viville D, Biron P, Granier A, Dambrine E, Probst A (1993) Interception in a mountainous declining spruce stand in the Strengbach catchment (Vosges, France). *Journal of Hydrology*, **144**, 273 - 282.

- Vose JM, Dougherty PM, Long JN, Smith FW, Gholz HL, Curran PJ (1994) Factors influencing the amount and distribution of leaf area of pine stands. *Ecol Bull (Copenhagen)* 43: 102-114.
- Wang K, Kellomäki S, Zha T, Peltola H (2005) Annual and seasonal variation of sap flow and conductance of pine trees grown in elevated carbon dioxide and temperature. *Journal of Experimental Botany*, 56, 155 - 165.
- Ward EJ (2012) Improving models of forest carbon and water cycling: revisiting assumptions and incorporating variability. Dissertation. University Program in Ecology. Duke University, Durham NC USA.
- Ward EJ, Oren R, Bell DM, Clark JS, McCarthy HR, Kim H-S, Domec J-C (2013) The effects of elevated CO<sub>2</sub> and nitrogen fertilization on stomatal conductance estimated from 11 years of scaled sap flux measurements at Duke FACE. *Tree Physiology*, 33, 135 - 151.
- Wardle DA, Zackrisson O, Hörnberg G, Gallet C (1997) Influence of island area on ecosystem properties. *Science*, 277, 1296 - 1299.
- Waring RH, Running SW (1998) Forest Ecosystems. *Concepts and Management*, 2<sup>nd</sup> edn. Academic Press, London.
- Waring RH, Whitehead D, Jarvis PG (1979) The contribution of stored water to transpiration in Scots pine. *Plant, Cell & Environment*, 2, 309 – 317.
- Waring RH, Landsberg JJ, Williams M (1998) Net primary production of forests: a constant fraction of gross primary production? *Tree Physiology*, 18, 129 – 134.
- Warren JM, Meinzer FC, Brooks JR, Domec J-C (2005) Vertical stratification of soil water storage and release dynamics in Pacific Northwest coniferous forests. *Agricultural and Forest Meteorology*, 130, 39-58.
- Warren JM, Norby RJ, Wullschlegel SD (2011) Elevated CO<sub>2</sub> enhances leaf senescence during extreme drought in a temperate forest. *Tree Physiology*, 31, 117 - 130.
- Way DA, Montgomery RA (2014) Photoperiod constraints on tree phenology, performance and migration in a warming world. *Plant, Cell & Environment*, DOI: 10.1111/pce.12431.

- Whitehead D, Kelliher FM (1991) Modeling the water balance of a small *Pinus radiata* catchment. *Tree Physiology*, **9**, 17 - 33.
- Whitehead D, Edwards WRN, Jarvis PG (1984) Conducting sapwood area, foliage area, and permeability in mature trees of *Picea sitchensis* and *Pinus contorta*. *Canadian Journal of Forest Research*, **14**, 940 - 947.
- Whittaker RH, Woodwell GM (1969) Structure, production, and diversity of the Oak-Pine forest at Brookhaven, New York. *J. Ecol.* **57**: 155 – 174.
- Wijk MTV, Dekker SC, Bouten W, Bosveld FC, Kohsiek W, Kramer K, Mohren GMJ (2000) Modeling daily gas exchange of a Douglas-fir forest: comparison of three stomatal conductance models with and without a soil water stress function. *Tree Physiology*, **20**, 115 - 122.
- Williams M, Rastetter EB, Fernandes DN, Goulden ML, Shaver GR, Johnson LC (1997) Predicting gross primary productivity in terrestrial ecosystems. *Ecological Applications*, **7**, 882 – 894.
- Williston HL (1972) Shortleaf and loblolly pine growth in the mid-South. *Journal of Forestry*, **70**, 290-291.
- Wilsey BJ, Polley HW (2006) Aboveground productivity and root-shoot allocation differ between native and introduced grass species. *Oecologia*, **150**, 300 - 309.
- Wilson KB, Baldocchi DD (2000) Seasonal and interannual variability of energy fluxes over a broadleaved temperate deciduous forest in North America. *Agricultural and Forest Meteorology*, **100**, 1 – 18.
- Wilson KB, Hanson PJ, Mulholland PJ, Baldocchi DD, Wullschleger SD (2001) A comparison of methods for determining forest evapotranspiration and its components: sap-flow, soil water budget, eddy covariance and catchment water balance. *Agricultural and Forest Meteorology*, **106**, 153–168.
- Wong SC, Cowan IR, Farquhar GD (1979) Stomatal conductance correlates with photosynthetic capacity. *Nature*, **282**, 424 – 426.

- Wonn HT (2001) Height:Diameter ratios and stability relationships for four northern Rocky mountain tree species. *Western Journal of Applied Forestry*, **16**, 87 - 94.
- Woodward FI (1987) *Climate and Plant Distribution*. Cambridge Univ. Press, Cambridge.
- Woodward FI, Smith TM, Emanuel WR (1995) A global land primary productivity and phytogeography model. *Global Biogeochemical Cycles*, **9**, 471 - 490.
- Wullschlegel SD, Meinzer FC, Vertessy RA (1998) A review of whole-plant water use studies in trees. *Tree Physiology*, **18**, 499–512.
- Wullschlegel S, Gunderson C, Hanson PJ, Wilson K, Norby R (2002) Sensitivity of stomatal and canopy conductance to elevated CO<sub>2</sub> concentration - interacting variables and perspectives of scale. *New Phytologist*, **153**, 485 - 496.
- Xiao CW, Yuste JC, Janssens IA, Roskams P, Nachtergale L, Carrara A, Sanchez BY, Ceulemans R (2003) Above- and belowground biomass and net primary production in a 73-year old Scots pine forest. *Tree Physiol* 23: 505 – 516.
- Xu Q, Liu S, Wan X, Jiang C, Song X, Wang J (2011) Effects of rainfall on soil moisture and water movement in a subalpine dark coniferous forest in southwestern China. *Hydrological Processes*, DOI: 10.1002/hyp.8400.
- Yi C, Ricciuto D, Li R et al. (2010) Climate control of terrestrial carbon exchange across biomes and continents. *Environ Res Lett* 5: 034007, 10 pp.
- Yu G, Song X, Wang Q, Liu Y, Guan D, Yan J, Sun X, Zhang L, Wen X (2007) Water-use efficiency of forest ecosystems in eastern China and its relation to climatic variables. *New Phytol* 177: 927 – 937.
- Zaehle S, Medlyn BE, De Kauwe MG *et al.* (2014) Evaluation of 11 terrestrial carbon-nitrogen cycle models against observations from two temperate Free-Air CO<sub>2</sub> Enrichment studies. *New Phytologist*, DOI: 10.1111/nph.12697.
- Zeller K, Nikolov N (2000) Quantifying simultaneous fluxes of ozone, carbon dioxide and water vapor above a subalpine forest ecosystem. *Environ Pollut* 107: 1-20.
- Zha T, Xing A, Wang K-Y, Kellomäki S, Barr AG (2007) Total and component carbon

fluxes of a Scots pine ecosystem from chamber measurements and eddy covariance. *Ann Bot* 99: 345 – 353.

Zhang Y, Oren R, Kang S (2011) Spatiotemporal variation of crown-scale stomatal conductance in an arid *Vitis vinifera* L. cv. Merlot vineyard: direct effects of hydraulic properties and indirect effects of canopy leaf area. *Tree Physiology*, **32**, 262–279.

Zheng G, Moskal LM (2009) Retrieving leaf area index (LAI) using remote sensing: theories, methods and sensors. *Sensors*, **9**, 2719 – 2745.

Zimmermann R, Oren R, Schulze E-D, Werk KS (1988) Performance of *Picea abies* (L.) Karst. Stands at different ages of decline. II. Photosynthesis and leaf conductance. *Oecologia*, **76**, 513 - 518.

Zimmermann R, Schulze E-D, Wirth C, Schulze E-E, McDonald KC, Vygodskaya NN, Ziegler W (2000) Canopy transpiration in a chronosequence of Central Siberian pine forests. *Global Change Biology*, **6**, 25 – 37.

## Biography

Pantana (Poy) Tor-ngern was born on September 3, 1985 in Khon Kaen (~440 km away from Bangkok to the northeast), Thailand. In 2004, she graduated from Mahidol Witthayanusorn high school in Nakhon Pathom (~50 km west of Bangkok) and won a scholarship from the Royal Thai government to continue her higher education in USA. She obtained her bachelor's degree in Electrical Engineering and Physics (second major) from Duke University in 2009. In the same year, she matriculated in a PhD program in Electrical and Computer Engineering at Duke and was granted the John Chambers fellowship for her first year. In summer 2011, she realized that her interest shifted from making nano-lasers to resolving environmental impacts on earth. Fortunately, she was given an amazing opportunity to pursue her bold interest by Professor Ram Oren. For her first project, she examined the decade-long impact of elevated CO<sub>2</sub> concentration on water use of a forest under the free-air CO<sub>2</sub> enrichment experiment at Duke Forest (Duke FACE). The study titled "Increases in atmospheric CO<sub>2</sub> have little influence on transpiration of a temperate forest canopy" was published in *New Phytologist* in January, 2015. In summer 2012, she joined the Department of Forest Ecology and Management at Swedish University of Agricultural Sciences in Umeå, Sweden for research assistantship and as a part of her PhD study, leading to the other three projects presented in this dissertation.